

Three New measuring spark gaps and the development of means for their calibration.

Author:

Medina, Leo

Publication Date:

1958

DOI:

<https://doi.org/10.26190/unsworks/4924>

License:

<https://creativecommons.org/licenses/by-nc-nd/3.0/au/>

Link to license to see what you are allowed to do with this resource.

Downloaded from <http://hdl.handle.net/1959.4/56314> in <https://unsworks.unsw.edu.au> on 2024-04-17

THREE NEW MEASURING SPARK GAPS AND THE DEVELOPMENT OF MEANS
FOR THEIR CALIBRATION.

by
L. Medina

A thesis submitted for the degree of Master of Engineering.

The N. S. W. University of Technology

September 1958.



UNIVERSITY OF N.S.W.

27922 26.FEB.75

LIBRARY

DECLARATION.

I declare that the work described in this thesis or any part of it has not been submitted to any other University or Institution for the purpose of gaining a degree, diploma or certificate.

Signed:

Date :

S U M M A R Y.

An investigation and the design of a crossed cylinder measuring gap using 5 cm diameter tubes for a range of 20 to 140 KV_p is described. This gap is easier to manufacture than a sphere gap for the same range, it is less influenced by the proximity of other objects, it requires less space and its sparkover voltage is remarkably consistent. The polarity effect at 140 KV_p is less than 1/5 of that of the equivalent sphere gap and one calibration table suffices for A.C., A.C. symmetrical, D.C. and 1/50 microsecond impulse waves of either polarity.

In the second part, the performance of this gap as well as of sphere gaps using high value series resistors is described. A guarded and corona free arrangement ensures satisfactory performance at 50 c/s, in the range 30 to 140 KV_p, on waveforms to be expected in practice. The max. discharge current is less than 5 mA r.m.s. and the gap which may be left sparking for a considerable time, without danger of electrode pitting, is the nearest approach to a voltmeter.

Pitting may also be avoided by diverting, after a short time, the current from the measuring gap to another gap, pitting of which has no effect on the accuracy of measurement. A special trigatron gap developed for this purpose is described in the third part. It is a fixture requiring no adjustment for a 3:1 voltage range and no additional equipment with the exception of two resistors. It may also be used to shorten the time of current flow when carrying out dielectric strength tests of liquids. By avoiding excessive carbonisation many tests may be made on one sample. An arrangement having a range of 20 to 60 KV. r.m.s. which is particularly suitable for transformer oil tests is described.

For the calibration of the spark gaps in terms of the Commonwealth primary standards, apparatus and techniques were developed which are of general interest for measurement work. These are described within the thesis and in appendices.

LIST OF CONTENTS.

	<u>Page</u>
1. Introduction	1
2. Comparison between gaps using spheres or crossed cylinders and some design considerations	3
3. The gap type "A".	6
3. 1. Performance on 50 c/s with one cylinder grounded	6
3. 1. 1. Voltage source and control	6
3. 1. 2. Method of voltage measurement	7
3. 1. 2. 1. Measurement of peak voltage on the tertiary	8
3. 1. 2. 2. Testing of the peak volt meter	10
3. 1. 2. 3. Monitoring of the high voltage wave-form	12
3. 1. 2. 4. Proposed procedure for ratio determination	13
3. 1. 2. 5. Remarks regarding the ratio of a three winding transformer	13
3. 1. 2. 6. Bridge circuit for the measurement of the fundamental voltage ratio	15
3. 1. 2. 7. Results of the determination of fundamental ratio.	17
3. 1. 2. 8. Estimated order of difference between fundamental and peak voltage ratio	19
3. 1. 2. 9. Measurement of peak voltage ratio	20
3. 1. 2. 10. Precautions taken in the determination of the peak voltage ratio	22
3. 1. 3. Preparation of spark gap electrodes	25
3. 1. 4. Preliminary tests	25
3. 1. 5. Perturbation tests	27
3. 1. 5. 1. Remarks on the proximity of other objects	31
3. 1. 6. Calibration data	33
3. 2. Performance on D.C. with one cylinder grounded	35
3. 2. 1. D.C. voltage generation and indication	35
3. 2. 1. 1. An estimate of ripple voltage and a simple method of measurement without the use of high voltage components	37
3. 2. 2. D.C. test results	40

3. 3.	Performance with $1/50$ microsecond impulse waves, one cylinder grounded	40
3. 3. 1.	The impulse generator	40
3. 3. 2.	Test results with impulse waves and polarity effect	43
3. 4.	Performance on symmetrical A.C. (transformer centre tap grounded)	45
3. 4. 1.	Voltage generation and measurement	45
3. 4. 2.	Test procedure and results	46
3. 4. 2. 1.	Spark gap capacitance and arrangement for constant capacitive loading	47
3. 5.	Comments on relative humidity and irradiation .	49
3. 6.	Conclusions re gap type "A"	50
3. 7.	References re gap type "A"	52
4.	The gap type "B"	58
4. 1.	The influence of a large series resistor . . .	58
4. 1. 1.	Observations	58
4. 1. 2.	Design requirements	59
4. 2.	Performance tests	61
4. 2. 1.	Discussion of performance	62
4. 3.	Applications	63
4. 4.	Two simple discharge current indicators	64
4. 5.	Conclusions re gap type "B"	65
4. 6.	References re gap type "B"	65
5.	The gap type "C"	66
5. 1.	Preliminary work	66
5. 2.	The trigatron diverter gap	68
5. 2. 1.	Circuit description	70
5. 2. 2.	The shape of the main electrodes	70
5. 2. 3.	The hole diameter and the needle position . . .	71
5. 2. 4.	The time lag	74
5. 2. 5.	Choice of values for R_1 and R_2	75
5. 2. 6.	Discussion of performance	76
5. 3.	Extension of the voltage range	76

5. 3. 1.	The use of two diverter gaps	77
5. 3. 2.	Other applications of gap type "C"	78
5. 4.	Conclusions re gap type "C"	81
5. 5.	References re gap type "C"	81
6.	Acknowledgements	83
7.	Appendices	84

<u>Appendix 1:</u>	Standard resistors wound with controlled tension on pyrex glass formers	84
	a) The influence of the former	84
	b) Physical concept of compensation	85
	c) General expression for the fictitious load coefficient of the former	86
	d) Methods of load coefficient measurement	89
	e) Experimental verification and performance of resistors built	92

<u>Appendix 2:</u>	The crossed rectangle parallel plate three terminal capacitor	96
	a) Capacitance change as a function of geometrical configuration for square, circular and rect- angular plates	96
	b) Suggested explanation of good results obtained when deliberately rough workmanship was employed	97
	c) Methods of testing	98

<u>Appendix 3:</u>	Computation and measurement of the self-capacitance of multiple layer coils	101
	a) The "VA" rule	101
	b) Derivation of an expression for coil self- capacitance	101
	c) A practical method of measuring the self- capacitance of very large iron cored coils	103

	<u>Page</u>
<u>Appendix 4:</u>	
The design of optimum "Q" reactors. (Hysteresis not neglected)	105
a) Condition for maximum "Q"	105
b) The "General Radio" method	106
c) Improvement on the "General Radio" method . .	106
d) Derivation of equations	107
e) Typical data and a sample design	107
f) A simple bridge for the measurement of "L" and "Q"	108
 <u>Appendix 5:</u>	
A crossed cylinder high voltage three terminal aircapacitor	110
a) The electrode configuration for an experimental model	110
b) A simple bridge for capacitance measurement . .	111
c) Capacitance and perturbation tests	113
d) High voltage tests and comparison with computation	116
e) Discussion and applications	118
 <u>Appendix 6:</u>	
A simple method of impulse wave chopping	122
a.) Review of known methods	122
b) Description of new circuit and analysis	123
c) Performance and applications	126
 <u>Appendix 7:</u>	
The use of corona detection apparatus for finding, at low voltage, the voltage distribution on high voltage insulators and the detection of internal sparking in high voltage resistors	128
 8.	
References pertaining to the appendices	135
9.	
A general remark, clarifications and recent changes in the equipment described	136



1. Introduction.

The use of crossed cylinders in a measuring spark gap has been suggested by Schwaiger (1) and several workers (2, 3, 4, 5) have published the results of A.C. breakdown tests of this electrode configuration in atmospheric air because of its general importance in the design of high voltage apparatus. This importance stems from the fact that the configuration "cylinder in a torus" may be approximated as a case of crossed cylinders.

In order to ascertain if such a gap has worthwhile advantages over the commonly used sphere gap, a gap was constructed and its performance tested on A.C., D.C. and impulse waves.

A mechanically and electrically sound design was aimed at with a view to use this gap for the calibration of testing transformers in situ during N.A.T.A. assessments and because of the interest of a manufacturer in the commercial production of this gap.

The maximum voltage was fixed at 140 KVp for three reasons. Firstly, the majority of Australian manufacturers (electrical, chemical, plastics, Radio and T.V.) require test voltages below 140 KVp. Secondly, preliminary work has shown that a gap for higher voltages would lead to an awkward structure. Thirdly, the maximum voltage available for experimental work on A.C. was 140 KVp.

Although in practice spark gaps are mostly used with one electrode grounded both cylinders were isolated because, sometimes, in small factories, for reasons of economy, A.C. test voltage is obtained either by means of a transformer with earthed centre tap or by series connecting the high voltage windings of two transformers with graded insulation. This gap which is thus also suitable for use on symmetrical alternating voltages is subsequently designated as "type A".

In common with other spark gaps a protective device (fuse or overload-relay) is necessary in order to interrupt the supply on spark-over. If the setting of this protective device is such that it can cope with large testing currents - e.g. in cable testing - the series resistor of the spark gap, which is always used to damp out dangerous

r.f. oscillations, must be small to ensure interruption on sparkover. The discharge current is therefore large and quickly causes pitting of the electrodes.

An investigation was therefore made on the influence of a series resistor which is so large that it prevents interruption of the supply and which limits the current to so low a value that pitting will not occur even if the gap is left sparking for a considerable time. A gap with a large series resistor has also been constructed and it is subsequently designated as "type B".

Its practical importance was brought home forcibly by the following incident. A very valuable cable was tested by its manufacturer for 15 minutes at the prescribed voltage as read on the primary voltmeter of a testing transformer. Due to partial resonance of the cable capacitance with the leakage inductance the actual test voltage was nearly twice as high. Although the cable passed the test it failed in service after two weeks because of the erosive damage done by internal ionisation during the pressure test. This led to the development of "type B" gap which permits convenient measurement of the actual voltage on the cable without expensive equipment.

Instead of limiting the current through the gap the time of current flow may be kept short by diverting the current from the measuring gap to an auxiliary gap pitting of which has no influence on the accuracy of peak voltage measurement.

A trigatron diverter gap which neither requires auxiliary electronic apparatus nor a change in spacing for a 3:1 voltage range and which therefore can be a fixture added to a measuring spark gap has been developed and it is subsequently designated as "type C".

This diverter gap may also be used in connection with a standard oil test cell. It will prevent carbonisation and permit several breakdown tests to be carried out on one sample of oil.

2. Comparison between gaps using spheres or crossed cylinders and some design considerations.

The advantage of stock size tubing requires no comment as far as ease of manufacture is concerned.

A less obvious advantage is the greater wall thickness of tubes as compared with spheres which are usually spun and thin walled. The thicker tubes are not only less sensitive to denting but they quickly conduct the heat away from the sparking area. This is important because successive discharges produce heat and decrease the airdensity of the layer of air in contact with the electrodes. Consequently the sparkover voltage is lowered. The effect is much less pronounced with crossed cylinders. (See section 3. 1. 4.).

The electric performance may qualitatively be assessed by comparing the field strength at the surface of the two electrode configurations. Let (F) be the field strength in V/cm and (a) the shortest spacing in cm of two electrodes the potential difference of which is (V).

$$F_{max} = \frac{V}{a} \cdot \frac{1}{\gamma}$$

..... 1.

wherein $1/\gamma$ is the stress multiplication factor. For spheres of radius (r) in cm and $a/r < 2$, Russel (6) found :

$$\frac{1}{\gamma} = 1 + \frac{a}{3r} + \frac{a^2}{45r^2} + \frac{2a^3}{945r^3} + \dots$$

..... 2.

For crossed cylinders Schwaiger (1) found experimentally that the breakdown voltage is nearly independant of the angle between the cylinders and the well known expressions for the fieldstrength on the surface of parallel cylinders have been used for crossed cylinders. However, even if the breakdown values experimentally obtained are identical for crossed and parallel cylinders it is regarded erroneous to assume

that $1/\eta$ is the same for crossed or parallel cylinders because the puncture strength of air which is known to depend on the electrode configuration may be different for the two cases. Clearly, only if $1/\eta$ can be computed for crossed cylinders the puncture strength of air for this configuration would be known from the measured breakdown value. At the author's instigation Harper and O'Dwyer (7) showed that for crossed cylinders :

$$\frac{1}{\eta} = 1 + \frac{a}{6r} - \frac{a^2}{90r^2} + \dots \quad \text{..... 3.}$$

and for parallel cylinders :

$$\frac{1}{\eta} = 1 + \frac{a}{6r} - \frac{a^2}{180r^2} + \dots \quad \text{..... 4.}$$

Inspection of equations 2 and 3 shows that for the same ratio of a/r the field is much more uniform for crossed cylinders. However this comparison is incomplete. A sphere gap for 140 KVp can be made with spheres of 10 cm diameter as shown in B.S.S. 358/1939 (8). Cylinders of this diameter would weigh more because they would have to be of sufficient length to avoid end effects and to prevent corona at the ends rounded caps would have to be fitted. Such a gap would, owing to its more uniform field perform better - e.g. it would have less polarity effect on D.C. - but it would be an awkward structure and the simplicity claimed for the cylindrical gap would be lost.

A more realistic comparison is to compare 10 cm diameter spheres with 5 cm diameter tubes, turned down from 2 inch O.D. material.

For 140 KVp the spacing of 10 cm diameter spheres can be interpolated from Table 2 of the B.S.S. 358 as 5.67 cm. Table 2 has been chosen because this Table is valid for equal and opposite potential of the electrodes and this is the assumption made in the derivation of the expressions by Russel and Harper and O'Dwyer. a/r is then 1.135. For cylinders of 5 cm diameter a spacing of 5.5 cm can be

expected from the work of Pankow (4). a/r is here 2.20. Putting these values in equations 2 and 3 yields a stress multiplication factor of 1.41 for spheres and 1.31 for crossed cylinders, indicating a more uniform field in the latter case.

In a precision measuring gap sparkover must precede corona in the sparking area. Corona would not only make the sparkover value strongly depending on the atmospheric humidity (10) and increase the scatter of results but it would cause a spark delay which would render the gap useless for measuring impulse voltages.

According to Peek (9) corona will not precede sparkover on spheres if $a/r < 2.04$ and on parallel cylinders if $a/r < 3.85$. These figures are arrived at by assuming an increase in diameter due to corona - "halo-effect" - and give the critical ratio at which the reduction in surface gradient due to the increased radius is just equal to the increase in surface gradient due to the reduced distance. Thus, these expressions are independent of the puncture strength of atmospheric air and it seems permissible to use, for the purpose of this comparison, the figure $a/r < 3.85$ also for crossed cylinders because according to equations 3 and 4 the difference in $1/\eta$ between parallel and crossed cylinders is only in the third term amounting to about 2% for an a/r value of 2. In both cases 10 cm diameter spheres as well as 5 cm diameter cylinders, a/r is approx. 60% of the limiting case for corona. The corona safety factor is therefore about the same in both cases.

Preliminary tests (see Section 3.1.4.) have shown that slight corona emanates from the semi-spherical ends of the cylinders above 130 KVp. Tests described later show this to be harmless at 140 KVp but this corona would set a lower limit to the diameter of the cylinders. A smaller diameter would still give sufficient safety against corona in the sparking area but other than semi-spherical endcaps would be necessary. As this is mechanically inelegant and as the 5 cm diameter cylinders give a more uniform field this diameter was decided upon.

The gap "type A" has slightly higher capacitance than a similarly constructed sphere gap for the same range. Typical values (for details

see Section 3.4.2.1.) for a horizontal gap with one cylinder grounded and connected to a 6 by 3 ft earth plane are 16.3 and 20.5 pF for 5.5 cm and 0.5 cm spacing respectively. The capacitance of a spheregap using 10 cm diameter spheres was found to be 3 to 4 pF less. This is quite insignificant as far as loading of testing transformers or impulse generators is concerned but it is slightly disadvantageous for a gap with a large series resistor.

3. The gap "type A".

The main details are shown in Fig 1 and plate 1. Spacing is being measured by a linear scale subdivided in mm and a vernier. The scale and vernier have been engraved on a linear dividing engine in the division of metrology C.S.I.R.O. Zero spacing is checked before use with an ohm-meter which indicates touching of the cylinders. The scale has elongated mounting holes which permit precise adjustment of the zero reading. A magnifying glass is used to read the vernier.

3.1. Performance on A.C. 50 c/s with one cylinder grounded.

3.1.1. Voltage source and control.

The testing transformer used in this work is rated 30 KVA. It has 2 identical 240 V windings and one 100,000 V r.m.s. secondary winding. One of the 240 V windings is subsequently designated primary and the other tertiary, the latter being used for metering. The core cross-section is 40 sq. inches and there are 6V/turn. The winding D.C. resistances are 0.019 and 2590 Ohms respectively at 20 degr. C. Further data are given in Section 3.1.2.7.

Coarse voltage control is effected by 3 paralleled variacs each rated 7 KVA. See Fig. 2. A balancing choke ($N = 10$, $A = 1.9$ sq. inches) was designed to restrict to less than 2 Amperes the circulating current caused by about 2 Volts unbalance of the variacs.

The overcurrent trip device of the available air circuit breaker did not permit adjustment over a wide range of currents, was slow in operation and considerable physical effort was required to close the breaker after tripping. In view of an anticipated 20,000 operations during the course of this investigation this was an important considerat-

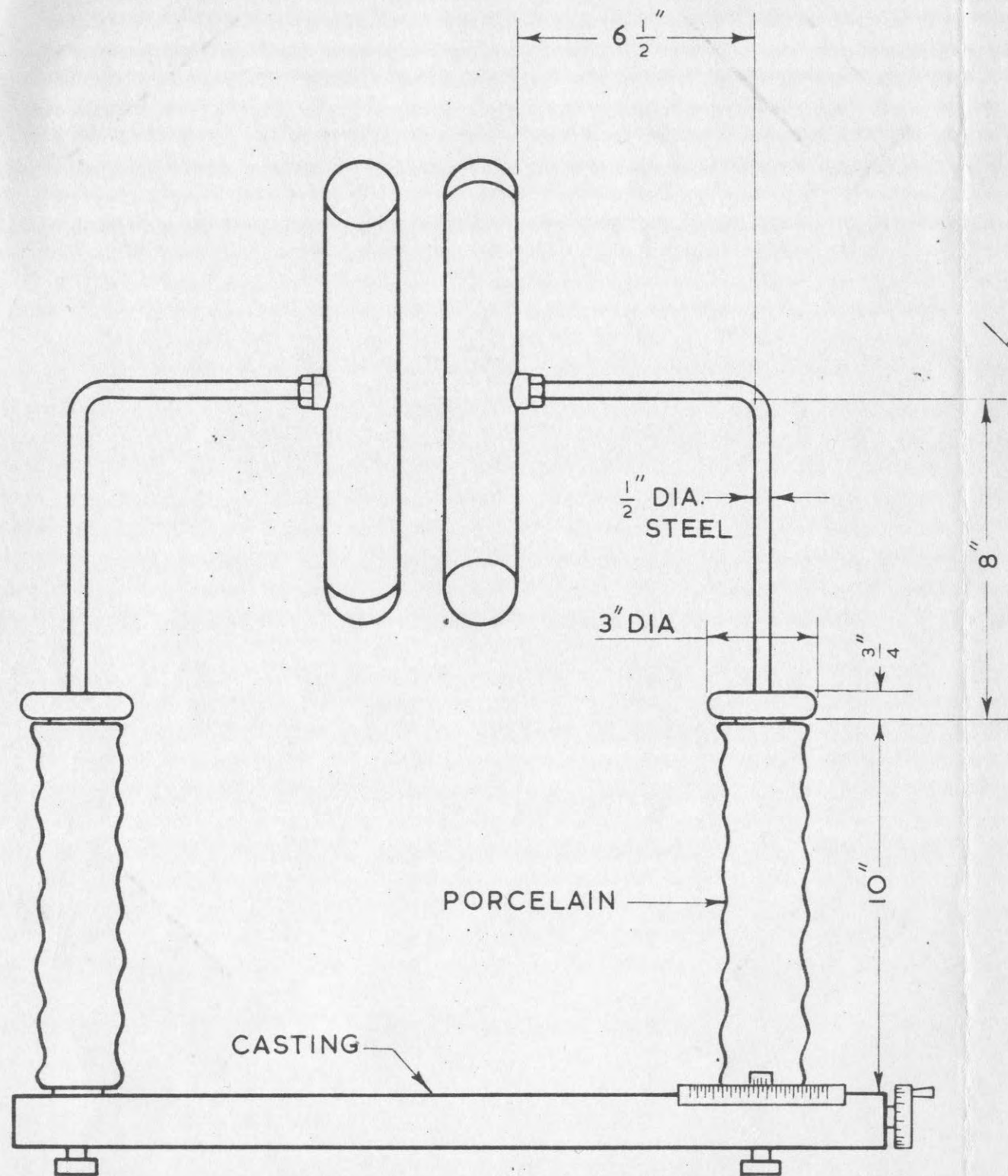
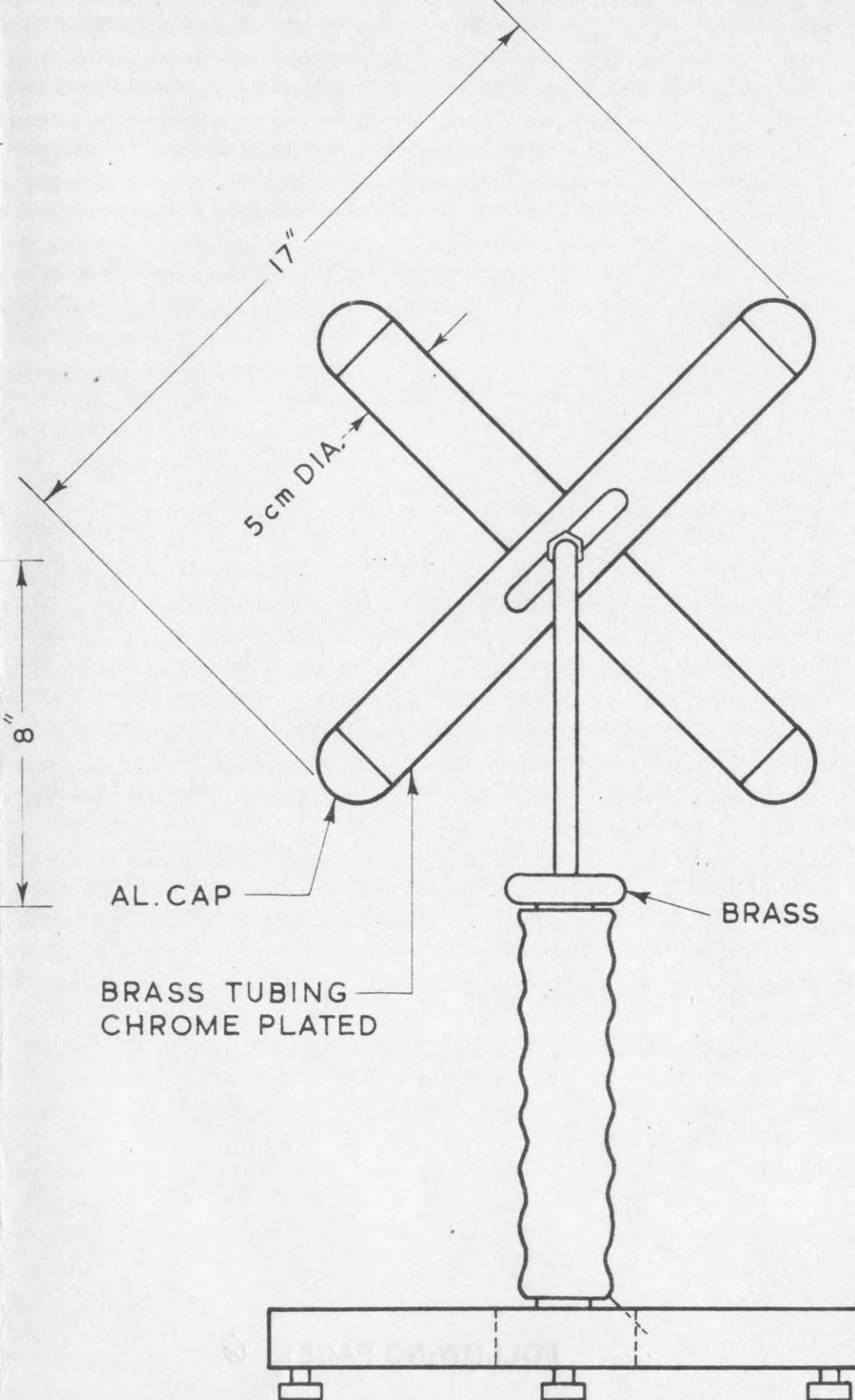


Fig. 1.



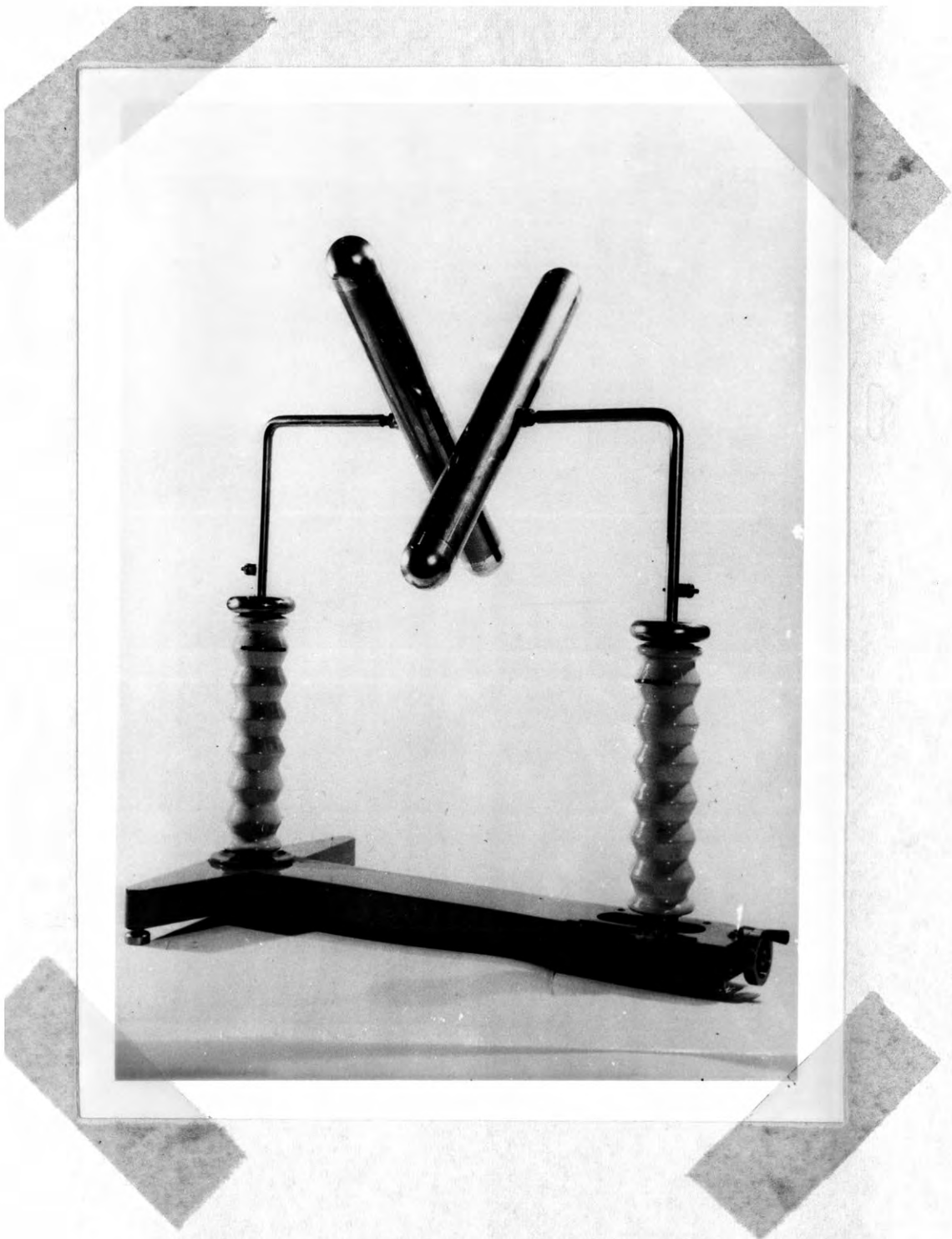


Plate 1. The gap type "A".

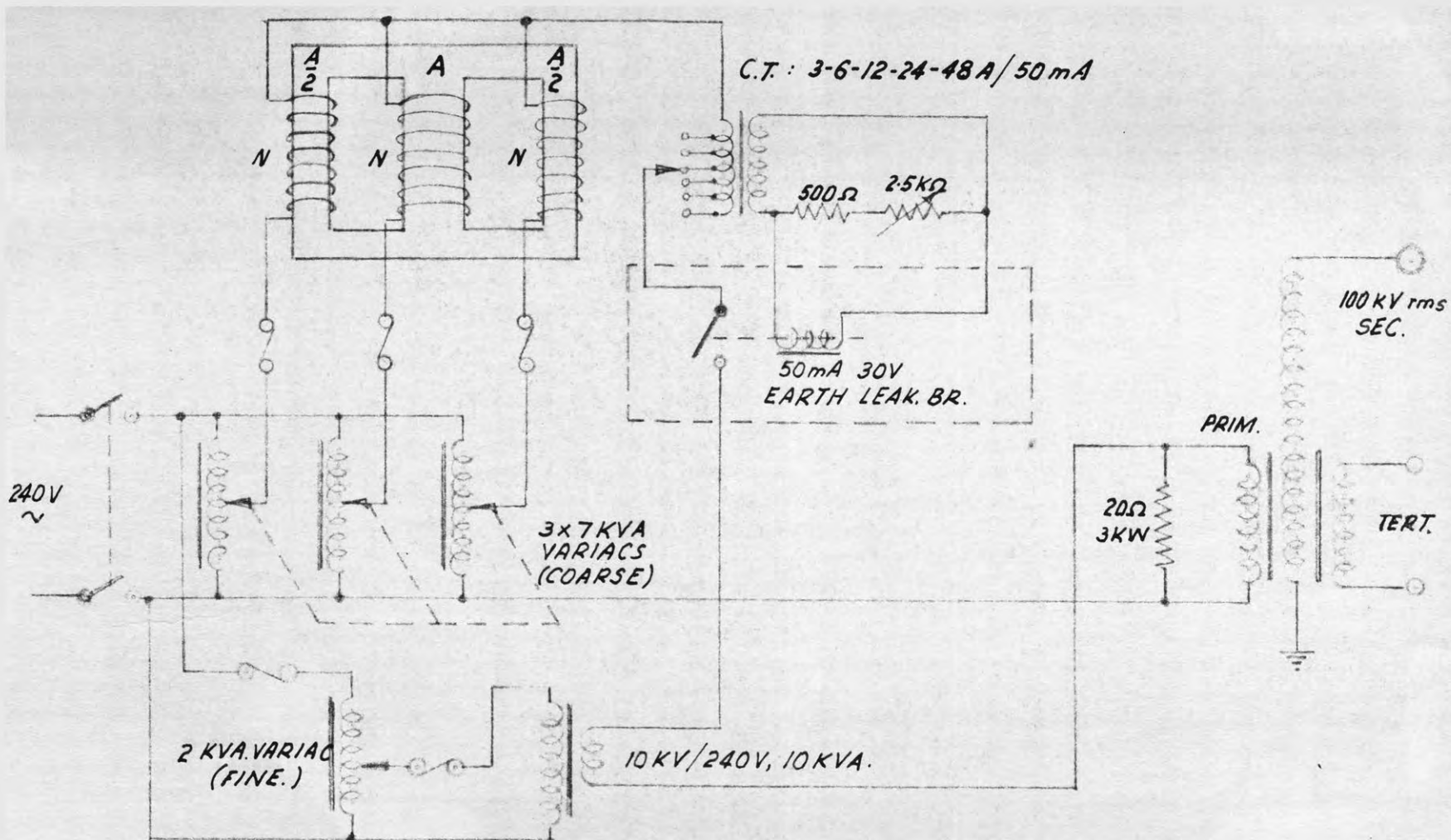


FIG. 2 : VOLTAGE CONTROL CIRCUIT.

ion because physical energy could be better used to concentrate on reading meters. The solution adopted consisted of the use of an electromagnetically tripped earth leakage breaker with a current transformer supplying the tripping current. Coarse control of the tripping current was by taps (see Fig. 2) and fine control by means of a variable resistive shunt. The current transformer designed for this purpose has a cross-sectional area of 1.9 sq. inches, a primary of 16 turns tapped at 1, 2, 4 and 8 turns and 960 secondary turns. The unit is small and inexpensive and can be used for general laboratory work instead of fuses.

A 20 Ohm - 3 KW resistor was solidly connected across the primary terminals of the testing Transformer. It served to dissipate the magnetic energy stored in the core and to prevent dangerous switching surges.

3.1.2. Method of voltage measurement.

The most unambiguous way of measuring the peak voltage applied to the gap under investigation is to measure directly at the high voltage terminals of the testing transformer. In precise work this is usually done by putting a low voltage peak voltmeter across the low voltage arm of a voltage divider, the divider being either resistive or capacitive. Such a divider, which for high voltages is a complex piece of apparatus, was not available. The only stable high voltage component at the author's disposal was a capacitor, 5 pF, rated 85 KV r.m.s. designed for corona investigations and described before. (11). Plate 2 shows a photograph of this capacitor.

Measurement at the secondary had to be abandoned owing to the insufficient voltage rating of the capacitor in favour of measuring the peak voltage of the tertiary and multiplying it with the Ratio. This ratio is not the turns ratio and not the fundamental voltage ratio as determined in a bridge circuit using a tuned detector but the peak voltage ratio.

While a large amount of work could have been avoided had a high voltage divider been available it is considered that the investigation

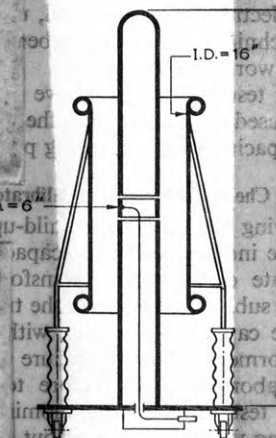
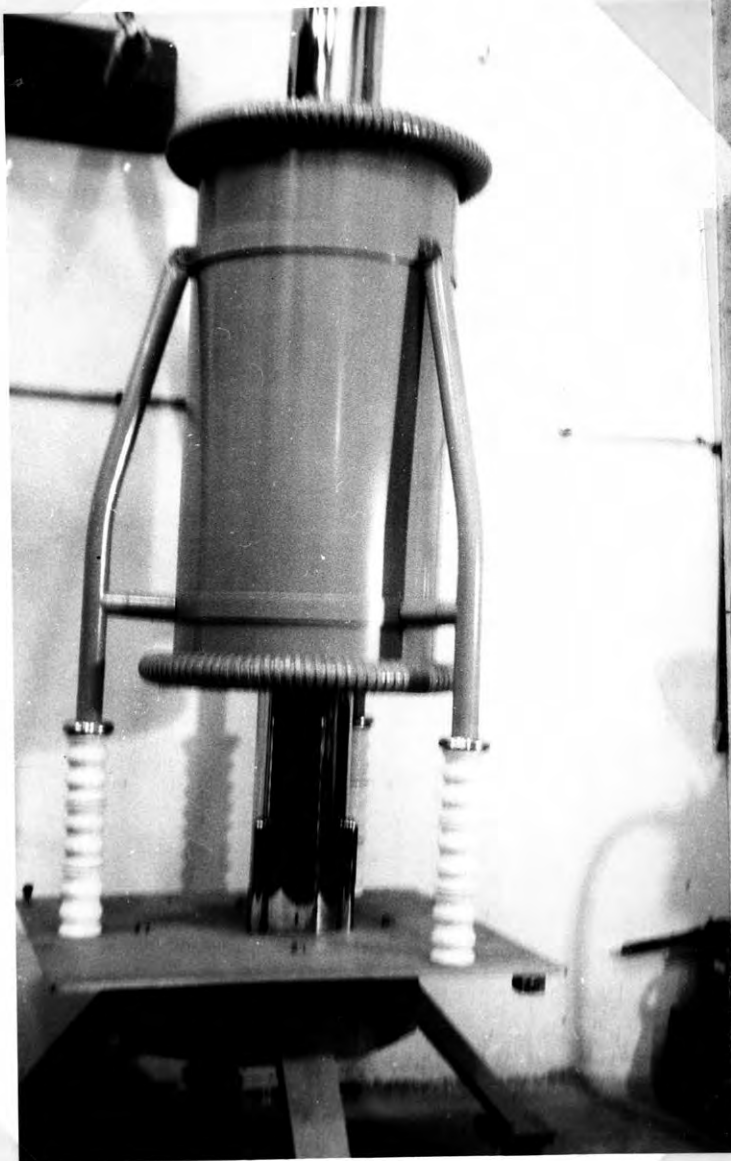


Plate 2. 5 pF, 85 KV r. m. s. , three terminal air capacitor.

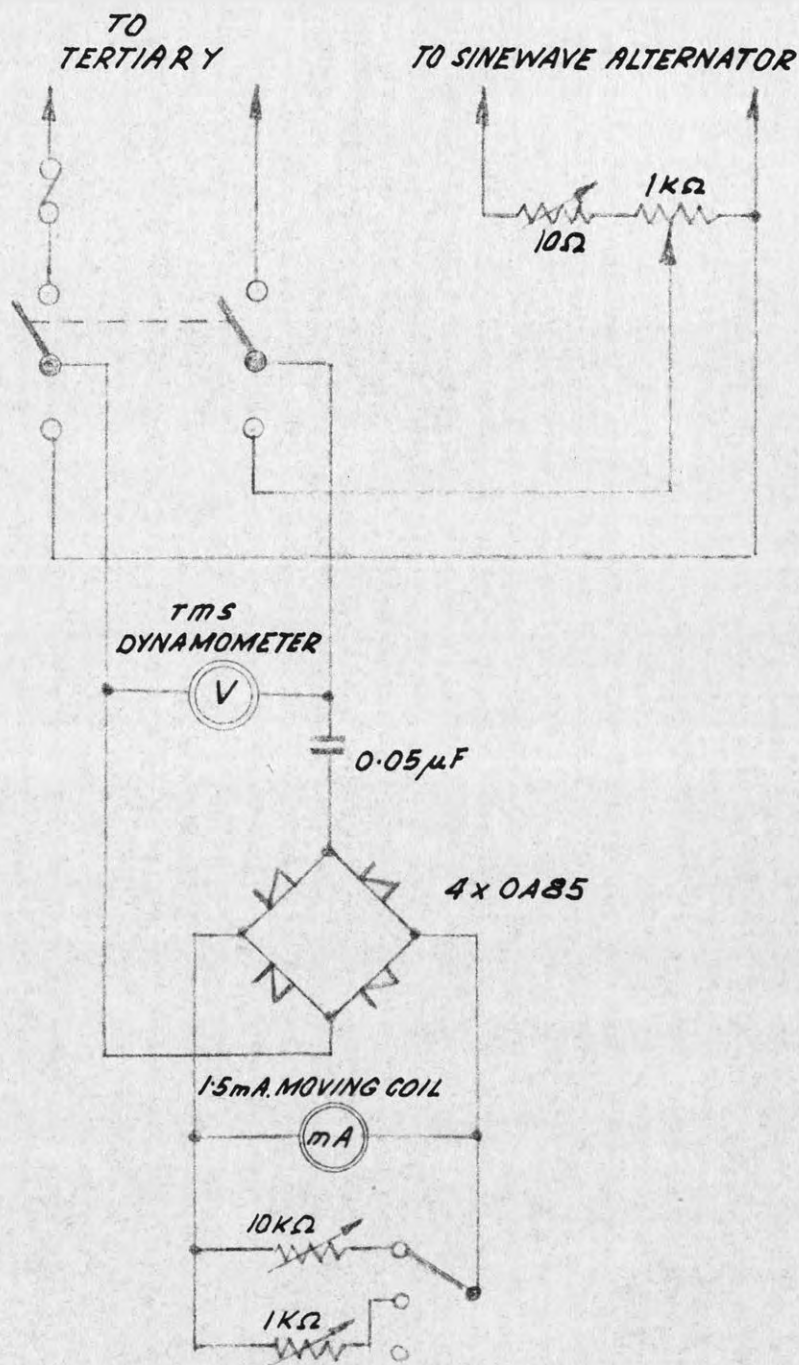
was worth while. Firstly, experience gained since 1947 in the design, testing and use of inductive ratio arms could now be extended to a testing transformer which in principle is an inductive ratio arm and it was also hoped to make use of additional knowledge gained for N.A.T.A. assessments. Secondly, a method believed to be novel for the determination of the peak voltage ratio was developed. Thirdly, if precise measurements - at least on open circuit - can be done from the tertiary, the convenience of this outweighs the initial work.

Peek, nearly half a century ago, with the primitive means at his disposal must have found this, because he very much favoured testing transformers with tertiaries.

3.1.2.1. Measurement of peakvoltage on the tertiary.

Fig. 3 shows the circuit employed. Two paralleled meters could be switched either to the tertiary or to the output terminals of a sine wave alternator which operated at nearly no load and the distortion of which did not exceed 0.05%. One instrument was r.m.s. reading and consisted of a first grade dynamometer the corrections of which were less than 0.3% and were known to a few parts in 10,000 by calibration against the A.C. standard voltmeter of the Division of Electrotechnology C.S.I.R.O. This standard meter is a multi-cellular electrostatic voltmeter with a useful range of 50 to 100 volts. A voltage divider was designed for use at higher voltages. Fig. 4 shows the circuit. Highly stable resistors made of bare wire and wound under tension on strain-free pyrex formers have been developed for this divider. Their theory, construction and performance are described in Appendix 1. Voltages below 50 volts are measured by means of mu-metal cored step-up transformers. Their design is conventional and is based on the exact knowledge of W/lb and VAR/lb as a function of fluxdensity. This has been described before. (21).

The peak reading instrument was a substandard moving coil meter (1.5 mA) which was used to measure the charging current of a high grade mica capacitor of 0.05 microfarad capacitance, rectification being effected by four OA 85 germanium diodes. The theory of this method



$$V_{max} = \frac{I_{AV}}{4 \cdot C \cdot f} = \frac{1.5 \cdot 10^{-6}}{1000 \cdot 4 \cdot 0.05 \cdot 50} = 150 V_{peak}$$

FIG. 3 : PEAK-VOLTMETER CIRCUIT.

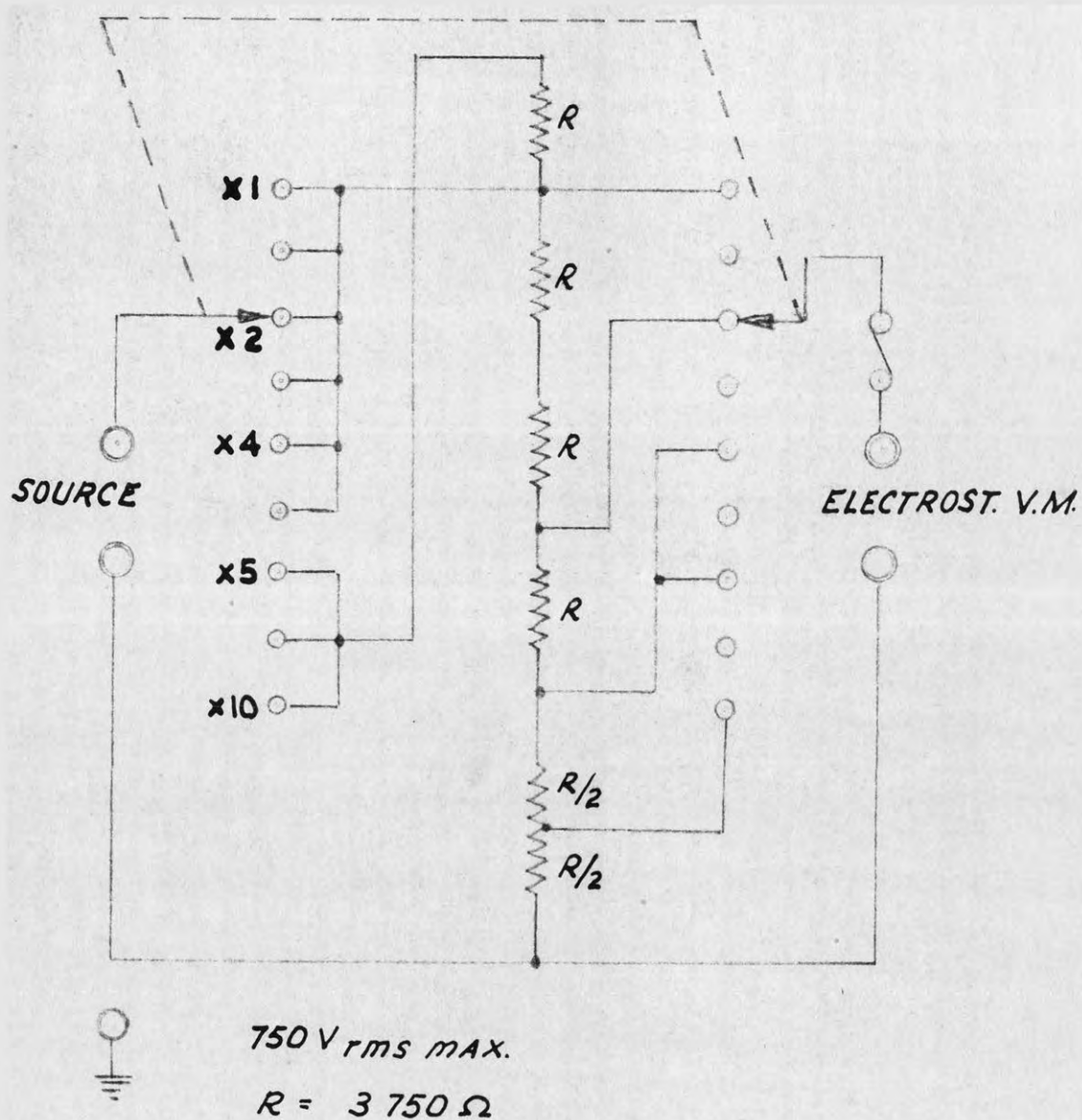


FIG. 4 : RESISTIVE VOLTAGE DIVIDER

(SEE APPENDIX I FOR DETAILS OF RESISTORS)

has been investigated by numerous workers and it is now described in textbooks. (12). The use of germanium or silicon diodes in this arrangement is much better than the use of electron tubes. Although the error from the current due to the initial velocity of emission can be nullified by a counter e.m.f. the advantage of avoiding this is obvious. The D.C. meter was also equipped with a finely variable resistive shunt. A Helipot was used for this. Both meters were first connected to the sine wave alternator and by means of a variable resistive divider the r.m.s. meter was adjusted to give a reading at a calibration point approx. as expected at breakdown of the gap at the particular spacing to be investigated. The D.C. meter was then adjusted by means of its shunt to give a reading at a convenient cardinal point, if possible, in the upper half of its scale. Thus the peak voltmeter was spot calibrated before and after each series of measurements in terms of r.m.s. value $\times \sqrt{2}$. This procedure was found to be very useful because it does not necessitate interpolation between calibration points on the dynamometer, the calibration point being transferred to an instrument with a linear scale. The deviation from linearity of a moving coil meter over a small part of its scale is certainly less than the uncertainty between calibration points of the dynamometer. It should be noted that the voltage of the sine wave alternator was adjusted by a resistive divider and not by a variac in order to avoid distortion of the wave.

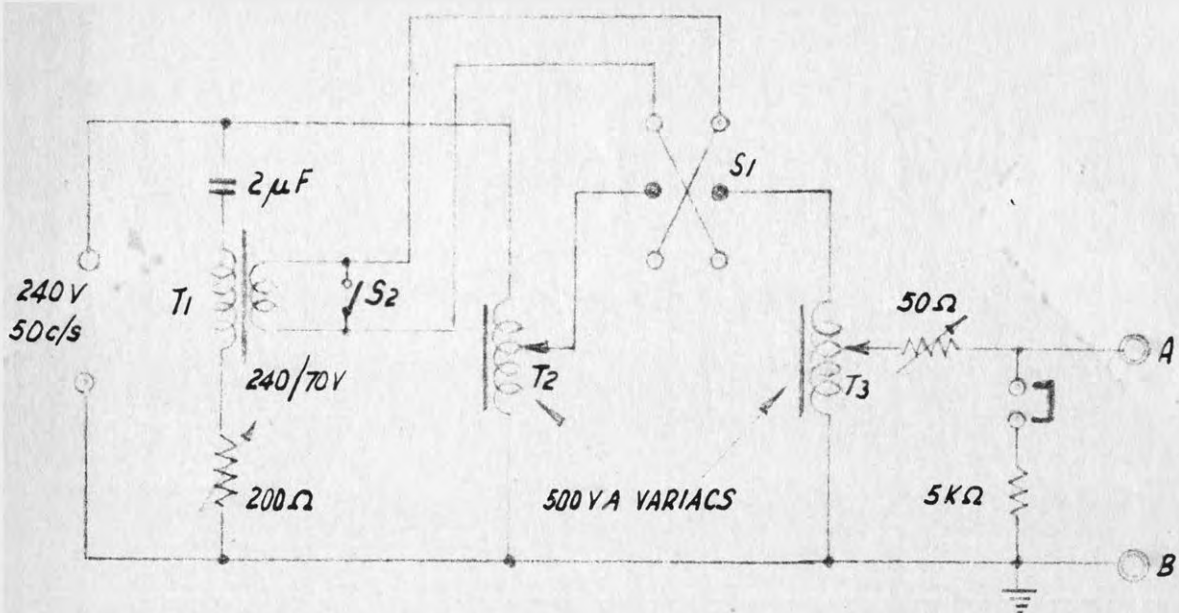
It may be speculated why the peak voltmeter with long time constant which "holds" the peak reading (13) was not used in this investigation. The reasons were twofold. Firstly it was found that the 20 Ohm resistor (see Fig. 2) does not completely suppress overvoltages, and on tripping an overvoltage of about 1% has occasionally been observed. While this is insignificant for routine tests on dielectrics it is not good enough for the work envisaged here. Secondly, a suitable movement of substandard repeatability for use in the electronic instrument described in reference 13 was not available.

It should also be stressed that the standard voltmeter mentioned before is an A.C./D.C. transfer device and it is calibrated with D.C. in terms of the Commonwealth standards of e.m.f. and resistance. As the dynamometer was calibrated by means of the standard voltmeter and as

the peak voltmeter was spot calibrated by means of the dynamometer it follows that the spark gap was calibrated in terms of the Commonwealth standards.

3.1.2.2. Testing of the peak voltmeter.

The scheme for testing if the peak voltmeter is in fact peak reading is based on observing if the meter gives the same deflection independent of waveform if fed with waves of exactly equal amplitude. The apparatus required for this (14) are a distortion generator and an indicator of amplitude. Fig. 5 shows the circuit of the distortion generator developed during class work in the conversion measurements course, school of electrical engineering, the N.S.W. University of Technology, in order to show the students the performance of various instruments on nonsinusoidal waves. Because of partial resonance the voltage on the 240 V primary of T_1 is higher than 240 V and the magnetising current is very distorted. This distorted current flows through the 2 microfarad capacitor and causes a distorted waveform on T_1 even if the source of supply has a sinusoidal voltage wave form. This is shown in oscillogram No. 1 of Plate 3. It was found that other waveforms, e.g. oscillograms 2, 3 and 4 may be obtained by adding the sinusoidal voltage from Variac T_2 to the voltage of T_1 . The waveform may be changed by altering the position of the brush on T_2 . Waveforms 5 and 6 are obtained by reversing. (Switch S_1). Undistorted output is obtained by shorting T_1 with S_2 . The second variac T_3 serves for coarse and the 50 Ohm resistor for fine output control. It is not possible to use the mathematical treatment given by Klinkhamer (15) for the solution of the partial resonance problem because this intrinsically difficult task is still more complicated in this case because the voltage on T_1 must have only one peak. Only then is it possible to obtain the typical waveforms shown in Plate 3 by the simple expedient of adding a sinewave. Adjustment for a single peak in oscillogram No. 1 is carried out by means of the 200 Ohm resistor. If iron with more than 1.2 W/kg at 10 kilogauss is used the resistor is not necessary. In operation the r.m.s. voltage on T_1 is approx. 350 V and approx. 550 V on the capacitor. With the data given in the circuit the generator will deliver slightly



T_1 : 17/1.5 Ω D.C.; 960/280 TURNS; AREA = 1.9 SQ. IN.

FIG. 5: DISTORTION GENERATOR

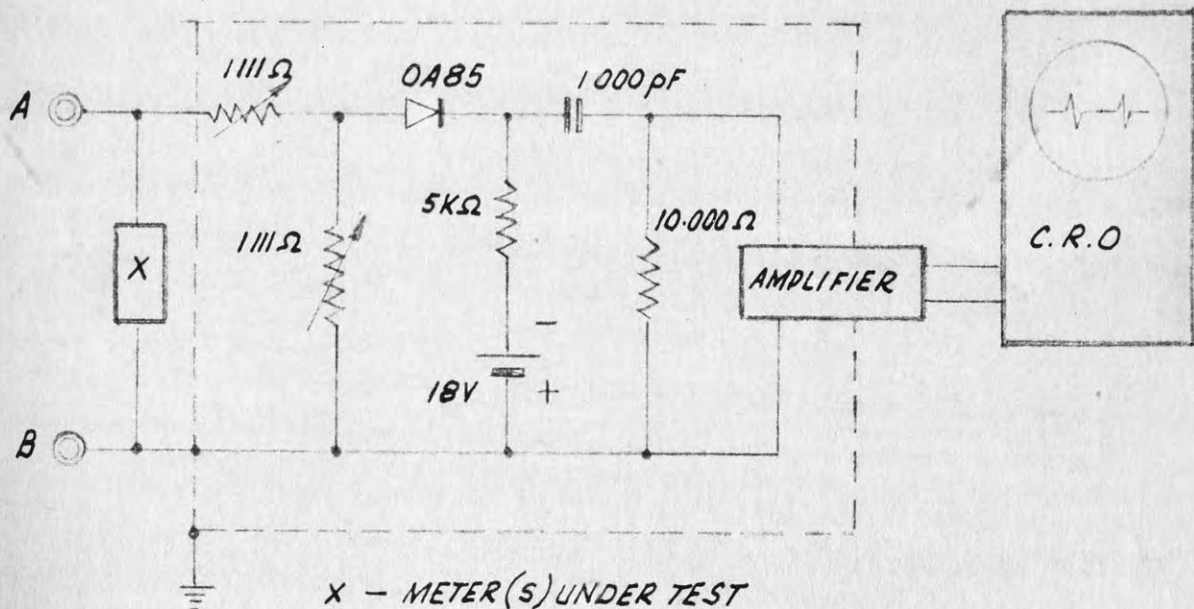


FIG. 6: AMPLITUDE INDICATOR

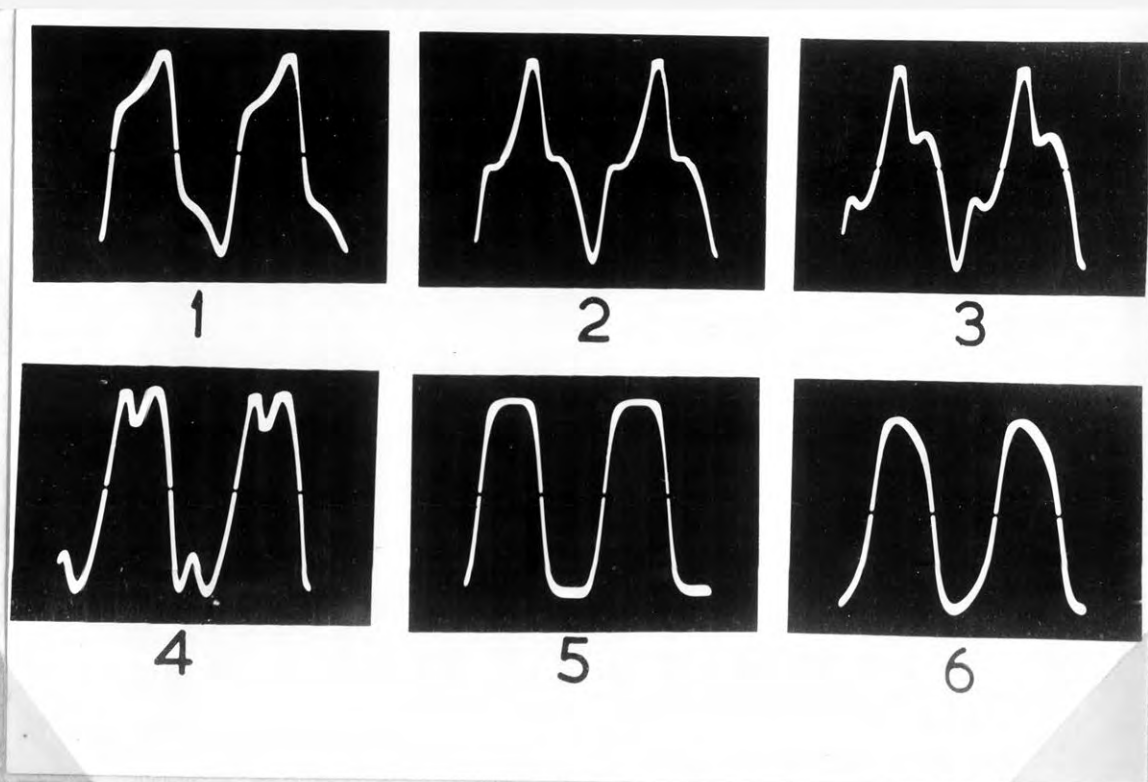


Plate 3. Typical waveforms obtainable with the distortion generator of Fig. 5.

more than 100 V peak on a load of 500 Ohms in parallel with 4 microfarad or 1.75 H μ without appreciable change in waveform. The peakfactor $V_{\max} / V_{\text{rms}} \sqrt{2}$ is adjustable within the limits 0.81 to 1.35.

To test the peakvoltmeter, the amplitude indicator shown in Fig. 6 and the meter under test are connected to the output terminals of the generator. With S_2 shorting T_1 the peak voltmeter is adjusted by means of T_3 to a convenient scale point. The low inductance decade resistance boxes 1111 Ohm are then adjusted till conduction through the biased off diode occurs at the peak of the wave. This can be observed on the C.R.O. by the occurrence of sharp spikes. The sensitivity of the amplifier and C.R.O. together are such as to give an oscillogram one inch high for 100 microvolt r.m.s. sine wave on the amplifier input. The waveform is now changed till the spikes again just appear. The meter reading should then be the same as before. For greater accuracy this test was carried out first by observing the meter deflection and then by replacing the D.C. meter with a resistor of about the same value as the movement and measuring the voltage on it with a vernier potentiometer. The difference observed between waveform 2 (Plate 3) and waveform 5 was approx. 0.1%. Part of this may be explained by the sensitivity limit of the amplitude indicator which was tested as shown in Fig. 7. When S is operated the change in voltage applied to the amplitude indicator is $\frac{1}{2} \times 0.25/240 \sim 0.05\%$. This could just be seen, giving a spike 1/16 inch high. It is suspected that the error of 0.1% or part of it is due to the mica capacitor the capacitance of which would be different at the harmonic frequencies. (16). Substitution of it by a capacitor with polystyrene dielectric gave some improvement but it appeared that with this simple apparatus the limit of experimental error had been reached. However, in actual use the waveforms would be far less distorted and the error was therefore deemed insignificant for the purpose. As was to be expected, large errors were observed on waves 3 and 4 because this type of peak voltmeter gives wrong readings on waves with more than one peak. (17).

The amplitude indicator described here was decided upon after tests on gas discharge lamps which were found to require artificial ageing. The improvement obtained by replacing the germanium Diode

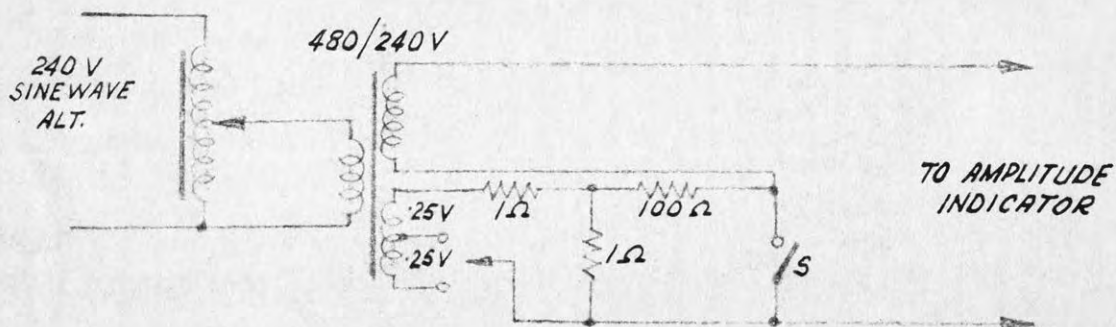


FIG.7: TEST FOR SENSITIVITY OF AMP. INDICATOR

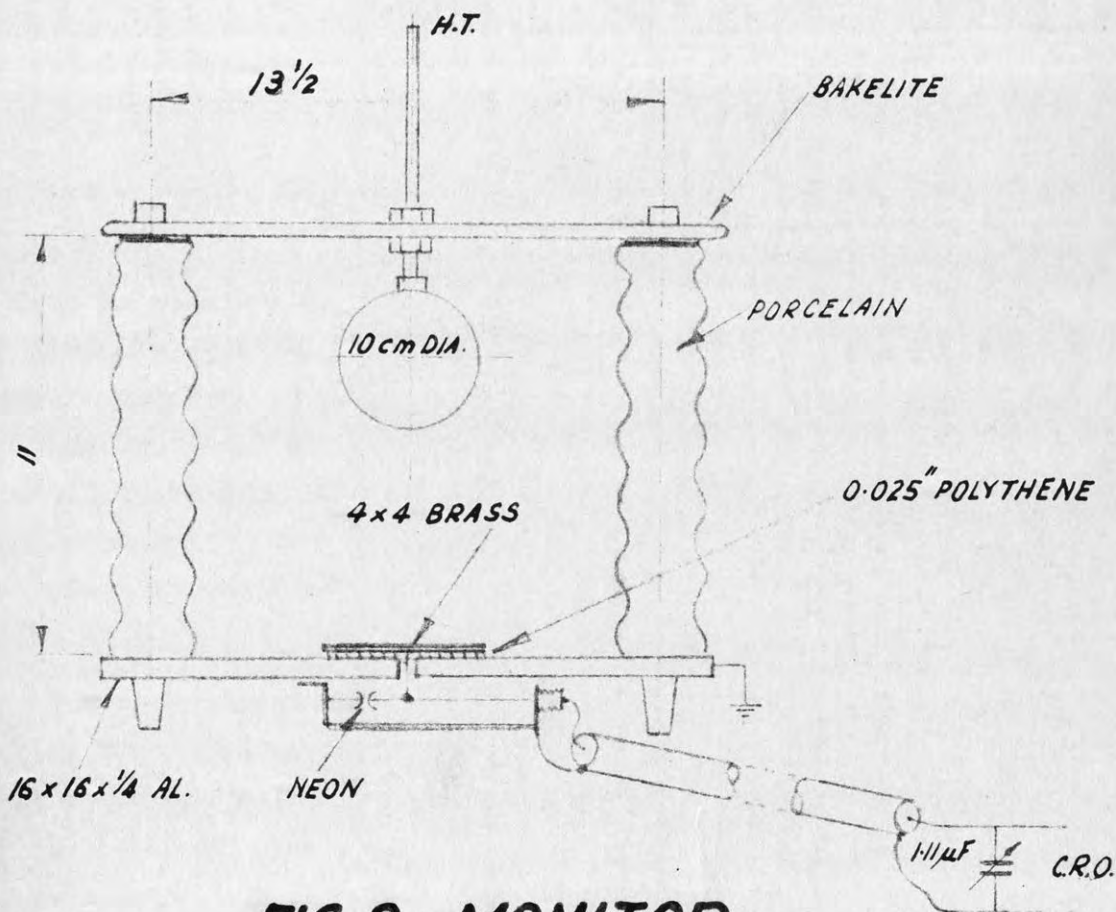


FIG.8: MONITOR

FOLLOWING PAGE: 11

by a silicon diode was only slight.

3.1.2.3. Monitoring of the high voltage waveform.

This is necessary to check that the waveform has only one peak. Fig. 8 shows the arrangement built for this purpose. A cathode ray oscillograph is connected across the low voltage arm of a capacitance divider the high voltage part of it consisting of a 10 cm diameter sphere and a 4 x 4 inch flat plate. This flat plate is insulated from a much larger base plate by a thin sheet of polythene. Thus, a guarded arrangement is provided and all insulation leakage is to earth and does not influence the oscillogram. For 140 KVp, the maximum voltage envisaged, the spacing was 12.5 cm, breakdown then occurring at about 145 KVp. The correctness of this was checked using data given by Schwaiger (1). On page 469 of his book "Theory of Dielectrics"

η is plotted as a function of $1 + a/r$ for the case sphere - plane. In our case $1 + a/r = 1 + 12.5/5 = 3.5$ and $\eta = 0.32$.

The puncture strength would then be :

$$F = \frac{V}{a} \cdot \frac{1}{\eta} = \frac{145}{12.5 \cdot 0.32} = 36.2 \text{ KVp/cm.}$$

No data on puncture strength of air for the sphere plane configuration are directly available but on page 466 Schwaiger gives data on the puncture strength of air in case of spheres as a function of a/r . By applying the image concept the puncture strength of air for a sphere spaced 12.5 cm from an earthed plane should be the same as for two spheres spaced 25 cm. For this case $a/r = 25/5 = 5$. The graphs show a puncture strength of 36 KVp/cm for spheres with 5 cm radius. This agrees closely with the figure computed from measurement.

The capacitance at 12.5 cm spacing is about 0.45 pF. The capacitance of the lower arm was about 200,000 pF giving a voltage ratio of about 450,000. The voltage fed to the C. R. O. was then $140,000/450,000 \sim 0.3$ V peak. For lower voltages the spacing was reduced keeping the voltage on the C. R. O. input above 0.2 V peak. The reactance of

200,000 pf at 50 c/s is about 16,000 Ohms and in order to avoid phaseshift between the fundamental and the harmonic frequencies the resistive component of the input impedance of the C. R. O. must be very much greater than 16,000 Ohms. An instrument with cathode follower input having an effective input resistance of more than 10 Megohms was therefore used.

It should be noted that this monitor is not suitable for precise voltage measurements although in some cases the oscillograph has been replaced by an amplifier and peak-reading vacuum tube voltmeter. Due to lack of shielding the capacitance is not properly defined it being slightly influenced by the position of connecting leads and surrounding objects.

3.1.2.4. Proposed procedure for Ratio determination.

Although it was stated before that the peak voltage ratio is the only ratio of interest in this investigation it is proposed to measure the fundamental ratio first and draw an equivalent diagram. The fundamental ratio measurement can be done by bridge methods which are inherently more accurate and convenient. At the same time the influence of capacitive loading may be studied and from this an estimate of the order of difference between the fundamental ratio and the peak voltage ratio should be possible. Direct peak voltage measurement could then be confined to checks at a few voltages only.

3.1.2.5. Remarks regarding the ratio of a threewinding transformer.

The equivalent diagram is shown in Fig. 9 which differs from the usual textbook diagrams only by the inclusion of the excitation shunt impedance Z_p . Only the ratio E_s/E_t is of interest for the present investigation and no statement need be made regarding L_p , R_p and Z_p . Two sources of error must be considered viz: the no load ratio error and the error due to loading. Normally in equivalent diagrams it is assumed that the no load error is zero and that at any instant the ratio E_s / E_t equals the turnsratio. This could only be true if the two

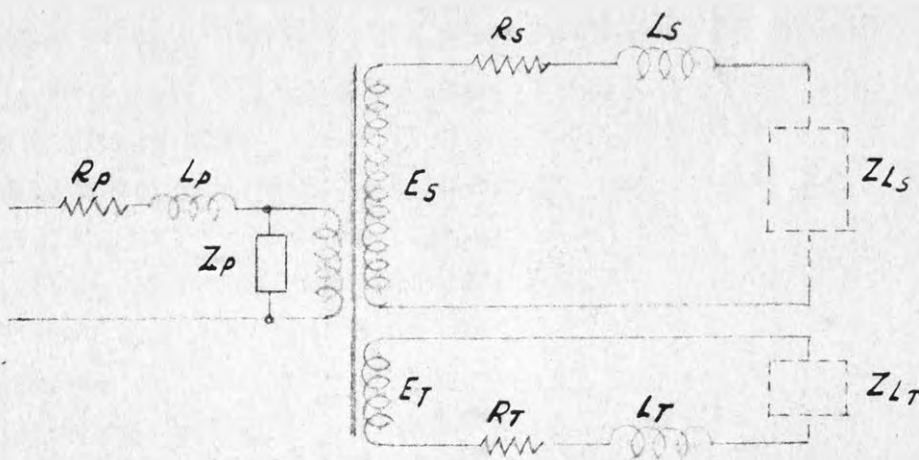
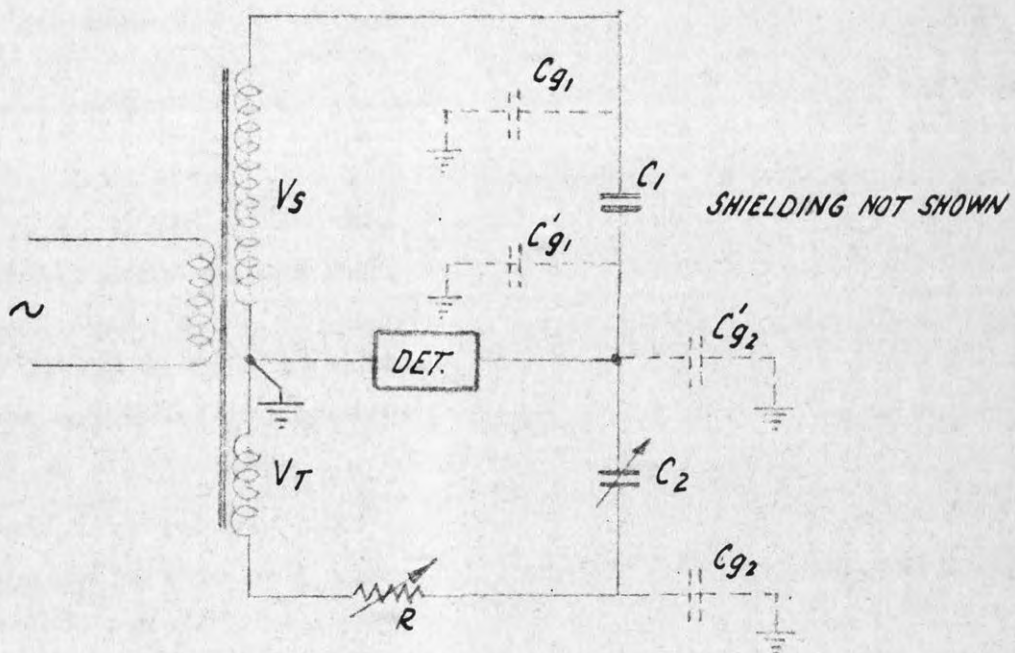


FIG. 9
EQUIVALENT DIAG. OF 3 WINDING T'FORMER



C_1 : 5 pF. 85 KV rms

C_2 : 1000 pF FIXED + 1250 pF VARIABLE

R : 1111 Ω

DET. : 100 μ V. rms / INCH AT 50 c/s.

FIG. 10: MEASUREMENT OF FUNDAMENTAL RATIO

FOLLOWING PAGE: 13

windings in question were completely intermingled so that all the turns of both windings were linked with all the flux lines and if there were no loading error due to selfcapacitance. In a high voltage transformer intermingling of the low and high voltage windings is not practical. Flux shunting the main magnetic circuit may therefore link with one and not with the other winding. Generally this flux will be larger the lower the permeability of the iron e.g. at higher fluxdensity. This "iron leakage" will therefore depend in a nonlinear manner on voltage and frequency or, at one frequency, on voltage and harmonic content. It cannot conveniently be represented in an equivalent circuit. In small 50 c/s three-winding transformers this no load error due to iron leakage was sometimes found to approach 0.1%. Iron leakage depended to a marked degree on the arrangement of the primary (excitation winding) and it was particularly pronounced at the corners of the window space. Magnetic shielding helps in this regard but is quite impractical for large transformers. Results of no load error measurements for the 30 KVA testing transformer will be given in Section 3.1.2.7.

In Fig. 9, R_s and R_t are the winding resistances which at 50 c/s are practically equal to the D.C. resistances and L_s and L_t are leakage inductances which are nearly constant because of the large proportion of air to iron in the winding leakage path. R_s , R_t , L_s and L_t cause the error due to loading. L_s or L_t can be negative depending on the winding arrangement.

Intermingling reduces both errors because, as stated before, the iron leakage influences both windings more equally and the leakage inductances are reduced. Alternatively, for a given permissible error the frequency range can be extended by better intermingling. (18a, 18b, 19).

If the secondary is loaded by a capacitance C , $1/\omega C$ being very much larger than ωL_s , and if this loading causes a change in ratio of $p\%$, L_s may be computed from :

$$\omega L_s / \frac{1}{\omega C} = \omega^2 L_s C \approx \frac{p}{100}$$

$$\therefore L_s \approx \frac{p}{100 \omega^2 C}.$$

This, of course, affords a simple way of measuring the relevant leakage inductances by observing the change in ratio due to capacitive loading. Because of a recent publication without acknowledgment it is wished to state here that this method was used by the author for the design and testing of numerous inductive ratio arms since 1949. See Section 3.1.2.7. for values obtained.

3.1.2.6. Bridge circuit for the measurement of fundamental ratio.

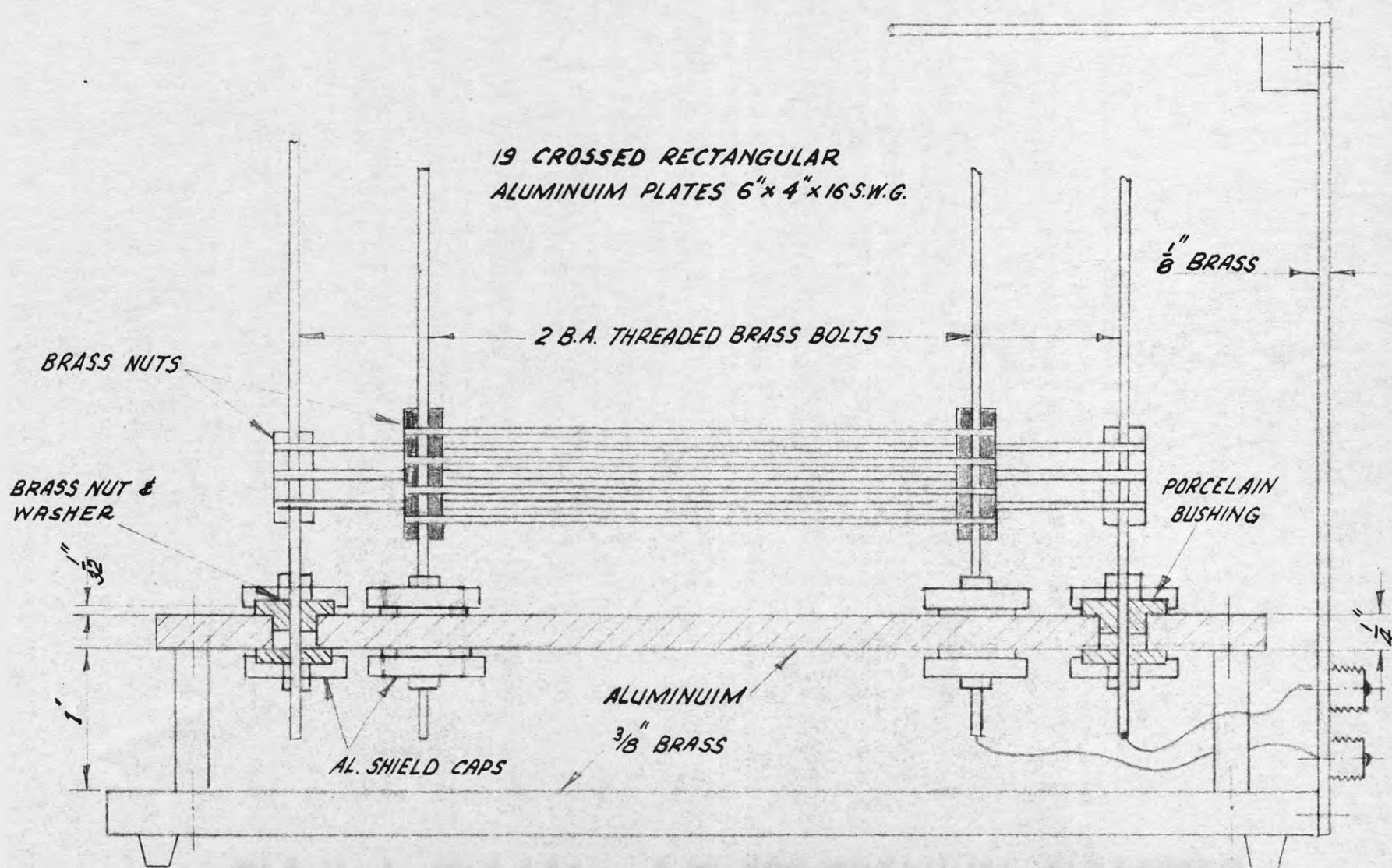
The test circuit shown in Fig. 10 is a simplified version of a circuit developed for instrument transformer testing. (20). C_1 is a 5 pF three-terminal aircapacitor (11) and C_2 is a Muirhead variable three-terminal aircapacitor type D-14-A of 1250 pF in parallel with a 1000 pF three-terminal aircapacitor the design principle of which is shown in Fig. 11. This capacitor is not of the type mentioned in reference 20 and it is of extremely simple design. It's construction required no precision work whatever. For tests and theoretical details see Appendix 2. Owing to the oxide film on the aluminium plates its phaseangle is about 2 parts in 100,000 at 50 c/s instead of zero, which is quite insignificant for the purpose, and could be allowed for, but the lower weight of the plate assembly so achieved was found to materially reduce its sensitivity to irreversible changes caused by shock. The capacitance value has changed by less than 0.05 pf in one year although the capacitor is transported frequently.

It is obvious from inspection that for small phaseangles $V_s/V_t = C_2 / C_1$. The guardcapacitances C'_{g1} and C'_{g2} and any leakage resistances are in parallel with the detector and have no influence on the measured ratio. The guardcapacitance C_{g1} and C_1 load V_s and their influence will have to be investigated. As

$1/\omega(C_{g2} + C_2) \gg R$, C_{g2} and C_2 capacitively load the tertiary. The phaseangle between V_s and V_t is given by:

$$\tan \theta \approx \theta \approx R \omega (C_2 + C_{g2})$$

the phaseangle of the three-terminal aircapacitors being assumed to



be zero. The circuit for phase balance is much simpler than that given in reference 20 but it has the disadvantage on depending on an intrinsically unstable capacitance viz: C_{g2} . However, as the value of phaseangle is not required for this investigation the simpler circuit was preferred.

The tuned detector amplifier is of a type described before for A.C. bridge work. (21, 22). Fig. 12 shows a block diagram using modern tubes. The particular merits of this amplifier are its noncritical components, its broad selectivity curve and its very high attenuation of harmonics. The effective "Q" value of an amplifier with a parallel "T" network in its negative feedback path is proportional to the loop gain. For good selectivity "Q" and therefore the gain must be high. This necessitates stable components in order to prevent changes of values which may lead to oscillation. Also, such an amplifier with a parallel "T" network in a feedback loop, or one with several stages with a network for each stage all being tuned to the same frequency, is nearly useless when the bridge is fed from the mains because small frequency changes cause large amplitude changes due to the sharp selectivity curve. On the other hand, high selectivity is necessary in power frequency bridge work to achieve a third harmonic attenuation of at least 3000 relative to the fundamental. While much can be done by the use of iron cored filters the convenience of "R-C" components is considerable because magnetic screening is not required. These considerations led to the solution shown in Fig. 12. A plug in parallel "T" network tuned to 50 c/s and placed between grid and plate of the first tube provides feed-back at the harmonic frequencies over one stage only. The selectivity curve is broad and no trouble is experienced on the mains. The first stage is followed by an "R-C" low pass filter which attenuates the higher harmonics plus a 150 c/s parallel "T" rejection filter which attenuates the third harmonic which is the strongest. The rejection factor of this harmonic is about 3000 and that of the other harmonics about 500, but these are much weaker and high attenuation is not required. For work at other frequencies, say 1000 c/s, another filter is plugged in and the rejection filters shorted. Much less harmonic attenuation is

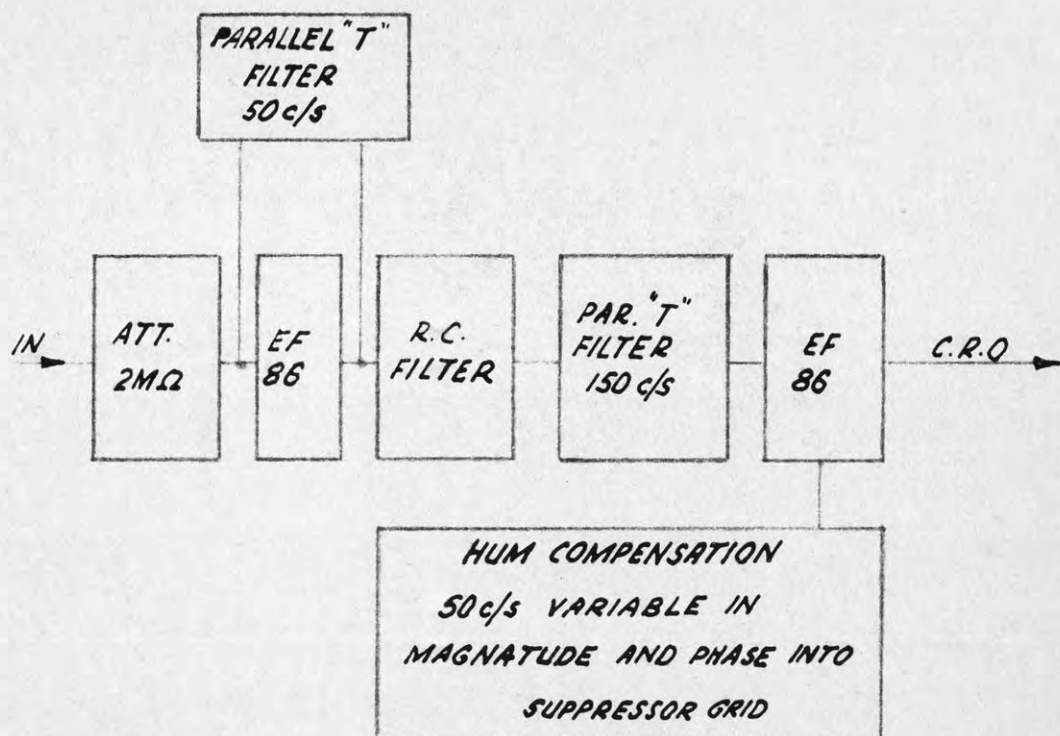


FIG. 12: BLOCK DIAG. OF DETECTOR AMP.

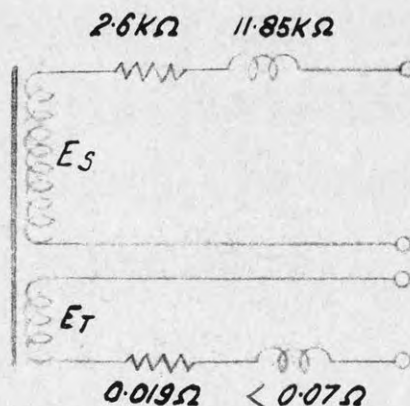


FIG. 13: EQUIVALENT DIAGRAM OF TESTING TRANSFORMER WITH MEASURED 50 c/s IMPEDANCE VALUES

usually required at 1000 c/s. The amplifier may also be used "flat" by omission of the first filter and shorting of the rejection filters. The sensitivity is 100 microvolts r.m.s. at 50 c/s, per inch. The noise voltage referred to the input is less than 10 microvolts. Several of these amplifiers have been built and some have given more than 10 years service.

3.1.2.7. Results of the determination of fundamental voltage ratio.

The ratio was found to vary by less than 0.1% over a range of secondary voltages from 200 to 100,000 V r.m.s. and by about 0.03% over the range 10 to 100 KV r.m.s. Owing to the voltage limit on the 5 pF capacitor, tests at 100 KV r.m.s. 50 c/s could not be made but the magnetic conditions in the transformer were approximated by testing at 80 KV and 40 c/s. The phase angle was nearly constant. R was 700 Ohms and $C_2 + C_{g2}$ was 2490 pF, giving a phaseangle :

$$\Theta \approx \omega R (C_2 + C_{g2}) = 314 \cdot 700 \cdot 2490 \cdot 10^{-12}$$

$$\approx 5.5 / 10^4 \text{ Rad} \approx 1.9 \text{ min}$$

The small change of ratio over such a large voltage variation which must have caused a large change in permeability is pleasing. It is of the same order as in smaller transformers and it may be inferred that the iron leakage causes a negligible ratio error. It is now likely that the main difference between fundamental and peak voltage ratio will be due to capacitice loading effects. This would also be in line with observations on small ratio arms that a small voltage coefficient of ratio is accompanied by a small frequency coefficient of ratio.

The secondary was then loaded with a capacitor C_L of 2200 pF rated 30 KV. This increased the ratio by $p = 0.82\%$ and the setting of R changed from 700 to 2990 Ohms. L_s may now be computed.

$$L_s \approx p / 100 \omega^2 C = 0.82 / 100 \cdot 314^2 \cdot 2200 \cdot 10^{-12} =$$

$$37.8 \text{ Hy}$$

and : $\omega L_s = 11850 \Omega$.

The D.C. winding resistance previously measured with a D.C. bridge was $R_s = 2590$ Ohms and this can now be checked from the change in phaseangle.

$$\Delta \Theta = \Delta R \omega (C_2 + C_{g2}) = R_s / \frac{1}{\omega C_L}$$

$$\therefore R_s = \Delta R (C_2 + C_{g2}) \cdot \frac{1}{C_L} =$$

$$\frac{(2990 - 700) \cdot 2490 \cdot 10^{-12}}{2200 \cdot 10^{-12}} = 2590 \Omega.$$

The agreement with the D.C. value provides a valuable check on the soundness of the practical execution of the bridge set up. Owing to the many sources of error in A.C. bridges viz: Pick-up, mutual coupling, circulating currents due to more than one earth etc, an independent check is important.

A sufficiently large capacitor to load the tertiary was not available but based on experience and knowledge of construction of the transformer it was assumed that L_t could not be greater than L_s divided by the square of the turn_s ratio.

$$L_t < 37.8 / \left(\frac{240}{100,000} \right)^2 < 215 \mu H.$$

$$\omega L_t < 314 \cdot 215 \cdot 10^{-6} < 0.07 \Omega.$$

Accurate knowledge of L_t is not necessary because in practice the tertiary would be loaded with an impedance in excess of 1000 Ohms and the loading error incurred would only be a few parts in 100,000. See also Fig. 13.

The 5 pF capacitor and its guardcapacitance constitute a load of about 100 pF. As 2200 pF cause a ratio error of 0.82%, this load would

lead to a ratio $100/2200 \times 0.82\% = 0.04\%$ too large. The actual ratio measured in terms of the capacitance ratio, which by calibration against standard capacitors was known to 0.01%, was found to be 417.7₅ which represents the mean of 10 ratios measured between 10 and 100 KV r.m.s. The turns ratio which was known to be correct was $100,000/240 = 416.66$, the difference being 0.26%. From above, this is too large by 0.04% which brings the difference to 0.22% which may be explained by a bushing plus self capacitance loading of $0.22/0.82 \times 2200 = 600$ pF. This figure appears of the right order. Roth (23) quotes the self-capacitance of a comparable testing transformer as 765 pF. The capacitance was computed from dimensions and also measured. The measurement of self capacitance was carried out by resonating at two frequencies. "L", provided it is constant, need then not be known. Unconventionally however "L" was the leakage inductance and not the shunt inductance. This firstly ensures that "L" is constant (mainly air) and secondly, the shunt inductance is usually so large and its "Q" so low that resonance is difficult to observe. The calculation of capacitance and details of the technique developed for measuring it are described in Appendix 3.

The influence of leakage resistance on the ratio is negligibly small. This resistance was nearly 1000 Megohms but even if it would drop to 10 Megohms the ratio change would only be :

$$\Delta \text{RATIO} = \frac{R_s}{R_L} \cdot 100 \% = \frac{2590}{107} \cdot 100 \sim 0.026 \%$$

3.1.2.8. Estimated order of difference between fundamental and peak voltage ratio.

The following is in no way rigorous because without knowledge of the phase relationship and the amplitudes of the harmonics no computation can be made. However it helps to obtain an order of magnitude. If, 600 pF loading at 50 c/s cause an error of 0.22%, then, at 150 c/s the error would be $(150 / 50)^2 \times 0.22 \sim 2\%$. However as the third harmonic amplitude would be less than 5% of the fundamental amplitude the error would not exceed $5 / 100 \times 2 / 100 \sim 0.1\%$. At highly distorted waves as used in tests on gap type "B" the

third harmonic amplitude may be 15% and the error therefore in the order of 0.3%. Higher harmonics have been neglected for this rough estimate of order only. This remains now to be confirmed by direct peak voltage ratio measurement.

3.1.2.9. Measurement of peak voltage ratio.

Fig. 14 shows the test circuit. When the change-over switch is in position 1, the current through C_1 (5 pF, 85 KV r.m.s.) causes a drop on C_3 . As $C_3 \gg C_1$, $i \sim V_s \omega C_1$. The drop on C_3 is amplified in a Mullard type 20 W amplifier (24) the 15 Ohms output terminals of which are connected to the amplitude indicator as described in Section 3.1.2.2. and Fig. 6. Onset of conduction will be at about 18 V peak. An amplifier output voltage of 18 V peak requires $18/80 \sim 0.23 V_p$ at the input, 80 being the gain of the amplifier. At a V_s of say 46 KV_p the value of C_3 is:

$$C_3 \sim \frac{C_1 V_s}{0.23} = \frac{5 \cdot 46000}{0.23} \sim 10^6 \mu F = 1 \mu F \ll C_1$$

With the switch in position 2, at the onset of the spikes :

$$i = V_t \omega \frac{C_2 C_3}{C_2 + C_3}$$

wherein C_3 is the actual capacitance of C_3 plus guardcapacitances. These are made equal for the two positions of the switch by means of the compensating capacitors C_c . Equating the two expressions for "i" yields :

$$K = \text{peak voltage ratio} = V_{sp}/V_{tp} = C_2/C_1 \times C_3 / C_2 + C_3.$$

$C_3 / C_2 + C_3$ is nearly unity because :

$C_2 = 5 \times 417.75 \sim 2100 \text{ pF} \ll C_3$. An incorrect adjustment of C_c is therefore hardly significant.

The measurement is carried out by adjusting V_t to the desired value and adjusting C_3 in position 1 of the switch till the spikes just commence. The switch is then operated and C_2 simultaneously varied till the spikes just appear in both positions of the switch. The peak voltage ratio is thus obtained in terms of precisely known capacitances. For greater convenience, a vibrating type change over switch, e.g. a "Carpenter" relay, suggests itself but was not used because the measurement is carried out only on rare occasions.

Alternatively, and particularly when a stable source of voltage, e.g. an electronically controlled sine wave alternator (29), is not available it was found easier to use the following procedure. At voltage, V_{t1} and V_{t2} respectively, when the spikes just start :

$$i = V_s \omega C_1 = V_{t1} K \omega C_1 = V_{t2} \omega C_3 C_2 / C_3 + C_2.$$

$$\therefore K = V_{t2} / V_{t1} \times C_2 / C_1 \times C_3 / C_3 + C_2.$$

In this case C_2 is left unaltered and the fine voltage control adjusted till the spikes occur at V_{t2} and then at V_{t1} . From the ratio of two meter readings, which differ only little from each other and the values of the capacitors, "K" may be computed.

The peak voltage ratio was tested at several voltages up to the voltage limit of C_1 . When the sine wave alternator was used, e.g. when the distortion of the secondary voltage wave due to transformers and various series impedances did not exceed 3% the peak voltage ratio was found to equal the fundamental ratio within the limits of accuracy of measurement, viz. approx. $\pm 0.1\%$. A typical peaky wave was then produced by means of the arrangement shown in Fig. 15 in which the peaky excitation current of a reactor caused a drop on a resistor in series with the primary of the testing transformer. The peakfactor was about 1.15. In this case the peakvoltage ratio was about 0.3% higher. Repeat results varied between the limits 0.2 and 0.4%.

3.1.2.10. Precautions taken in the determination of peak voltage ratio.

Besides the usual precautions, like avoiding electromagnetic and electrostatic couplings, tests were made to ensure that the amplifier faithfully reproduces the high voltage wave-form. The capacitors C_1 , C_2 and C_3 must have a negligible phaseangle in order to avoid a change in the phase relationship of the harmonics. C_1 and C_2 were above suspicion. C_3 was a first class mica capacitor but it was shunted by guardcapacitances, the screened leads of C_1 and C_2 and the inputresistance of the amplifier. The only significant offender was found to be the inputresistance of the amplifier. The original gridleak of 1 Megohm was changed to 5 Megohms and the heater voltage of the first tube was reduced. As the value of C_3 was usually greater than 1 microfarad (3180 ohms at 50 c/s) its shunt resistance was more than 1000 times greater.

Harmonic distortion in the amplifier was checked as shown in Fig. 16. The distortion of the sine wave alternator was reduced to less than 0.01% by the L/C Filter shown. L was an optimum "Q" reactor designed as outlined in Appendix 4. The only noteworthy point of the 50 c/s parallel "T" filter connected between the amplifier output terminals and a vacuum tube voltmeter is its output network. For any frequency between 130 and 1000 c/s the attenuation is constant and its value is 10. Thus, if V_o is the r.m.s. output voltage of the amplifier and V_v the r.m.s. reading of the vacuum tube voltmeter, at balance of the filter, the total harmonic distortion is $10 V_v / V_o \times 100\%$. The amplifier was found to have about 0.04% distortion at 13 V r.m.s. output ($13 \times \sqrt{2} = 18$) when loaded with the amplitude indicator as is the case when used for peak voltage ratio determination. With 26 W supplied to a resistive burden the distortion was 0.2% and this broadly agrees with the makers claims.

Phaseshift was checked using the circuit shown in Fig. 17. The distortion generator described in Section 3.1.2.2. and Fig. 5 was used to supply the amplifier. The input voltage to the amplifier was made to be in phase with the supply voltage by the use of a resistance divider free of phase defect at audio frequencies. If the input

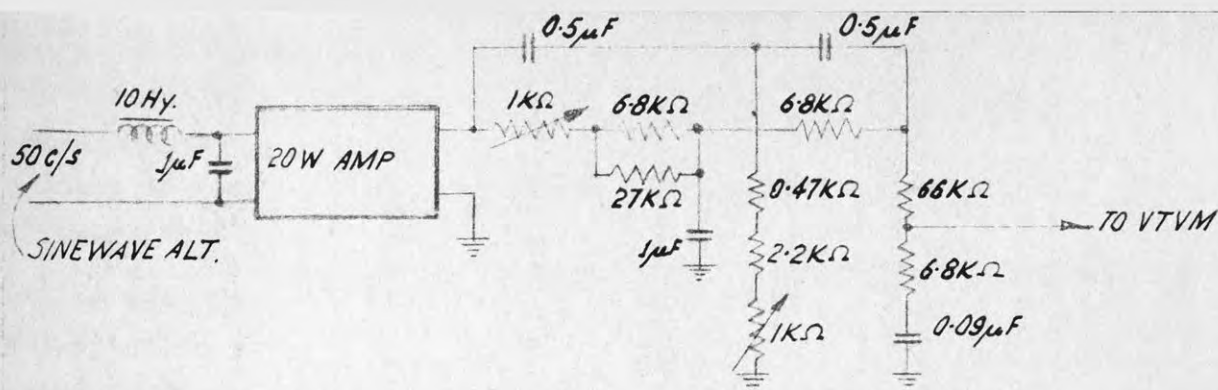


FIG.16: SET-UP FOR DISTORTION TEST OF THE 20W AMPLIFIER

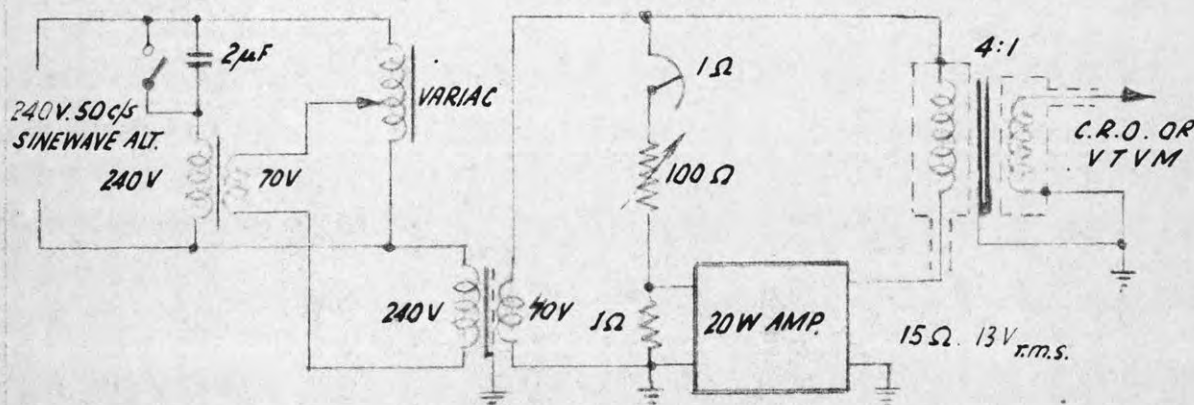


FIG.17: SET-UP FOR PHASE-SHIFT TEST OF THE 20W AMPLIFIER

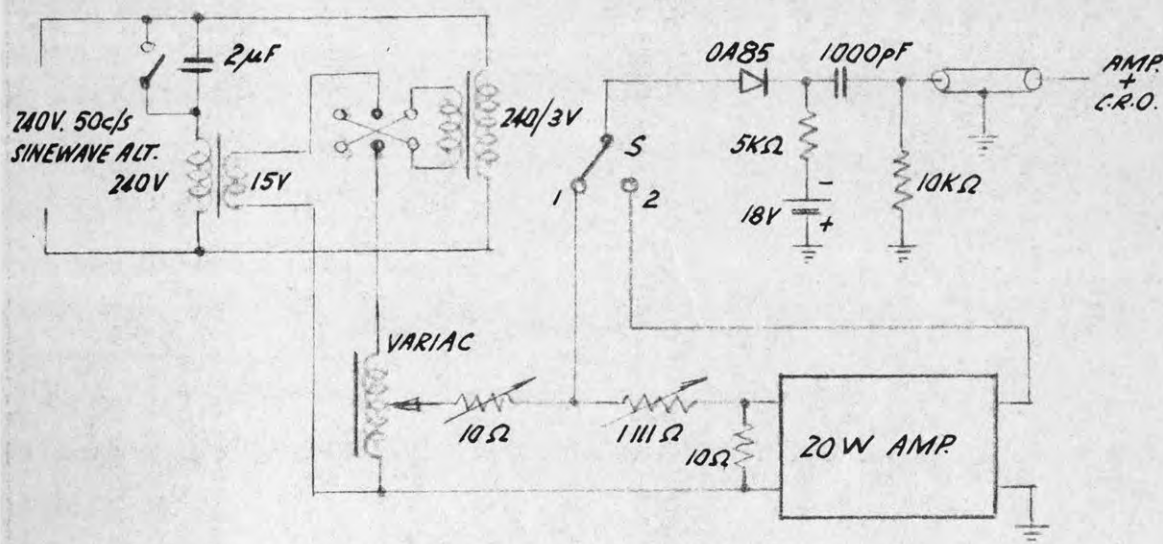


FIG.18: TEST FOR CHANGE OF AMPLITUDE WITH WAVEFORM

voltage is adjusted to a value $1/A$ whereby A is the gain of the amplifier, no potential difference should exist between the output voltage of the amplifier and the supply voltage (winding marked 40) if there were no distortion and phaseshift in the amplifier.

A potential difference is indicated on a C. R. O. or V.T.V.M. connected to the secondary of a magnetically and electrostatically shielded differential transformer with 40 Hy primary inductance the direct winding to winding capacitance was less than 0.0002 pF. Each winding of this transformer is enclosed in a slit brass box, the two boxes being on opposite legs of a mu-metal core type transformer with $\frac{1}{4}$ sq. inch cross-sectional area. In order to reduce the leakage inductance of this configuration a single layer winding linking the two legs is arranged outside the shielding boxes. The primary, secondary and link windings have 1800, 450 and 35 turns respectively, the wire gauges being 39, 33 and 20 S.W.G. This transformer represents a mechanically simpler and electrically more favourable design than e.g. the "General Radio" bridge transformer type 578.

The residual observed on the C.R.O. was nearly a sine wave, even when the amplifier was fed with distorted waves, indicating that the main phaseshift occurred at 50 c/s, the lowest frequency, as would be expected. Referred to the primary the residual voltage was about 0.13 V or 1% of the output voltage. As the distortion was previously found to be very small this was taken as caused by a phaseshift of about 35 minutes at 50 c/s. Because 35 min. could not be dismissed as entirely negligible a further test was made.

Two waves of equal amplitude and not too dissimilar shape were fed into the amplifier and the difference in amplitude after amplification was observed. The test circuit is shown in Fig. 18. The distortion generator was used again, the two different waveshapes being obtained for the two positions of the reversing switch. The variac, the fine control and the decade resistance box were adjusted for the spikes to just occur in positions 1 and 2 of the changeover switch. The setting of the decade resistance box was noted and the experiment then repeated for another waveform. In both cases the same setting

of the decade box was obtained viz: 803 Ohms. The settings 802 or 804 gave a very distinct difference. This test showed the suitability of the amplifier particularly as the waveshapes which were used in this test differed far more from each other than did the voltages of the secondary and tertiary of the testing transformer. When the latter ones were displayed on a double beam C.R.O. no difference could be observed visually. This indicated that the above test was more severe than required in practice although it was only an overall qualitative test in which the phase relationships of the harmonics were not defined. In order to test the amplifier further - even if not required for the present purpose - a sinusoidal wave and a very peaky wave (No. 2 of Plate 3) of equal amplitude were compared using the circuit shown in Fig. 18 but with different secondary voltages of the two 240 V transformers. A 0.3% difference in the output amplitudes could then be observed.

3.1.3. Preparation of spark gap electrodes.

The cylinders were cleaned with "Searchlight" metal polish and a cotton cloth. They were then washed with alcohol and wiped dry. This was repeated after about every 100 flashovers.

3.1.4. Preliminary tests.

It was mentioned before that corona at the semispherical ends could be observed in the vicinity of the range limit of the gap. First, it was desired to make sure that corona indeed started at the semispherical ends and not at other parts of the electrodes. The ends were covered with plasticine and corona which previously started at 128 KV_p now commenced at 137 KV_p. When the semispherical ends were replaced by 10 cm diameter spheres, joined to the cylinders with plasticine, corona did not commence at 150 KV_p, the highest peak voltage available. Having ascertained that no other part nearer to the sparking area caused corona it was thought important, owing to the paucity of published information, to find out if corona on the semispherical ends should occur and if some confirmation for this observation could be found.

One cylinder of the spark gap was removed and a large earthed plate was fixed 12.5 cm from the semispherical end of the cylinder. The mean of 10 breakdown measurements carried out on this configuration was 110 KV_p. Using for convenience the graphs for η in Schwaigers book (1) page 469 :

$$\eta = 0.18 \text{ for } 1 + \frac{a}{r} = 1 + \frac{12.5}{2.5} = 6$$

The surface gradient which must be the puncture strength of air at the surface of the semispherical end is :

$$F = \frac{V}{a} \cdot \frac{1}{\eta} = \frac{110}{12.5} \cdot \frac{1}{0.18} = 49 \text{ KV}_p / \text{cm}$$

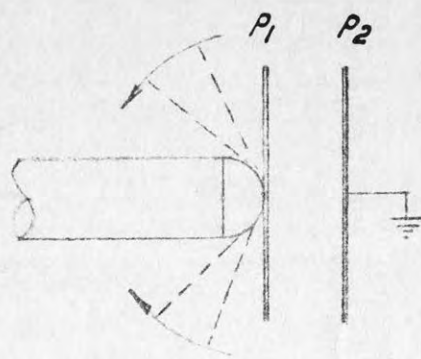
This figure has no absolute meaning because in the derivation of η a full sphere has been assumed and not a semisphere at the end of a

cylinder. That the cylinder must have a slight influence can be visualized from Fig. 19. If an infinite plane P_1 is assumed touching the semispherical end, $1/\gamma = 1$ and the gradient smallest. The stress multiplication factor $1/\gamma$ would be a maximum for the sphere without the plane P_1 . If P_1 is now spun back gradually, $1/\gamma$ must increase, and the case cylinder with semispherical end is the limiting case of this spinning back process. In practice, as could be found from breakdown tests on spheres over half of which a cylinder was slipped, the influence is small and in engineering calculations it is usually neglected. However, the required confirmation for corona may be obtained by making the same erroneous assumption twice. The gradient at the surface of the smaller of two concentric spheres with radii R and r is :

$$F = V \frac{R}{(R-r)^2}$$

If the outer sphere is very large, $R \gg r$, $F = V/r$ which must be the surface gradient on a single far away sphere. When corona occurred V was 128 KV_p and $V/r = 128/2.5 = 51$ KV/cm. Again, this is not correct, but as before the result is obtained under the assumption of a full sphere. The relative agreement 49 against 51 KV/cm may be regarded as satisfactory. In view of the assumptions made and some uncertainty in the value 110 KV_p due to corona preceding sparkover it appears that the occurrence of corona on the semispherical ends is natural and to be expected. Onset of corona was tested as described before (25,25a).

Another preliminary test was carried out in order to determine the minimum possible time interval between successive sparkovers of the gap. As heating of the electrodes causes a change in airdensity a copper constantan thermocouple was attached to the inside of one cylinder. It was separated from the sparking point only by the cylinder wall of 0.06 in. thickness. The cylinder was earthed and the thermocouple leads were brought out through the slot which can be seen in Fig. 1 and Plate 1. A "Philips" D.C. vacuum tube voltmeter type GM 6010 on its 1 mV range was used for temperature indication. The input resistance of the instrument is very large (order of 1 Megohm) as compared with the resistance of the thermocouple and the



$\frac{1}{\eta}$ INCREASES THE MORE P_1 IS SPUN BACK.

FIG. 19

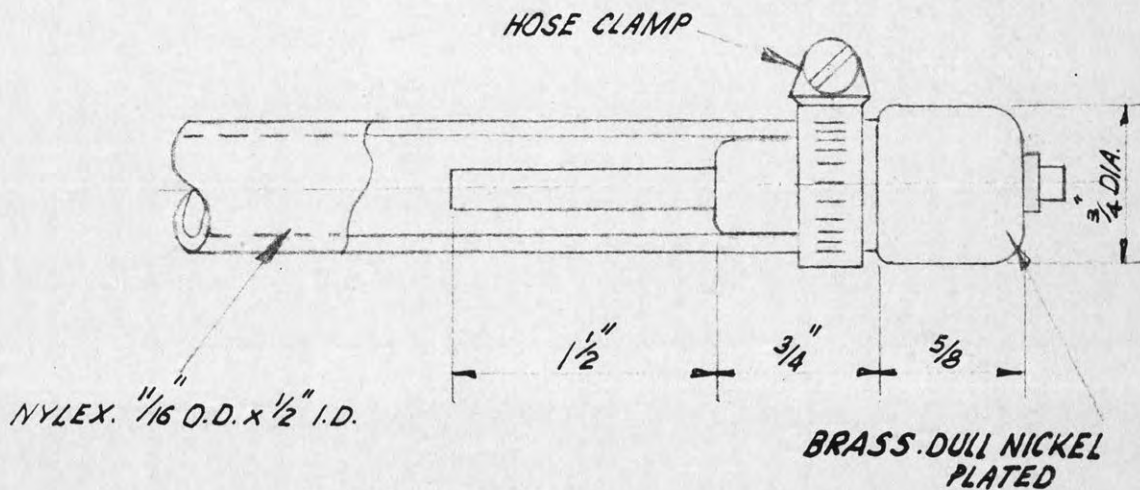


FIG. 20: WATER-RESISTOR

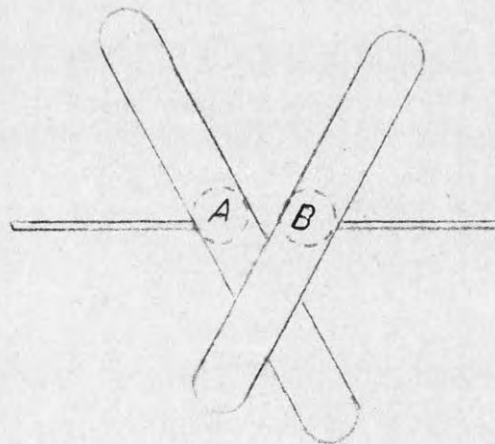


FIG. 21: PHYSICAL PICTURE OF SHIELDING DUE TO CYLINDERS

thermal e.m.f. can thus be measured far more conveniently than with a potentiometer. As the couple generates $40 \mu\text{V}/^\circ\text{C}$, and 1 div of the meter is $10 \mu\text{V}$, 1 div $\sim 0.25^\circ\text{C}$. By working as fast as the circuit-breaker could be operated, 12 sparkovers were made at 130 KVp during 1 minute. The series resistor of the gap was 100,000 Ohms and the temperature rise less than 1°C . As a time of 30 to 60 seconds per sparkover must elapse in practice, in order to read meters and record the result, the temperature rise can be neglected. When spun 10 cm diameter copper spheres with 0.015 inch wall thickness were used in the identical set up, the temperature rise was about 5°C for 12 sparkovers in one minute. This rise could also be noticed by touching the spheres immediately after the test.

Preliminary tests were also made regarding irradiation of the gap. This is summarized in Section 3.5.

3.1.5. Perturbation tests.

Before an actual calibration was made, the influence of nearby objects and the required accuracy of mechanical alignment was tested. As disturbances will have a greater effect at larger spacings the tests were made at a spacing of 5 cm which is close to the maximum spacing of 5.5 cm. The latter was avoided for these tests because it was thought that the results may be masked by the slight corona occurring at the semispherical ends. It was later found that this was not justified but there was another practical reason, actually more a hunch, for avoiding a large number of sparkovers at 140 KV_p . Before the start of this investigation, by courtesy of the Sydney County Council, the testing transformer was cleaned and its oil filtered. When the transformer was out of its tank it could be inspected. From experience obtained when measuring the impulse voltage distribution on similar transformers by means of a recurrent surge oscillograph built by one of the author's students (26, 26a) it was known that the transformer would be very vulnerable to surge stressing and it was thought wiser not to use the transformer too often for spark gap work at the highest voltage, although it was realised that the series resistor should afford some protection. A failure of this

major piece of test equipment would have meant the end of the work described in this thesis.

The gap was placed on an aluminium sheet 6 x 3 ft. which served as an earth plane. The series resistor, details of which are shown in Fig. 20 consisted of a clear "Nylex" tube filled with water and a copper sulphate solution of very low concentration. Its resistance value measured at 50 c/s was 100,000 Ohms. Resistors of this type are used throughout this investigation and they will subsequently be designated "water resistor".

The connecting leads between transformer and resistor and between resistor and gap were of 26 S.W.G. tinned copper wire. The lead between resistor and H.T. electrode of the gap was short. Corona hiss on the leads could be heard but there was no "spitting". The fine wire was used deliberately because users of the gap would regard it as impractical to employ large diameter tubing for corona free connections. These tubes would not only be inconvenient but would require auxiliary supports as otherwise the gap would be strained by their weight and the electrode separation changed. According to Peek (27) the puncture strength of air rises considerably for small diameter wire electrodes (e.g. it is 90 KV_p for 26 S.W.G. wire) and the corona onset voltage for fine wire is relatively higher as compared with wire of larger diameter. More important still is that the wire is so fine that it can be smoothed out with a cloth. It was often observed that a tube too large in diameter to be smoothed out properly (e.g. refrigeration tubing) gave more spits from surface irregularities than the fine wire. Thin wire appears to be universally used in high voltage laboratories as has also been confirmed by Liao and Kresge (28).

The effect of ionised air surrounding the connecting wires on the operation of the spark gap and on the voltage measurement has been checked as described at the end of this section.

For each type of test 5 preliminary discharges were made and then readings taken on 10 further discharges. The voltage was adjusted coarsely to within a few % of the expected breakdown value and then

finely till breakdown occurred. The fine control was advanced as quickly as the meter could be read. For reliable results it was found important not to leave the gap at high voltage longer than necessary as, it is believed, fibres being attracted into the field caused anomalous flashovers.

A sine wave alternator, the frequency and voltage of which was electronically controlled (29) was used as power supply.

All breakdown figures given below in Table I and in subsequent sections have been corrected for 20° C and 760 mm mercury as outlined in the B.S.S. 358/1939. See also Section 3.5.

The peak voltage was obtained by multiplying the tertiary peak voltage with 417.7. This takes into account a capacitive loading of about 50 pF due to the gap, the monitor and the leads. See also Section 3.1.2.7.

Table 1.

Test No.	Type of Test	Mean of 10 Readings KV _p
1.	Movable cylinder grounded, earthplane 6 x 3 ft	130.1
2.	Fixed " " " "	130.0
3.	Movable cylinder grounded. Gap on wooden platform 10 inch. above bench, no earth plane	130.1
4.	As test 3 but fixed cylinder grounded	129.7
5.	Repeat 1	130.05
6.	As 1, but a vertical grounded plate 20" x 28" arranged parallel to base of gap and symmetrical to sparking point. Distance from semispherical end = 9"	129.9
7.	Repeat 1	130.0
8.	Repeat 1 some time later, the cylinders having been cleaned with metal polish. Relative humidity 5% higher	130.4
9.	Vertical ebonite rod, 2" in diameter, 21" long placed 5" from sparking point. Otherwise as 1	130.3
10.	As 1, but shank of H.T. cylinder thickened by attaching to it a helix of 16 SWG wire, 6" long, 1 $\frac{1}{4}$ " O.D. turns spaced 2 wire diameters	130.2
11.	Repeat 1	130.2
12.	Shank of fixed H.T. cylinder turned 15 degrees in a horizontal plane, bringing the sparking point much nearer to the semispherical end	124.0
13.	As 12 but tilted cylinder moved in slot provided for this experiment in order to increase the distance between the sparking point and the end	128.5
14.	As 13 but tilt removed	128.6
15.	Repeat 1	130.2

The tests 12 to 14 show that the change in spark over voltage is caused by endeffect and not by misalignment. It appears therefore inadvisable to use shorter cylinders. No effect could be detected when the test No. 12 was repeated at 1 cm spacing in which case the endeffect would be negligible.

The increase in sparkover voltage apparent in test No. 8 is believed to be caused by repolishing. A gradual decrease is shown in tests No. 9, 10, 11 and 15. According to the B.S.S. 358 a high degree of polish should be avoided. Stress concentration in tiny crevices is believed to be important for repeatable sparkover values.

The gap was also found to be quite insensitive to the angle between the crossed cylinders as has been found by Schwaiger (1) and is to be expected from the work of Harper and O'Dwyer (7).

It should be noted that in all tests concerning misalignment, the sparking distance was measured by slip gauges.

In repeating test No. 1, the corona on the connecting leads was several times artificially increased by hanging on them pieces of wire with sharp ends. Also, Test No. 1 was repeated using carefully supported large diameter connecting tubes with plasticine covering bends and surface irregularities. No other effect than the usual differences of 0.1 to 0.2 KV_p for repeat tests could be observed.

3.1.5.1. Remarks on the proximity of other objects.

The tests described show the gap quite insensitive to nearby objects. Particularly, Test No. 6 indicates that the spacing between the gap and a conducting body need not be greater than that required to prevent sparkover. In fact, during the tests which were commenced with 8" spacing, sparkover to the vertical plate sometimes occurred and the spacing was then changed to 9". Physically, the insensitivity to nearby objects is believed to be due to the shielding effect of the cylinders which may be visualized as shown in Fig. 21. The cylinders are seen to shield two imaginary spheres A and B. If an infinite number of cylinders were attached to each sphere the electrode system

would become similar to the uniform field spark gap used by Bruce (30), which is known to be very much less sensitive to outside disturbances than the sphere gap, due to the guarding action of the curved edges which shield the uniform field between the central areas from distortion by surrounding objects. The crossed cylinder gap is therefore regarded as a gap in which part of the uniform field electrode system is missing.

It is interesting to compare this crossed cylinder gap with other spark gaps regarding the minimum distance to nearby objects. According to test No. 6 the distance of the sparking point to the conducting plane was :

$$\frac{17}{2} \cdot \frac{1}{\sqrt{2}} + 9" = 15" \sim 38 \text{ cm}$$

(the $\sqrt{2}$ is due to the 45 deg. inclination of the cylinders). For 10 cm spheres the minimum recommended distance to the sparking point is 12 x spacing. (31). With one sphere earthed, at 130 KV_p, the spacing is 5.5 cm as per Table I of the B.S.S. 358/1939. The minimum distance is therefore 12 x 5.5 = 66 cm. The difference is not very large but high voltage enclosures are often too small and any saving in distance is helpful.

Bruce (30) recommends that the clearance between the edges of the electrodes and the nearest earthed conductor should not be less than 4 x gap spacing. For 130 KV_p this spacing is slightly less than 2" and the clearance required is therefore 8". Bruce's electrodes for the equivalent voltage range are only 6.5 inches in diameter and the distance between the centre of these electrodes and an earthed body is : $6.5 / 2 + 8 = 11.25" \sim 29 \text{ cm}$. This is less than for the crossed cylinder gap and broadly confirms the contention that the crossed cylinder gap lies between the sphere gap and the uniform field gap. It is believed that the latter gap has not found widespread practical use because of its precise contour required.

During these tests the idea was conceived to use several crossed cylinders for a guarded three terminal high voltage capacitor of extremely simple design. Work on this is proceeding and it is hoped

to give at least preliminary results in Appendix 5 of this thesis. The influence of nearby objects will be apparent as a capacitance change which is much easier to measure precisely than breakdown voltage.

3.1.6. Calibration data.

The results of a calibration at 50 c/s are shown in Table II. The values are corrected for 20° C and 760 mm mercury and the test conditions are as outlined for Test No. 1 in Section 3.1.5.

The puncture strength of air for 5 cm diameter crossed cylinders is given in Column 3 of the Table. It was computed from equation 1 in Section 2 using for $1/\gamma$ the values calculated from equation 3 in Section 2 and for V and a the values given in Column 1 and 2 of the Table below :

Table II

Spacing	Mean of 10 readings	Puncture strength of air
cm	KV _p	KV _p /cm
0.5	16.9	34.9
1.0	31.6	33.6
1.5	45.6	33.3
2.0	59.1	33.3
2.5	72.0	33.3
3.0	84.4	33.3
3.5	96.6	33.4
4.0	108.0	33.4
4.5	119.2	33.5
5.0	130.0	33.5
5.5	139.3	33.2

The maximum deviation from the mean value was approx. 1% for the spacings 0.5 cm and 5.5 cm and approx. 0.5% for the other spacings. Plotting sparkover voltage as a function of spacing gives a smooth curve but on reasonable size graph paper the reading accuracy is low. Fig. 22 shows a plot in which the difference against a straight line is plotted as a function of spacing a (cm). The sparkover voltage V_b in KV_p is : $V_b = 26 a + y$, whereby $y = f(a)$ is shown in Fig. 22.

As far as the accuracy of this calibration is concerned it is not regarded correct to estimate the error of each piece of apparatus and then use the mean or root mean square value to estimate the overall experimental error. This hardly allows for operators fatigue which for such a large number of measurements is considerable and was mentioned earlier (Section 3.1.1.). A different approach to the assessment of experimental error lies in finding out how much the actual result differs from some known law of nature. In this specific case it is known from Peek's work (9) that at larger spacings the puncture strength of air for the parallel cylinder case is constant for one constant value of radius. It is most likely that this should be so also for crossed cylinders. In any case, it is unthinkable that the puncture strength, if plotted against spacing should be a ragged line and not a smooth curve. It is further known that in a uniform field the puncture strength rises enormously at small spacings (32). Using now the values for puncture strength in Column 3 of Table II it seems rational to neglect the small spacings of 0.5 and 1 cm as for these the case of a uniform field is approached. The arithmetic mean of the other values is $33.35 \text{ KV}_p/\text{cm}$ and the maximum deviation from this value is : $(33.35 - 33.2) / 33.35 \times 100 \sim 0.5\%$. This appears a more realistic appraisal of accuracy which, if anything, is too pessimistic. It can be noted that at 5.5 cm spacing the puncture strength is $33.2 \text{ KV}_p/\text{cm}$. It may well be that this figure is too low. Firstly there may be a lowering of the breakdown value due to the slight corona at the semispherical ends or an endeffect due to the finite length of the cylinders and secondly equation 3 in Section 2 has only 3 terms. If the fourth term were known its sign would be positive making $1/\eta$ larger. This would be more significant at the

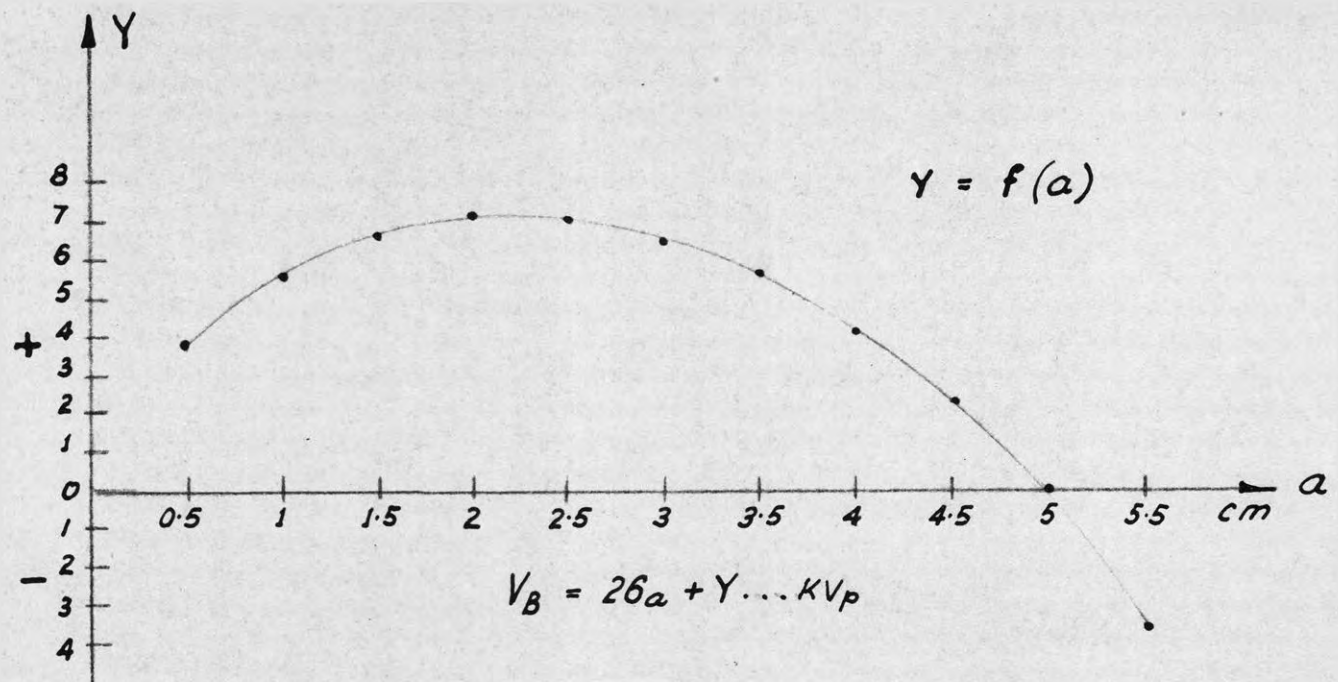


FIG. 22: 50 c/s CALIBRATION OF GAP "A"

larger spacings. Thus $F = V / a \times 1/\eta$ may in reality be slightly larger.

It is also interesting to observe that for spacings up to and including 2.5 cm the figures in Table II agree with those for 10 cm spheres in the B.S.S. 358/1939 and they are within 0.1 KV_p of the latest values for 10 cm spheres made available by courtesy of the I.E.C. spark gap Committee. This is fortunate because many users will be able to use the B.S.S. 358 for gap type "A".

3.2. Performance on D.C. with one cylinder grounded.

An absolute calibration on D.C. was considered unnecessary. If the gap is to measure correctly 1/50 microsecond impulse voltages, the calibration for negative D.C. cannot differ from the calibration at 50 c/s where, at the peak of the wave, the voltage changes by less than 0.25% during 400 microseconds. The main interest is the difference between positive and negative spark-over voltage for crossed cylinders. For sphere gaps the positive sparkover voltage is greater at the larger spacings. (33).

Generally, the D.C. test was regarded as a guide as to what to expect at the far more important tests with impulse voltages.

3.2.1. D.C. voltage generation and indication.

The 100 KV testing transformer used for the A.C. calibration has graded insulation of the H.T. winding and it was used in a half wave rectifier circuit to charge a capacitor of 0.062 microfarad, rated 120 KV - D.C. via 22 S.T.C. 5 mA selenium rectifiers type K 8 / 200. The rectifiers were mounted zig zag on a perspex panel measuring 36 x 13 inches. The wire ends of the rectifiers were connected to 1 inch diameter aluminium cylinders with semispherical ends which acted as stress-distributors and the panel itself fitted into a wooden frame situated on top of the capacitor. By turning it upside down the polarity could be changed conveniently.

The normal way to measure the D.C. voltage would have been to put a moving coil substandard instrument at the earthy side of a stable



Plate 4. The charging unit and the electrostatic Voltmeter.

FOLLOWING PAGE: 35

bleed resistor in parallel with the capacitor. Unfortunately such a resistor was not available and only recently a gift of wire wound resistors was received which, when mounted in an oil-filled bakelite tube, will provide a 100 Megohm resistor. An Abraham-Villard type attracted disk electrostatic voltmeter was therefore used to indicate the D.C. voltage. This meter had excellent repeatability, and in the open part of its scale it could be read to nearly 0.1% by means of a telescope from outside the H.V. cage. Four ranges, 15, 30, 60 and 120 KV D.C. or A.C. could be adjusted by altering the spacing between its electrodes. As the meter was not supposed to flash over at the limit of its range, 120 KV r.m.s. (170 KV_p), no reason could be seen why it should not be used at D.C. voltages higher than 120 KV with appropriate alteration in electrode spacing.

Tests were carried out as to the influence of nearby live conductors on the indication of the instrument. 100 KV r.m.s. was applied to the meter and a wire at 40 KV r.m.s. above earth was brought to within 18 inches of the electrodes. The wire was fed from another transformer connected to the same supply as the 100 KV transformer in order to ensure a small phase difference between the two voltages. About 0.2% total change in indication could be observed when the polarity of the 40 KV transformer was reversed. A distance of 5 ft. from other live wires was then considered to give negligible error. For the work described here the electrostatic instrument is used only as an indicator and not absolutely. It is only required to indicate the difference in breakdown voltage with changed polarity.

Although the ordinary polarity effect of electrostatic voltmeters which is brought about by contact potential on its electrodes would be entirely negligible when indicating high voltages, past experience has shown that H.V. electrostatic voltmeters sometimes show a different reading when the polarity is changed. This was found to be due to corona emanating from a sharp edge, a surface irregularity or dust on the surface. When ions from one electrode hit air molecules a mechanical movement of the electrode follows. (This can be observed on transmission lines which may vibrate violently due to corona).

The effect was observed in those meters in which one earthed vane

moves between two fixed ones. While there is no evidence that this also occurs in attracted disc type meters an attempt was made to overcome the uncertainty whether the meter shows differently at changed polarity or if the spark gap has a breakdown value depending on polarity. When investigating the gap at D.C. 10 readings were taken at one and 10 at the other polarity and all 20 tests repeated with the meter leads reversed. Also up to 60 KV D.C. the polarity effect of the meter itself could be checked using borrowed resistors and a D.C. milli-ampere meter. It was fortunate that the effect was negligible because for the much more important impulse tests the charging voltage of the generator did not exceed 60 KV and there was therefore no uncertainty as to the polarity effect of the meter itself.

The electrostatic voltmeter measures the r.m.s. value of the D.C. $\hat{+}$ ripple voltage, while the spark gap under test is responsive to the peak value. A negligibly small ripple voltage was aimed at. Although this investigation is only concerned with the difference between positive and negative sparkover it is erroneous to assume that the ripple voltage would be the same for both polarities. In such a rectifier plant of the "string and sealing wax" type it is not practical to avoid all corona and, due to the difference in magnitude of positive and negative corona currents, the loading of the rectifier plant may vary when the polarity is changed. As the ripple voltage is directly proportional to load current (see next Section) it was thought better to estimate the amount of ripple voltage and confirm this by measurement.

3.2.1.1. An estimate of ripple voltage and a simple method of measurement without high voltage components.

In Fig. 23, with simplifying assumptions, the current i flowing through the load resistor R_L multiplied by the discharge time t must equal the change in voltage E multiplied by the capacitance C . $i \times t = \Delta E \times C$, and as ΔE = twice the amplitude V_{rp} of the ripple voltage superimposed on the D.C. voltage : $V_{rp} = \frac{1}{2} \times i \times t / C$. The time t depends on the ratio R_S / R_L and lies in practice between 80% of T if $R_S / R_L = 0.03$ and 65% if $R_S / R_L = 0.3$. (By courtesy of

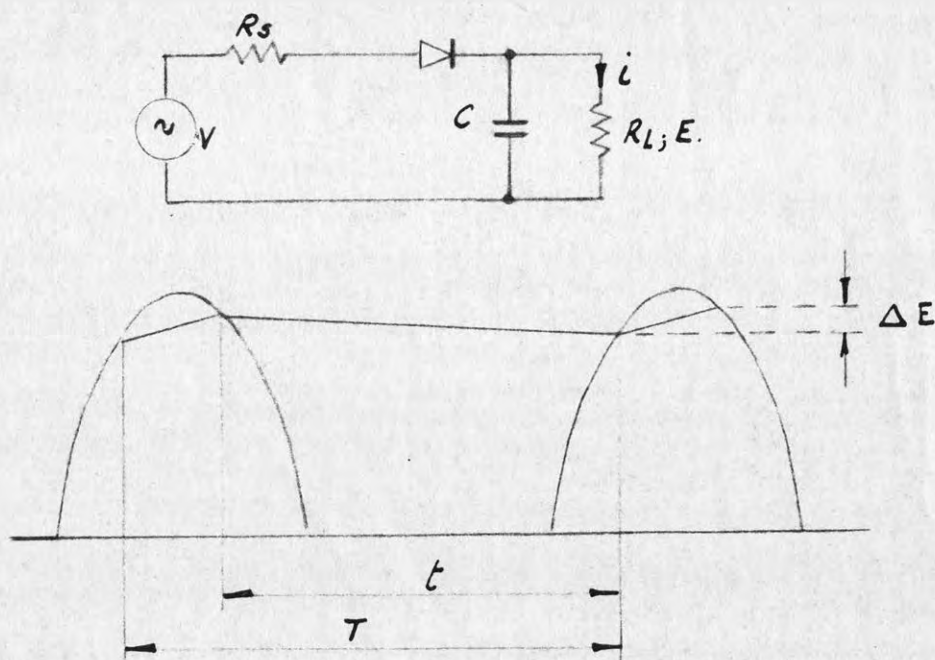
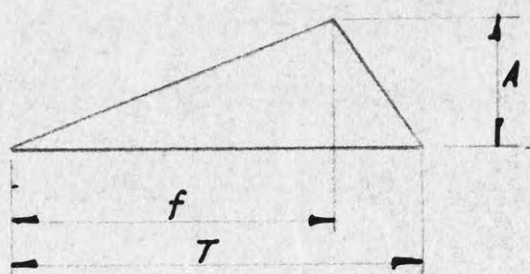


FIG. 23: PERTAINING TO ESTIMATE OF RIPPLE VOLTAGE



$$A_{AV} = \frac{A}{2}$$

C_n = AMPLITUDE OF n^{th} HARMONIC

$$C_n = \frac{2 \cdot A_{AV} \cdot T}{\pi^2 n^2 f (1 - \frac{1}{n^2})} \sin \frac{\pi f}{T}$$

FIG. 24: SAW TOOTH WAVE NOMENCLATURE AS IN REFERENCE 34

Mr. A. van Sluiter, Eindhoven 1935). Using the first figure, $V_{rp} = \frac{1}{2} \times i \times 0.8 \times T/C = 0.4 \times i / C \times f$ and for $f = 50$ c/s, i in mA and C in microfarad, $V_{rp} = 8$ V peak \times mA / microfarad.

For full wave rectification V_{rp} becomes 3 V peak \times mA / microfarad, because t is approx. 30% of T .

In order to check these simple expressions by means of published information it is necessary to know the amplitude of the fundamental component of the ripple voltage. In published data this figure is usually given because normally the ripple at the first capacitor of a capacitor input filter is attenuated by further filtering and the harmonics are attenuated more than the fundamental component which is thus the most significant one.

If the exponential charging and discharge curves of Fig. 23 are approximated by a saw tooth wave shown in Fig. 24 the parameters may be computed. (34). In our case $n = 1$, $T = \pi$, introducing $k \times T = f$ and setting $\pi^2 = 10$,

$$C_n = \frac{\sin(\pi k)}{10(1-k)} A$$

For $k = 0.2, 0.25$ and 0.3 , $C_n = 0.37 \times A, 0.38 \times A$ and $0.39 \times A$ respectively. As A represents twice the amplitude of the ripple voltage, the amplitude of the fundamental is $0.74 \times V_{rp}$ assuming as before that the discharge time is 80% of the period T , viz: $k = 0.2$

A convenient check is now afforded by comparing data published (35) for the U 52 / 5U4 G rectifier tube : $i = 250$ mA, $E = 470$ V, $C = 16$ microfarad, $F = 50$ c/s, ripple = 15%. Now : 15% of 470 V is 70 V. This is the r.m.s. value of the ripple voltage fundamental. V_{rp} would then be : $70 \times \sqrt{2} / 0.74 = 134$ V. The simple expression for V_{rp} yields, $8 \times 250 / 16 = 125$ V. The agreement is fair for such a simplified calculation. Checks for full wave rectification gave even better results and good agreement was also obtained by using the figures given by Terman (36) if consideration is given that his data are for 60 c/s.

Measurement of ripple voltage was first carried out as shown in Fig. 25. In link position 1 an oscillogram was obtained and then in position 2 the variac was adjusted to give an oscillogram of equal amplitude. The ripple voltage can then be deduced from the reading of the voltmeter VM.

The main disadvantage of this arrangement is the necessity of a high voltage blocking capacitor. It's connection requires high voltage leads which are needed only during the ripple voltage measurement. If those leads or the capacitor fitting corona the ripple voltage measurement will be wrong because the additional loadcurrent due to corona will not be present in the actual use of the D.C. supply.

Fig. 26 shows an improved arrangement requiring no H.V. components and no corona-free high voltage plumbing. Here, the fundamental component of the ripple current is measured as a drop on the resistor R. The harmonics are suppressed in the tuned amplifier. See Section 3.1.2.6. and Fig. 12. If, e is the r.m.s. voltage measured on R, the amplitude of the fundamental of the ripple voltage is given by :

$$\frac{e}{R} \cdot \frac{1}{\omega C} \sqrt{2}$$

and V_{rp} may be obtained by dividing this by 0.74.

$$V_{rp} = \frac{e}{R} \cdot \frac{1}{\omega C} \cdot 1.9$$

To quote only one test result : i was 0.75 mA, R was 5000 Ohms and when the oscillograms in switch positions 1 and 2 had the same amplitude e was 5.4 V, r.m.s.

$$V_{rp} = \frac{5.4}{5000} \cdot \frac{10^6}{314 \cdot 0.062} \cdot 1.9 \sim 106 \text{ V}$$

From the simplified expression we obtain : $8 \times 0.75 / 0.062 \sim 97 \text{ V}$, again a fair agreement.

In the computation, and again to a lesser degree in the measurement (factor 0.74) the back resistance of the rectifiers was assumed infinite. Measurements with 12 KV D.C. on each rectifier gave a mean back resistance of about 10 Megohms. The value 12 KV was chosen

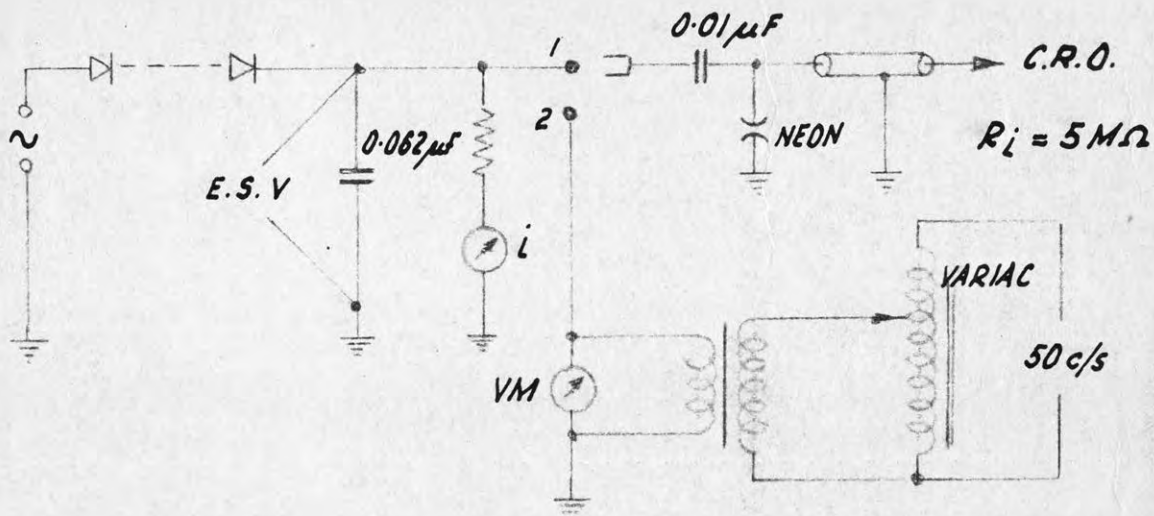


FIG. 25: RIPPLE VOLTAGE MEASUREMENT

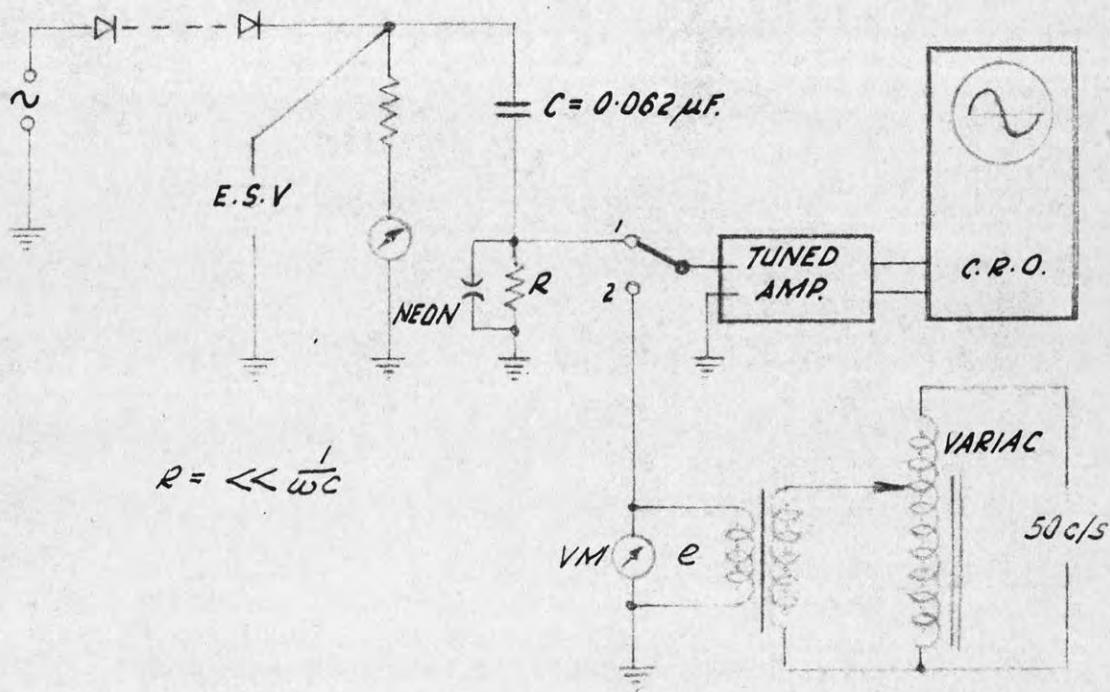


FIG. 26: IMPROVED METHOD OF RIPPLE VOLTAGE MEASUREMENT

because the max. peak inverse voltage per rectifier was slightly smaller than this value. Compared with the reactance of the filter capacitor (approx. 50.000 Ohms at 50 c/s) the back-resistance of 22 rectifiers may be neglected as far as ripple is concerned.

Generally, when the D.C. plant was used the ripple voltage amplitude was less than 0.15% of the D.C. voltage. Even allowing for a difference in negative and positive corona current, the error due to ripple in the determination of the gap polarity effect would thus be less than 0.1%.

3.2.2. D.C. test results.

The tests were made using a 100,000 Ohm series resistor (water type) with the gap resting on a 6 x 3 ft. earth plane.

The polarity effect was tested at a spacing of 4.8 cm because the available D.C. voltage was insufficient to cause spark-over at larger spacings. With the H.T. cylinder positive, the breakdown voltage was approx. 0.5% higher than with negative polarity. Using the same test equipment, a sphere gap with 10 cm spheres was then substituted. The spacing was 4.8 cm and the shanks as well as the height above the earth plane were nearly the same as for the crossed cylinder gap. In this case the positive spark over voltage was 4% higher than the negative one. According to the B.S.S. 358 a difference of 5% should have been measured, but it is known that the values of Table III in the B.S.S. 358 are not quite certain and as in any case the polarity effect depends on the capacitance asymmetry of the structure (33) it may not be justified to expect closer agreement.

3.3. Performance with 1/50 microsecond impulse waves with one cylinder grounded.

3.3.1. The impulse generator.

The circuit of the generator built for the work described in this thesis is shown in Fig. 27. Plate 5 shows the physical arrangement. At the left of Fig. 27 is the charging unit and the electrostatic

TO 100 kV
T'FORMER

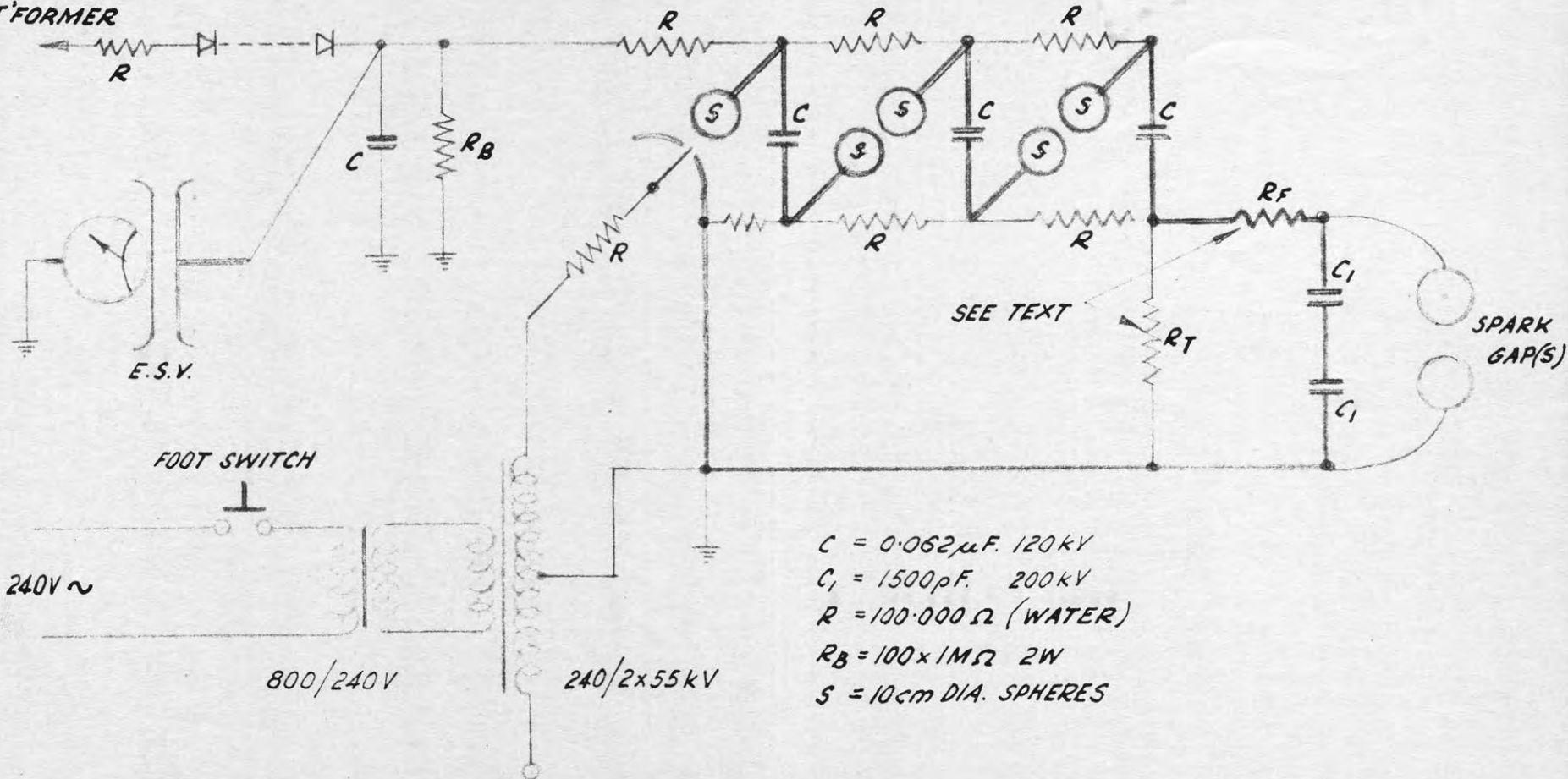


FIG. 27: CIRCUIT OF IMPULSE GENERATOR

FOLLOWING PAGE: 40

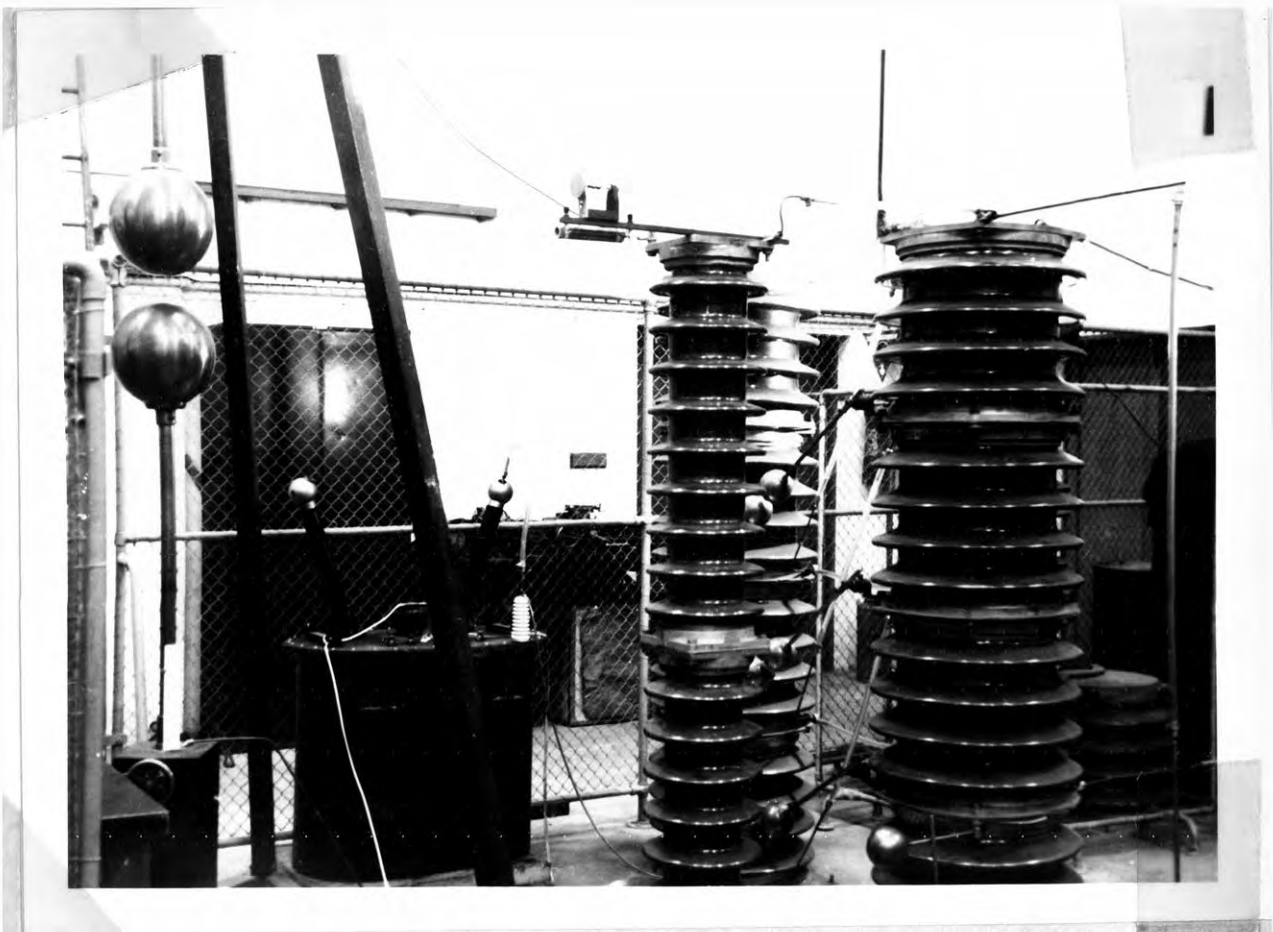


Plate 5. The impulse generator.

voltmeter described in Section 3.2.1. 100, 1 Megohm resistors form a discharge resistor for the D.C. supply. D.C. is fed to the impulse generator via a transmission line indicated by the dashed line in Fig. 27. The generator itself has three stages and employs the "Goodlet" circuit (37) which permits grounding of the trigger electrode. Triggering is carried out by means of a foot-switch closing of which applies A.C. voltage to the trigger-pin of the trigatron spark gap shown in the circuit. The reason for two transformers in the trigger circuit is that no single transformer with the required voltage of 10 to 15 KV r.m.s. was conveniently available. The tail resistor R_t precedes the front resistor R_f as this connection gives slightly higher output voltage than with R_t after R_f . This is advantageous because the charging voltage is smaller and there is less corona and radio interference. Physically, the generator has 2 columns carrying capacitors alternating with spacers and a third column consists of the two 1500 pF capacitors of the pulse forming network. The generator rests on a large aluminium plate to which all earth connections are made. When this method of earthing was proposed some time ago scepticism was encountered. It was therefore pleasing to find that this way of making inter-generator earth connections, which is quite obvious to r.f. workers, appears now to be good overseas practice. (38).

The resistors R_f and R_t were computed from approximate equations given by Striegel (39).

$$t_F = \frac{1}{10^6} \sim 2.5 R_F \frac{C_g C_L}{C_g + C_L}$$

wherein C_g is the generator capacitance, in our case 62000/3 pF and C_L is the output capacitance, in our case approx. 800 pF. With reference to Fig. 27 this is the series capacitance of the two capacitors marked C_1 plus 50 pF for the capacitance of the test object, which sometimes consisted of two spark gaps in parallel. R_f was 520 Ohms and was a water resistor as per Fig. 20 filled with a water and salt solution. R_t was computed from :

$$t_T = \frac{50}{10^6} \sim 0.72 (C_g + C_L) R_T$$

The actual value was 3200 Ohms. (Water resistor). The circuit as shown and used for the tests does not permit a convenient check of the wave form. For this purpose the circuit of Fig. 28 was used. R_t'' was a 4400 Ohm, I.R.C. MPO resistor placed in oil and R_t' was a 9000 Ohm water resistor. The front duration of the wave for this case is:

$$t_F = 2.5 \frac{R_F R_T''}{R_F + R_T''} \cdot \frac{C_g \cdot C_L}{C_g + C_L}$$

which yields 0.9 instead of 1 microsecond. Owing to the large tolerances permitted in the standard waveform this was neglected.

Fortunately a modern high speed C.R.O. could be borrowed to check the waveform. This instrument has a time base with negligible delay in starting and a special helical cored delay cable of several feet length which provides a delay of approx. $\frac{1}{4}$ microsecond within its passband of 30 Mc/s, between the input terminals and the "Y" plates. The signal first triggers the time base and is delayed in reaching the "Y" plates thus permitting the time base to start. With such a C.R.O., in which the delay cable gives negligible distortion, the method of triggering the generator becomes unimportant and any delay in the action of the trigatron has no effect on the oscillography. Trigatron delay will be discussed when describing the gap type "C" later on. The waveform was clean without overshoot and spurious oscillations. A sweep speed of 0.8 microseconds per inch was used to observe this and there was no irregularity at or in the vicinity of the peak of the wave. Near the tail end a slight "wriggle" could be observed which could not be resolved during the time the C.R.O. was available, but this could not have had any influence in spark gap tests. It was particularly pleasing that splitting up of the front resistor was apparently not necessary. This would have been inconvenient as all parts of the impulse generator with the exception of the water resistors and the selenium rectifiers were on loan.

Some time after the tests, during an investigation on cable terminations for the Sydney County Council, Mr. W. Williams checked the waveform on a different C.R.O. with identical results.

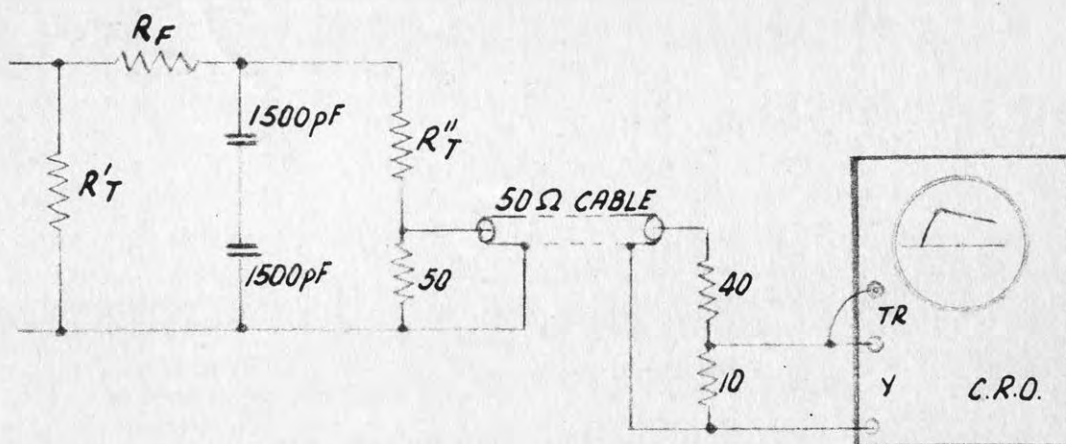


FIG.28: CHECK ON IMPULSE WAVEFORM

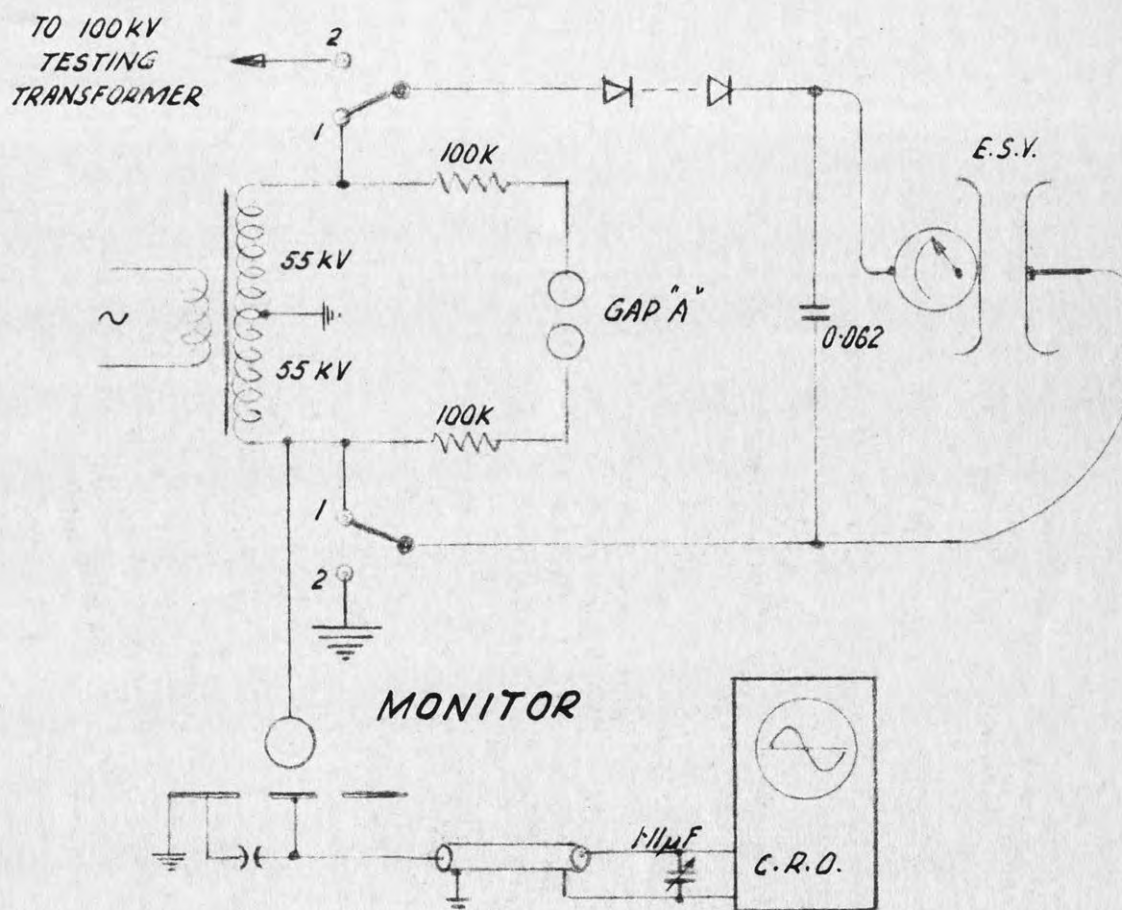


FIG.30 UNSUCCESSFUL TEST METHOD

The generator was found very convenient to use. Without changing the gap spacing a 1: 1.7 voltage range could be covered by altering the charging voltage. The telescope for reading the electrostatic meter was firmly attached to the box containing the voltage controls. The foot switch for triggering the generator and the overload trip reset were arranged within easy reach so that a large number of measurements could be made without leaving the seat in front of the control box. The overload protection described in Section 3.1.1. and Fig. 2 was suitable to interrupt the supply to the charging unit on impulse flashover.

A vertical sphere gap with 25 cm diameter spheres the lower sphere of which was earthed formed part of the impulse testing equipment.

It was not found necessary to draw probability curves for 50 or 90% flashover, as, after initial discharges the 25 cm sphere gap as well as the crossed cylinder gap gave very consistent performance. For example, flashover occurred consistently at say 50.0 divisions of the meter but not at 49.9. It is believed that the reduced scatter as compared with A.C. or continuous D.C. tests is due to the fact that there is unlimited time to set and read the meter accurately and that while doing this the gap is at zero potential and does not attract fibres.

3.3.2. Test results with impulse waves and polarity effect.

The gap rested on a 6 x 3 ft. Aluminium sheet and was connected to the generator without series resistor.

An absolute calibration was carried out at spacings 2, 3, 4, 5 and 5.5 cm. For each setting the reading of the charging voltmeter was noted for negative impulse spark over. Let this reading be V_i . The 25 cm sphere gap was then substituted without change of the physical position of either gap. Its spacing was adjusted, by trial and error, for negative impulse spark over to occur at about the same reading of the charging voltmeter. Let this reading be V_i' . In both cases 30 to 40 sparkovers were made for each gap spacing. (40). Both gaps were then calibrated in situ on 50 c/s as described in Section 3.1.2.

The values so obtained, V_{50} and V_{50}' respectively gave check readings on the results shown in Table II and it was found that for all spacings tested :

$$V_1 / V_1' = V_{50} / V_{50}' (1 \pm 0.005)$$

indicating that the crossed cylinder gap is just as suitable to measure impulse voltages as a sphere gap. The calibrations agreed to within approx. 1% with the B.S.S. 358 as determined from the spacing of the 25 cm spheres.

The polarity effect of the crossed cylinder gap is shown in Table III and a comparison of the crossed cylinder gap with a 10 and 25 cm sphere gap is shown in Fig. 29.

Table III

Spacing cm	KV pos / KV neg
4.5	1.000
5.0	1.005
5.5	1.010
6.0	1.025
6.5	1.035

A 10 cm diameter sphere gap spaced 4.8 cm and substituted for the crossed cylinder gap gave a difference of approx. 4% between positive and negative sparkover, while a 25 cm sphere gap the spacing of which was adjusted to give about the same reading on the charging voltage meter as was the case for the crossed cylinder gap at a spacing of 6.5 cm showed a difference of 0.8%. From the B.S.S. 358 a difference of 0.6% may be computed and although, owing to the rounding off to the nearest KV, this figure is somewhat uncertain it serves as a check on the method and accuracy of measurement.

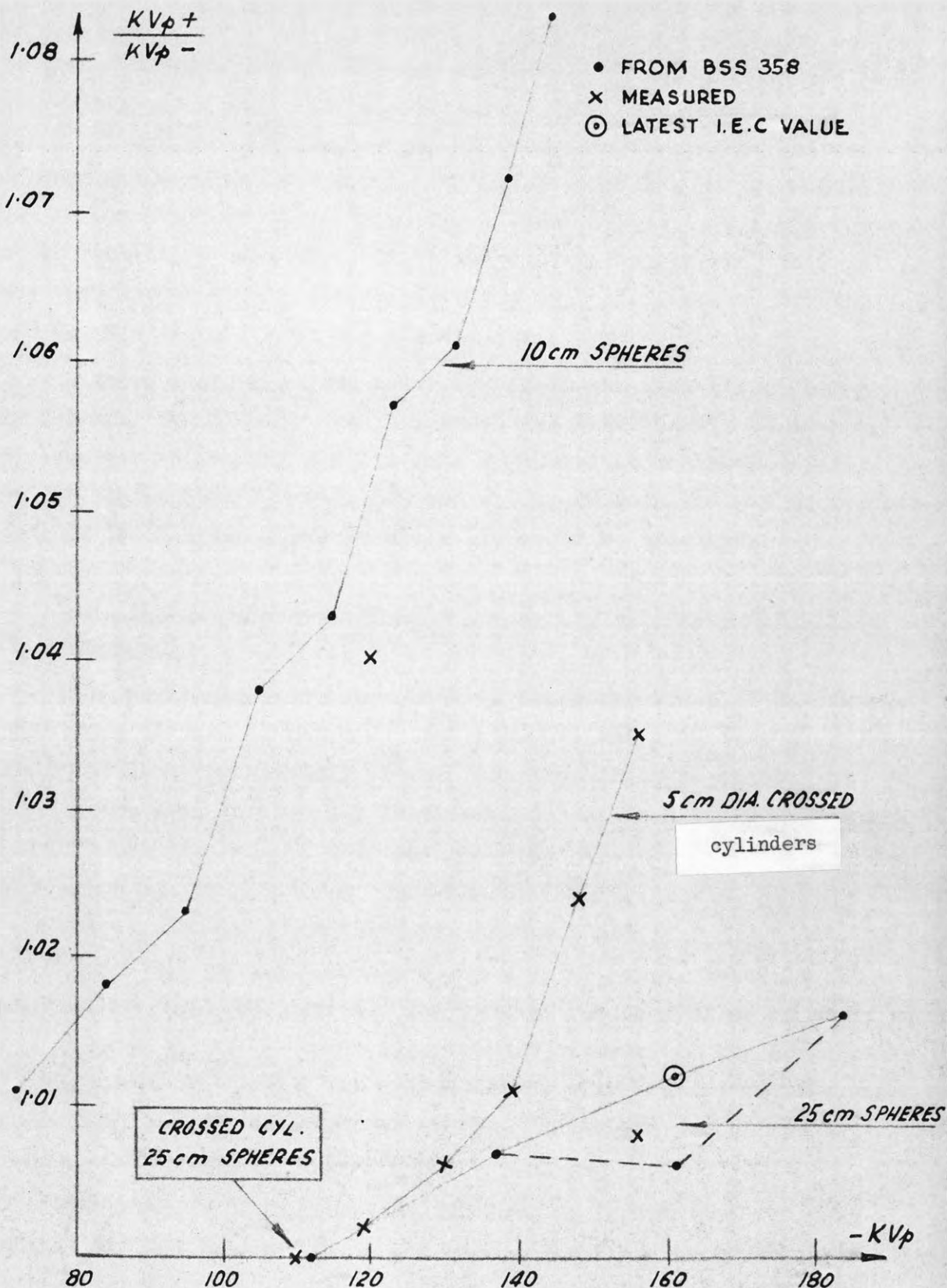


FIG. 29: POLARITY EFFECT
 10cm & 25cm SPHERES; 5cm CROSSED CYLINDERS
 FOLLOWING PAGE: 44

The polarity effect measured previously on continuous D.C. fits also the results given in this section. It should be noted that at the limit of its range, viz : 5.5 cm, the polarity effect of the crossed cylinder gap is approx. 1% while, according to the B.S.S. 358 the polarity effect at the same spark over voltage is 7 to 8% for a 10 cm diameter sphere gap. It is interesting to observe, in Fig. 29, that the slopes of the graphs referring to 10 cm diameter spheres and the crossed cylinder gap are similar.

A further check on the polarity effect was made using longer cylinders. The diameter was 2 inches, the total length 27 inches, the gap was horizontal and its axis 25 inches above the 6 x 3 ft. ground plane. The spacings 5.5 and 6.5 cm were tested but no improvement on the figures given in Table III could be obtained.

3.4. Performance on symmetrical A.C. (Transformer centre tap grounded).

From Whitehead's work on which is based the B.S.S. 358 little difference between symmetrical and unsymmetrical A.C. (one electrode grounded) is to be expected if the polarity effect is small. As this is the case for the gap described, it was considered sufficient to carry out the test at only one spacing, viz : 5 cm.

3.4.1. Voltage generation and measurement.

An "X" ray transformer 240 V / 2 x 55 KV r.m.s. rated 10 KVA was used as a voltage source. The voltage was controlled as shown in Fig. 2, Section 3.1.1. Each high voltage terminal of the transformer was connected to the gap via a 100,000 Ohm water resistor. The earth plane was a 6 x 3 ft. Aluminium sheet. The centre tap of the H.V. winding was connected to this sheet.

Considerable trouble was encountered in determining the peak voltage in this connection of the gap. A tertiary being not available, it was planned to use the measuring circuit shown in Fig. 30. The procedure was to have been to record the readings of the electrostatic voltmeter for 10 spark overs with the high voltage change over switch in position 1 and then to switch over to position 2 and determine, as described in Section 3.1.2. the peak voltage which gives the same

reading on the electrostatic voltmeter. When this was tried it was found impractical to suppress corona sufficiently. The D.C. current flowing through the secondary of the transformer caused core saturation and clipping of one half of the wave. This could be observed by means of the monitor described in Section 3.1.2.3. The transformer must have an enormous number of turns as evidenced by a secondary resistance of $2 \times 25,000$ Ohms, and it is believed that the rating of 10 KVA is a short time rating only. With the available equipment and 22 selenium rectifiers no solution to this could be found and the scheme, described in the next Section, was evolved in which the spark gap under test is also used as its own measuring device.

3.4.2. Test procedure and results.

The gap was first calibrated at a spacing of 5 cm with one cylinder grounded as described in Section 3.1.2. using the 100 KV testing transformer as before. The mean of 10 spark over values obtained was 129.6 KV_p which served as a check on the previously measured value of 130.0 KV_p . Connection was then made to the 2×55 KV transformer. The peak voltmeter described in Section 3.1.2.1. was connected to the primary terminals of the transformer. After initial discharges the readings of this meter were noted for 10 spark overs. Let the mean of these readings be D_o . The gap was then connected to one half of the transformer secondary and the electrode spacing reduced until breakdown occurred close to the mean of the previously obtained reading. Ten discharges were recorded and then, without change in spacing, the high voltage cylinder of the gap was connected to the other half of the transformer, ten discharges again being recorded. Let the mean of the readings so obtained be D_a and D_b . At this spacing the gap was then calibrated as described in Section 3.1.2. using the 100 KV testing transformer. Let the peak voltage so obtained be V_1 . The sparkover value for symmetrical A.C. could then be computed from the results of the measurements described above :

$$V_p (\text{sym}) = V_1 (D_o / D_a + D_o / D_b)$$

wherein D_o/D_a and D_o/D_b differ but little from 1.000.

The value obtained was 129.9 KV_p. Owing to the many steps required to obtain this result the accuracy of measurement must have suffered but it appears certain that for practical purposes, the figures given in Table II should suffice.

The operating fluxdensity of the transformer was abnormally low and the voltage drop on the primary resistance \hat{r} leakage inductance was much smaller than 0.1% of the applied voltage. The harmonic content of the exciting current was about 20% and as the total no load primary impedance drop was \ll 0.1% the error made due to the slight departure of D_o / D_a and D_o / D_b from 1.000 was considered negligible.

From the value of the total impedance referred to the primary, viz : $(0.42 + 0.90 j)$ Ohms at 50 c/s it could be deduced that the error due to the different capacitive loading for the two connections of the gap would be nearly negligible. However, an attempt was made to keep the loading nearly constant by means of two 15 cm diameter spheres connected to the H.V. terminal of that half of the transformer which was not in use. This is described in the next Section.

3.4.2.1. Spark gap capacitance and arrangement for constant capacitive loading.

The capacitances of the spark gap were measured as shown in Fig. 31 by measuring voltage and current and computing C from $C = i / V\omega$. This method while crude and susceptible to wave form error is very convenient in the H.V. laboratory. The meter M was enclosed in a metal box suspended from the ceiling by a string and it could be read by means of a telescope from outside the H.V. enclosure through a grille in the box. The meter, with a nominal full scale deflection of 100 microamperes D.C. showed a full scale deflection ^{or} 230 microamperes A.C. instead of the theoretical value, $100 \pi / \sqrt{2} = 222 \mu A$.

Its indication was sufficiently linear as could be proved by obtaining identical results with various values of V. Usually V was between 5 and 20 KV. An overall "absolute" check was made by measuring the capacitance of a 12.5 cm diameter sphere suspended on a Nylon thread and spaced more than 3 ft. from the nearest object. A capacitance of

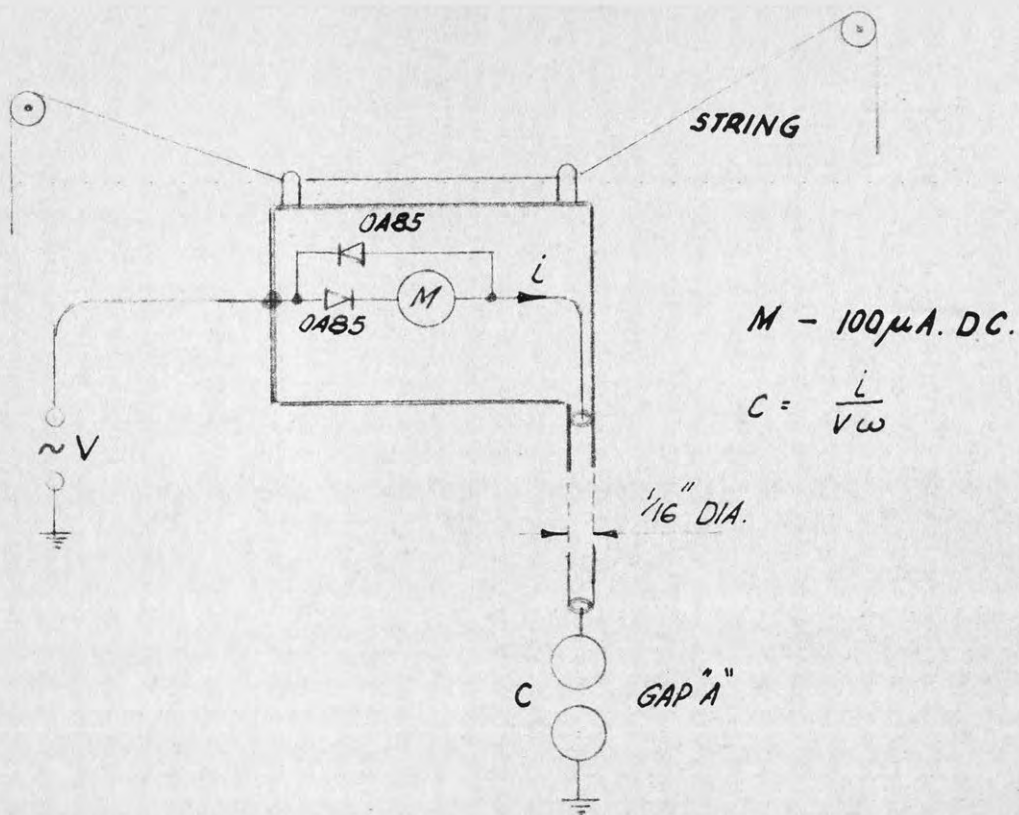


FIG. 31: SET-UP FOR GAP CAPACITANCE MEASUREMENT

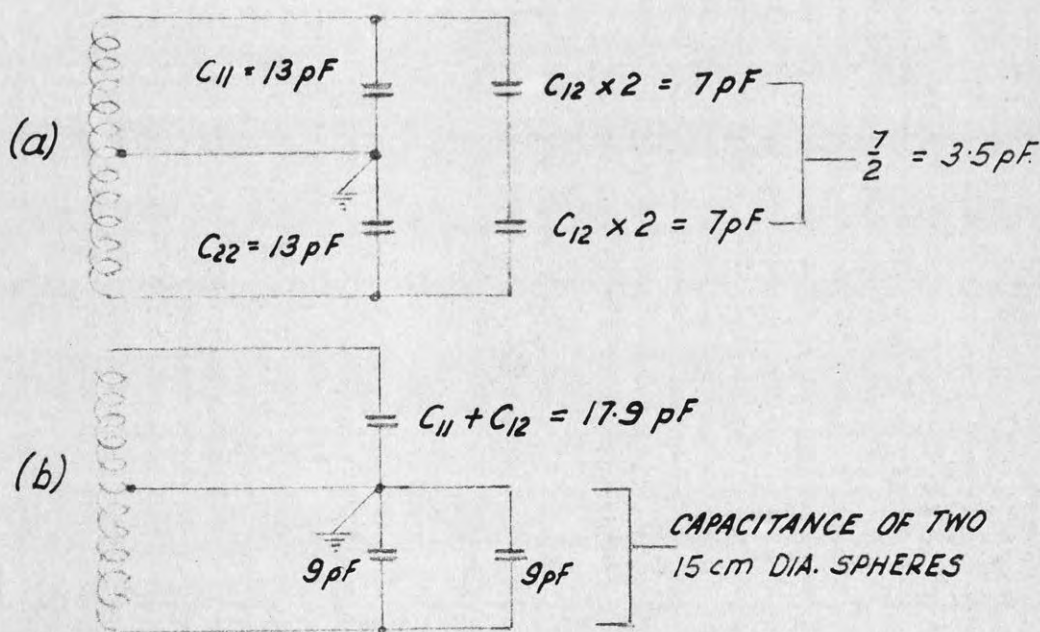


FIG. 32: CAPACITIVE LOADING OF THE 2x55 KV TRANSFORMER

7.0 pF was measured instead of 1.11 $r = (12.5 / 2) \times 1.11 = 6.9$ pF. A probe type capacitance meter, which must have caused more field distortion than the thin shielded lead shown in Fig. 31, indicated 6.8 pF. (41).

If C_{11} and C_{22} are the ground capacitances of each cylinder and C_{12} the mutual capacitance, the value $C_{11} + C_{12}$ is obtained when one cylinder is grounded. $C_{11} + C_{12}$ measured as a function of spacing is shown in Table IV.

TABLE IV.

a (cm)	$C_{11} + C_{12}$ (pF)
0.5	20.5
1	19.0
2	18.0
3	17.5
4	17.0
5	16.5
6	16.0

The capacitance $C_{11} + C_{22}$ was measured by joining both cylinders. The values obtained at a spacing of 5 and 2 cm were 26 and 25 pF respectively. Owing to the symmetrical arrangement $C_{11} = C_{22} = 13$ pF at 5 cm spacing. From Table IV $C_{11} + C_{12} = 16.5$ pF and C_{12} therefore 3.5 pF. The loading diagram for the case when the gap was across the total secondary winding may now be drawn as shown in Fig. 32a. Fig. 32b shows the loading diagram for the gap across $\frac{1}{2}$ the winding. The spacing in this case was about 2.2 cm and from Table IV, $C_{11} + C_{12}$ may be interpolated, 17.9 pF. The two loading spheres were on shanks which explains the capacitance value of 9 pF instead of $(15 / 2) \times 1.11 = 8.3$ pF per sphere. It was important to separate the spheres by about 2 ft. as otherwise, due to field distortion, the total capacitance was less than the sum of the

individual capacitances.

The loading diagrams show that in one case each half of the transformer was loaded with 20 pF and in the other case with 18 pF. This is quite negligible when referred to the primary and compared with the reactance values.

3.5 Comments on relative humidity and irradiation.

In all tests the relative humidity was between 40 and 60%, the temperature between 17.5 and 20.0 centi-degrees and the barometric pressure between 750 and 770 mm mercury.

Up to quite recently it was believed by many workers that the influence of humidity can be neglected. Systematic tests require obviously elaborate experimental facilities and no work has been done on this aspect for this thesis. It is understood however that at present Prof. Bruce is preparing an experimental investigation of that nature. Schroeder (42) has recently tested uniform field electrodes up to 5 cm spacing and found that a change in absolute humidity from 4 to 13 mm mercury increased the sparkover voltage linearly by about 1½% and it is most likely that this should be valid for the spacings encountered in gap type "A". At 20° C where the vapour pressure of water is 17.5 mm mercury the figures quoted above correspond to a change in relative humidity from : $(4 / 17.5) \times 100 = 23\%$ to $(13 / 17.5) \times 100 = 74\%$. For a 10% change in relative humidity an increase in sparkover voltage of $1.5 \times 10 / 74 - 23 = 0.3\%$ approx. can therefore be expected. This figure would amply explain the few tenths of one percent difference observed when doing repeat checks at various times.

Irradiation by means of a 30 W mercury vapour lamp, the ultra-violet radiation of which was checked by means of uranium glass, did not have any apparent effect. At a spacing of 0.5 cm, at A.C., there appeared to be some influence but this was too small and uncertain to influence the result given in Table II. The lamp used approximated closely the type recommended by the I.E.C. spark gap Committee.

In case of impulse tests the explanation may be that the light of

the generator gaps provided irradiation for the gaps under test. Owing to the rather limited space screening was not attempted. Another reason may be that the air pumped into the laboratory passes through precipitrons or it may have happened that, as was the case in Hueter's work (43) ionised ground air ("Bodenluft") made additional irradiation superfluous.

3.6 Conclusions re gap type "A".

For the range investigated, 140 KV_p, the gap performs better than the equivalent sphere gap. It is less influenced by the proximity of other bodies and the ground plane, its polarity effect is very much less and it is easier to build. For practical purposes one calibration is sufficient for A.C., A.C. symmetrical, D.C. of either polarity and impulse voltages of either polarity. It is believed that the polarity effect of this electrode configuration has not been investigated before. The puncture strength of atmospheric air for the crossed cylinder configuration was found to be independent of spacing at 33.3₅ KV/cm for 5 cm diameter cylinders.

To ascertain the performance, measurement methods and apparatus were developed which are not restricted to the calibration of spark gaps only, viz : Convenient voltage control and overload protection equipment, a peak voltmeter and a method for its calibration, a distortion generator, an amplitude indicator, economically producible high and low voltage three terminal air capacitors, a convenient 50 c/s Detector amplifier to replace vibration galvanometers, a resistive divider with highly stable resistors virtually free of load coefficient, a method for measuring the peak voltage ratio of a testing transformer, a practical method of measuring the self-capacitance of large iron cored coils, a method of measuring the ripple voltage of a high voltage D.C. supply with low voltage components, an easily producible bridge detector transformer with extremely low interwinding capacitance, a simple high voltage wave-form monitor and a method of using a spark gap to test its performance on symmetrical A.C.

As a by-product, experience was gained regarding the performance of testing transformers which should be of direct value for N.A.T.A. and at a time when no impulse generator was working in N.S.W. the impulse generator built for the purpose of this thesis gave valuable service in the development and testing of commercially produced electrical equipment.

3.7. References re gap type "A".

- (1) A. Schwaiger
Elektrische Festigkeitslehre.
2nd ed. Springer, Berlin, 1925.
In English : Schwaiger - Sorensen
Theory of Dielectrics
John Wiley & Sons, 1932.
- (2) A. Pen - Tung - Sah
Studies on sparking in air.
Journal A. I. E. E. Vol. 46, 1927, p.1073
- (3) E. Werner
Gekreuzte Zylinder als Funkenstrecke.
Arch. f. Elekt. Vol. 22, No. 1 1929, p. 1.
- (4) W. Pankow
Die Durchschlagsspannung zwischen zylindrischen Leitern in Luft.
Deutsche Elektrotechnik Vol. 6, No. 3, March 1952, p.109.
- (5) F. Obenaus
Durchschlagwechselspannung von Luftstrecken von 10 - 30 KV.
Deutsche Elektrotechnik Vol. 10, No. 6, June 1956, p.212.
- (6) A. Russel
A treatise on the theory of alternating currents.
Vol. 1, p.256, Cambridge press 1914.
- (7) P.G. Harper and J.J. O'Dwyer
Electric field strength between crossed and parallel cylinders.
I. E. E. Monograph No. 235, May 1957.

- (8) Measurement of Voltage with sphere gaps.
British Standard 358 / 1939.
- (9) F.W. Peek
Dielectric Phenomena in high voltage Engineering.
2nd ed. 1920, McGraw - Hill, New York.
- (10) A. Roth
Hochspannungstechnik.
3rd ed. p.383, Springer, Berlin 1950.
- (11) L. Medina,
The detection of corona discharges in high voltage air capacitors.
Austr. J. appl. Sc. Vol. 6, No. 4, p.453, 1955.
- (12) E.W. Golding
Electrical Measurements
3rd ed. p.428, Pittman 1942.
- (13) L. Medina
A peak voltmeter with a long time constant.
Austr. J. appl. Sc. Vol. 5, No. 2, p.141, 1954.
- (14) L. Medina
A simple distortion generator with adjustable waveform for investigating the waveform error of indicating instruments at 50 c/s.
E. T. Z. Vol. 79, 11/3/1958, p. 180.
- (15) H.A.W. Klinkhamer
Equivalent network with highly saturated iron cores with special reference to their use in the design of stabilisers.
Philips Techn. Rev. Vol. 2, 1937, p.276.
- (16) B. Hague
Alternating current bridge methods
Pitman 1945, 5th ed. p.194.

- (17) R. Davies, G.W. Bowdler and W.G. Standring
The measurement of high voltages with special reference to the measurement of peak voltages.
J. I. E. E. Vol. 68, 1930, p.1222.
- (18a) L. Medina
The computation of the inductance of bifilar strips
E. T. Z. (A) Vol. 76, No. 23, 1. 12. 1955.
- (18b) The method described in reference (18a) was used to design a 100 c/s to 4 Mc/s inductive ratio arm for Dr. A.B. Hope.
A.B. Hope
The electric properties of plant cell membranes
Austr. J. Biol. Sc. Vol. 9, No. 1, 1956 p. 55.
- (19) The N.S.W. University of Technology
Ann. Exam. 1957, Prof. elect. - Electrical measurements.
Exam. question No. 1.
- (20) W.K. Clothier and L. Medina
The absolute calibration of voltage transformers.
Proc I. E. E. Part A, Vol. 104, No. 15, June 1957, p.204.
- (21) L. Medina
On the measurement of the no load losses of small transformers at 50 c/s
E. & M., Vol. 67, No. 4, 1950, p.99.
- (22) L. Medina
An instrument for the detection of shorted turns in coils
Proc. I. R. E. (Aust.) Vol. 12, No. 11, Nov. 1951, p.329.
- (23) As (10) but p.386.
- (24) Mullard
High quality sound reproduction
Mullard Ltd., Century House, London W.C.2.

- (25) L. Medina
Prevention of ionisation in small power transformers.
Proc. I. R. E. (Aust.) Vol. 15, No. 5, May 1954, p.114.
- (25a) L. Medina
Apparatus for the detection of corona discharges in the insulation of electrical equipment
Proc. I. R. E. (Aust.) Vol. 17, No. 6, June 1956, p.218.
- (26) F.C. Hawes
A recurrent surge oscillograph
Proc. I. R. E. (Aust.). *Vol 18, Dec 1957, p 462.*
- (27) As reference (9) but page 46.
- (28) T.W. Liao and J.S. Kresge
The detection of corona in oil at very high voltages
Power apparatus and systems, No. 15, Dec. 1954, p.1389.
- (29) B.V. Hamon
Precise frequency and voltage control of a sine wave alternator set
Austr. J. appl. Sc. Vol. 2, No. 1, 1951, p. 1.
- (30) F.M. Bruce
Calibration of uniform field spark gaps for the measurement of high voltages at power frequencies.
J. I. E. E. Part II. Vol. 94, 1947, p. 138.
- (31) Private communication from Mr. Hylten-Cavallius (Sweden),
Secretary spark gap Committee of the I. E. C.
- (32) As reference 1, page 465.
- (33) S. Whitehead
A note on standard calibrations for sphere gaps
J. I. E. E. Vol. 84, 1939, p.408.

- (34) Federal Telephone and Radio Corporation, New York
Reference Data for Radio Engineers
2nd ed. p.285.

- (35) A.W.V. Sydney
Radiotron valve data book, p.265.

- (36) F.E. Terman
Radio Engineers Handbook
McGraw - Hill New York, 1943, p.603.

- (37) F.S. Edwards, A.S. Husbands and F.R. Perry
The development and design of high voltage impulse generators
Proc. I. E. E. Part 1, Vol. 98, 1951, p. 155.

- (38) N. Hylten Cavallius
Impulse tests and measuring errors
Asea Journal, No. 5, 1957.

- (39) R. Striegel
Electrical impulse strength
Springer Berlin, 2nd ed. 1955, p.130.

- (40) W. Bauman
Statistical error in the determination of the 50% flashover value
E. T. Z. (A), Vol. 78, 1.6.1957, p. 369.

- (41) L. Medina
Two probe type capacitance meters
Proc. I. R. E. (Aust.) Vol. 14, No. 8, Aug. 1953, p. 193.

- (42) G.A. Schroeder
The influence of atmospheric humidity on the breakdown voltage of
a uniform field spark gap
Annalen der Physik, Vol. 18, No. 5 - 8, 1956, p. 385.

(43) E. Hueter

On the measurement of the peak value of power frequency voltages by means of the spark gap

E. T. Z. Vol. 57, 28.5.1936, p. 621.

(26 a) The N. S. W. University of Technology

Exam. question 7

Annual examination 1955, Professional elective, Electrical Measurements.

(19 a) as above but question 2 c.

4. The gap type "B".

4.1. The influence of a large series resistor.

Although the use of a large series resistor, to prevent pitting, is obvious only little information on this could be found. In nearly all published work relating to spark gaps a value of $\frac{1}{2}$ to 2 Ohms per Volt is recommended and only one report (44) deals briefly with the effect of a 4 Megohm and an 8 Megohm resistor in connection with a 2 cm diameter sphere gap spaced 2 cm. An increase in sparkover voltage of 1% and 2 $\frac{1}{2}$ % respectively was observed and the performance was described as erratic.

Only recently, the I.E.C. Spark Gap Committee has considered higher values of series resistors, the value being based on

$$\frac{1}{2} \omega^2 R^2 C^2 < 0.1\%$$

wherein R is the series resistance, C the effective capacitance of the gap and $\omega = 314$.

4.1.1. Observations.

Experiments were first carried out on an experimental horizontal gap using 10 cm diameter spheres. The construction of the gap was similar to the one shown in Fig. 1 and Plate 1. A 20 Megohm series resistor the ceramic body of which was $1\frac{1}{8}$ inch in diameter and $6\frac{1}{2}$ inches long was mounted horizontally and connected to the gap externally. The resistor was in a perspex trough filled with transformer oil. All work on gap type "B" was made at 50 c/s.

At spacings between 1 and 4 cm the results were reasonably consistent but the spark-over values were higher than expected from the calculated voltage drop in the resistor due to the capacitance of the gap $C_{11} + C_{12}$ (see Section 3.4.2.1.) plus $1/3$ of the ground capacitance of the resistor. For proof of the figure $1/3$ see Appendix 3. Also, when repeated at times of high relative humidity the sparkover values were higher still and results up to 5% higher

than expected were not uncommon. At spacings above 4 cm, even at low relative humidity, the results were higher than computed. At spacings below 1 cm and particularly below 0.5 cm the sparkover was erratic and the scatter of results was approaching 30%. In fact, it was difficult to assign a value to the spark over voltage. For example, at a certain setting of the voltage control sparking would occur, then become extinguished on its own accord and sometimes occur again after a few seconds, often at a much lower voltage.

4.1.2. Design requirements.

The discouraging performance mentioned above could be improved by a radical change in the design of the gap. It was found that the insulation resistance of the porcelain insulators dropped to below 1000 Megohm in humid weather and that corona on the connecting lead and the fitting caused a significant voltage drop on the series resistor. The gap was also found less erratic when used vertically probably because, in the horizontal position, rising hot air tends to extinguish the rather feeble spark, an action similar to the one occurring in arc horns.

In order to be quite independent of the state of the insulation, an important consideration for use in factories, the high tension electrode was fixed to the series resistor as shown in Fig. 33 and Plate 6, the resistor being housed in an oil filled tube of synthetic resin bonded paper. Leakage current over the wooden framework is harmless as it is supplied by the source of voltage and leakage across the insulating tube alters only the effective value of the series resistor. This is quite insignificant as evidenced by the performance figures given in Section 4.2. The vertical arrangement has the additional advantage of slightly less earth capacitance and temperature rise of the resistor. Crossed cylinders were used instead of spheres for the reasons outlined in Section 2 and because it was desired to obtain check-readings on a differently constructed crossed cylinder gap.

The shank of the H.T. electrode must not be too short in order to avoid field distortion but must not be too long for reasons of

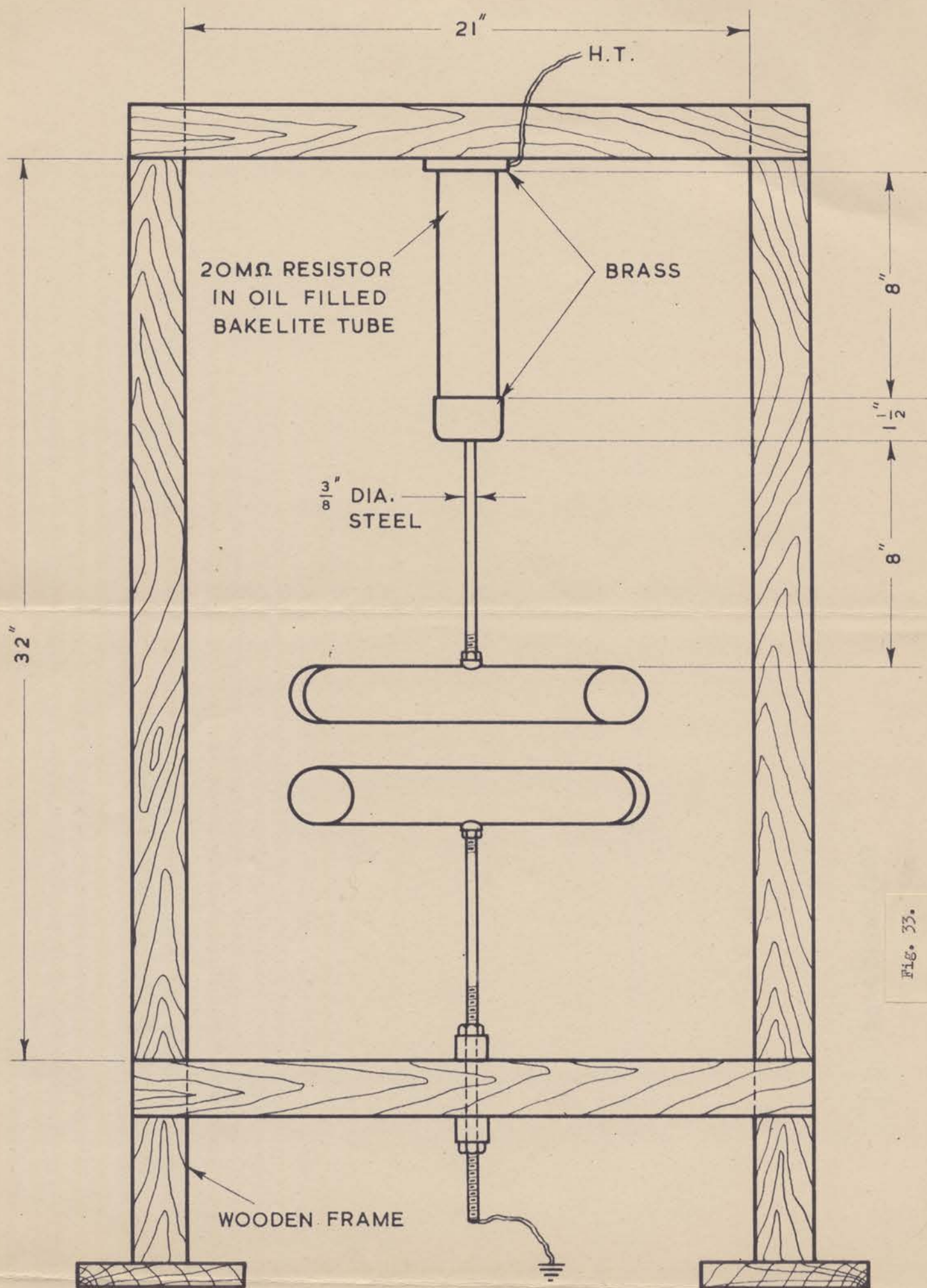
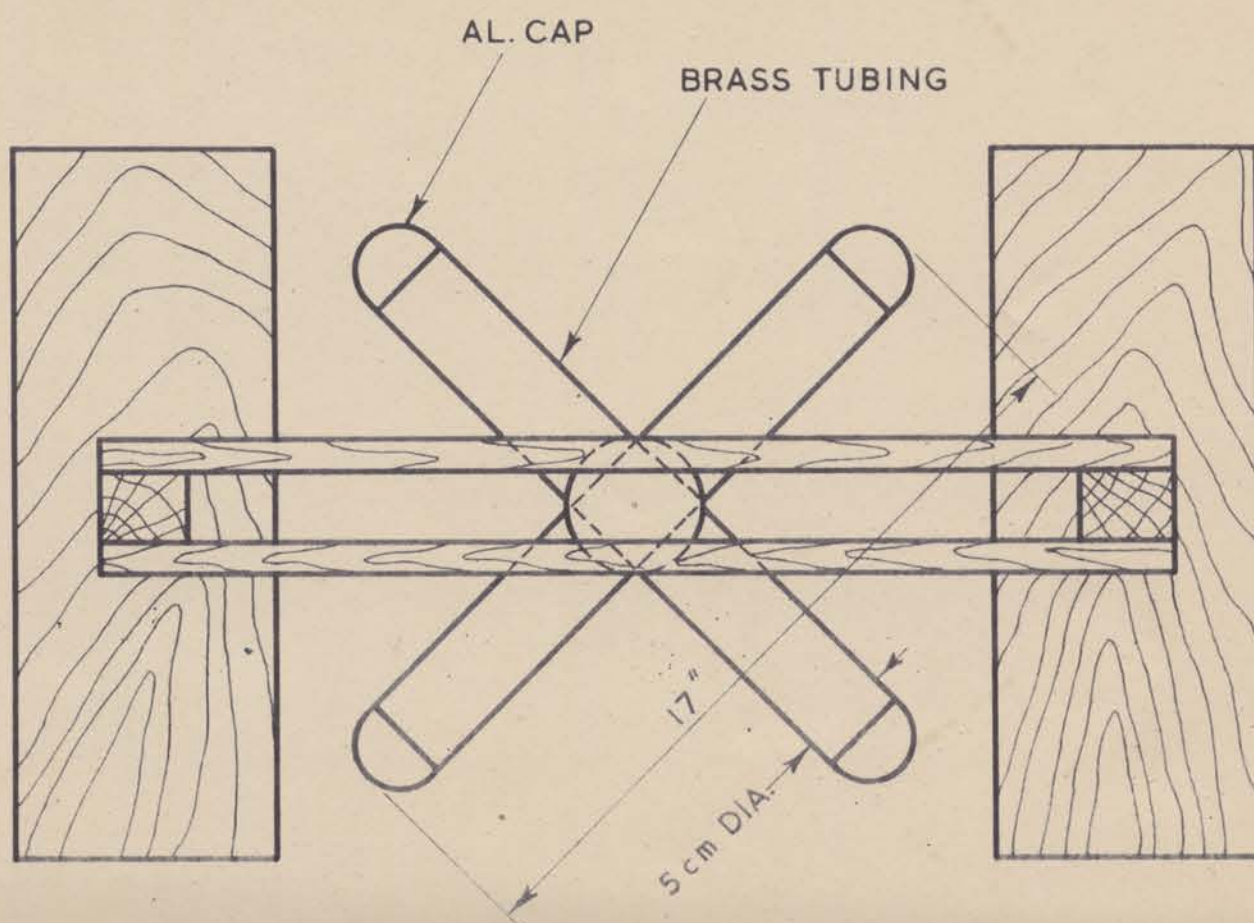


Fig. 33.



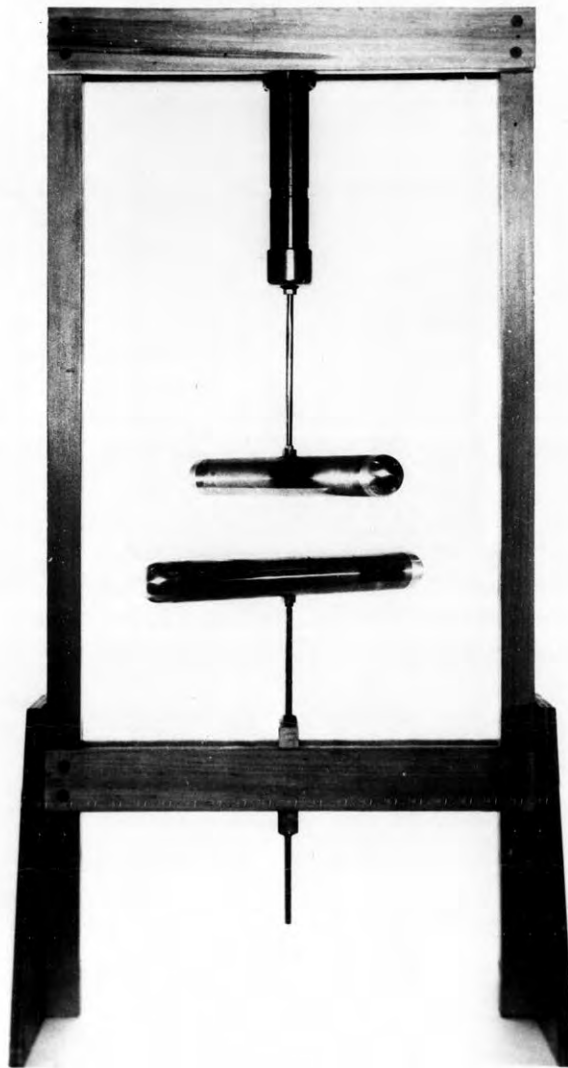


Plate : 6 .

The Gap Type " B " .

FOLLOWING PAGE: 59

mechanical stability and to avoid corona. Due to the shielding effect of the cylinder on one side and the rounded metal cup at the end of the insulating tube on the other side of the shank, corona does not form on the shank in the working range of this gap viz: 30 to 140 KV_p. Preliminary tests regarding this point were made as shown in Fig.

34. Various lengths of $\frac{3}{8}$ inch diameter rod were screwed into a $1\frac{1}{2}$ inch diameter corona free transmission line connected to the 100 KV testing transformer. The rod was terminated by a 10 cm diameter sphere and the line by a 15 cm diameter sphere. For rod lengths of 4 and 8 inches corona onset could not be detected and was assumed to be above 140 KV_p. At 12 inches, onset was at 128 KV_p and at 28 inches at 113 KV_p. The latter figure was checked by computation because it could be assumed that the shielding effect of the ends would be negligible at this length. From published data on transmission lines (45) of $\frac{3}{8}$ inch diameter (0.48 cm radius) the surface gradient g_s for corona onset is 43 KV_p / cm in atmospheric air. From $g_s = V_p / r \cdot 2.3 \cdot \log d/r$, wherein d is the spacing between the wire and its image, V_p can be computed. In our case the distance to earth was not clearly defined because several heavy objects could not be moved but $d/2$ was between 50 and 100 cm. Putting these values in the expression for g_s yields 110 and 124 KV_p respectively. This agrees broadly with the observed value of 113 KV_p and the measurements show clearly the increase in corona onset voltage due to the shielding effect of the ends.

Corona at the semispherical ends, at spacings above 5 cm, (see Section 3.1.4.) has a slight influence only as will become apparent from Table V in the next Section.

Various values of series resistance have been tried with 1.9 and 10 cm diameter spheres and 5 cm diameter crossed cylinders.

In all cases it was found that - provided the precautions regarding leakage and corona as outlined above were observed - the gaps performed consistently and gave a continuous spark discharge at 50 c/s if $V_{rms} / R \geq 1$ mA. For 1.9 cm diameter sphere gaps ($\frac{3}{4}$ inch phosphor bronze ball bearings) to be used in the range 10 to 40 KV_p

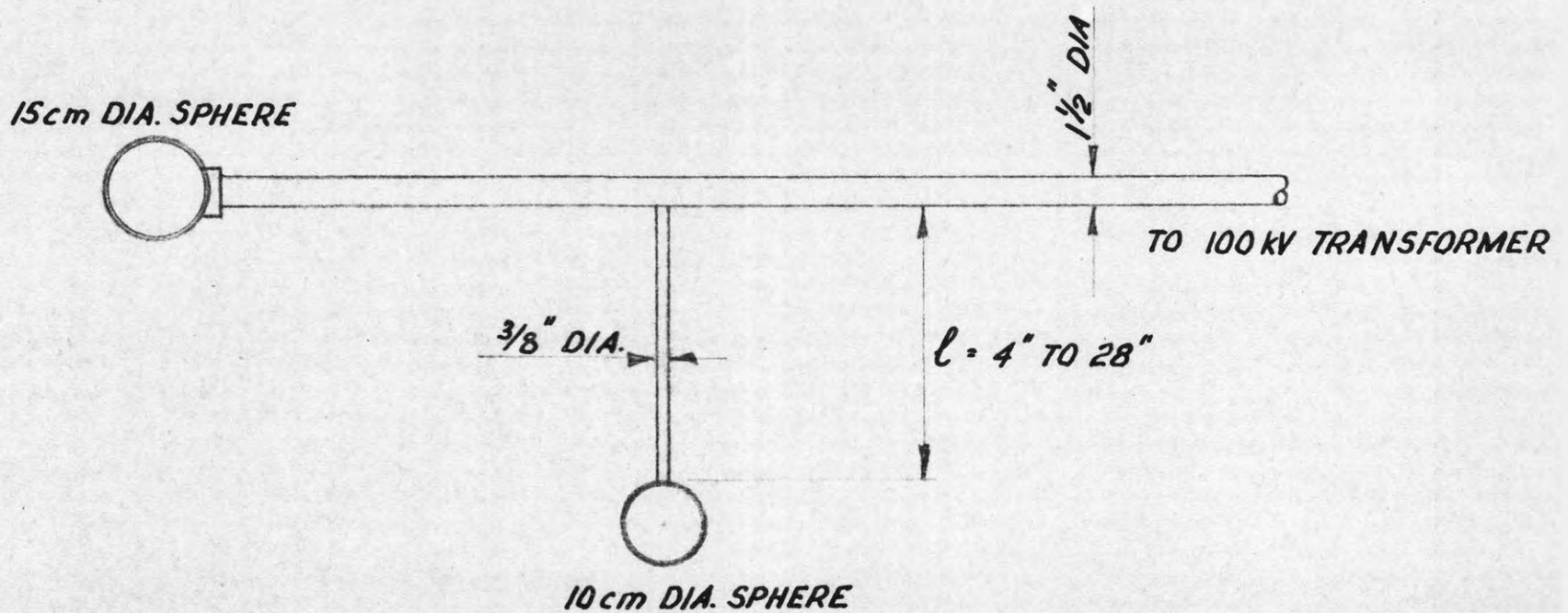


FIG.34. ARRANGEMENT FOR MEASURING CORONA ONSET ON $\frac{3}{8}$ " DIA. ROD AS A FUNCTION OF l

FOLLOWING PAGE: 60

the series resistor should therefore be 5 Megohms. A value of 20 Megohms is suitable for gaps with a range 30 to 140 KV_p.

The observation of erratic behaviour if the short circuit current falls below 1 mA appears to agree, as far as order of magnitude is concerned, with data published by Gaenger (46) who states that a luminous channel can only form if, in the time it takes for spark-over, the initial electron has increased to 10^9 electrons. Assuming now $\frac{1}{4}$ microsecond as time to breakdown and knowing that 1 Amp = 0.6×10^{19} electrons / sec, a current of 0.7 mA can be computed.

4.2 Performance tests.

A calibration of gap type "B" at 50 c/s corrected to 20 degr. C. and 760 mm mercury is shown in Table V. The lower electrode was earthed as intended when using this gap. The calibration was carried out in the manner described previously for gap type "A". Spacing was measured with slip gauges. A thin springy brass strip was used to short the series resistor without altering the electrode spacing. All figures given in one line of Table V were measured before the spacing was changed.

Table V. Mean of 10 readings, KV_p.

Spacing (cm)	20 Megohm resistor shorted	20 Megohm resistor in circuit. sine wave	20 Megohm resistor in circuit. Peakfactor of wave 1.15.
1	31.6	31.9	32.1
2	59.1	59.6	60.0
3	84.4	85.1	85.6
4	108.0	109	110
5	130.0	131	132
5.5	139.3	141	142

4.2.1. Discussion of performance.

Column 2 of Table V agrees with the calibration for gap type "A" as given in Table II. This is gratifying because one gap was horizontal and the other vertical and the electrodes of gap type "A" were chromium plated while those of gap type "B" were natural brass, acid dipped. It appears therefore that the figures of Table II are not restricted to one particular design only.

Except at a spacing of 5.5 cm at which corona at the semi-spherical ends causes a drop in the series resistor, the breakdown values, with the 20 Megohm resistor in circuit are 0.9% higher at 1 cm spacing and 0.7% higher at 5 cm spacing. From $\frac{1}{2} \omega^2 R^2 C^2$ this could be explained by an effective gap capacitance of 22 and 19.7 pF respectively. When the earth capacitance of the series resistor is taken into account these figures agree with capacitance measurements, within the limits of experimental error and rounding off.

Column 4 shows the values obtained on a typical peaky wave (for its generation see Fig. 15) the peakfactor of which was 1.15 and thus much higher than would be tolerated for commercial testing. In practice the error would be insignificant if 1% higher values than those given in Table II for gap type "A" would be used for gap type "B".

The series resistor had a carbon track consisting of 46 turns with a spacing of 1 mm between turns. No sign of sparking could be observed at 140 KV_p. For this test the resistor was placed in a translucent vessel filled with oil and it could be observed from outside the H.V. enclosure by means of a telescope and suitably placed mirrors.

However, as a decision of some responsibility had to be made for N.A.T.A. a sensitive electrical method of spark detection in resistors was devised. This is described in Appendix 7.

The temperature of the oil in the oil-filled tube rose from 17 degr. C. to 44 degr. C. when the gap was left sparking for 1 minute at 140 KV_p. Only very slight discolouration of the brass tubes could be

observed after the test. When $\frac{3}{4}$ inch phosphor bronze balls were used at 40 KV_p with a series resistor of 10 Megohms slightly more discoloration was observed after 1 minute continuous sparking. In both instances moderate application of metal polish restored the original surfaces.

4.3. Application.

Normally, in spark gap work, several discharges are necessary before reliable readings can be taken. In the gap with large series resistor this conditioning can be achieved by letting the gap spark for several seconds.

The following procedure was used to adjust the actual test voltage of a piece of electrical equipment, say a cable, by means of gap type "B". The spacing was adjusted for a sparkover voltage which was 5% less than the required test voltage of the cable. The cable and the gap in parallel were then connected to the testing transformer and its voltage raised till the gap sparked over. After a few seconds of conditioning the voltage was lowered and then raised again till the gap just sparked over. The primary voltmeter of the testing transformer was read and its reading noted. The voltage was then reduced to zero, the gap disconnected and the pressure test, which lasted 15 minutes, carried out using the primary voltmeter only but the voltage was adjusted to a value 5% higher than the one previously noted. This procedure permits conditioning of the gap, which may require slightly higher voltage, without exceeding the specified test voltage of the cable.

Owing to the general reluctance of management to incur expense for test equipment the design of gap type "B" has been kept simple and inexpensive by omitting the precise lead screw and scale provided in gap type "A". In practice this is no great disadvantage because a factory usually requires only a few specified test voltages and gauges for the required spacings are easily made.

Sometimes, when the control room was some distance away from the test bay and particularly at the smaller spacings, it was found

difficult to see or hear the spark discharge. Simple discharge current indicators in which a thyatron operates a signal lamp are described in the next Section.

4.4. Two simple discharge current indicators.

Fig. 35 shows the first circuit. A.C. bias and A.C. plate voltage are employed. A current of either polarity flowing through the gap produces a positive D.C. voltage which fires the thyatron. The lamp in the plate circuit lights when the current through the 5000 Ohm resistor exceeds 0.35 mA, r.m.s. By attaching sharp ended wires to one or the other cylinder a strong polarity effect could artificially be produced and checks carried out if the lamp lights up at the crest of either cycle. However this circuit was found to be unnecessarily complicated for the purpose and the simplified version shown in Fig. 36 is now being used. Superficially, it would seem that the thyatron can only fire if breakdown occurs in the positive half wave. In practice the polarity effect of the gap is small, as shown before, and the first breakdown occurs at random in the positive or negative half wave. Furthermore, with a large series resistor, the extinction voltage was found to be a few percent lower than the striking voltage indicating that even if there were a small polarity effect sparkover would occur shortly also in the other half wave. A third reason is that, due to unavoidable stray capacitance and inductance, the circuit is oscillatory and positive voltage for firing the thyatron reaches its grid even if breakdown occurs in the negative cycle.

This circuit has been extensively tested with the gap shown in Fig. 33 and with a smaller gap using 1.9 cm diameter spheres plus a 5 Megohm series resistor. A large number of readings could be taken in a very short time and a good mean value was arrived at. The voltage control was advanced till the red signal lamp - which may be situated adjacent to the indicating meter - lit up, a meter reading taken, and this was repeated as often as desired.

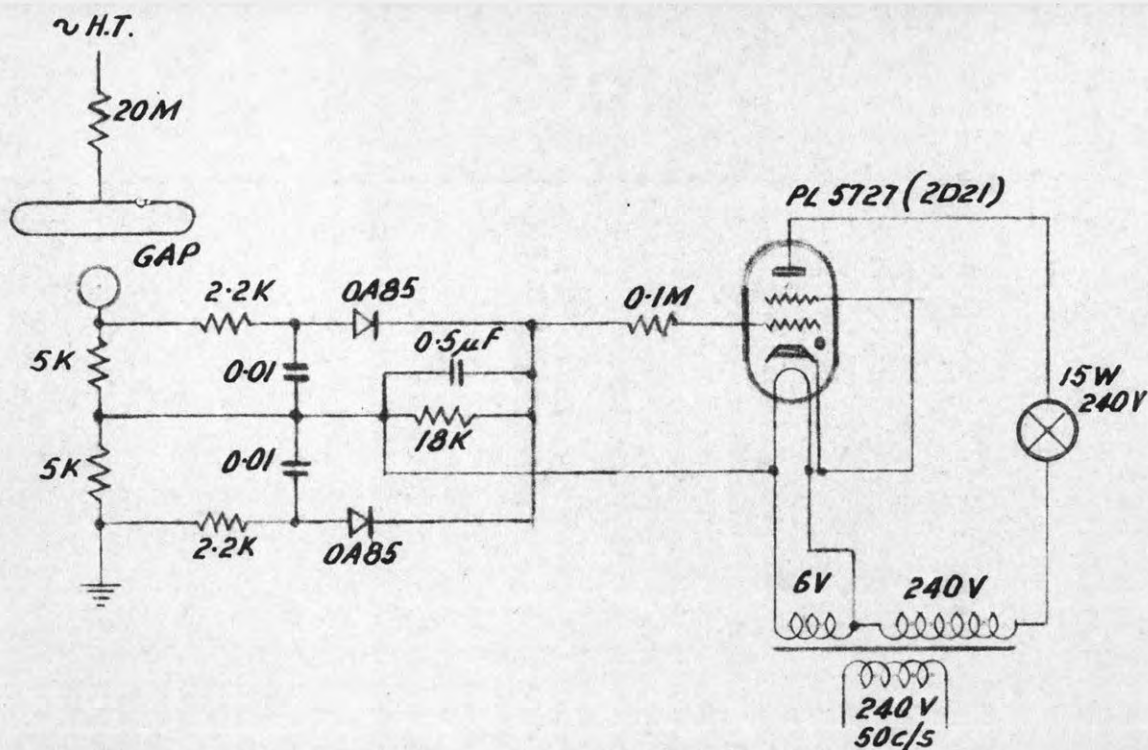


FIG. 35. POLARITY INDEPENDENT DISCHARGE CURRENT INDICATOR

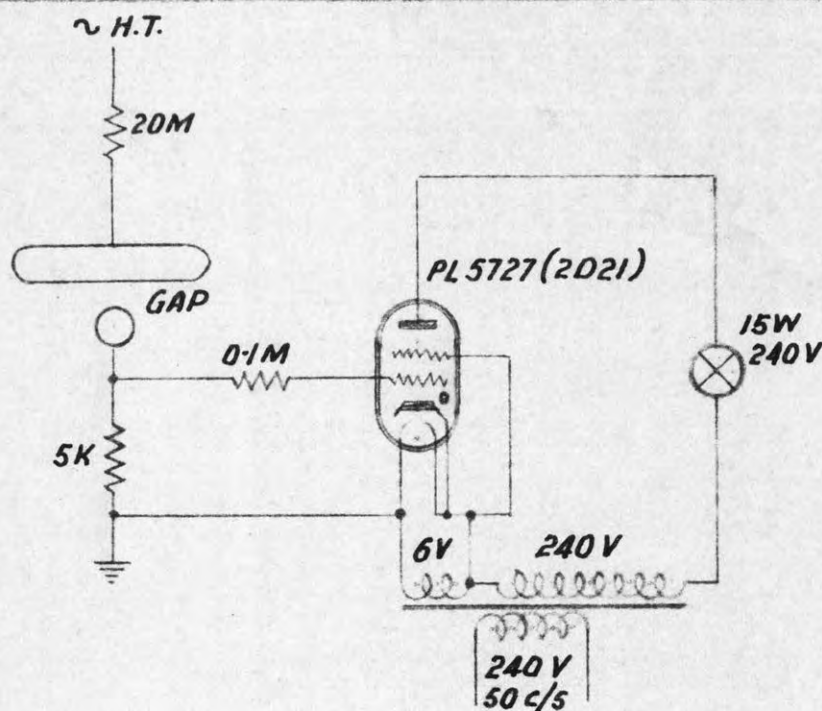


FIG. 36. SIMPLIFIED INDICATOR

4.5. Conclusions re gap type "B".

For the voltage ranges considered viz: 10 to 40 KV_p and 30 to 140 KV_p at 50 c/s a gap with spheres or crossed cylinders may be furnished with a large series resistor provided that :

- a. the short circuit current exceeds 1 mA r.m.s.
- b. the gap is vertical
- c. a guarded arrangement is used which nullifies the effect of insulator leakage
- d. corona on the connection between the high voltage electrode and the series resistor is avoided.

For practical purposes a constant percentage correction to the calibration with small series resistor suffices to allow for the large series resistor and moderately distorted waveforms.

There is no electrode pitting and the gap may be left sparking for one minute.

Together with a simple electronic discharge current indicator such a gap is the nearest approach to a high voltage voltmeter and it is particularly suited for industrial testing. The cost of construction is trivial.

4.6. References re gap type "B".

(44) E.R.A. report L/T 16, 1926 (no author given).

(45) A. Roth.

Hochspannungstechnik

3rd ed. p.178, Springer, Berlin, 1950.

(46) B. Gaenger

The electric breakdown of gases, p. 261.

Springer, Berlin, 1953.

5. The gap type "C".

A diverter gap for the protection of a measuring gap from pitting must not in any way influence the accuracy of the measuring gap and should, if possible, fulfil the following requirements:

- a) For reasons of simplicity auxiliary apparatus like pulse transformers, thyratrons, amplifiers, and high voltage capacitors as used by Watson and Higham for oil testing should be avoided (47).
- b) The diverter gap should be a fixture. Adjustment of spacing as employed by Baker (48) in his oil testing apparatus should not be necessary, at least for a 3 : 1 voltage range of the measuring gap.
- c) In order to "add" the diverter gap to existing gaps no structural change of the measuring gap, e.g. isolating a previously earthed electrode should be required.
- d) The diverter should operate as soon as possible after the sparkover of the measuring gap.

A voltage range of 10 to 30 KV r.m.s. sine wave (14 to 42 KV_p) was selected for experimental ease, compactness of design and because an investigation of a diverter gap working in atmospheric air at these voltages was hoped to be a greater contribution than work at higher voltages which have been favoured by other investigators. However, extension of the voltage range is described in Section 5.3.

The measuring gap used was a small sphere gap with 1.9 cm phosphor bronze balls as shown in Plate 7. It is not intended to give a calibration of this gap, sufficient applicable data having been published by Hardy and Broadbent (49), but to describe the work done on the diverter gap.

5.1. Preliminary Work.

A manufacturer who regularly had to check two test voltages viz: $15 \times \sqrt{2}$ and $27 \times \sqrt{2}$ KV used a 2 cm diameter sphere gap which had been approved by the inspectors of his customers. Because of the low series resistor which was chosen in accordance with the relevant B.S.S. and a rather slow acting circuit breaker pitting was severe and the measuring accuracy very doubtful. As the "officials" did not permit any deviation from the B.S.S. a diverter gap consisting of three $\frac{1}{4}$ inch diameter

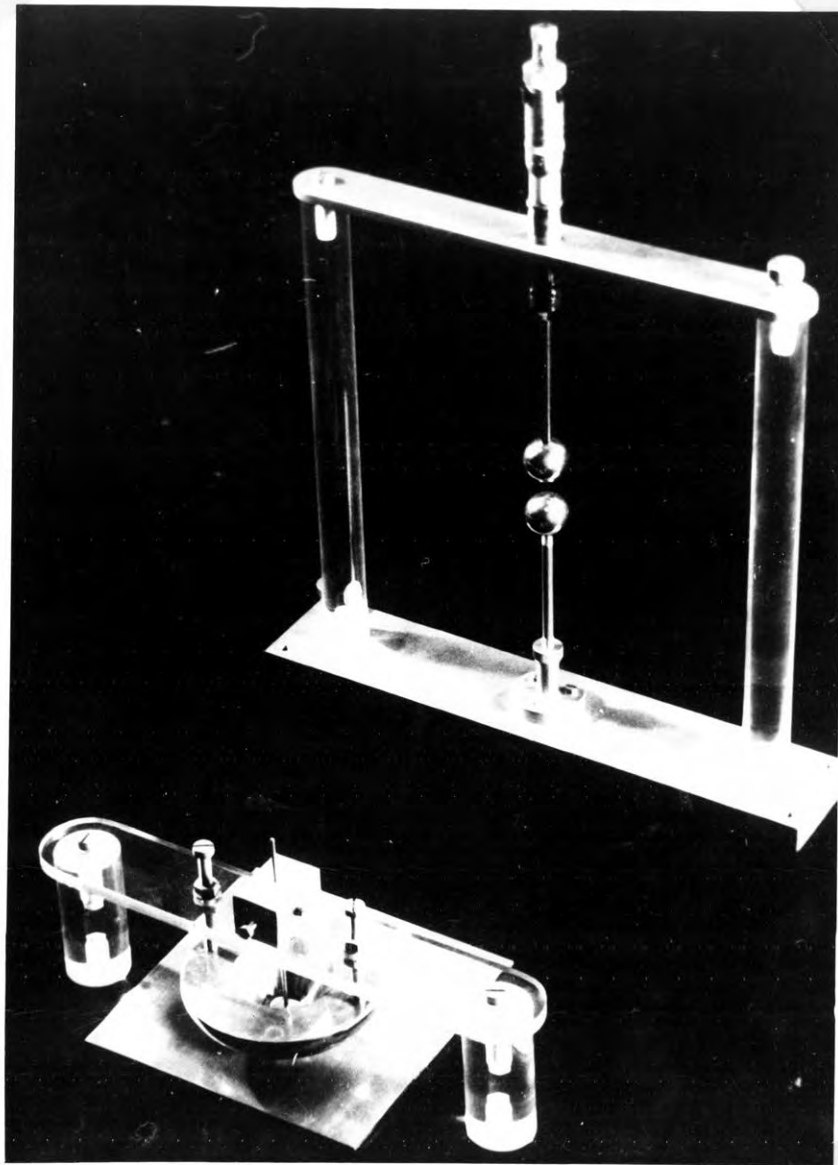


Plate : 7. The Gap Type " C ".
The diverter gap is in the foreground.

FOLLOWING PAGE: 66

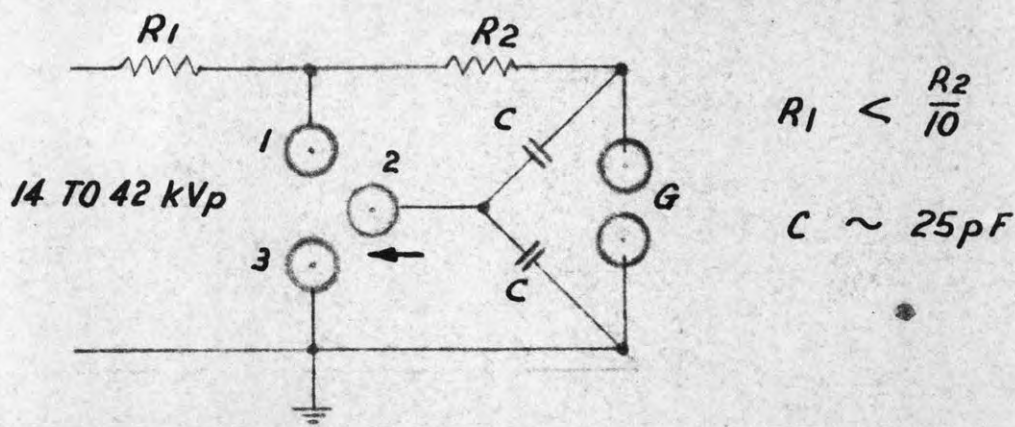


FIG. 37. CIRCUIT OF 3-SPHERE DIVERTER GAP

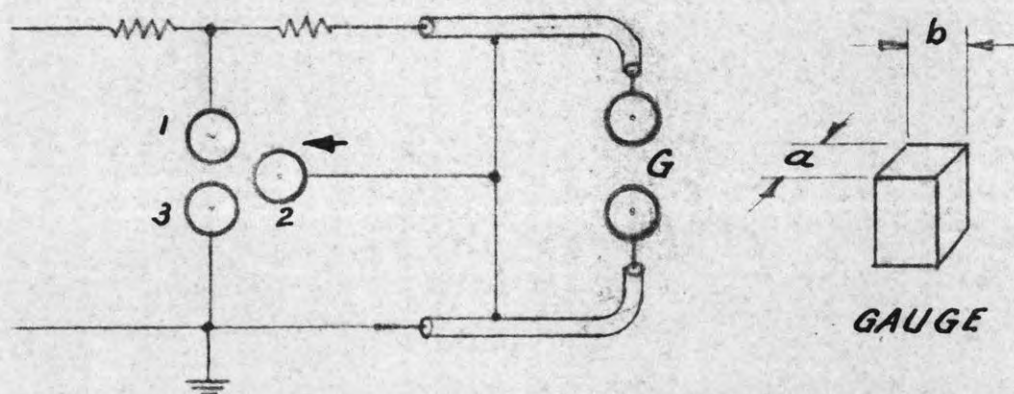


FIG. 38. 3 SPHERE DIVERTER GAP WITH CAPACITORS MADE OF POLYTHENE CABLE

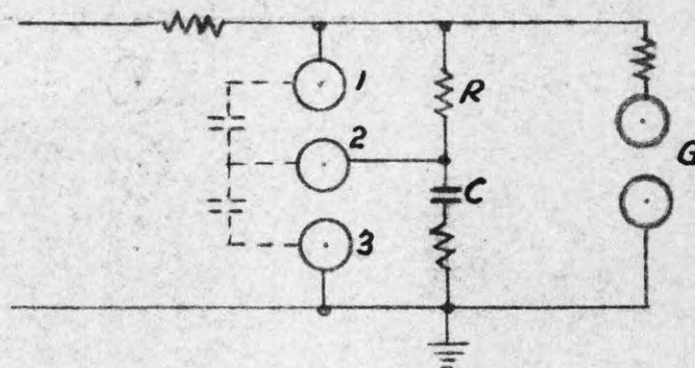


FIG. 39. UNSUITABLE DIVERTER GAP

balls (1, 2 and 3 in Fig. 37) was added to the existing measuring gap G. The centre ball 2 was kept at a potential $V/2$ by means of the two capacitors C. The spacing 1 ... 2 equals the spacing 2 ... 3 and it was $\frac{1}{2}$ of that of the measuring gap G. If, as in the present case, all balls have the same diameter, two series connected gaps each with a spacing S have a larger breakdown value than one gap with a spacing $2 \times S$. This follows from equation 2 in Section 2 and Page 467 of Schwaigers book (1). Therefore, when on sparkover of G the potential of the centre sphere dropped to zero, sparkover occurred from 1 to 2 and then from 2 to 3, thus shorting the measuring gap. Capacitors were used to define the potential of the centre sphere for three reasons. Firstly resistors each of value R would have to be rated $V^2 / 4 R$ because it may happen that the testing officer applies test voltage, insufficient to cause sparkover, for a considerable time. Secondly, these resistors, which for a reasonable wattage rating would be of rather high value, would together with the circuit and sphere capacitances introduce a time delay. Thirdly, capacitors for the required voltage rating could be made cheaply from two 15 inch lengths of concentric polythene insulated cable. See Fig. 38. The adjustment of the gaps was carried out by means of two identical gauges as shown in Fig. 38. The gap spacings for the lower voltage were a and $2 \times a$ and for the higher voltage, b and $2 \times b$.

The performance was quite satisfactory. The diverter gap caused the spark in the measuring gap to become very thin and sometimes hard to see. Pitting was completely eliminated.

While this was successful for one particular application the three ball gap cannot be a fixture requiring no adjustment for a large voltage range.

A diverter gap as shown in Fig. 39, which after a time determined by R and C breaks down between 3 and 2 and then between 2 and 1, is unsuitable. This gap operates independently of G at a voltage which may not have caused sparkover in G.

However, this arrangement was found eminently useful for the production of chopped waves for impulse testing. In that case 2 was a

sphere added to the always existing measuring gap and C was the ground capacitance of 2 and its shank. Details of this scheme in which expensive high voltage capacitors are not required and which provides much better controlled chopping than the commonly used rod gap are described in Appendix 6.

5.2. The Trigatron Diverter Gap.

The requirements set out in Section 5 (a to d) can only be met by a trigatron type diverter gap.

This investigation was hampered by the fact that, when work commenced, the references (50) and (51) were now known. This was due to the use of surface mail and the long interval which elapses between publication of a paper and its record in an abstracting journal.

From the study of the book by Craggs and Meek (52) and the references mentioned there it was learnt that apparently the diameter of the hole of the drilled electrode is unimportant. For example, Craggs, Haine and Meek (53) state that an alteration in the form of the electrodes gives no appreciable improvement. While this may be a general remark and not applicable to the hole diameter no specific mention of the influence of the hole diameter could be found. That there should be no influence was hard to understand from the following consideration.

Assuming an electrode system as shown in Fig. 40 consisting of a sphere B, a drilled plane C and a needle A, the maximum voltage $V_{bc \text{ max}}$ which can be applied before breakdown occurs between B and C must be smaller for larger holes because B "sees" a point instead of a plane. Conversely, V_{bc} would be larger for smaller holes but, whatever the trigatron breakdown mechanism may be due to, field distortion (as per reference 53 but disproved in reference 50) irradiation, or the production of a local region of hot low density gas ejected into the gap, these effects would be expected to be influenced by the hole diameter and affect the minimum voltage $V_{bc \text{ min}}$ required between B and C to cause sparkover when the trigger gap fires.

In order to find out if there is an optimum hole diameter giving the largest ratio $V_{bc \text{ max}} / V_{bc \text{ min}}$ a preliminary test was made using the

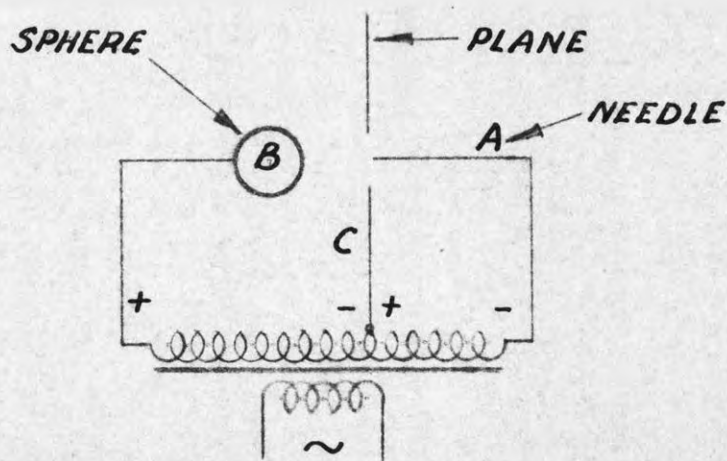


FIG. 40. PERTAINING TO INFLUENCE OF HOLE SIZE ON TRIGATRON OPERATION

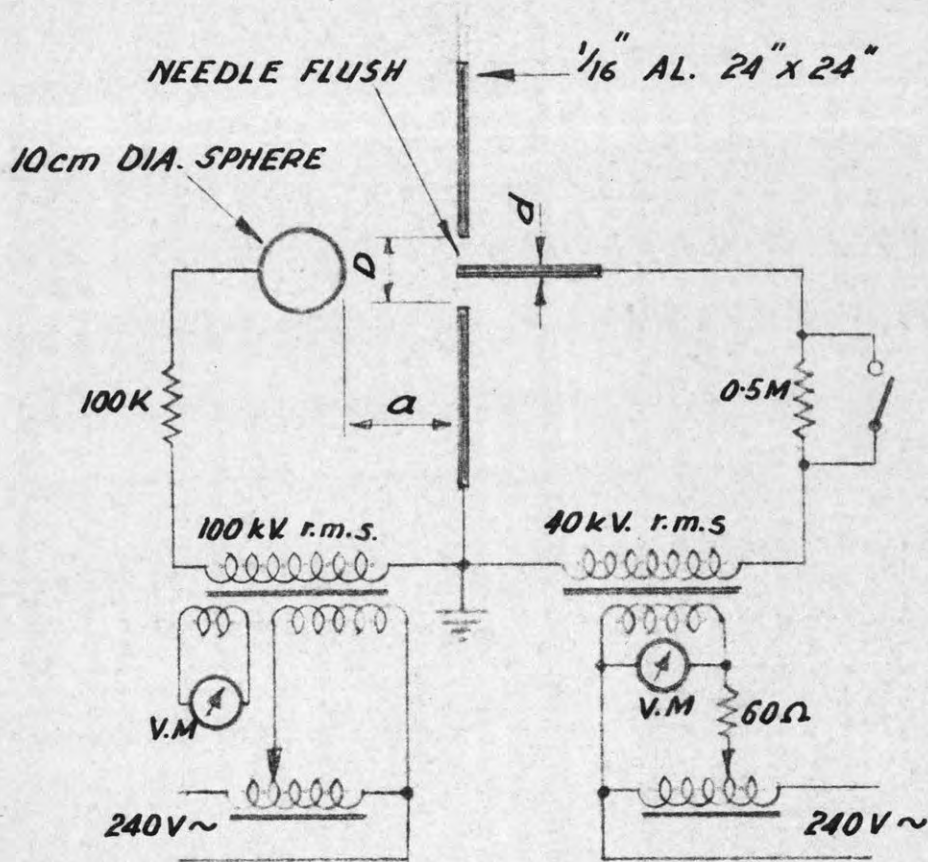


FIG. 41. TRIGATRON TEST CIRCUIT

A.C. 50 c/s FOLLOWING PAGE: 68

circuit of Fig. 41 A.C. voltages series aiding were employed and it was realised that this preliminary test could not show up any polarity effect. The 100 KV transformer was controlled as shown in Fig. 2 Section 3.1.1. The secondary voltage of the 40 KV transformer was nearly 180 degrees out of phase with the voltage of the 100 KV transformer because at the trigger voltages required for this test the voltage drop on the 60 Ohm series resistor was very much smaller than the primary voltage.

In all subsequent data, V_s is the self triggering voltage. This is the voltage which causes breakdown of the main gap (in this case sphere to plane) without a trigger voltage. V_L is the minimum voltage at which breakdown of the main gap occurs when a voltage is applied to the needle which causes breakdown between it and the drilled electrode. In order to find V_L the voltage between the sphere and the plane was decreased from the V_s value in small steps and at each step triggering was tried by winding up the variac controlling the 40 KV transformer. The results for various spacings (1 to 7.5 cm), three hole diameters viz: $\frac{1}{4}$, $\frac{1}{2}$ and 1 inch, and two needle diameters, viz: $\frac{1}{16}$ and $\frac{1}{4}$ inch are given in Table VI.

TABLE VI

<u>d</u> DIA. INCH	<u>D</u> DIA. INCH	SPACING (cm)														
		1			2			3			5			7.5		
		V _S	V _L	V _S /V _L	V _S	V _L	V _S /V _L	V _S	V _L	V _S /V _L	V _S	V _L	V _S /V _L	V _S	V _L	V _S /V _L
1/16 SQUARE TIP	1/4	21	6	3.5	36	14	2.6	51	20	2.5	70	35	2.0	84	50	1.7
	1/2	14	6	2.3	28	7	4.0	46	12	3.8	70	24	2.9	84	45	1.9
	1	11	6	1.8	23	7	3.3	35	10	3.5	58	28	2.1	78	45	1.7
1/4 ROUNDED TIP	1	16	6	2.7	36	6.5	5.5	50	10	5.0	70	22	3.2	84	30	2.8

MEAN OF 5 TESTS; V_S AND V_L IN kV_{r.m.s} SINE WAVE
REFER TO FIG. 41

The figures show that the effect of "seeing" the needle becomes smaller at the larger spacings. For a 1/16 inch diameter needle V_S / V_L is a maximum for a 1/2 inch diameter hole except, owing to the effect mentioned above, at a spacing of 1 cm. An optimum hole diameter appears therefore to exist. The ratio V_S / V_L became smaller when the polarity of the 40 KV transformer was reversed. It was also noticed that V_L depended on the energy in the trigger spark, which could be altered by putting a resistor in series with the needle or by adjusting the trigger voltage to a higher voltage than that which was required to produce the trigger spark. The test with the 1 inch hole and rounded tip, while interesting, is of no value for a 10 to 30 KV r.m.s. diverter gap because the trigger voltage required exceeded 10 KV r.m.s.

Owing to the uncertainty due to the influence of the trigger spark energy it was decided to construct a prototype diverter gap with provision to alter the hole diameter and test it fully on D.C. so that the polarity effect could also be studied.

5.2.1. Circuit Description.

The diverter gap was constructed as shown in Fig. 42 and Plate 7. The circuit is shown in Fig. 43. When the measuring gap breaks down a trigger spark occurs between the cup shaped electrode 1 and the needle 2. This spark initiates the breakdown in the main gap between 1 and an earthed plate 3 on which the gap rests. R_1 is the series resistor of the measuring gap. R_2 serves to maintain the voltage between 1 and 3 after breakdown of the measuring gap. Without R_2 a path would exist from H. T. via 1 to 2 and the measuring gap to earth. The voltage drop on the source impedance would reduce the voltage between 1 and 3 and prevent breakdown of the main trigatron gap. See also Section 5.2.5. If not otherwise stated R_1 equals R_2 and each resistor consisted of 5 cracked carbon resistors, 0.1 Megohm, 2 W, submerged in oil. The circuit fulfils the condition set out in Section 5 c viz: The diverter gap may be attached to an existing gap one electrode of which is grounded.

5.2.2. The Shape of the Main Electrodes.

It seems certain that hot gas of low density ejected into the space between the main electrodes (51) forms a major part of the breakdown

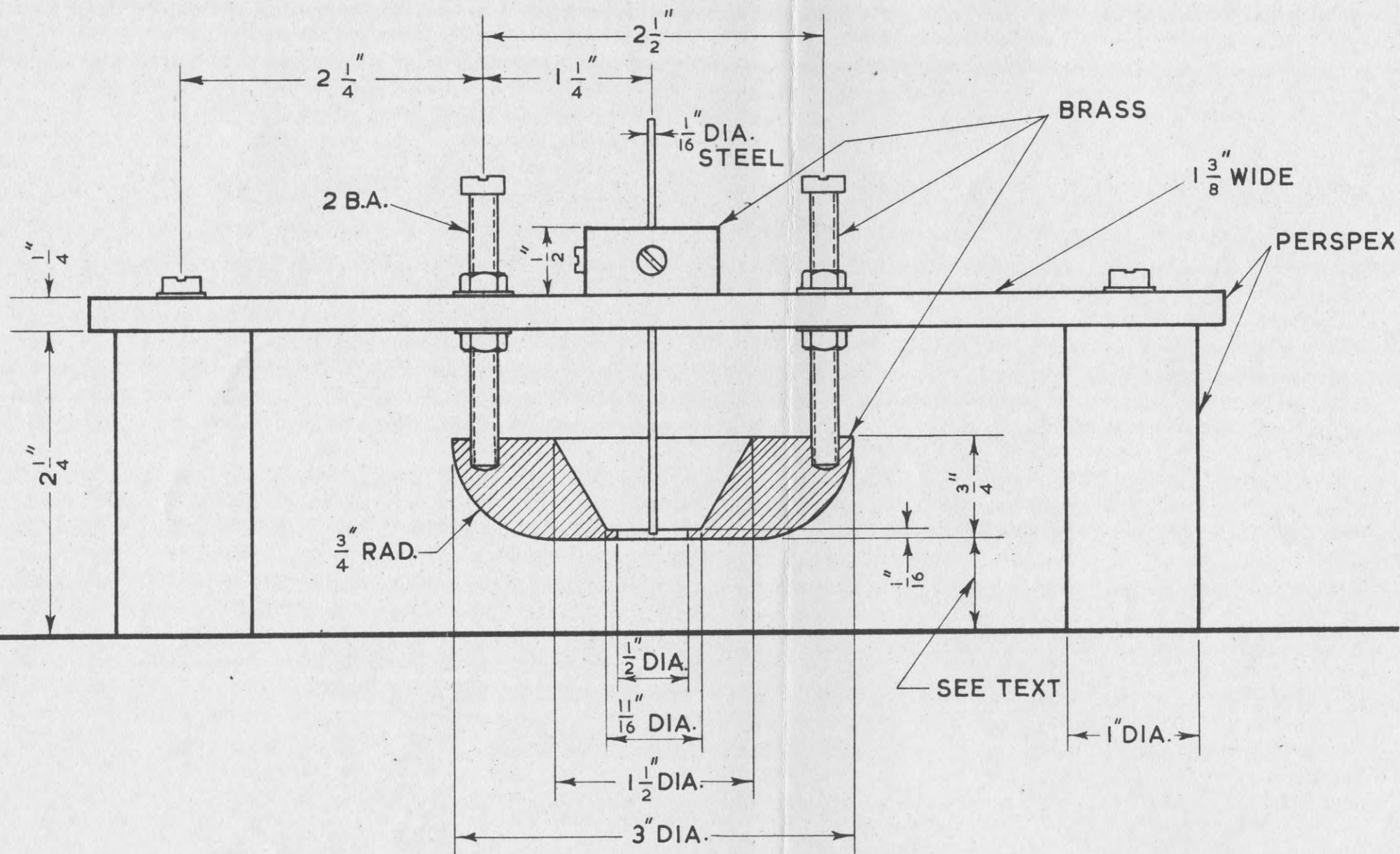
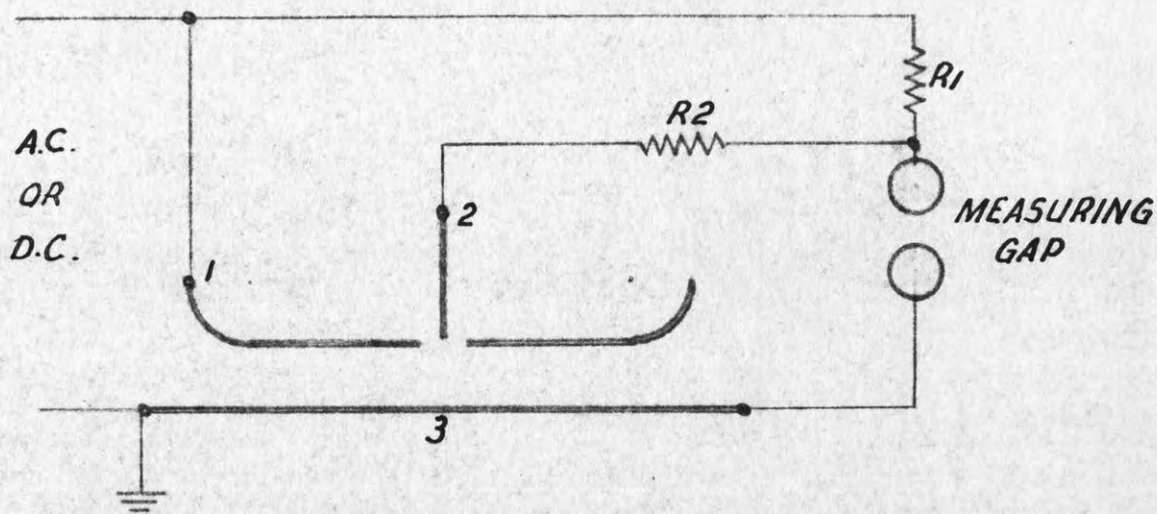


Fig. 42.



**FIG. 43. CIRCUIT OF GAP TYPE "C"
SHOWING THE CONNECTIONS OF THE
DIVERTER GAP TO THE MEASURING
GAP**

mechanism. This seems also to be confirmed by Broadbent (50) who found similarity in the breakdown mechanism between a thermally triggered gap (54) and the trigatron. Now, if hot gas travels into the main gap space, it is reasonable to assume that the largest ratio V_s / V_L will be obtained with electrodes which give the highest value of V_s at the smallest spacing - everything else being equal.

Comparing the "near uniform field" electrode system shown in Fig. 42 with a 5 cm diameter sphere and assuming that each electrode is spaced 1.6 cm from an infinite plane yields :

- a) From Bruce (30) the breakdown voltage in a uniform field gap,
 $V_b = 24.22 \times a + 6.08 \times a^{\frac{1}{2}}$ which in our case is 46.5 KV_p.
- b) From spheres with a ratio of spacing / radius of $2 \times 1.6 / 2.5$
 $= 1.28$, we find from Schwaiger (1) page 466 the puncture strength of air, 38.7 KV_p / cm. (For image concept see before, Section 3.1.2.3.). Now, $1 + a/r = 1 + 1.6/2.5 = 1.64$, and from page 469 $\gamma = 0.68$. V_b is therefore $1.6 \times 0.68 \times 38.7 = 42.2$ KV_p.

The chosen electrode form gives a higher breakdown voltage and besides that it is also easier to make than a sphere. The spacing of 1.6 cm has been selected after tests described in the next Section. It will be shown that the calculated value of 46.5 KV has nearly been obtained in practice although the electrode has a hole in the centre. At this spacing it was not found necessary to use the "Bruce" or "Rogowski" contour because breakdown always occurred at the edge of the hole.

It should be recorded that Hardy and Broadbent (55) have unsuccessfully tried the uniform field electrode system. It is believed that full use of this configuration in a trigatron can only be made by recessing the needle as shown in the next Section.

5.2.3. The hole diameter and the needle position.

The test circuit is shown in Fig. 44. A brass insert, also shown in Fig. 44, could be dropped into the cup shaped electrode in order to investigate the performance with a $\frac{1}{4}$ inch diameter hole. The needle was 1/16 inch in diameter, of stainless steel with a square end. The test circuit includes a 0.5 Megohm resistor in series with the needle as is

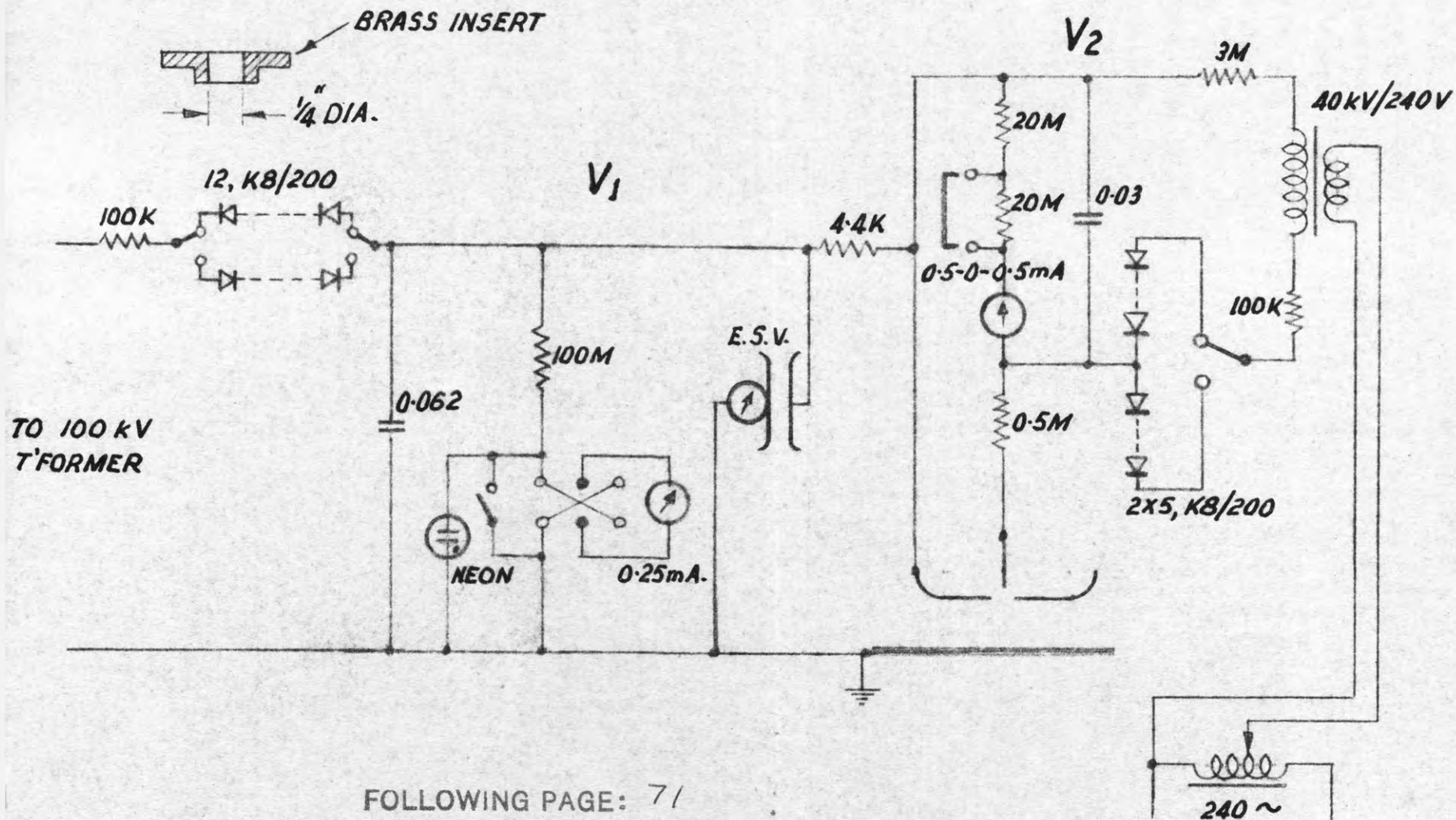


FIG. 44 D.C. TEST CIRCUIT OF DIVERTER GAP

the case in actual use of the diverter gap. V_1 , the voltage applied between the cup-shaped electrode and earth, could be measured with the attracted disc electrostatic voltmeter mentioned before, and, at voltages below its useful range by means of the 0.25 mA moving coil meter. V_1 was increased in 1 KV steps and at each step the trigger voltage V_2 was increased till breakdown occurred between the needle and the cup. The value of V_1 which caused sparkover of the main gap was noted. The mean of 5 readings is given in Table VII for the various conditions of test listed there. By connecting the needle to the cup, with V_2 at zero, the V_s values could be measured. Breakdown of the gaps could be observed visually and on the meters.

The tests 6, 12 and 18 show that in all cases V_L is highest when the cup is positive relative to earth and the needle negative relative to the cup. This is unfortunately the case in practice (compare Fig. 43) if the measuring gap sparks over in the positive half cycle of an A.C. wave.

By comparing tests 9 and 10 with tests 3, 4, 15 and 16 it can be observed that V_s is highest with the needle recessed. Recessing does not increase V_L as much as V_s thus giving a better ratio of V_s / V_L .

The $\frac{1}{2}$ inch hole is quite unsuitable giving a much higher value of V_L . The irregularity in the polarity effect as evidenced in test 15 and 16 for the practically useless case of a protruding needle and $\frac{1}{2}$ inch hole may be either due to an experimental error (e.g. error in adjustment of protrusion) or caused by the difference in sharpness of the needle tip and hole edge.

It is remarkable that very large ratios of V_s / V_L could be obtained, e.g. in test 11, when the needle had the same polarity relative to the cup as the cup relative to earth. In practice this could only be obtained by a device giving phase reversal. Although not directly applicable to the present case the electrode configuration and needle position used here should give a great improvement in those diverter gaps where electronic means for phase reversal are no objection.

Table VIII gives the final result of the gap type "C" at the finally chosen spacing of 1.6 cm. V_s / V_L exceeds 3. Thus a 3 : 1 voltage range has been achieved without change in spacing.

TABLE VII. BREAKDOWN VOLTAGE CUP TO EARTH.
kV D.C. (V_i IN FIG. 44)

* RELATIVE TO EARTH;

RELATIVE TO CUP.

TEST	CONNECTION		HOLE 1/2" DIA.			HOLE 1/4" DIA.		
			SPACING cm					
			1	1.5	2	1	1.5	2
1	NEEDLE REMOVED; CUP - *		31	43	53	31	43	54
2	" " CUP +		31	43	54	31	43	54
3	NEEDLE FLUSH	NEEDLE CONNECTED TO - CUP	21	35	43	30	42	53
4		" " " + "	23	36	44	30	43	54
5		CUP + * NEEDLE + *	3	6	10.5	5.5	12	21
6		" + " -	7	11.5	17	12.5	18	23.5
7		" - " +	3	6	10	8.5	13	19.5
8		" - " -	< 3	3	7	5	8.5	14.5
9	NEEDLE RECESSED 1mm	NEEDLE CONNECTED TO - CUP	30	40	52	31	42	53
10		" " " + "	31	41	53	31	42	54
11		CUP + NEEDLE +	3.5	6.5	11.5	8	13.5	23
12		" + " -	8	12.5	18	16	20	26
13		" - " +	4	6.5	10.5	12	15	22.5
14		" - " -	< 3	3	8.5	6.5	9	15.5
15	NEEDLE PROTRUDING 1mm	NEEDLE CONNECTED TO - CUP	18.5	28	40.5	25	29	47.5
16		" " " + "	19	27	39	26	31	48.5
17		CUP + NEEDLE +	3.5	6	10.5	7.5	10	20
18		" + " -	8	11.5	15.5	20	25	42
19		" - " +	4	5.5	9.5	8	11	18
20		" - " -	< 3	3	6.5	4.5	8.5	15

TABLE VIII

BREAKDOWN VOLTAGE CUP TO EARTH

SPACING. 1.6 cm.

NEEDLE. STEEL. $\frac{1}{16}$ " DIA. 1mm RECESSED

HOLE. $\frac{1}{2}$ " DIA.

CONNECTION	kV. D.C.
NEEDLE CONNECTED TO - CUP	43 = V_s
" " " + CUP	44
CUP + NEEDLE +	7.5
" + " -	13.5 = V_L
" - " +	7
" - " -	3

$$V_s / V_L > 3$$

FOLLOWING PAGE: 72

The required trigger voltage V_2 could also be measured in the setup shown in Fig. 44. V_1 was at zero and the spacing of the main gap was found to have negligible influence on the needle to cup breakdown voltage. Table IX shows the results. Assuming the worst polarity condition, 10.5 KV trigger voltage is required for our case. This is sufficiently below 14 KV the lower limit of the range.

TABLE IX
TRIGGER VOLTAGES (V_2 IN FIG. 44)
 (BREAKDOWN NEEDLE TO CUP. KV.D.C.)

HOLE DIA.	NEEDLE POSITION	NEEDLE + REL. TO CUP	NEEDLE - REL. TO CUP
$\frac{1}{2}$ "	FLUSH	10.7	8.1
	1mm RECESSED	10.5	7.9
	1mm PROTRUD.	11.3	8.7
$\frac{1}{4}$ "	FLUSH	4.7	3.8
	1mm RECESSED	4.6	3.8
	1mm PROTRUD.	5.2	4.7

5.2.4. The time lag.

Time lag was measured as shown in Fig. 45 with the C.R.O. mentioned in Section 3.3.1. using its sweep calibration. There was considerable scatter of results at the lower voltage limit particularly when the cup was positive. The values given in Table X below were reasonably repeatable and they are representative for both polarities.

TABLE X.

KV _p + or -	Lag Microseconds
14	1700
18	1000
25	500
31	200
36	30

The large time lag was not believed at first. A different C.R.O. and a check of the sweep speed calibration failed to show a gross error. Increasing the time lag by artificially doubling the needle to ground capacitance resulted in an increase of a few microseconds only as would be expected. A further test, without any C.R.O. was then made at 25 KV. A resistor of 50,000 ohms was put between earth and the measuring gap. Otherwise the circuit was as shown in Fig. 43. In parallel with this resistor was a tiny spark gap ($\frac{3}{8}$ inch balls) with its 100,000 Ohm series resistor. The spacing of this gap was adjusted to just give sparkover when the measuring gap broke down. The spacing was measured with a feeler gauge and then reduced to $\frac{1}{2}$ of its former value. The small gap was then shunted by a capacitor, the value of which was altered by trial and error until, at 25 KV, the small gap again just sparked over. Now, assuming that the current pulse through the measuring gap was of rectangular shape* its duration could be computed from: $t_{\text{charge}} = 2.3 R C \log V_{\text{max}} / V_{\text{max}} - V$ wherein the voltage values were known from

* Footnote: This is approx. justified because the discharge time constant of the supply is large viz: 0.062 microfarad x two paralleled 0.5 Megohm resistors, approx. 15000 microseconds.

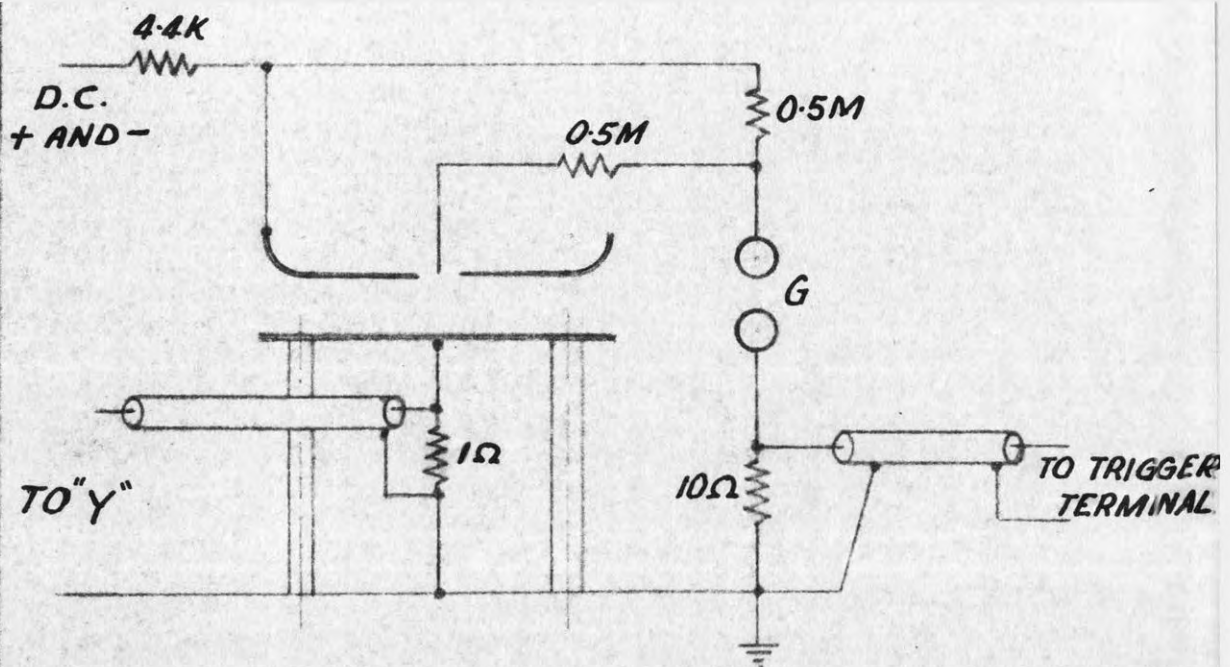


FIG. 45. ARRANGEMENT FOR MEASURING OF TIME LAG

the measured spacings of the small gap. The result obtained was within 100 microseconds of the value given in Table X indicating that there was no gross error in the measurement. Finally, Fig. 8 of reference 51 came to hand showing the enormous difference in time lag when a 1000 Ohm resistor was inserted between the needle and the source of trigger voltage.

It seems that the time lag of the described diverter gap is mainly due to the trigatron mechanism itself and brought about by a trigger spark, not powerful enough to eject the hot gas at high velocity, and limited in its number of charge carriers. It was possible to reduce the lag to less than 800 microseconds at 14 KV when the distance was reduced. In this design this can be done simply by placing a metal plate, $\frac{1}{4}$ inch thick on the earth plate on which the gap rests.

5.2.5. Choice of values for R_1 and R_2 . (Fig. 43).

By artificially increasing the internal impedance of the supply with external series resistors, R_1 and R_2 were found to depend on the source impedance. For the D.C. supply, source impedance is defined as that fictitious impedance in series with a zero impedance source which would give the same voltage drop as caused by the discharge of the 0.062 microfarad capacitor via the measuring gap path in parallel with the trigger gap path.

Generally these resistors must be large enough to cause only a small voltage drop on the source impedance because otherwise the voltage Cup to ground is reduced and V_L is increased. With R_2 at 0.5 Megohm, R_1 could be increased to 10 Megohms without significantly changing the diverter gap performance. This is as expected, because, once the measuring gap has broken down the trigger spark current depends mainly on R_2 . However, with such a large value of R_1 the gap reverts to type "B" making the diverter superfluous. With R_1 at 0.5 Megohm, changing of R_2 to 50,000 Ohms increased V_L to 18 KV and the time lag at 25 KV was nearly doubled. When R_2 was increased to 5 Megohms the diverter did not work at 14 KV and the resistor had to be decreased to 2 Megohms to ensure operation, but with increased time lag. This is also as expected because a larger resistance value thins the trigger spark.

$R_1 = R_2 = 0.5$ Megohms appears to be a good compromise which ensures a small drop on the source impedance as well as sufficient trigger energy. The tests were also repeated at 50 c/s where the values were found to be even less critical, probably because of the lower source impedance.

Attempts to replace R_2 with a capacitor were not successful. A capacitor large enough to give the required ratio of V_S / V_L caused the spark in the measuring gap to become much thicker thus offsetting the advantage of the diverter.

5.2.6. Discussion of performance.

In cases where a powerful trigger spark is not available, as in the diverter described here, the hole diameter, the needle position and the electrode shape are important. Without an effort to obtain the longest possible trigger spark the diverter with a 3 : 1 voltage ratio could not have been realised. This is not in contradiction to the findings of other workers who firstly did not aim at such a large range and who used trigger sparks in which a large amount of energy was dissipated.

Nevertheless, the price paid for the simplicity of the present design is its larger time lag. While this is disappointing the diverter fulfills the task of protecting a spark gap. In the upper part of its range the time lag is small and the spark in the measuring gap becomes so fine that it can only be observed against a dark background. It is fortunate that the lag is small at those voltages where damage due to pitting would be most severe.

Several 100 discharges at 15, 25 and 35 KV_p have caused only a slight discolouration which could easily be cleaned off.

5.3. Extension of voltage range.

From reference (55), Table VI of this thesis and from test 12 of Table VII (2 cm spacing) a smaller ratio V_S / V_L may be expected for a, say, 20 to 60 KV, r.m.s. range of the diverter. Tests made on an experimental electrode system shown in Fig. 46 confirmed this. The circuit was the same as that shown in Fig. 43 but the measuring gap was the gap type "A" described in Section 3. Two water resistors, 0.5

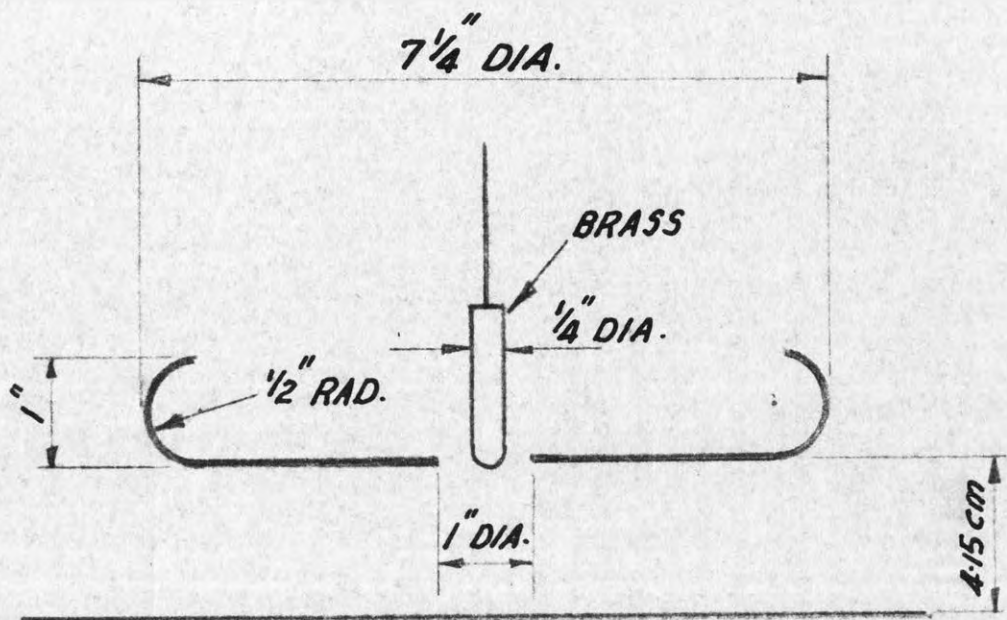


FIG. 46. MAIN DIMENSIONS OF DIVERTER GAP FOR 85KV_p MAX.

Megohm each, were used. The Electrode was made by spinning back the edges of an aluminium soup plate of $1/32$ inch thickness.

When tested on D.C., V_s was 86 KV and V_L about 43 KV at the worst polarity combination. The ratio V_s / V_L was thus reduced from 3 to 2 for twice the upper voltage limit of the previous diverter. On A.C. 50 c/s V_L could be reduced to 29 KV_p by reducing the source impedance of the 100 KV transformer set up, viz: shorting the fine control and the current transformer feeding the overload relay. V_s / V_L was nearly three in this case viz : 86/29.

At V_s flashover occurred at the edges of the one inch diameter hole, but there was little margin, because, when the spacing was increased from 4.15 to 4.30 cm flashover occurred at the rounded edges of the electrode. It is probable that slightly better results could have been achieved by using a thicker (but hard to make) electrode, rounded edges of the one inch hole, smaller spacing and Bruce or Rogowski edges.

5.3.1. The Use of two diverter gaps.

Realising that the diverter shown in Fig. 42, which can be so easily turned on a lathe, has very favourable dimensions, it was thought that it may be possible to increase its upper voltage limit by circuitry, leaving its dimensions constant.

For a small voltage range the circuit of Fig. 47 in which a two ball gap is placed in series with the diverter gap was found to work well. This arrangement is similar to the one proposed by Sletten and Lewis (51). The potential of the plane "E" was fixed only by the stray capacitances but no trouble was experienced on A.C. 50 c/s. It is however obviously impossible to obtain a large ratio of V_s / V_L without changing the spacing of the two ball gap.

The circuit of Fig. 48 in which the diverter was placed across $\frac{1}{2}$ of a centre tapped transformer gave no trouble regarding a 3 : 1 voltage range but the thinning out of the spark in G left much to be desired. It was suspected that this trouble may be connected with the rather terrible surge voltage distribution of this transformer (see Fig. 4 of reference 26) but it was not investigated further partly because at the

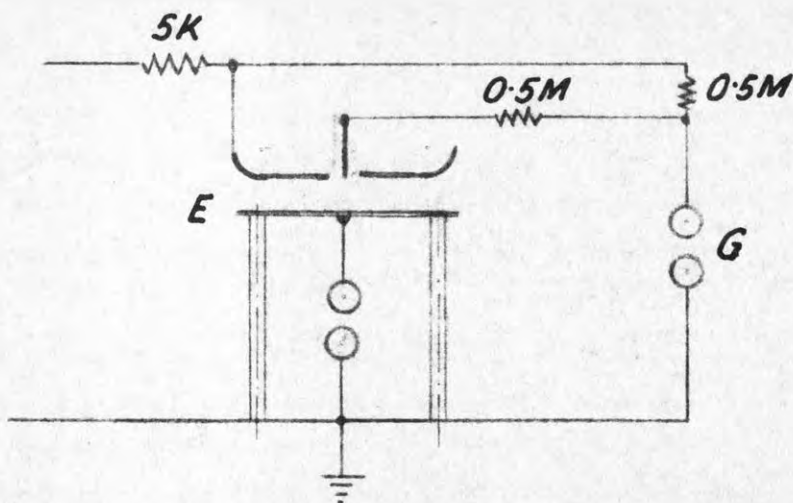


FIG.47. SERIES CONNECTION OF THE DIVERTER AND A TWO ELECTRODE GAP

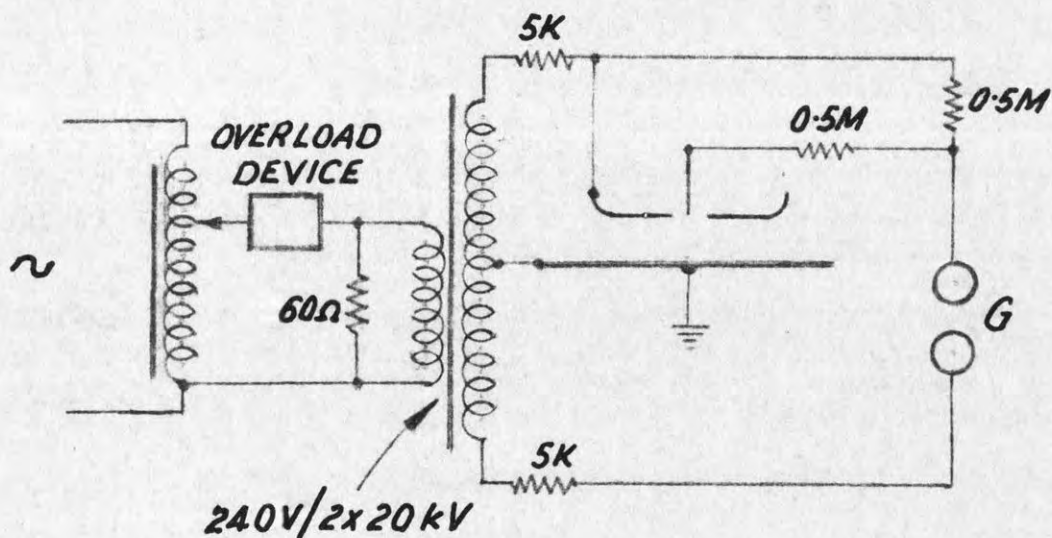


FIG.48. EXTENSION OF UPPER VOLTAGE LIMIT BY PLACING THE DIVERTER ACROSS HALF OF A CENTRE TAPPED TRANSFORMER

time when this test was set up the high speed C.R.O. was not available and partly because the circuit of Fig. 49 was thought of, the performance of which would be independent of the supply transformer.

It should be stressed that the tests were made in the range 20 to 40 KV r.m.s. instead of 20 to 60, because the available transformer was rated 2 x 20 KV. This was regarded as no limitation because trouble was never experienced near V_g but always at the lower limit of the range near V_L .

Two diverter gaps of identical construction (Fig. 42) were placed on an earthed plate as shown in Fig. 49. As each diverter is across $\frac{1}{2}$ of a centre tapped transformer the range of the circuit is twice that of a single diverter. In each half cycle one or the other of the two gaps works under more favourable polarity conditions (see Table VII) and this is believed to be the reason for the good results obtained.

The disadvantage of having to use two gaps instead of one is small owing to the simple construction and the use of inexpensive resistors. For a specific purpose, e.g. dielectric strength testing as described in the next Section, a centre tapped transformer is usually not more expensive because two bushings for $\frac{1}{2}$ the voltage are less costly than one bushing for the full voltage and because core type construction with windings on two legs lends itself to a design requiring only small insulation clearances. It must be admitted however that for the purpose of spark gap protection the circuit of Fig. 49 does not fulfill the requirements set out in Section 5 c.

5.3.2. Other applications of gap type "C".

Both the single diverter and the two as per Fig. 49 have been used to prevent carbonisation of transformer oil when testing it in the standard B.S.S. test cell (56). Up to 12 tests could be made on one sample of oil before a trace of carbonisation became visible. Without the diverter fresh oil has to be used after every breakdown. A much better mean value could thus be obtained. For good oil breakdown at the standard spacing of 4 mm between $\frac{1}{2}$ inch diameter spheres occurs at voltages above 40 KV r.m.s. When the 40 KV transformer was used the spacing was therefore reduced to 2.5 mm and the mean breakdown value

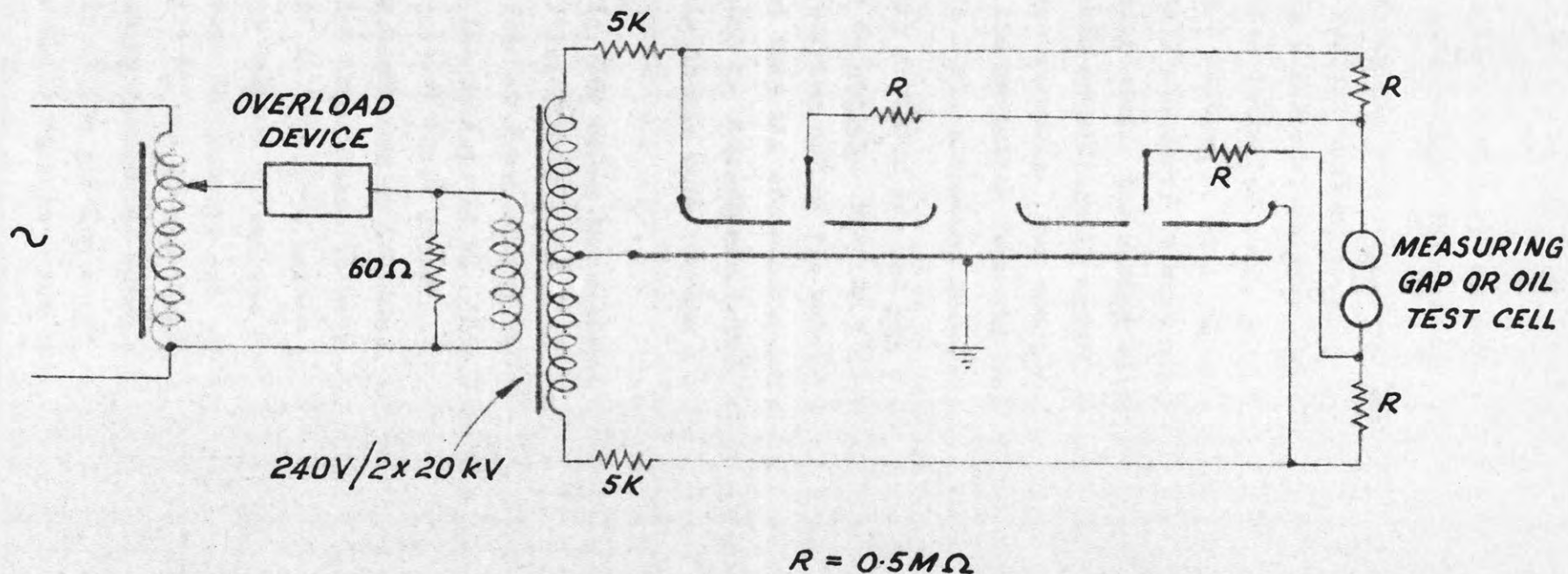


FIG. 49. SERIES CONNECTION OF 2 DIVERTER GAPS

FOLLOWING PAGE: 78

multiplied with 1.485 to obtain the value which would have been obtained at 4 mm spacing. This factor is taken from Reference (57).

While the time lag of the diverter is greater than that of diverters used for oil testing by other workers who employ electronic means to obtain a powerful trigger spark or an adjustment of spacing, the circuits described meet, as far as could be observed, the needs of routine testing of oil. It should be stressed that with any system it is still necessary to wait about 30 seconds till bubbles have left the sparking area. The saving of testing time is therefore not as great as would superficially appear but the convenience and increased accuracy are considerable. For example, in a typical test on medium quality oil, the deviation from the mean did not exceed 5% when 12 determinations of the 1 min withstand value were made.

The diverter gap has not as yet been used for dielectric strength tests on solids. This is planned for the future and it is hoped that the "burning up" of the material under test will be reduced to such an extent that the cause of breakdown is not obliterated and may be detected by microscopic investigation. While this is outside the scope of this thesis some remarks can be made on the electrodes developed for this work.

Fig. 50a shows the standard B.S.S. electrodes for testing paper, insulating fabrics, sheet material etc. (M in Fig 50a). The author has often observed sparks emanating from the H.V. electrode and gliding along the surface of M. This was particularly noticable at higher voltages and thick material of high dielectric strength. These sparks may be explained as follows: A small annular area "A" on the surface of M has capacitance to both electrodes. Usually C_2 is much larger than C_1 , "A" is therefore nearly at earth potential and a spark can bridge the gap between it and the H.V. electrode. Thus, the H.V. electrode has grown in diameter and the same mechanism may now occur between "A" and "A'", and so on. These gliding or cascading sparks, so dreaded by bushing designers, cause premature breakdown of the material. If the tip of the gliding spark is positive, ionised channels will appear in the solid because electrons are drawn out. These channels may be regarded as sparks penetrating the solid material.

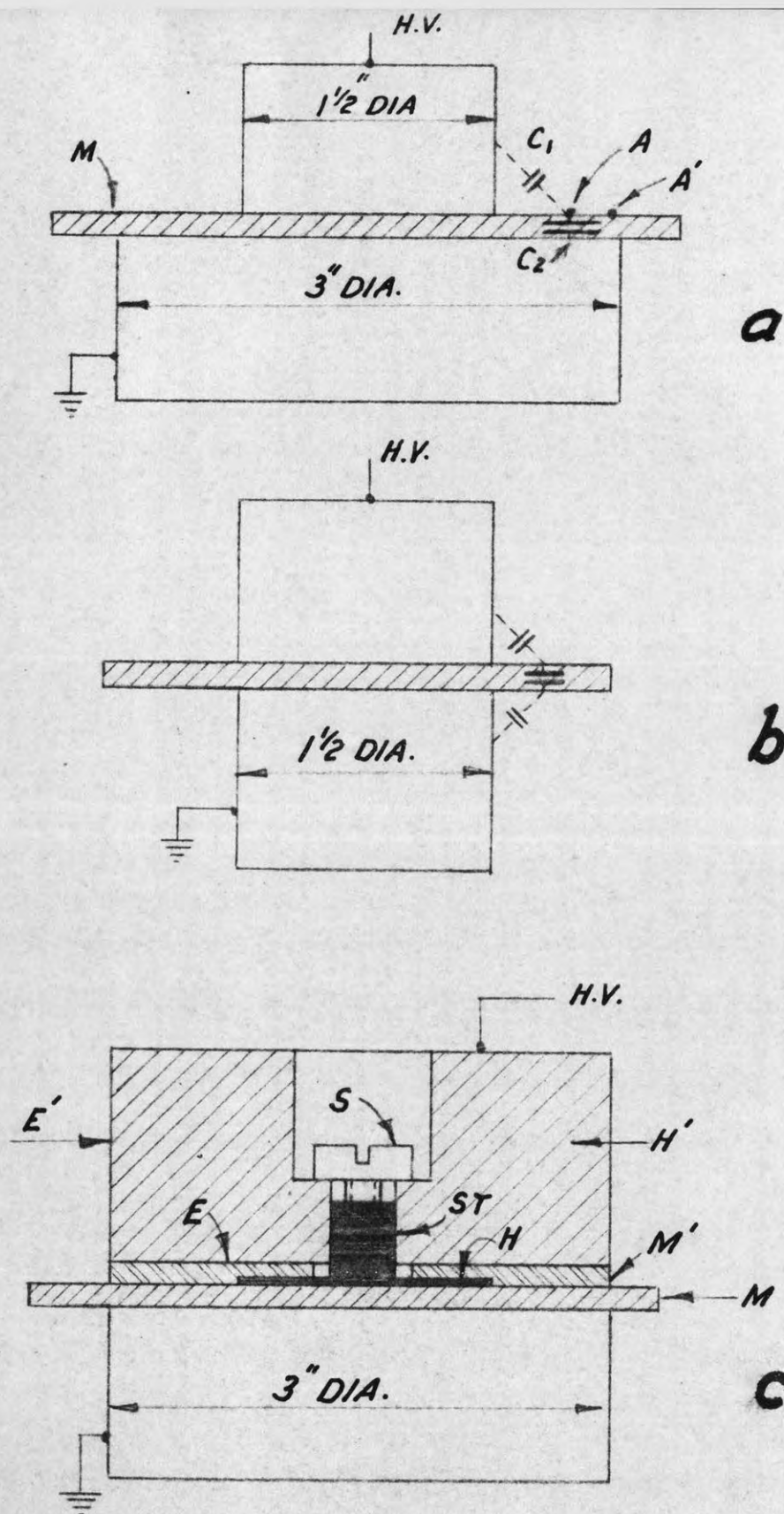


FIG. 50. ELECTRODE FORMS FOR DIELECTRIC STRENGTH TESTS ON SHEET MATERIAL

Gliding sparks are obviously avoided with the electrodes shown in Fig. 50b. Paper, vacuum impregnated in oil, gave about the same dielectric strength figures when either the electrodes of Fig. 50a or 50b were used as long as its thickness was below 0.006 inches. With the electrodes as shown in Fig. 50b higher figures were obtained at those thicknesses which required voltages above the onset level of the gliding sparks. The downward bend in the plot, voltage as a function of thickness, was significantly reduced when the electrodes of Fig. 50b were used. Expressed in a different way, at the larger thicknesses the dielectric strength did not fall as much as with the B.S.S. electrodes indicating an obvious influence of the method of test. Some doubt as to the validity of published figures therefore exists.

In both types of electrodes there is an edge - effect and some uncertainty if a breakdown, occurring at the edge, is not caused by stress concentration. For the tests in conjunction with the diverter gap another electrode system has been conceived and this is shown in Fig. 50c and Plate 8.

The earthed electrode is the same as in Fig. 50a. The high voltage electrode H is $1\frac{1}{2}$ inch in diameter and $1/32$ inch thick. This electrode is turned from the full to provide a stud St. Due to distortion it was found not possible to solder the stud to H. The electrode H is recessed in a bakelite ring M', H and M' being flush. The Stud slide fits into H', which, like all other metal parts is made of brass. The height of H' is chosen such as to give 1 kg contact pressure when in oil. Rings (not shown in Fig. 50c) may be attached to increase the weight to 2 or 3 kg. By means of the screw S, H, St and M' are attached to H'. The thickness of M' is $3/32$ inch. The material under test is M.

It can be seen that gliding sparks are not likely to occur because the condition C_2 much larger than C_1 of Fig. 50a no longer exists. Edge effect is virtually eliminated because the edge of H is guarded by E, the edge of H'. Edge effect at the outer edge E' is harmless, increased insulation thickness being provided there.

When H' was suspended 0.1 inch above a plane in air, the breakdown values for a uniform field gap were obtained (computed as per reference 30) indicating the efficacy of guarding the edge. Much lower values

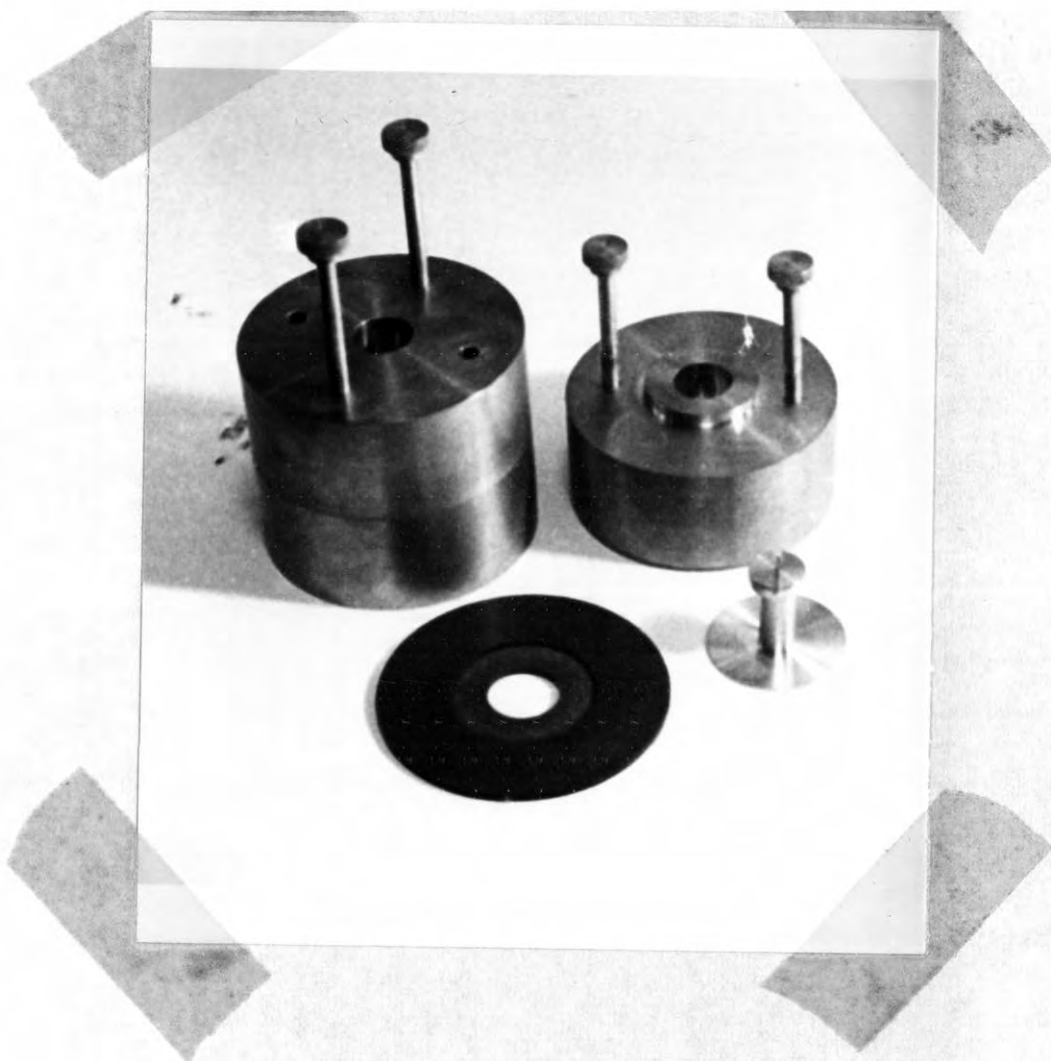


Plate : 8. The streamer - free and guarded electrode system of Fig. 50 c.

FOLLOWING PAGE: 80

were obtained with the standard electrode.

5.4. Conclusions re gap type "C".

A diverter gap has been described for the voltage range 10 to 30 KV r.m.s. (14 to 42 KV_p). In this range the diverter is a fixture requiring neither adjustment of spacing nor additional apparatus with the exception of two resistors. The time lag is higher than desirable but adequately small to protect a spark gap from pitting. At higher voltages the 3 : 1 range cannot be realised except in a series arrangement of two diverter gaps.

The most important application besides the protection of a measuring gap appears to be the prevention of carbonisation during routine tests on transformer oil.

It has been shown that by careful attention to the electrode shape, the hole diameter and the needle position the trigatron may be made to break down at an astoundingly small fraction of that voltage which would be required for a two electrode gap of the same shape.

Byproducts of the investigation are : A simple and inexpensive new chopping circuit for impulse generators (Appendix 6), new electrodes for dielectric strength tests on sheet material and a method in which a spark gap is used to approximately determine the time lag of a diverter gap.

5.5. References re gap type "C".

- (47) P.K. Watson and J.B. Higham
Electric breakdown of transformer oil
Proc. I. E. E., vol. 100, part II A, March 1953, p.168.
- (48) W. Baker
The non-destructive testing of electric strength of liquids
Proc. I. E. E., vol. 103, part A, August 1956, p.337.
- (49) D.R. Hardy and T.E. Broadbent
The effect of irradiation on the calibration of 2 cm diameter
sphere gaps
Proc. I. E. E., vol. 101, part II, August 1954, p.438.

- (50) T.E. Broadbent
The breakdown mechanism of certain triggered spark gaps
Brit. J. appl. Phys. vol. 8, February 1957, p 37.
- (51) H.M. Sletten and T.J. Lewis
Characteristics of the trigatron spark gap
I. E. E. Monograph 193 M, August 1956.
- (52) J.D. Craggs and J.M. Meek
High voltage laboratory technique
Butterworth Scientific publications
London, 1954.
- (53) J.D. Craggs, M.E. Haine and J.M. Meek
The development of triggered spark gaps for high power modulators
J. I. E.E. vol. 93, part III A, p 963.
- (54) T.E. Broadbent and J.K. Wood
A thermally triggered spark gap
Brit. J. appl. Phys. vol 6, 1955, p 368
- (55) D.R. Hardy and T.E. Broadbent
The control of high voltage impulse generators
The Beama Journal, vol. 62, February 1955, p.63
- (56) E.W. Golding
Electrical Measurements
3rd ed. p. 458, Pitman 1942
- (57) H. Josse and Y. Enault
Le mesure de la rigidite dielectrique des huiles isolantes
Bull. de la Soc. Franc. de Electriciens.
Vol. 4, Sept. 1954, p. 536

6. Acknowledgments.

Of prime importance, during the work described, was encouragement because for a middle-aged lone worker the burden, at times, became rather heavy.

It is therefore not just courtesy if I wish to record my gratitude to Prof. R.E. Vowels, head of the school, for his interest, advice and understanding.

I also wish to thank Mr. R.M. Huey and Dr. H.A.S. Rosenthal. When, in a colloquium on high voltage measurements given in October 1956, I outlined my hopes and ideas regarding spark gaps, these two gentlemen were so encouraging that I gained enough confidence to start in earnest the research described in this thesis.

My wife Martha not only helped with the reading of the manuscript but, with angelic tolerance, put up with a very preoccupied husband for a long time.

Persons who made specific suggestions or whose work was used are acknowledged in the text or in the references.

VII. Appendices.

Appendix 1.

Standard resistors wound with controlled tension on pyrex glass formers.

(a) The influence of the former.

- 1) Requirements: If, in a voltage divider, all resistors show the same change of resistance as a function of temperature (either ambient or created by the load) the voltage ratio would remain constant and it would not matter if the resistors changed in value. In practice this condition is hard to meet because, when mounted in a box, one resistor heats the other thus making the individual temperature rises different. It is preferable to use resistors which change little due to the heat created by their load current and thus also with ambient temperature. It was aimed at to develop resistors of reasonable size, for a rating of 5 to 10 W, with values between 1000 and 5000 Ohms which would not change by more than 10 parts in a million from zero to full load and which would remain stable to 1 to 2 parts per million per year. Their manufacture was to be easy and economical so that they could also be used industrially as standards in the measuring or sensing circuits of automatically controlled processes. It was also thought desirable that this performance should be achieved in atmospheric air without oilfilling or sealing.

- ii) Remarks on properties of resistors: A length of bare resistance wire which is completely unrestrained will change with temperature as computed from the temperature coefficient of resistance of the material. Indeed, such a wire represents the best possible resistor. If silk covering is used the resistance will increase with rising humidity while cotton insulation causes a decrease. The change may be irreversible. Leeds & Northrup (U.S.A.) have patented a resistor having silk plus cotton insulation to cancel the effect mentioned above. In the humid climate of Australia attention to the influence of humidity is imperative. Worse still is the influence of a former. Bakelite cards swell and stretch the wire, causing irreversible changes. This may be reduced by winding the wire loosely but this is hardly an engineer-

ing solution. Mica cards with their edges sealed by means of polystyrene laquer are better but too fragile to permit the use of bare wire. Metal spools covered with empire cloth or similar insulation give irreversible changes due to dimensional changes of the organic material. It is for that reason that resistors for precise work are sealed in oil or dry gas and used in an oilbath at controlled temperature with the load on the resistors being kept very small. Another influence of the former is due to its coefficient of linear expansion. If the former expands more than the wire the latter will become stretched, perhaps above its elastic limit, or alternatively the wire may become loose if the former expands less. If this effect is cushioned by such unstable materials as oilsilk, empire cloth, polythene or waxed paper irreversible changes are unavoidable.

It should be noted that the order of the changes referred to rarely exceeds 0.1% but this is quite disastrous for a standard resistor.

From the above remarks it is obvious that the former can be used to control the performance of a resistor in a predictable manner provided there is no unstable material between former and wire. To the best of the author's knowledge this was suggested by W.K. Clothier as early as 1944. The author's work on the realisation of this suggestion commenced in 1946 culminating in the design of the divider shown in Fig. 4 and mentioned in Section 3.1.2.1.

(b) Physical concept of compensation.

In order to obtain control in an orderly fashion the formers are assumed to be thin-walled annealed pyrex glass tubes, freedom from internal strains having been checked by means of polarized light. When bare wire is wound under tension onto such a tube the wire is stretched and its resistance increased relative to the unstretched condition. Assuming now that the coefficient of linear expansion of the former is smaller than that of the wire the latter will become less stretched (thicker in diameter) when the temperature rises. Thus its resistance will fall. The former can therefore be said to cause a negative temperature coefficient of resistance. If now the wire has a positive temperature coefficient of resistance the two coefficients can be made to cancel by the proper choice of the temperature coefficient of the wire.

The assumptions made in the above simplified concept are that the wire is stretched to well below its elastic limit and that the temperature rise (either ambient or by the load) is not so high that the wire becomes loose and the former loses control. As long as the former retains control the exact amount of tension is of no importance and does not influence the compensation. It is further assumed that the temperature coefficient of resistance is constant in the temperature range concerned, viz: 15 to 50 deg. C. This is only approximately the case for constantan which was used for the resistors. For example in one case it was found to be $27 \text{ pp } 10^6$ per deg. C at 16 degrees and $25 \text{ pp } 10^6$ per deg. C at 47 degrees

For metallurgical reasons a copper nickel alloy is much more stable than alloys containing manganese. For example, it is a nuisance that manganin changes its resistance when exposed to air. It must be protected by varnish or sealing. It is wrong, but a popular misconception, to use manganin for all resistors. It should be used only on these low value D.C. resistors in which the higher thermal e.m.f. of constantan would become significant when compared with the voltage on the resistor. Manganin is out of place in all A.C. resistors and in high value D.C. resistors.

(c) General Expression for the fictitious temperature coefficient of resistance of the former (K_f).

i) Estimate of K_f : Although based on simplifying assumptions it was found that for bare wire in contact with the former, K_f may be approximated reasonably well by:

$$K_f = -S (C_w - C_f)$$

wherein C_w and C_f are the coefficients of linear expansion of the wire and former respectively. S is the strain coefficient defined as :

$$S = \Delta R/R : \Delta L/L$$

L being the length.

Taking now typical values : For constantan S is known from strain gauge work to be about 2, $C_w \sim 16.5/10^6$ per deg. C, and C_f is $3.5/10^6$ per deg. C for pyrex. $K_f = -2 (16.5 - 3.5) = -26 / 10^6$ per deg. C. Thus a

wire with a temperature coefficient of $+ 26 / 10^6$ per degr. C is required for compensation. In practice it was sometimes found that a slightly lower figure gave better compensation.

It should be stressed that the simple calculations made above and those to follow are engineering approximations which led to good results. Instead of investigating in detail the mechanical and electrical properties of the materials used, it is far less time consuming to wind a resistor, test it, and if not quite up to expectations correct for it in a second attempt.

ii) Calculation of critical temperature and tension required : It is of interest to work out the tension required. For the particular wire used which was of 36 B & S gauge the elongation $\Delta L/L$ was measured as described in Section (e) of this Appendix by means of a travelling microscope. It was found to be $135 / 10^6$ per 1 oz. This figure is only slightly lower than calculated from Young's modulus taken from tables of properties of materials. Let this elongation be e . For n ounces and considering that both the wire and the former expand, the critical temperature rise at which the wire would just become loose is :

$$t_{crit} = n \times e / (C_v - C_f).$$

the wire was found to be well within its elastic limit at $n = 4$ oz which represents $\frac{1}{4}$ of the breaking stress.

$$\therefore t_{crit} = 4 \times 135 / 16.5 - 3.5 \sim 41 \text{ degr. C.}$$

If the wire was wound onto the former at 20 degr. C, it would become loose at about 61 degrees.

In practice two types of resistors were wound both using 36 B&S Constantan, Eureka, Ferry or Cupron wire with approx. 1 Ohm/inch resistance. In one type 96 turns per inch were used and in the other 48. The rated wattage per inch of length of the $1\frac{1}{2}$ inch diameter former varied between 0.73 and 0.88 for the resistors with 96 turns per inch and it was 1.63 for the resistors with 48 turns per inch. The temperature rise was about 16 degr. C in the first and 25 degr. C in the latter case. The resistors were vertical in all cases and

enclosed

in a metal box with louvres. The temperature rise is thus well below the critical one even allowing for a higher ambient temperature than 20 degr. C. This was indirectly proved by repeatedly heat cycling the resistors which showed no sign of irreversible changes. See also Section 2 and Fig. 57.

(iii) Compensation if suitable wire is not available : From the above it is clear that for one former material there is only one temperature coefficient of resistance of the wire which will give a resistor virtually free of load coefficient, the order being $+ 26 / 10^6$ per degr. C. for pyrex formers. Unfortunately thin constantan wires are much more likely to have a negative temperature coefficient of resistance than a positive one. It is indeed hard to find a suitable wire to implement the principle outlined before. The task would become hopeless if a ceramic former were used. Because C_f is negative in this case, K_f has a large negative value and a nearly impossibly large positive temperature coefficient of resistance of the wire is required. Moreover even if a manufacturer is kind enough to supply say 50 reels of wire for the selection of one reel, - in this case O.H. O'Brien of Pitt Street, Sydney, was most helpful - it is often found that the temperature coefficient of resistance of a wire sampled from the outside of a reel may be different from a sample further down.

This difficulty may be overcome by a second compensation. The main part of the resistor consists of a wire with a temperature coefficient of more than $+ 26 / 10^6$ per degr. C and the remainder has a wire with a less positive temperature coefficient.

Let R_1 and R_2 be the two portions of the resistor wound with wire of the same thickness and resistivity but having temperature coefficients of resistance of a and b respectively :

$$R_1 (a + K_f) + R_2 (b + K_f) = 0.$$

$$\therefore R_1 / R_2 = -(b + K_f) / (a + K_f)$$

For example : Let K_f be $- 26 / 10^6$ as before and let wires with $a = + 29 / 10^6$ and $b = - 4 / 10^6$ per degr. C be available ;

$$R_1 / R_2 = - (-4 - 26) / 29 - 26 = 10$$

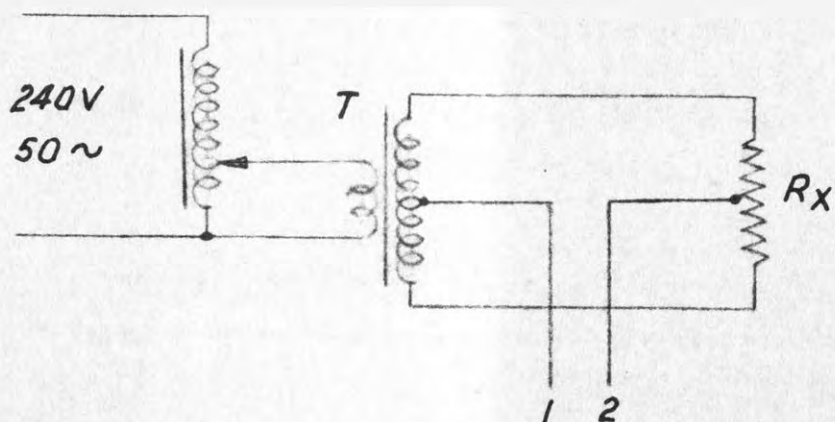
In practice the compensation so computed may not be quite correct because, depending on the relative position of R_1 and R_2 the temperature of the two parts of the resistor is different. This is shown in Section C, Fig. 57 b. This method of compensation was found quite stable with time and heat cycling and it is better than the two alternatives given below.

Compensation may also be achieved by winding part of the resistor with copper or Nichrome, both materials having large positive temperature coefficients of resistance. In the first case difficulty was experienced in obtaining good thermal contact of the few copper turns with the rest of the resistor and in the second case, Nichrome was found hard to precision wind without kinks because of the "curly" nature of the wire.

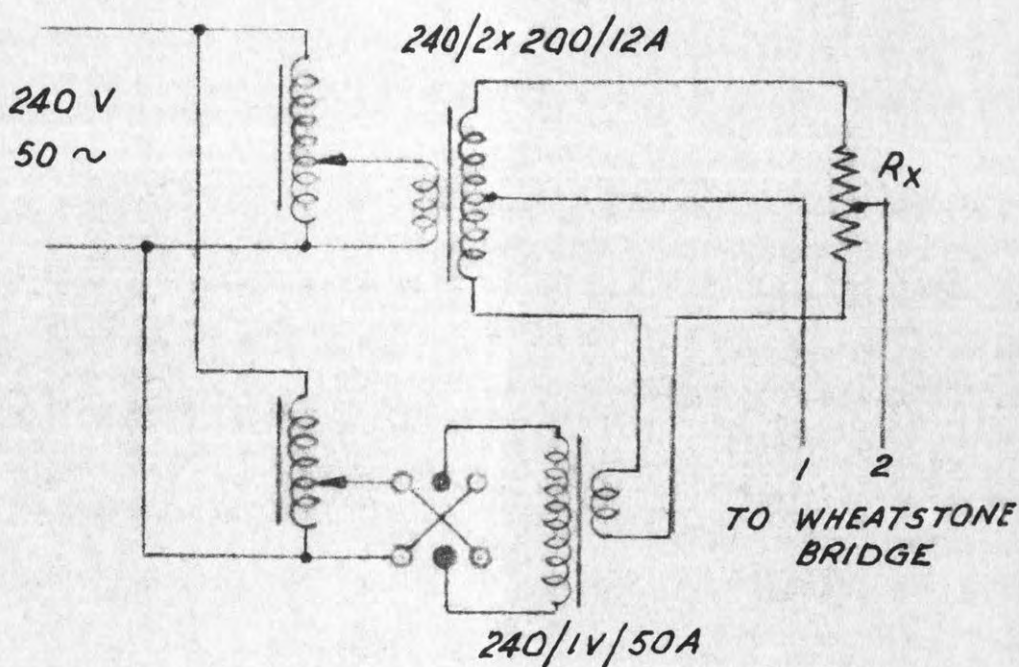
(d) Methods for the measurement of $\Delta R/R$.

1) Method 1 : A method was required to check experimentally the change of resistance as a function of time for various loads. The principle of the scheme devised is shown in Fig. 51 a. A centre tapped transformer T supplies the load current to the resistor R_x which must have a centre tap or must consist of two identical resistors. T and R_x form the 4 arms of an A.C. bridge and no potential appears between the centre taps, points 1 and 2. These points can therefore be connected to a D.C. Wheatstone bridge for the measurement of the two halves of R_x in parallel. Measurements can be made at any load, the resistor is always in circuit and its change can be observed continuously. Most resistors had centre taps but the necessity to use two identical resistors is usually no hardship. It is convenient to use a transformer T with very low secondary resistance. A temperature change will then cause a change in winding resistance which is negligible as compared with the change in R_x . During the tests a fan was used to cool the transformer and to reduce its temperature rise caused by the iron losses. In a typical case the total winding resistance was 0.5 Ohms, the resistance under test was 3750 Ohms and the temperature rise of the winding was $2\frac{1}{2}$ degr. C. The transformer was operated at about $1/3$ of its normal fluxdensity. Taking 0.4% per degr. C. resistance change for copper, the change due to $2\frac{1}{2}$ degr. C is 1% of 0.5 Ohms or 0.005 Ohms. The error so incurred was $0.005 / 3750 \sim 1.3$ in 10^6 which was neglected.

In practice the circuit was arranged as shown in Fig. 51 b. which



(a)



(b)

FIG. 51 METHOD OF CONTINUOUS MEASUREMENT OF $\Delta R/R$

permits balance of the A.C. bridge in case of assymetry^m in R_x or T. If the A.C. part was not properly balanced the light spot of the D.C. galvanometer became blurred.

During the development of these resistors a very large number of measurements were made and it was found convenient to arrange the Wheatstone bridge to be direct reading in pp 10^6 or pp 10^5 change of resistance. Fig. 52 shows the scheme and the relevant equations.

ii) Method 2. Although this was not used for the purpose of this thesis it is believed that this subsection may be more useful if two more methods are described.

When resistors or a bank of resistors had to be measured at high voltages the scheme of Fig. 51 was considered too dangerous for the operator. In this case the circuit of Fig. 53 was used. The high voltage change over switch S_1 is normally held in position A by the spring. In this position R_x is heated by the testing transformer T. Pulling the string connects R_x to the D.C. Wheatstone bridge. After S_1 has moved to B, S_2 shorts terminals 3 and 4 which are wired in series with the galvanometer. The test procedure is as follows: With S_1 at B the bridge is balanced. The string is then released and the required test voltage applied. Every two minutes or other time interval the string is pulled to B, the galvo deflection quickly read and the string released again. Before or after the test the galvo deflection is calibrated in pp 10^6 or pp 10^5 . The cooling during the measurement is kept as short as possible by not balancing the bridge but by quickly reading a deflection. A galvanometer with short period or an electronic galvanometer amplifier with a large amount of negative feedback (58) is helpful. A further artifice is to keep the deflection small and therefore the time to deflect short by anticipating the change. While S_1 is still at A the bridge setting is changed to a setting giving "near" balance based on experience and the results of a previous test. Thermals are allowed for by observing the galvo deflection with the bridge supply reversed.

iii) Method 3. Recently the load and voltage coefficients of 1000 Megohm oil immersed resistors had to be measured at 100 KV D.C. These resistors are

One arm of
Wheatstone
Bridge.

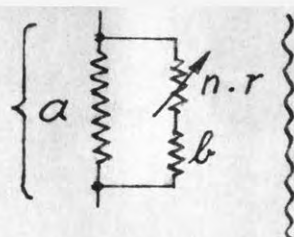


FIG. 52.

n steps of value r are required
to give fractional change d .

FOLLOWING PAGE: 90

$$d = \frac{\frac{a(b+nr)}{a+b+nr} - \frac{ab}{a+b}}{\frac{ab}{a+b}} = \frac{nra}{a+b+nr} \times \frac{1}{b}$$

$$= \frac{a}{b} \cdot \frac{1}{\frac{a}{nr} + \frac{b}{nr} + 1} ; \text{ for } \frac{b}{nr} \gg 1 \text{ and } \frac{a}{nr} \ll \frac{b}{nr}$$

$$d \cong (anr)/b^2 ;$$

$$b \cong (anr/d)^{1/2}$$

The error e in this approximation is :

$$e = \left(1 - \frac{\frac{anr/b^2}{\frac{a}{b} \frac{nr}{a+b+nr}}}{\frac{a}{b} \frac{nr}{a+b+nr}} \right) = \left(\frac{a+nr}{b} \right) 100\%$$

Example: $n = 100$, each step $= \frac{1}{10^6}$, $d = \frac{100}{10^6} = \frac{1}{10^4}$

Say: $r = 1 \Omega$, $a = 100 \Omega$

$$b = \sqrt{\frac{100 \cdot 100 \cdot 1}{\frac{1}{10^4}}} = 10^4 \Omega ; \quad e = \left(\frac{100 + 100 \cdot 1}{10^4} \right) \cdot 100 = 2\%$$

or $2/10^6$ total.

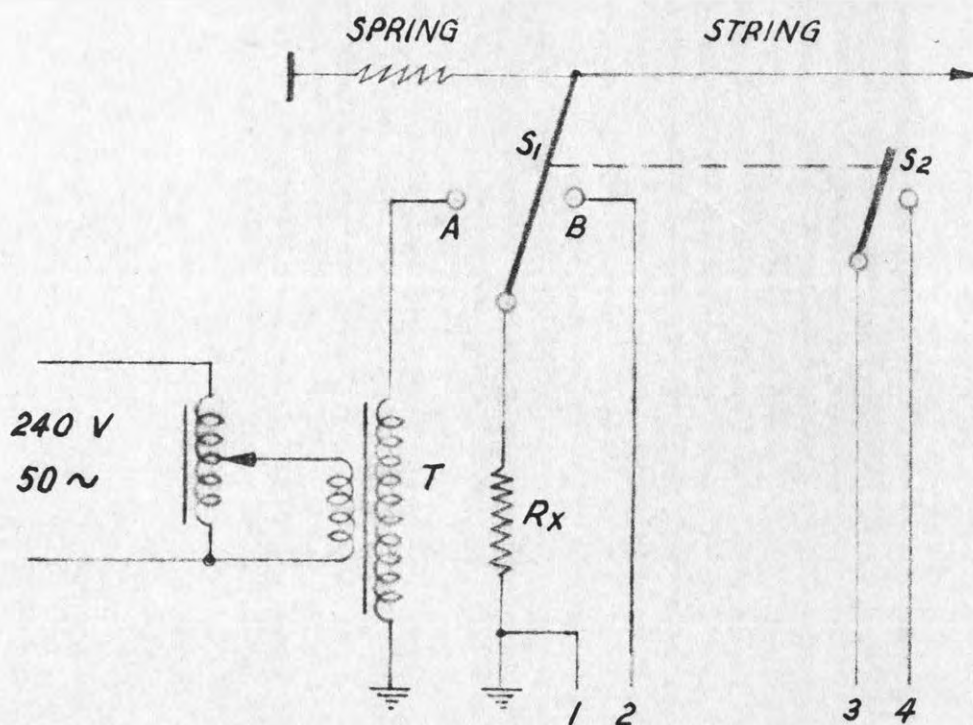


FIG. 53 MEASUREMENT OF $\Delta R/R$ BY SWITCHING R_x TO T OR TO WHEATSTONE BRIDGE (1,2). 3 AND 4 ARE IN SERIES WITH THE GALVANOMETER.

FOLLOWING PAGE: 90

used as series resistors to indicate on a meter with 100 microamperes full scale deflection the voltage during electrostatic painting.

Fortunately the 100 Megohm 100 KV wire wound resistor mentioned in Section 3.2.1. has been completed in the meantime and could be used as a standard. The D.C. supply mentioned in Section 3.2.1. and shown in Plate 4 was the voltage source. The circuit of the bridge used is shown in Fig. 54.

The bridge was first balanced at 10 KV and then at another voltage, say 100 KV. The test was then interrupted and after a time considered long enough for the resistor to cool down the test was repeated. The bridge was again balanced at 10 KV, the voltage was then quickly raised to 100 KV and balance quickly obtained. This was possible because the approximate dial readings were known from the previous test. Thus the change with voltage could be measured. After a while a new balance gave the change due to heating. This was repeated at various voltages and in this way the voltage and load coefficients could be separated.

R_x and R_{st} were mounted in oil-filled tubes of insulating material and it was imperative to provide guarding against surface leakage. However, besides guarding shielding of the detector circuit was necessary because due to unavoidable corona of the H.T. leads ions reached the detector terminals and caused completely erroneous results. For example, a model 3 Avometer on its 50 microampere range, with one terminal grounded, standing by itself in 3 ft. distance of the 100 KV wire showed a reading of 5 microamperes. The effect which can easily be dealt with by screening was expected from previous work on corona (11). While earthed metal shielding is the obvious engineering solution it is interesting to note that the ionic conduction path may be intercepted by an insulator and shielding by a sheet of perspex is possible. A search of the literature failed to provide any relevant information on D.C. bridges operating at so high a voltage. Bridges used for cable fault detection (59) do not belong in this category.

iv) A null detector using transistors: A simple attachment to the model 3 Avometer was built for use as a D.C. null detector. The circuit is shown in Fig. 55. The position 1 of the three position three circuit switch S is the "off" position. In position 2, the input terminals A and B are shorted

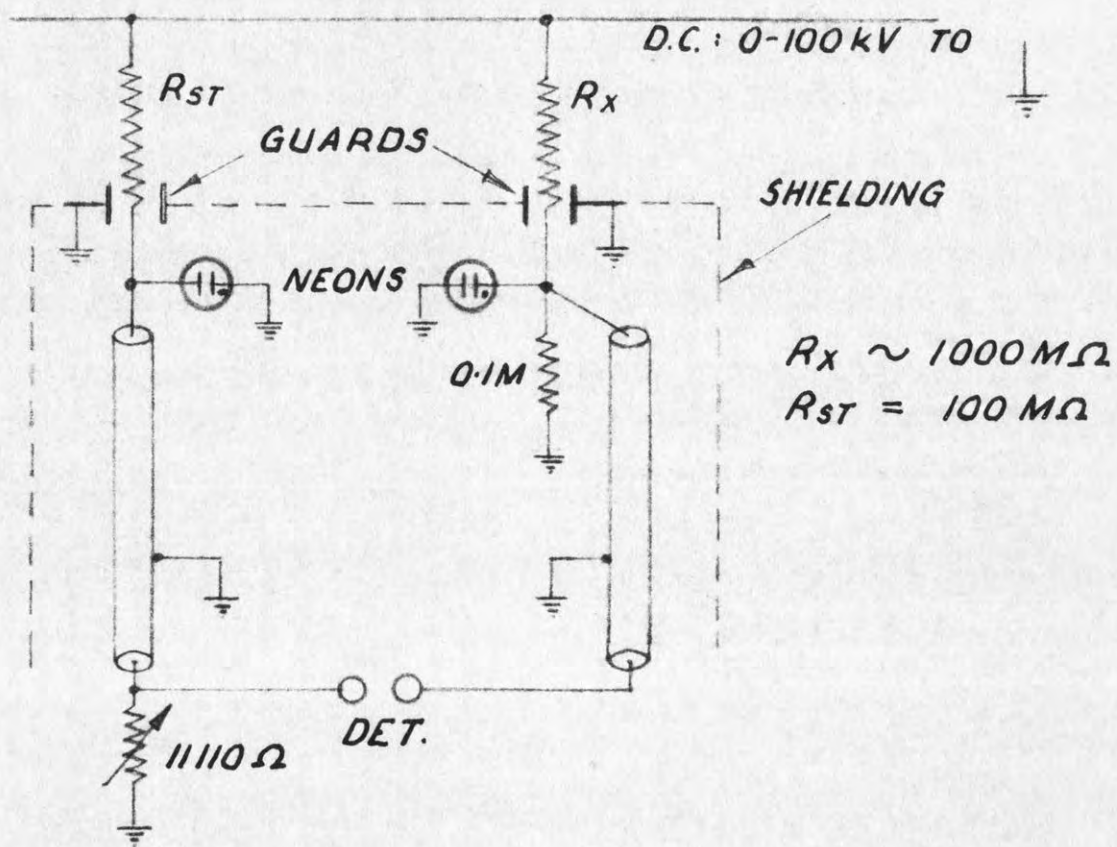


FIG. 54. HIGH VOLTAGE D.C. BRIDGE FOR LOAD AND VOLTAGE COEFFICIENT MEASUREMENT.

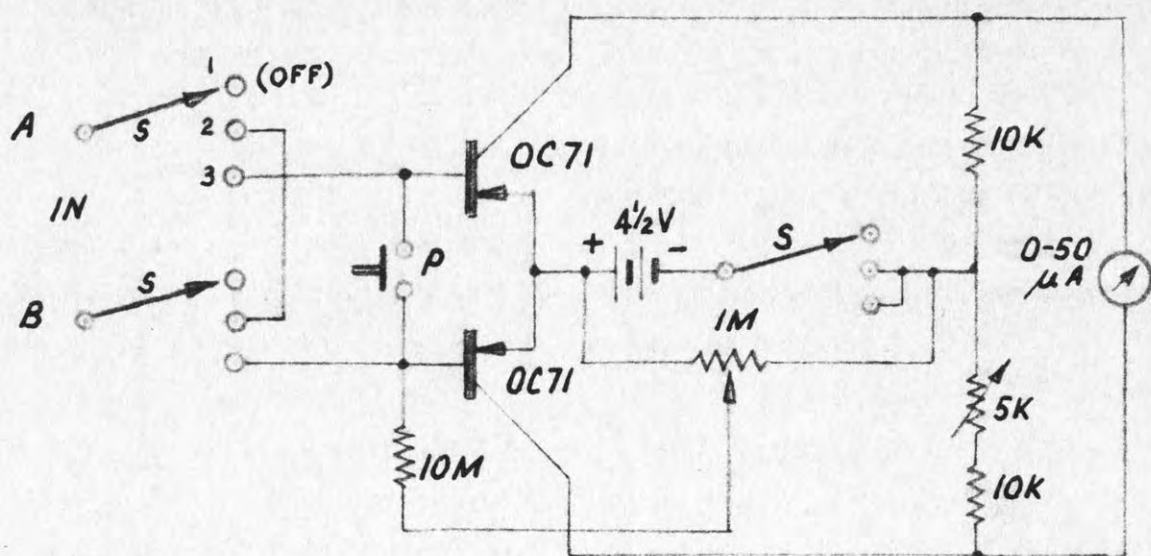


FIG. 55. D.C. NULL DETECTOR

and the meter can be adjusted by means of the 5 K variable resistor to read $\frac{1}{2}$ scale thus giving a convenient centre zero. In this position the 1 M potentiometer must be adjusted till pressing of P does not cause any meter deflection. This equalisation of base voltages is necessary because of the natural differences in the transistors and the collector circuit asymmetry. In the operating position 3 the input resistance is approx. 20,000 Ohms and the sensitivity is about 1×10^{-8} A per division of a 2 x 50 div. scale. The transistors are close to each other ($\frac{1}{8}$ inch) in holes drilled in an Aluminium block which itself is wrapped in foam plastic. Thus the drift trouble has been overcome.

(e) Experimental verification and performance of resistors built.

For reasons of space only a summary and typical examples are given here.

i) Measurement of strain and temperature coefficient: Fig. 56 shows schematically the set up for the measurement of the strain-coefficient of resistance wire. The mean value of S varied between 1.8 and 2.05 for the various brands of resistance wire available. All wires were 40 SWG or 36 B & S gauge. The temperature was 20 degr. C. and the load per wire was varied between 1 and 6 ozs.

The temperature coefficient of resistance of wire samples was measured conventionally in an oil-filled glass vessel fitted with an immersion heater and stirrer. The wire samples were about 50 Ohms each and they were wound loosely on mica cards.

ii) Constructional details of the resistors: Plate 9 shows typical resistors. Pyrex tubes with $1\frac{1}{2}$ inch O.D. and $\frac{1}{16}$ inch wall thickness were used, wound with constantan wire of 40 SWG or 36 B & S gauge at a tension of 4 oz. 96 or 48 turns per inch were employed. For the divider shown in Fig. 4 the number of turns per inch was 96. The wire was annealed at 100 degr. C before use. For this purpose the wire was wound on steel bobbins which expand less than the wire. The tensioning device was mounted on the tool carriage of the lathe used for winding. The wire was passed through two felt "filters" which removed surface dirt and slight kinks, Resin was used to fix

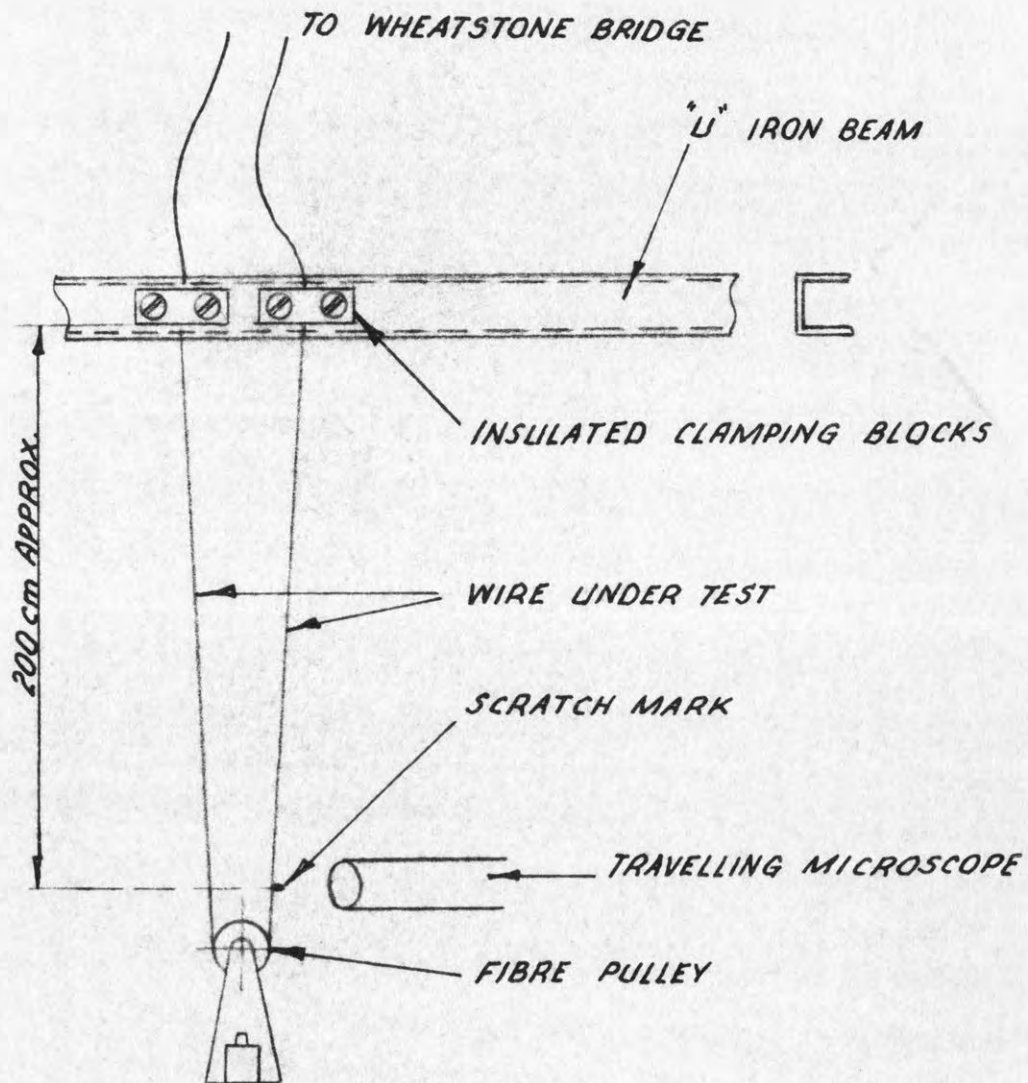


FIG. 56. SCHEMATIC ARRANGEMENT FOR THE MEASUREMENT OF STRAIN COEFFICIENT $\Delta R/R : \Delta L/L$.

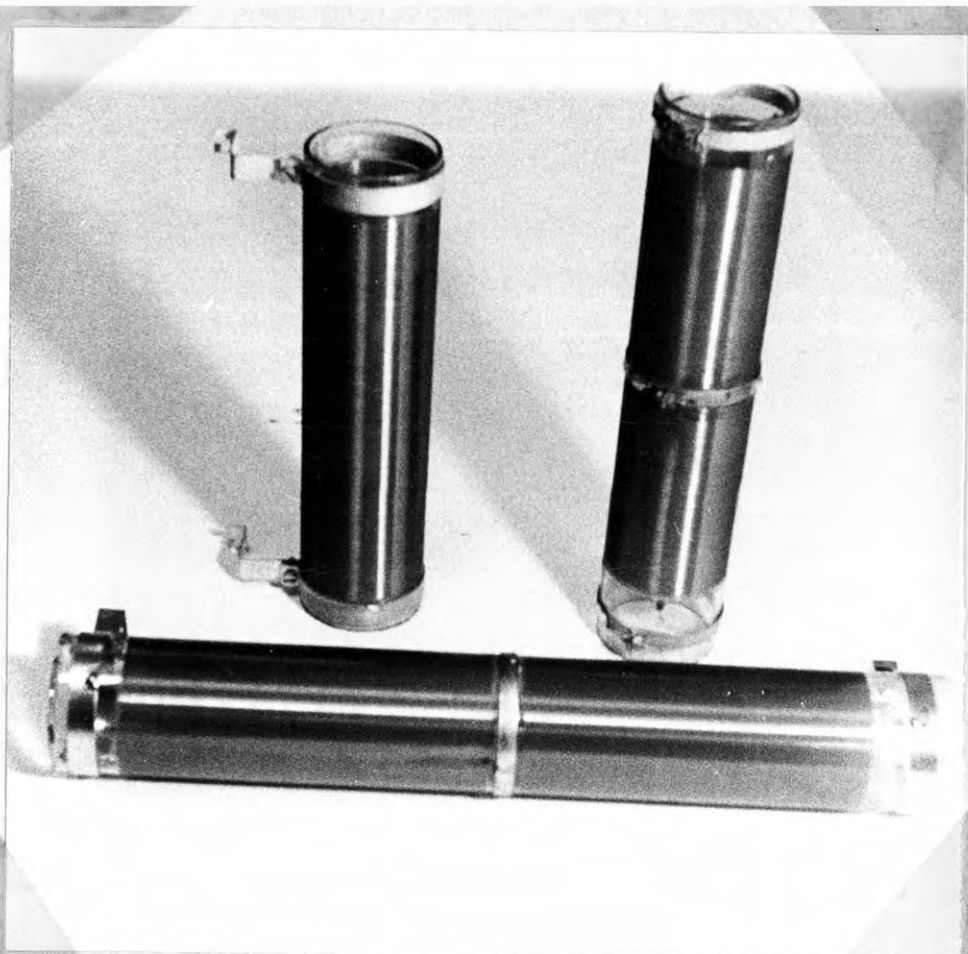


Plate : 9. Glass - Resistors.

FOLLOWING PAGE: 92

the wire ends to the former. After winding the resistors were given a coat of RD77 phenolic varnish approximately 0.0007 inch thick. This served as protection against dust and mechanical damage and it also permitted the removal of the end-turns which may not have had the correct tension. It was found absolutely essential that not a trace of varnish crept between the bare wire and the former. When this happened - and accidentally it did when an attempt was made to speed up the drying time by placing the resistors in an oven - the resistors showed irreversible changes of up to 2 parts in 10^4 and had to be destroyed. This may be regarded as proof of the dictum that unstable materials must not be allowed to take control of the resistance wire.

As the wires had about 1 Ohm per inch resistance and cutting to $1/16$ was quite easy, adjustment to $1/16 \times 3750 \sim 2 \text{ pp } 10^5$ was possible. In some cases when the wire was accidentally cut too short, a length of thicker gauge constantan wire was added externally. All resin residue of the solder joints between wire and terminal clamps (see Plate 9) was washed away with alcohol and all joints were inspected and scraped under a microscope to make sure that no solder crept along the wire giving dubious contact and that contact occurred in one well defined spot only.

iii) Performance tests for short term stability: The test for performance during the development and later of the final resistors consisted of balancing the Wheatstone bridge without A.C. load voltage (see Fig. 51) and then to record the change in resistance every few minutes with load applied. After equilibrium had been reached, say after 30 min., the load was removed and the cooling curve taken. A good resistor always returned to its original value and this was checked several times. However when this work was commenced great difficulties were encountered. A Wheatstone bridge stable to a few parts in a million for a period of several hours requires immersion of its arms in a temperature controlled oil bath. The author had no access to these facilities. Resource had therefore to be taken to place ordinary resistance boxes in large wooden containers filled with cotton wool to provide lag against temperature changes. With these primitive means the first glass resistors were developed and they in turn were then put in the bridge arms. Thus better glass resistors (compensated) could be made which again were used as bridge arms. Eventually a bridge was built which was

stable enough to take performance curves on glass resistors. Alternatively expressed, glass resistors had first to be made to build a bridge which was more stable than the product to be investigated.

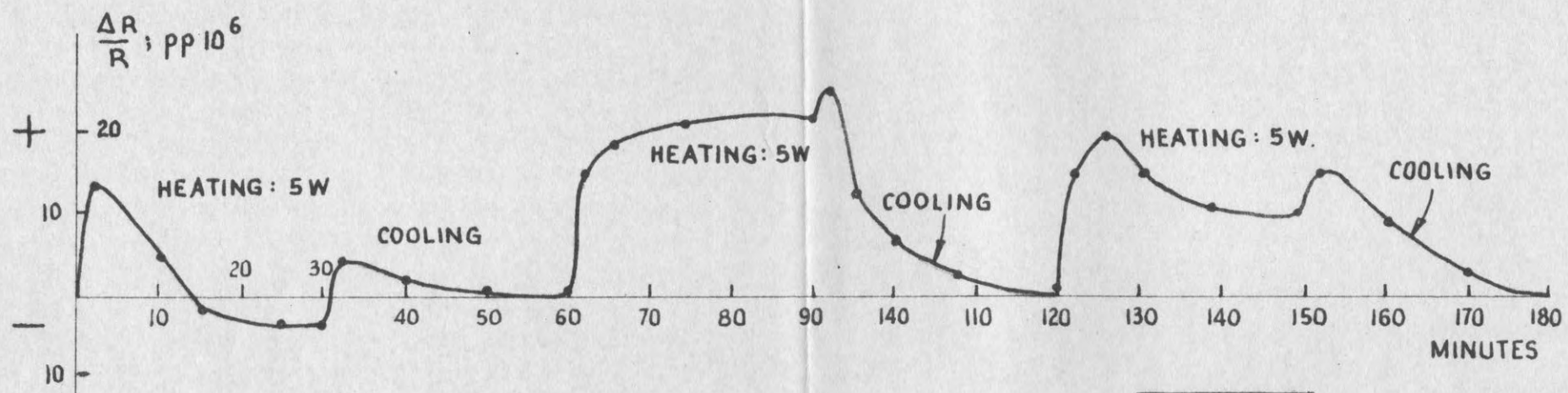
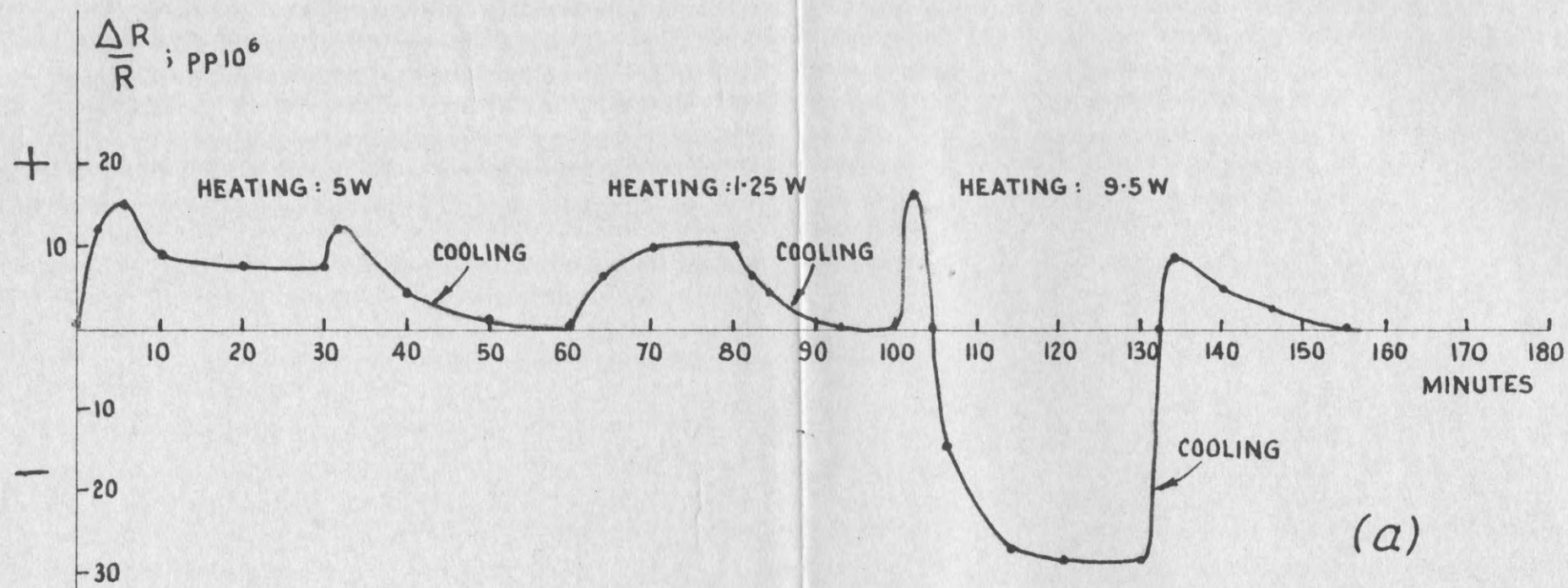
Fig. 57 shows typical results of 2500 Ohm resistors rated 5 W. Fig. 57a gives the result of cycling tests on a resistor the wire of which had a temperature coefficient of resistance of $+ 26 / 10^6$ per degr. C. The performance for various loads is given. Of particular interest is the last curve when 9.5 W were applied. The resistance change became negative as would be expected because the temperature coefficient of resistance of the wire falls at higher temperatures. Thus the fictitious negative temperature coefficient of resistance of the former (K_F) preponderates.

Fig. 57b gives the performance of a compensated resistor showing also the influence of the relative position of the two windings. The temperature coefficients of resistance of the two wires used were as given in the example in the previous Section.

Cycling tests carried out at near 100% humidity or in a very dry atmosphere (using a covered vessel the bottom of which was filled with either water or chlorcalcium) have definitely established that the resistors perform equally well under those conditions.

iv) The long term stability: 16 resistors of 1000 Ohm each were wound for comparison with a 1000 Ohm standard at 1 month intervals. Unfortunately it was found impossible to ascertain if the few parts per million change observed per year were due to the standard or the glass resistors. It was particularly unfortunate that the standard used showed inexplicable random variations. The tests had to be done in air while the history and properties of the standard were precisely known only when submerged in an oil-bath. It is regretted that owing to lack of access to equipment superior in long term stability to the objects to be tested this investigation had to be abandoned. However from time to time, for the purpose of calibrating volt ratio boxes at the actual operating load, 60 glass resistors of 2500 Ohm each have been lent to colleagues who have ascertained that their value has increased by about 10 parts in one million in 8 years.

v) Conclusion: It can thus be concluded with fair certainty that the



(b)
(COMPENSATED)

FIG. 57. 2500 Ω RESISTORS RATED 5W.

stability of these glass resistors is of the same order as that of commercial standards sealed in dry gas and suitable for about $1/10$ of one watt only. The glass resistors can be loaded with 5 to 10 watts for a change of less than 10 parts in a million, they require no sealing and can be operated under ordinary ambient conditions.

VI) Remarks: Although this development has been made known by word of mouth and by means of scientific exhibitions this appendix is the first publication giving details of the design, construction, testing and performance of glass resistors.

Mr. F.C. Attwood, a former student of the author, has shown commendable skill and patience in winding the resistors.

Appendix 2.

The crossed rectangle parallel plate three terminal capacitor.

(a) Capacitance change as a function of geometrical configuration for square, circular and rectangular plates.

1) Introductory remarks: To the best of the author's knowledge the most superb low voltage three terminal air-capacitors are those described by Clothier (60) who uses circular plates. For their construction facilities for highest precision grinding, milling and turning are required together with outstanding workmanship.

Because in engineering the best compromise between economy of effort and performance is always aimed at it was thought interesting to find out how much the performance, in this case the stability, would suffer if less skill and time consuming care were employed in the construction of capacitors. An opportunity arose several years ago when, for an urgent measuring task, a capacitor of "non-standard" value was required. For the construction the following rather extreme specification was laid down: Besides handtools like files and thread cutting tools only a bench vice, a guillotine and a drillpress were to be used. The work was to be carried out by a person without any trade qualifications who could best be described as a handyman. The construction was to be on the lines shown in Fig. 11.

The capacitor was built but the author was the target of so much derision that a detailed investigation was not made at the time. After calibration in situ the capacitor was quickly used and for fear of mechanical disturbances it rested on a sponge rubber pad.

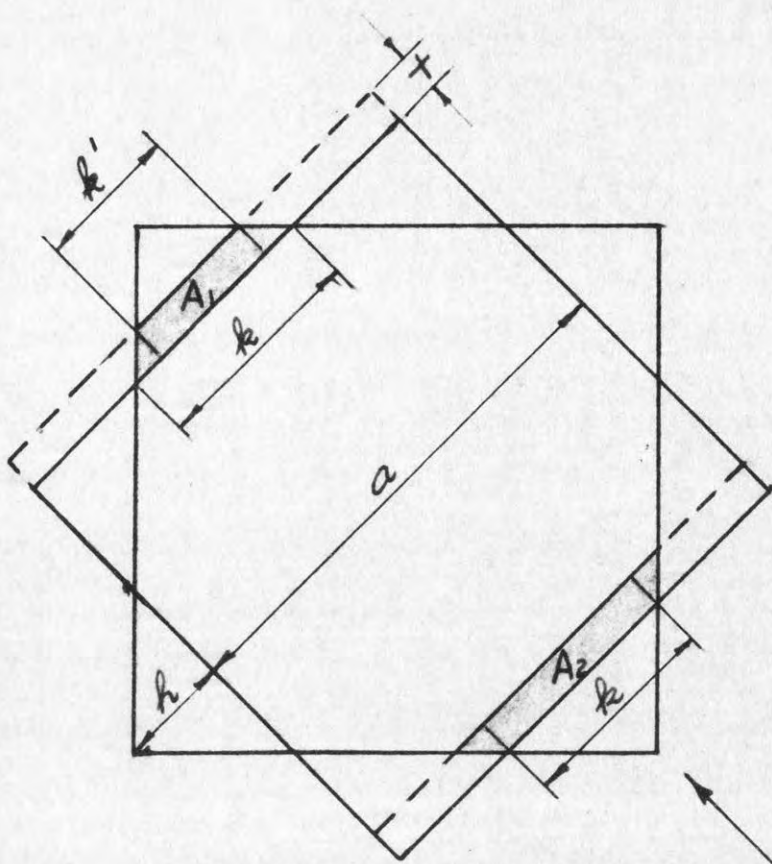
When for the purpose of this thesis capacitors of 1000 pF and 1300 pF (see Appendix 5) were required the old capacitor was tested as shown in Section (c) and it was found surprisingly stable. The 1300 pF capacitor shown in Plate 10 which can be changed to 1000 pF by removing plates was then built. This time the construction was carried out by a very rough handyman. The result was a stable capacitor as before.

It is the purpose of this appendix to suggest some reasons why capacitors as simply and economically constructed as shown in Plate 10 perform adequately in practice.

- ii) Square plates: An electrode system of crossed square plates is shown in Fig. 58. For a small movement (x) in the direction of the arrow the capacitance change which is proportional to the change in overlapped area is proportional to x^2 as shown in Fig. 58. A rather large change in the relative electrode position due to mechanical disturbances will therefore cause a small change in capacitance.
- iii) Circular plates of equal diameter: Fig. 59 shows two circular plates with their centres moved by a small distance (x). The equations and the example given show that this configuration is very sensitive to dimensional changes.
- iv) Crossed rectangles: From Fig. 60 it is obvious that a small movement in the directions marked 1, 2 or 3 will not alter the overlapped area and the capacitance. This configuration is not only simple to make but advantageous.

(b) Suggested explanation of good results obtained when deliberately rough workmanship was employed.

It is well known that in an electrode system consisting of one plate between two plates as shown in Fig. 61a the rate of change of capacitance is zero if plate 2 is situated equidistant from Plates 1 and 3. The error term x^2/d^2 (Fig. 61a) becomes large if the original position of Plate 2 is not equidistant. In Fig. 61a, any movement of the Plate 2 away from the centre increases the capacitance. Now, if a condition is assumed as in Fig. 61b, where the Plate is shown under an angle, a movement of the Plate in the direction of the arrow will increase $C_1 + C_1'$ (movement away from centre) but it will decrease $C_2 + C_2'$ (movement towards centre). In practice the plates were not flat and cut from sheet aluminium on a guillotine. The nuts used as spacers did not permit equidistant adjustment. It is therefore likely that the schematic representation of Fig. 61b applies, this being not limited



$$k' = k - 2x$$

$$A_1 = k'x + x^2 = kx - x^2$$

$$A_2 = kx + x^2$$

$$\Delta A = 2x^2 = 2n^2a^2 \text{ with } x = na.$$

$$h = \frac{a}{2}(\sqrt{2}-1)$$

$$C \propto \text{overlapped area } A \propto a^2 - 4h^2 \propto 0.83a^2$$

$$\frac{\Delta C}{C} = \frac{\Delta A}{A} = \frac{2n^2}{0.83}$$

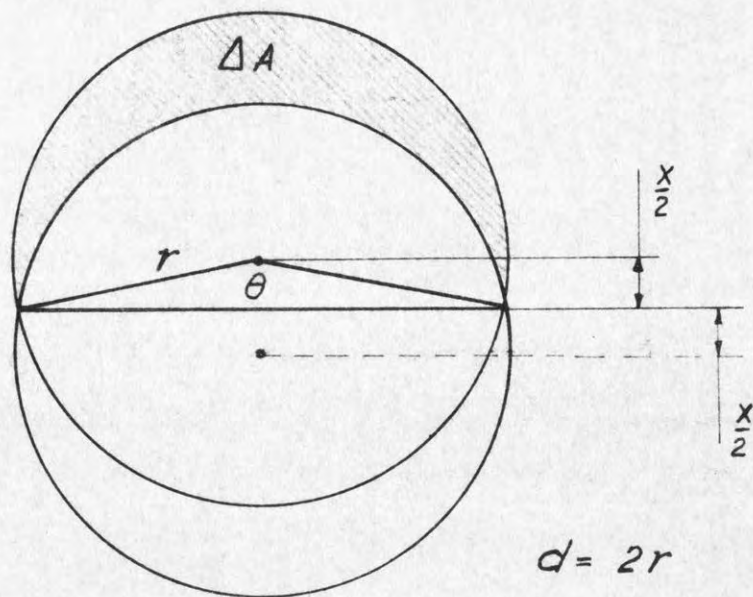
$$\text{Say: } a = 100 \text{ mm } (\sim 4''); x = 1 \text{ mm.}$$

$$\therefore n = 1/100$$

$$\frac{\Delta A}{A} = \frac{2}{8300} = 0.024 \%$$

FIG: 58

FOLLOWING PAGE: 97



FROM (61) : $\Delta A = r^2 \left(\pi - \frac{\pi\theta}{180} + \sin \theta \right) = r^2 \eta$

FOR $\frac{x}{d} < 0.3$, $\eta \sim \frac{4x}{d}$

$$\frac{\Delta C}{C} = \frac{r^2 \eta}{r^2 \pi} = \frac{4x}{\pi d}$$

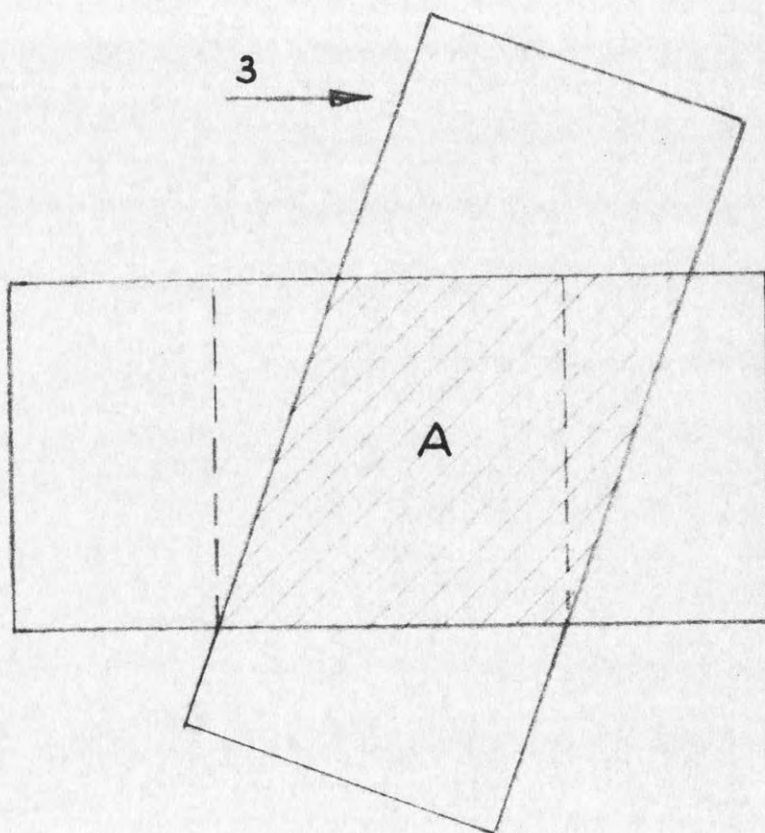
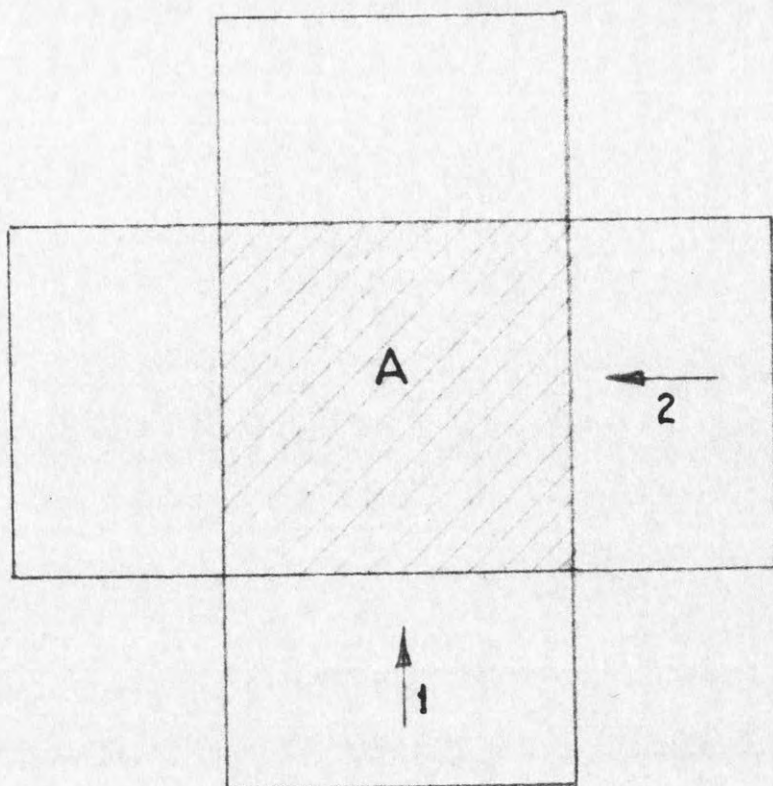
SETTING $x = nd$

$$\frac{\Delta C}{C} = \frac{4n}{\pi}$$

SAY : $n = \frac{1}{100}$ as before ;

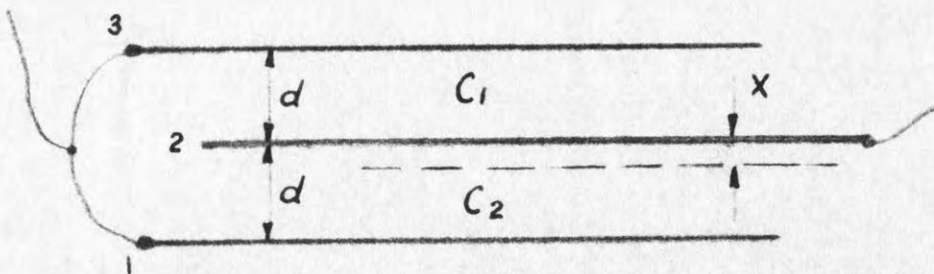
$$\frac{\Delta C}{C} = \frac{4}{100\pi} \sim 1.27\%$$

FIG. 59



FOLLOWING PAGE: 97

FIG. 60.



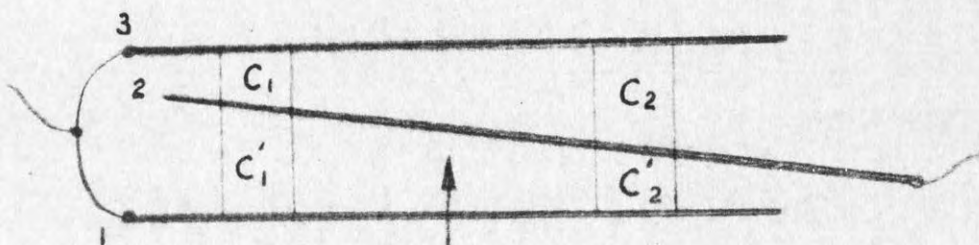
FOR EQUAL AREA AND PERMITTIVITY :

$$C = C_1 + C_2 = 2k/d.$$

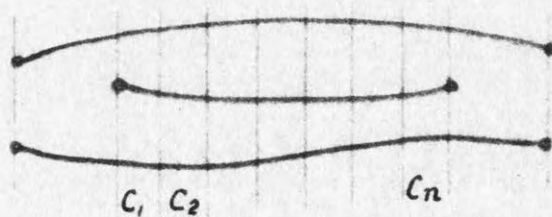
IF PLATE 2 DISPLACED BY SMALL AMOUNT x :

$$C = \frac{k}{d+x} + \frac{k}{d-x} = \frac{2k}{d} \left[1 + \left(\frac{x}{d} \right)^2 + \dots \right]$$

(a)



(b)



(c)

FOLLOWING PAGE: 97

FIG. 61.

to two dimensions. Thus it appears possible that owing to the infinite number of capacitances $(C_1 + C_1') + (C_2 + C_2') + \dots (C_n + C_n')$ as depicted in Fig. 6le cancellation of the changes occurs which together with the favourable electrode form may explain the good result.

From the first capacitor mentioned in Section (a, 1,) it was learned that an extremely strong box is required to prevent irreversible changes due to distortion when carrying the capacitor. Consequently, as shown in Plate 10 a very rigid base plate ($3/8$ inch) was used. The sides of the box are also rigid ($1/8$ inch) to prevent changing of the fringing field when pressing on the sides or the lid. The links between the baseplate and the mounting plate of the electrode assembly are relatively weak to prevent transmission of distortion of the base plate to the mounting plate. The relatively large plate spacing of approx. $1\frac{1}{2}$ m.m. is helpful and as it is large compared with the thickness of surface films it ensures a reasonably low power factor. The square metal bars which can be seen on Plate 10 between the porcelain bushings intercept flux from passing through solid insulation.

(c) Methods of testing.

1) Capacitance measurement: Owing to the temperature coefficient of capacitance and the influence of humidity and pressure on the permittivity of air a capacitor which is not sealed must be checked for mechanical stability under as constant ambient conditions as possible. Capacitance measurements were therefore made in an air-conditioned room. It is not intended to give complete details of the method of measurement because some data has been given in Section 3.1.2.6. and Fig. 10 of this thesis, in reference 20, and further techniques will be given in appendix 5. The principle of the procedure was as follows :

Glass resistors (see appendix 1) were arranged as a voltage divider to give a ratio 200/1. The phase angle of the divider was less than $1/10^3$ giving thus negligible magnitude difference between the A.C. voltage ratio and the ratio determined by conventional D.C. build up methods. Three capacitors, 5 pF/33 KV, (shown in reference 11 and 20, see reprints attached) and the 1000 pF capacitor to be tested in parallel with a micrometer capacitor (see appendix 5) formed also a 200/1 divider which could be

intercompared at 50 c/s with the resistive divider using a voltage of a few KV. By means of the capacitance divider a 22000/110 V Potential transformer could then be investigated for stability of ratio. As this ratio was found to be constant within $\pm 1/10^5$ over a period of one month and as furthermore the reading on the micrometer capacitor indicated a change of capacitance ratio of less than $1\frac{1}{2} / 10^5$ over the same period it was concluded that, in the air-conditioned room, the 22000/110 V transformer formed a suitable inductive ratio arm and that the 5 pF capacitor was a suitable standard for stability tests estimated to last several days.

The intercomparison with the resistive divider could have been omitted if it would not have been desired to check both arms independently. Alternatively the potential transformer could have been omitted and the resistance divider used only. However the inductive ratio arm bridge which requires no Wagner balance is more convenient when a large number of tests are to be made.

The capacitors were not sealed and changes due to humidity and pressure should have affected all air-capacitors equally. It would have been too much to expect that the temperature coefficients of capacitance were the same but this was of lesser importance owing to the rigid control of temperature. The test for capacitance changes was carried out by balancing the bridge and observing the change in the micrometer reading when the parallel plate capacitor was submitted to the tests described below.

(ii) Stability tests: Pressing rather hard at the top of the box caused changes of 1 to 2 in 10^5 which were completely reversible. Moderate blows with a wooden hammer had the same effect. Lifting the capacitor with both hands gave a completely reversible change of 3 in 10^5 . For this the C.R.O. display was calibrated first in parts in 10^5 . Hard knocks with a hammer or setting the capacitor down hard gave an irreversible change of 4 in 10^5 but one knock at another spot restored the original value. Turning the capacitor on it's side gave a change of 15 in 10^5 of which 1 in 10^5 remained irreversible. The capacitor was then carried to an oven, heated for six hours to 50 degr. C., cooled during the night and measured in the morning. This was repeated three times. The changes observed were within ± 3 in 10^5 of the original value. This was particularly pleasing because it is regarded as a

severe test for the detection of the effects of structural constraints. The mean temperature coefficient of capacitance in the range 20 to 40 degr. C. was found to be $3 \text{ pp } 10^5$ per degr. C. which is not very much higher than the coefficient of linear expansion of Aluminium.

Appendix 3.Computation and measurement of the self-capacitance of multiple layer and multiple pie coils.(a) The "VA" Rule.

If a network containing also capacitances C_1, C_2, \dots, C_n , the voltages on which are e_1, e_2, \dots, e_n is connected to a source of voltage V :

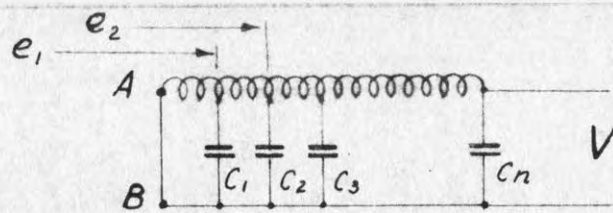
$$e_1^2 \omega C_1 + e_2^2 \omega C_2 + \dots = V^2 \omega C_x$$

wherein C_x is the capacitance seen by the source. Normally the voltages $e_1 \dots e_n$ will only be known if the capacitances $C_1 \dots C_n$ do not significantly alter the voltage distribution in the network. This is very often the case at low frequencies and the calculation of the effective value C_x of a distributed capacitance is thus possible.

(b) Derivation of an expression for transformer coil capacitance.

It is shown in Fig. 62a that for a single layer coil wound over a (static) shield or for a resistor having uniformly distributed ground-capacitance, $C_x = C/3$. C is the capacitance measured between shield and coil with the connection A...B open.

For a coil with N layers and a mean layer to layer capacitance of value C : $C_x = (N - 1) / N^2 \times 4/3 \times C$ as shown in Fig. 62b.



$$C_1 = C_2 = C_3 = \dots = \frac{C}{n}$$

$$e_1 = \frac{V}{n}; e_2 = \frac{2V}{n}; e_3 = \dots$$

$$VA_1 = \frac{V}{n} \cdot \frac{V}{n} \omega \frac{C}{n} = V^2 \cdot \frac{\omega C}{n^3} \cdot 1^2$$

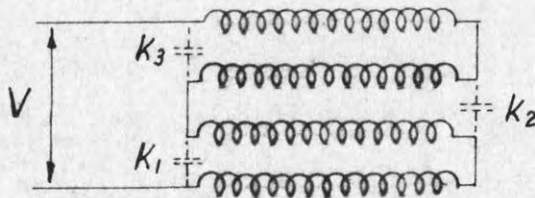
$$VA_2 = V^2 \frac{\omega C}{n^3} \cdot 2^2$$

$$1^2 + 2^2 + 3^2 + \dots + n^2 = \frac{n^3}{3} \text{ if } n \gg 1.$$

$$\sum VA = V^2 \frac{\omega C}{n^3} (1^2 + 2^2 + \dots) = V^2 \omega C x$$

$$\therefore \boxed{C_x = \frac{C}{3}}$$

(a)



N.... LAYERS

N-1...CAPACITANCES k_1, k_2 ... EACH OF VALUE $\frac{C}{3}$

VOLTAGE ON k_1, k_2 ... $\frac{2V}{N}$

$$\sum VA = (N-1) \left(\frac{2V}{N} \right)^2 \omega \frac{C}{3} = V^2 \omega C x$$

$$\therefore \boxed{C_x = \frac{N-1}{N^2} \cdot \frac{4C}{3}}$$

(b)

FIG. 62.

For simple layer wound coils this expression gives reasonable results, the limitation being the accurate knowledge of area, spacing and permittivity in the calculation of C . However in the 100 KV testing transformer mentioned in Section 3 the situation was much more complicated because the secondary consisted of 20 layer wound pie coils in series. Schematically the arrangement was as shown in Fig. 63a.

Neglecting the small voltage drop along one layer of one pie and assuming the low voltage primary and the tertiary which is interwound with it at earth potential the VA may be tabulated as in Fig. 63b.

Instead of calculating the capacitances C_{1a} , C_{2a} , and C_{1d} , C_{2d} , a reasonable approximation is to assume that, in Fig. 64, the inner and outer edges of the pies form two imaginary cylinders Z_1 and Z_2 having distributed ground-capacitances K_1 and K_2 . If further the second line in Fig. 63b is neglected the much simpler expression of Fig. 64 follows if one also assumes equal pie self-capacitances K_3 and inter pie capacitances K_4 . As all pies are equal and equally spaced this assumption is valid.

C_x must in practice be increased by the capacitance of the bushing. K_1 and K_2 were computed using the well known expressions for concentric cylinders, the tank being one electrode for K_2 . K_4 was computed as parallel plate capacitor and K_3 as shown in Fig. 62b for layer wound coils.

Such a calculation can, at the best, be only an intelligent estimate because of the simplifying assumptions made, the effect of fringing and the uncertainties mentioned before.

Throughout this thesis it was never intended to swell its volume by recording a large amount of arithmetical work and it is therefore thought superfluous to give more than the result of the computation. The computed value of C_x which included an estimate of the bushing capacitance was about 800 pF or approx. 25% higher than measured in Section (c). This disagreement is not too great considering that the effective permittivity of the various dielectrics was judged from experience on much smaller transformers.

(c) A practical method of measuring the self-capacitance of very large iron cored coils.

Fig. 65 shows the arrangement. The method is limited to transformers because a second winding is required.

The tertiary of the 100 KV testing transformer was bridged with a resistor of value 0.001 Ohm made from several paralleled strips of constantan. Voltage was applied from an audio oscillator via an amplifier and matching transformer T. At some frequency F_1, F_2, \dots series resonance occurs between the leakage inductance of T_x and the sum of self-capacitance C_x and load-capacitance C. Resonance is indicated by a maximum deflection of the V. T. V. M.

$$\omega_1^2 L_L C_x = 1; \quad C = 0$$

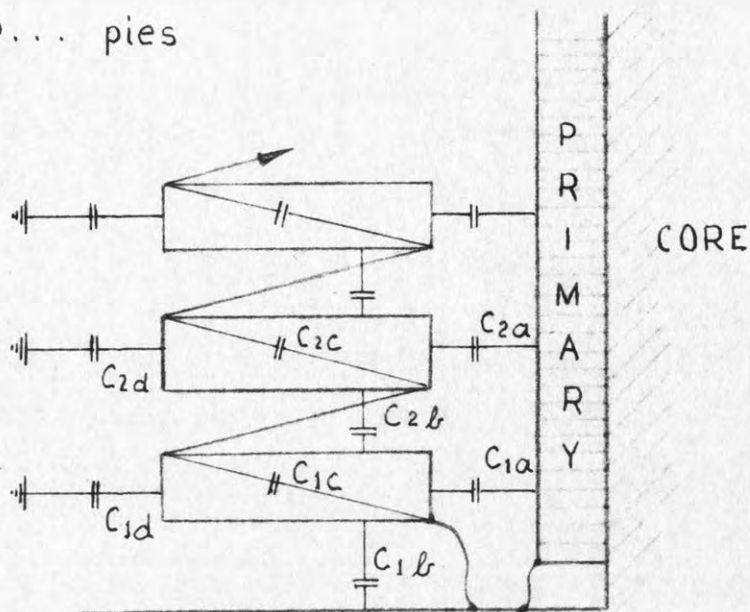
$$\omega_2^2 L_L (C_x + C) = 1$$

$$\therefore C_x = \frac{C}{\left(\frac{f_1}{f_2}\right)^2 - 1}$$

Fig. 65 gives also the results of tests on the 100 KV transformer. As the capacitance of the V. T. V. M. plus the zero capacitance of the decade capacitor box was 94 pF the true self-capacitance of the 100 KV transformer is $713 - 94 \sim 620$ pF which agrees closely with the expected value. See Section 3.1.2.7.

It should be stressed that this method in which resonance with the leakage inductance is established is superior to the well known scheme of resonating with the shunt inductance. The self-capacitance is associated with both inductances but as the change in ratio with capacitance is brought about by the effect of capacitance on the leakage inductance it is, for the

P... pies

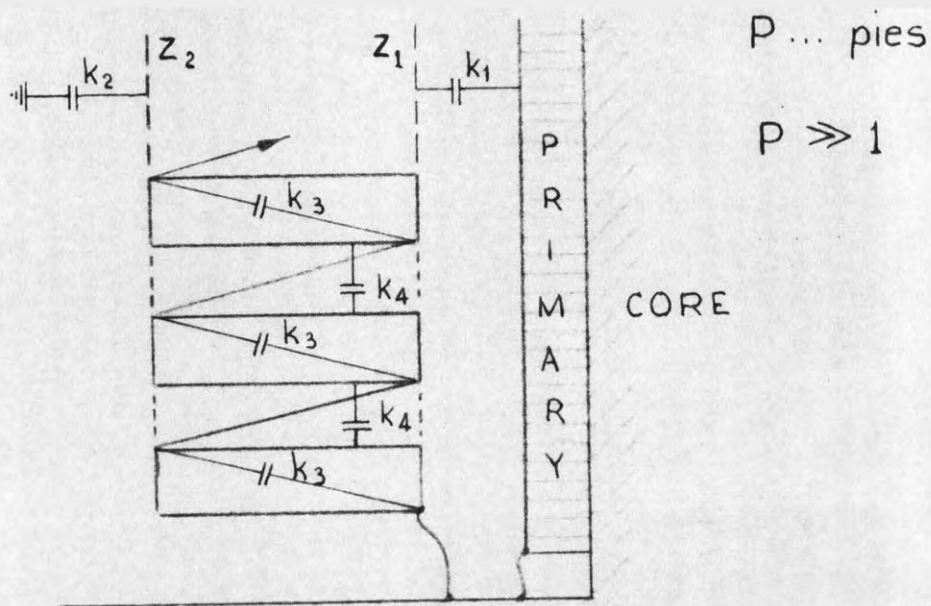


(a)

COIL	CAP.	EFFECTIVE	VOLTAGE	VA
1	C_{1a}	FULL	0	0
	C_{1b}	$\frac{1}{3}$	$\frac{V}{P}$	$\left(\frac{V}{P}\right)^2 \omega \frac{C_{1b}}{3}$
	C_{1c}	FULL	"	$\left(\frac{V}{P}\right)^2 \omega C_{1c}$
	C_{1d}	"	"	$\left(\frac{V}{P}\right)^2 \omega C_{1d}$
2	C_{2a}	"	"	$\left(\frac{V}{P}\right)^2 \omega C_{2a} \cdot 2^2$

(b)

FIG. 63.



$$\sum V_A \approx V^2 \omega \left(\frac{k_1 + k_2}{3} \right) + P \left[\left(\frac{V}{P} \right)^2 \omega k_3 + \left(\frac{V}{P} \right)^2 \omega k_4 \right]$$

FIG. 64.

- (c) A practical method of measuring the self-capacitance of very large iron cored coils.

Fig. 65 shows the arrangement. The method is limited to transformers because a second winding is required.

The tertiary of the 100 KV testing transformer was bridged with a resistor of value 0.001 Ohm made from several paralleled strips of constantan. Voltage was applied from an audio oscillator via an amplifier and matching transformer T. At some frequency F_1, F_2, \dots series resonance occurs between the leakage inductance of T_x and the sum of self-capacitance C_x and load-capacitance C. Resonance is indicated by a maximum deflection of the V. T. V. M.

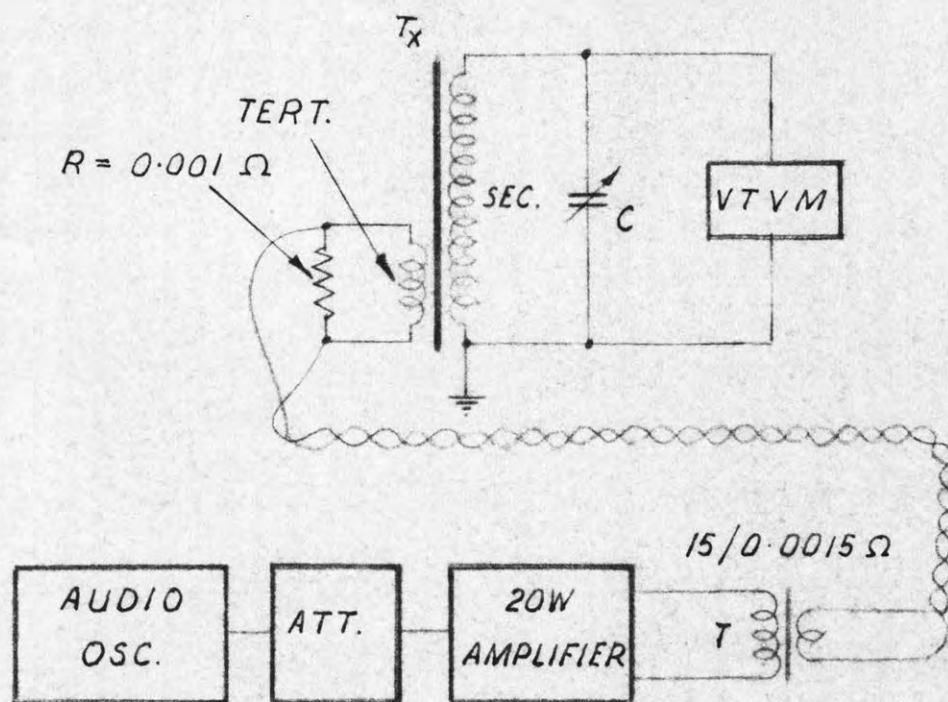
$$\omega_1^2 L_L C_x = 1; \quad C = 0$$

$$\omega_2^2 L_L (C_x + C) = 1$$

$$\therefore C_x = \frac{C}{\left(\frac{f_1}{f_2}\right)^2 - 1}$$

Fig. 65 gives also the results of tests on the 100 KV transformer. As the capacitance of the V. T. V. M. plus the zero capacitance of the decade capacitor box was 94 pF the true self-capacitance of the 100 KV transformer is $713 - 94 \sim 620$ pF which agrees closely with the expected value. See Section 3.1.2.7.

It should be stressed that this method in which resonance with the leakage inductance is established is superior to the well known scheme of resonating with the shunt inductance. The self-capacitance is associated with both inductances but as the change in ratio with capacitance is brought about by the effect of capacitance on the leakage inductance it is, for the



C pF.	f_1 c/s	f_2 c/s	C_x pF.
0	935	—	—
2000	—	477	705
5000	—	331	717
30 000	—	143	717

} MEAN 713 pF

FIG. 65

MEASUREMENT OF SELF-CAPACITANCE OF THE 100 kV TRANSFORMER AND RESULTS.

present purpose, more fundamental to use the latter one. Also, the "Q" of the leakage inductance is higher and sharp resonance is easy to obtain. Furthermore this inductance being mainly an air-inductance is nearly constant at different frequencies and the validity of the expression for C_x is ensured. By making R in Fig. 65 very much smaller than ωL referred to the winding to which R is connected the effect of R on "Q" can be made negligible.

Appendix 4.The design of optimum "Q" reactors (Hysteresis not neglected).(a) Conditions for optimum "Q".

Let (i) be the current through a coil of inductance (L) and series loss resistance (R) connected to a source of sinusoidal voltage (V).

$$i = V / (R^2 + \omega^2 L^2)^{\frac{1}{2}}$$

$$Q = \omega L / R$$

$$i = V / \omega L \left(1 + \frac{1}{Q^2} \right)^{\frac{1}{2}}$$

$$\text{For } Q > 5$$

$$i \approx V / \omega L$$

$$Q = \frac{VA}{W} = \frac{i V}{W_i + i^2 R_c}$$

wherein W_i are the iron losses and R_c the winding resistance. For constant fluxdensity and frequency :

$$\frac{dQ}{di} = \frac{(W_i + R_c i^2) V - V \cdot i \cdot 2 \cdot i R_c}{(W_i + i^2 R_c)^2} = 0$$

$$\therefore Q = \text{MAX if } W_i = i^2 R_c$$

For low frequencies and thin wire R_c equals the D.C. resistance and can readily be computed. The problem lies in the computation of the iron losses.

(b) The "General Radio" Method (62).

The assumption is made that the reactor is used at such a low level that the iron has its initial permeability and that the fluxdensity is very small. Under these conditions the hysteresis losses vanish and the remaining eddy current losses can be readily computed from the knowledge of frequency, iron volume, thickness of laminations and the resistivity of the iron. (See also Section c).

(c) Improvement on the "General Radio" method.

Often the assumption of low fluxdensity is not possible particularly in the design of reactors operating at 50 c/s.

Another method was developed some time ago and it has been used often since. While not being as direct as the G.R. method, with a little experience, even the first trial calculation is usually found to be correct.

From graphs provided by the manufacturers or from measurements the total iron loss in W/kg as a function of the fluxdensity (B) is known. The approximation is then made that at one frequency the losses are proportional to B^2 . This can easily be observed to be correct over a small range of (B) from published data on silicon iron, mu - metal and Radio-metal.

$$W_i = \frac{W}{kg} \cdot Vol \cdot g \cdot \frac{B^2}{B^2}$$

wherein "Vol" is the volume in cm^3 and "g" the density in kg/cm^3 .

Set :

$$\frac{W}{kg} \cdot \frac{1}{B^2} = K_m$$

$$W_i \approx K_m \cdot Vol \cdot g \cdot B^2$$

Because for optimum "Q" :

$$W_i \propto B^2 \propto \left(\frac{V}{N}\right)^2 = i^2 R_c \propto \left(\frac{V}{\omega L}\right)^2 R_c$$

the number of turns (N) may be determined without actual knowledge of "B" as in the G.R. method.

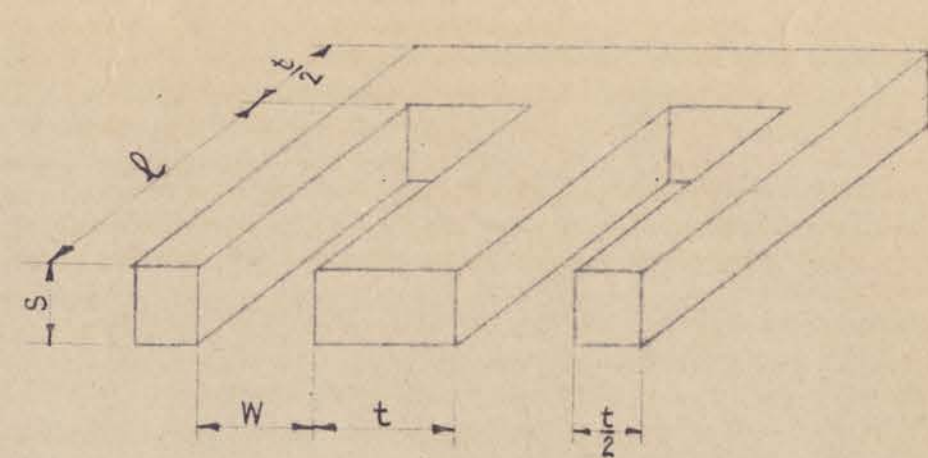
The procedure in practice rests on estimating a value of (B) and obtaining K_m by dividing the figure of W/kg taken from a graph by B^2 . If afterwards, after the turns have been computed, it is found that (B) lies between $\frac{1}{2}$ to 2 times the estimated value, no new calculation is necessary because $W \propto B^2$ is sufficiently close for this range. If however the estimate was wrong a second calculation will be quite close to the improved estimate.

d) Derivation of equations.

This is shown in Fig. 66 for "EI", "E \exists " or "E \neg " laminations. Expressions for the number of turns, the air-gap and "Q" are given. The air-gap formula is not derived because it directly follows from the general expression of the inductance of an inductor with air-gap. Fringing is neglected because in practice some adjustment to the computed gap is always necessary. If iron losses are to equal the copper losses the "Q" value as given follows. No allowance is made for stacking factor as this would only pretend fictitious accuracy, β the winding space factor being an estimate only. It should be noted that in high "Q" reactors the losses in the reactor capacitance may become significant. See example in Section (e).

(e) Typical data and a sample design.

The worked example concerns an inductor the author was asked to design for the Electricity Commission of New South Wales. This was to be the prototype compensating reactor for 66 KV capacitive potential transformers used in the protective system of the Hornsby-Ryde line. Its rating was: 1700 Ky at 8 mA r.m.s. and 50 c/s. The "Q" value was to exceed 20.



N Turns.

d Wire diameter, cm.

R_c Winding Resistance. Ω .

ρ Resistivity of copper, $1.75 \cdot 10^{-6} \Omega \text{ cm}$.

β Winding space factor.

W_i Iron losses, W.

B Flux density, lines/cm².

g Iron density, kg/cm³.

L Inductance, Hy.

V Voltage, V.

f Frequency, c/s.

K_m (W/kg) ($\frac{1}{B^2}$) See section C.

Mean turn: $2(s + t + \frac{W\pi}{2})$

$$R_c = \frac{N \cdot 2(s + t + \frac{W\pi}{2}) \rho}{\frac{d^2 \pi}{4}}$$

$$d^2 N = W \ell \beta$$

$$\frac{d^2 \pi}{4} = \frac{W \ell \beta \cdot \pi}{N}$$

$$R_c = \frac{N^2 \cdot 8 \cdot (s + t + \frac{W\pi}{2}) \rho}{W \ell \beta \pi}$$

$$i^2 R_c = W_i = K_m \cdot \text{Vol.} \cdot g \cdot B^2$$

$$i = \frac{V}{\omega L} ; (2\pi)^2 \sim 40 ; B = \frac{V \cdot 10^8}{4.44 f N s t}$$

$$\underbrace{\frac{V^2}{40 f^2 L^2}}_{i^2} \cdot \underbrace{\frac{N^2 \cdot 8 \cdot (s + t + \frac{W\pi}{2}) \rho}{W \ell \pi \beta}}_{R_c} = K_m \cdot \underbrace{2 s t (\ell + W + t)}_{\text{weight.}} \cdot \underbrace{g \cdot \left(\frac{V \cdot 10^8}{4.44 f N s t} \right)^2}_{B^2}$$

$$N^2 = 10^8 L \sqrt{\frac{K_m \pi (\ell + W + t) g W \ell \beta}{2 \rho s t (s + t + \frac{W\pi}{2})}}$$

$$Q = \frac{\omega L}{2 R_c}$$

Air Gap:

$$\mathcal{V} = \frac{4 \pi N^2 s t}{L 10^9} - \frac{\ell_m}{\mu}$$

$$\ell_m = \text{Iron path} = 2(\ell + W + t)$$

FIG: 66.

Because the cost of the reactor was only a very small fraction of the cost of the total arrangement a higher "Q" than 20 was aimed at to provide for production tolerances. Fig. 67 shows the use of the formulas given in Fig. 66. For brevity's sake the routine calculations connected with the winding build up are not shown. The fluxdensity was 50% higher than estimated but β was much lower, R_e therefore higher. The reason for this was that, in view of the importance of the project, large insulation clearances and rather thick wire insulation were chosen. The "Q" was therefore lower than computed. The actual value measured was 32 while from the check calculation of Fig. 67 a value of 34 was expected. This discrepancy was found to be due to eddy current loss in the rather substantial brackets and loss in the coil capacitance. This could be proved by measuring without brackets and by using a core connection in which the main effective loss capacitance appears across the detector of the bridge shown in the next Section. The actual reactors built were required to have taps for tuning purposes and it was found that the tap at 42500 turns and a slight change in the gap gave a better Q. This is as expected from Fig. 66 and 67.

Losses in the insulation reduced the "Q" much further when the reactor was exposed to a humid atmosphere. This was a nuisance during the development but of no importance in practice because the reactor was vacuum impregnated in oil and sealed in one container with the potential transformer.

For small 50 c/s inductors or small gapped tuned transformers made of mu-metal and using 0.015 inch thick laminations, a K_m value of 3×10^{-9} was found to be a good starting point for calculations.

(f) A simple bridge for the measurement of "L" and "Q".

An ordinary Maxwell or resonance bridge would require components of awkward value which would have to be suitable for high voltage in order to check the reactor shown in Fig. 67 at its rated voltage, viz : 4300 V.

Fig. 68 shows a resonance bridge devised for the purpose in which ordinary components were used in addition to inductive ratio arms. Further advantages are the absence of a Wagner balance and one earthed detector terminal which is convenient for electronic detectors of the type shown in Fig. 12. The inductive ratio arms were a 6600 /110 V standard potential transformer in cascade with a 110/11 V transformer. As the reactors were

$$L = 1700 \text{ Hy}; \quad i = 8 \text{ mA}; \quad f = 50 \text{ c/s}; \quad Q \cong 20.$$

Laminations 29# EΞ.

$$\begin{aligned} W &= 3.4 \text{ cm.} & \rho &= 1.75 \cdot 10^{-6} \Omega \text{ cm.} \\ t &= 4.6 \text{ cm.} & g &= 7.5 \cdot 10^{-3} \text{ kg/cm}^3 \\ S &= 6.3 \text{ cm.} & \beta &= 0.35 (\text{say}). \\ \ell &= 17 \text{ cm.} \end{aligned}$$

$$\begin{aligned} \text{Say: } B &= 1000 \text{ l/cm}^2 \rightarrow 18 \text{ mW/kg.} \\ K_m &= 18/1000 \cdot 1000^2 = 18 \cdot 10^{-9}. \end{aligned}$$

$$\ell + W + t = 25 \text{ cm}; \quad S + t + \frac{W\pi}{2} = 16.2 \text{ cm.}$$

$$N^2 = 10^8 \cdot 1700 \sqrt{\frac{18 \cdot \pi \cdot 25 \cdot 7.5 \cdot 3.4 \cdot 17 \cdot 0.35}{10^9 \cdot 10^3 \cdot 2 \cdot \frac{1.75}{10^6} \cdot 6.3 \cdot 4.6 \cdot 16.2}}$$

$$N^2 = 19.4 \cdot 10^8 \quad N = 44000 \text{ turns.}$$

$$R_c = \frac{19.4 \cdot 10^8 \cdot 8 \cdot 16.2 \cdot 1.75 \cdot 10^{-6}}{3.4 \cdot 17 \cdot 0.35 \pi} = 6900 \Omega$$

$$Q = \frac{314 \cdot 1700}{2 \cdot 6900} = 39$$

$$\ell_m = 2.25 = 50 \text{ cm}; \quad \mu: \text{ Say } 2000$$

$$\phi = \frac{4\pi \cdot 19.4 \cdot 10^8 \cdot 6.3 \cdot 4.6}{1700 \cdot 10^9} - \frac{50}{2000} \sim 0.4 \text{ cm}$$

Checks:

1: For gross error of turns. Assume zero reluctance of iron

$$L = \frac{1.26 N^2 S t}{\phi \cdot 10^8} = \frac{1.26 \cdot 19.4 \cdot 10^8 \cdot 6.3 \cdot 4.6}{0.4 \cdot 10^8} \sim 1770 \text{ Hy.}$$

2: For B:

$$V = i \omega L = 8 \cdot 10^{-3} \cdot 314 \cdot 1700 = 4300 \text{ V.}$$

$$B = \frac{V \cdot 10^8}{4.44 \cdot f \cdot S \cdot t \cdot N} = \frac{4300 \cdot 10^8}{4.44 \cdot 50 \cdot 29 \cdot 44000} = 1550 \text{ l/cm}^2$$

3: For equality of losses.

(a) Iron losses.

at 1550 l/cm² ---- 43 mW/kg
iron weight from weighing of one lamination: 11.3 kg
 $W_i = 43 \cdot 10^{-3} \cdot 11.3 = 0.48 \text{ W.}$

(b) Copper losses.

Wire # which can be wound on:
36 S.W.G. En. + 2 x silk.

Mean turn: $2 \times 16.2 = 32.4 \text{ cm} = 12.8 \text{ inches.}$

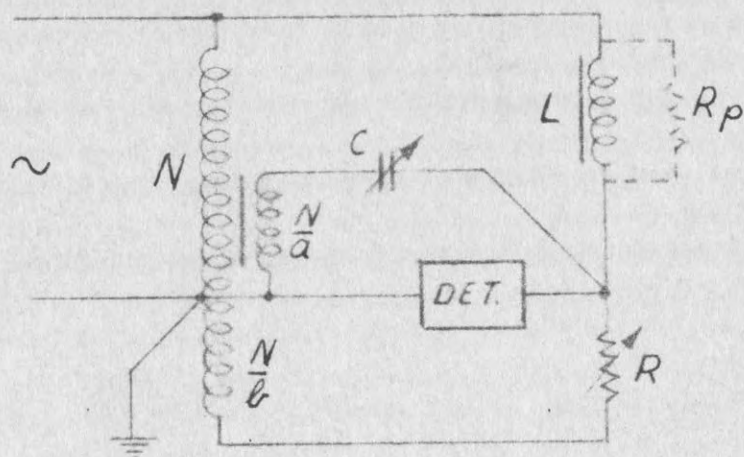
$$\frac{44000 \cdot 12.8}{36} = 15600 \text{ yds} \rightarrow 8250 \Omega$$

$$i^2 R_c = \left(\frac{8}{1000}\right)^2 \cdot 8250 = 0.53 \text{ W}$$

$$\therefore i^2 R_c \sim W_i$$

$$Q = \frac{VA}{W} = \frac{8 \cdot 10^{-3} \cdot 4300}{0.53 + 0.48} = 34$$

FIG. 67.



At resonance:

$$\frac{R_p}{R} = \frac{N}{\frac{N}{b}}$$

$$R_p = bR$$

$$Q = \frac{R_p}{\omega L} = \frac{bR}{\omega L}$$

$$LC' = \frac{1}{\omega^2}$$

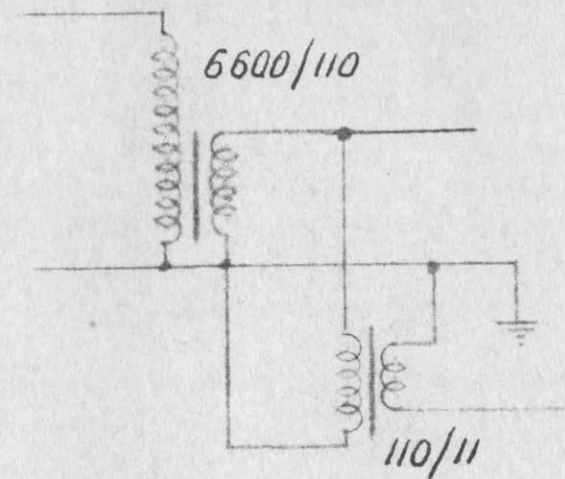
$$C' = \frac{C}{a}$$

$$L = \frac{a \cdot 10^6}{\omega^2 C}$$

$$Q = \frac{bRC\omega}{a \cdot 10^6}$$

} C in μF

For :



$$a = 60$$

$$b = 600$$

at 50 c/s; $\omega^2 \sim 10^5$

$$\therefore L \cong \frac{600}{C}$$

$$Q \cong \frac{RC}{314}$$

FIG. 68

HIGH VOLTAGE PARALLEL RESONANCE
BRIDGE WITH INDUCTIVE RATIO ARMS.

produced in a transformer factory the inductive ratio arms were much easier to obtain than high voltage components for more conventional bridges. The ratio error and phase angle of the combination was considerably smaller than 1% and the simple equations given in Fig. 68 could be used without corrections. For $L = 1700$ Hy and a "Q" of 30, at 50 c/s the order of component values were 0.35 microfarad for the capacitor and 27000 Ohms for the resistor. The voltage on R and C was approx. 7 and 70 V respectively. Thus ordinary laboratory equipment was suitable.

APPENDIX 5.A crossed cylinder high voltage three terminal air capacitor.a) The electrode configuration for an experimental model.1) Introduction.

A loss free high voltage capacitor is an important piece of equipment in any high voltage laboratory. The usual order of capacitance is 50 pF but owing to the use of high impedance electronic detectors and the use of the three terminal principle 1/10 or even 1/100 of this value is suitable for many purposes. Besides its more conventional use in high voltage Schering bridges and for the determination of the errors of potential - transformers (20) applications for such a capacitor are described in Sections 3.1.2.6. and 3.1.2.9. as well as in Section (e) of this Appendix.

Some 11 years ago an attempt was made to build a three terminal vacuum capacitor rated 5 pF / 200 KV_p. This resulted in failure. An arc occurred at $\frac{1}{2}$ the rated voltage, and worse still, a sharp increase in power factor was observed above 30 KV_p. The gradients were far too small to explain this by field emission and it is believed that, owing to the difficulty in degassing the structure with inadequate equipment and the necessity to introduce a getter, some getter material was deposited on the electrodes thus enormously lowering their work function. It was scant consolation that commercial two terminal vacuum capacitors and a transmitting triode used as a capacitor also showed the steep increase in power factor at low voltages and that it was learnt that a similar attempt at the P. T. R. (Berlin) also failed.

A compressed gas capacitor was then built and was actually working. Due to an oversight an explosion occurred. Nobody was hurt but the electrodes were wrecked.

Then, in despair, the air capacitor shown in Plate 2 was designed and built but its rating is only approx. 120 KV_p because a larger structure was unmanageable.

The crossed cylinder capacitor, an outcome of the work described in

this thesis has at last provided the author with a capacitor the voltage rating of which is higher than that of the testing transformer.

ii) The electrode configuration.

The simplest possible arrangement was aimed at in order to enable the author to build the capacitor himself and it was also required that assembly and dismantling should be very easy so that the capacitor could be packed into a suitcase for calibration work in the field. Plate 11 shows the rather unusual capacitor which has been nicknamed "organ-pipes".

An aluminium base plate carries an insulator of the same type and having the same dimensions as that shown in Plate 1 and Fig. 1 which in turn supports the shanks of two paralleled horizontal high voltage cylinders made of 3 inch diameter aluminium tubing. One vertical cylinder carries a centrally arranged wrap of 3 inch wide polythene and a 2 inch wide wrap of shim brass. Through a hole in the polythene and the cylinder this brass strip, which forms the low voltage electrode, is connected to a concentric connector. The connection is made inside the hollow vertical cylinder. The protruding polythene (white in the photo) is in the field and causes a small power factor. Owing to its small thickness ($\frac{1}{2}$ mm) as compared with the spacing (75 mm) this was neglected in this model but in the final model (Fig. 70) this power factor will be eliminated. The main dimensions of the experimental model are shown in Fig. 69.

The principle shown in Fig. 70 in which the solid insulation of the low voltage electrode is completely removed from the field is also employed in the capacitor shown in Plate 2. This type of construction permits high precision as only turned parts are required. T are the guard tubes and W is the working electrode. Proper spigotting ensures self-centering.

b) A simple bridge for capacitance measurement.

The capacitance aimed at was 0.5 pF but during the investigation into the properties of this capacitor capacitances up to 3 pF had to be measured. A minimum fractional accuracy of 1 part in 1000 was thought desirable.

The bridge operates at 50 c/s and contains an inductive ratio arm, a 1300 pF capacitor shown in Plate 10, Fig. 11 and described in Appendix 2 and

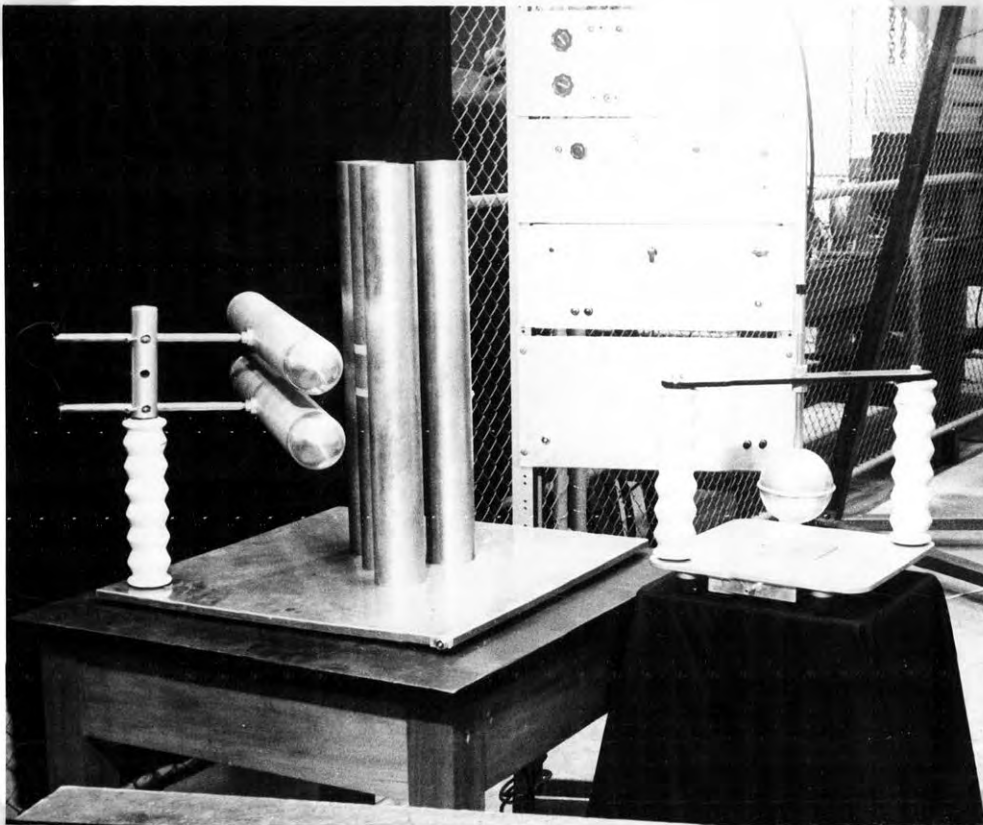
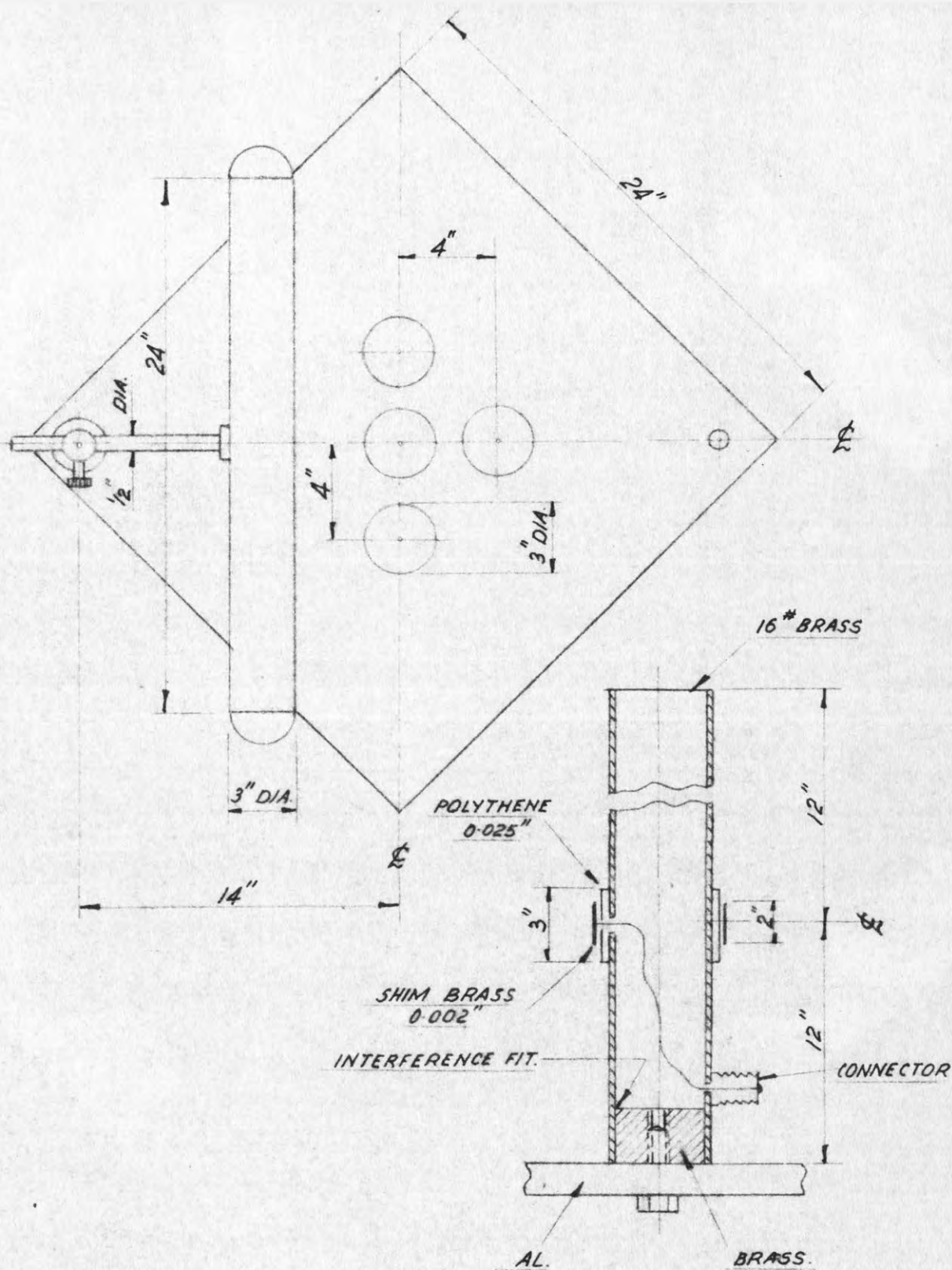


Plate 11. The experimental crossed cylinder capacitor



**FIG.69. MAIN DIMENSIONS OF EXPERIMENTAL
CROSSED CYLINDER CAPACITOR**

FOLLOWING PAGE: III

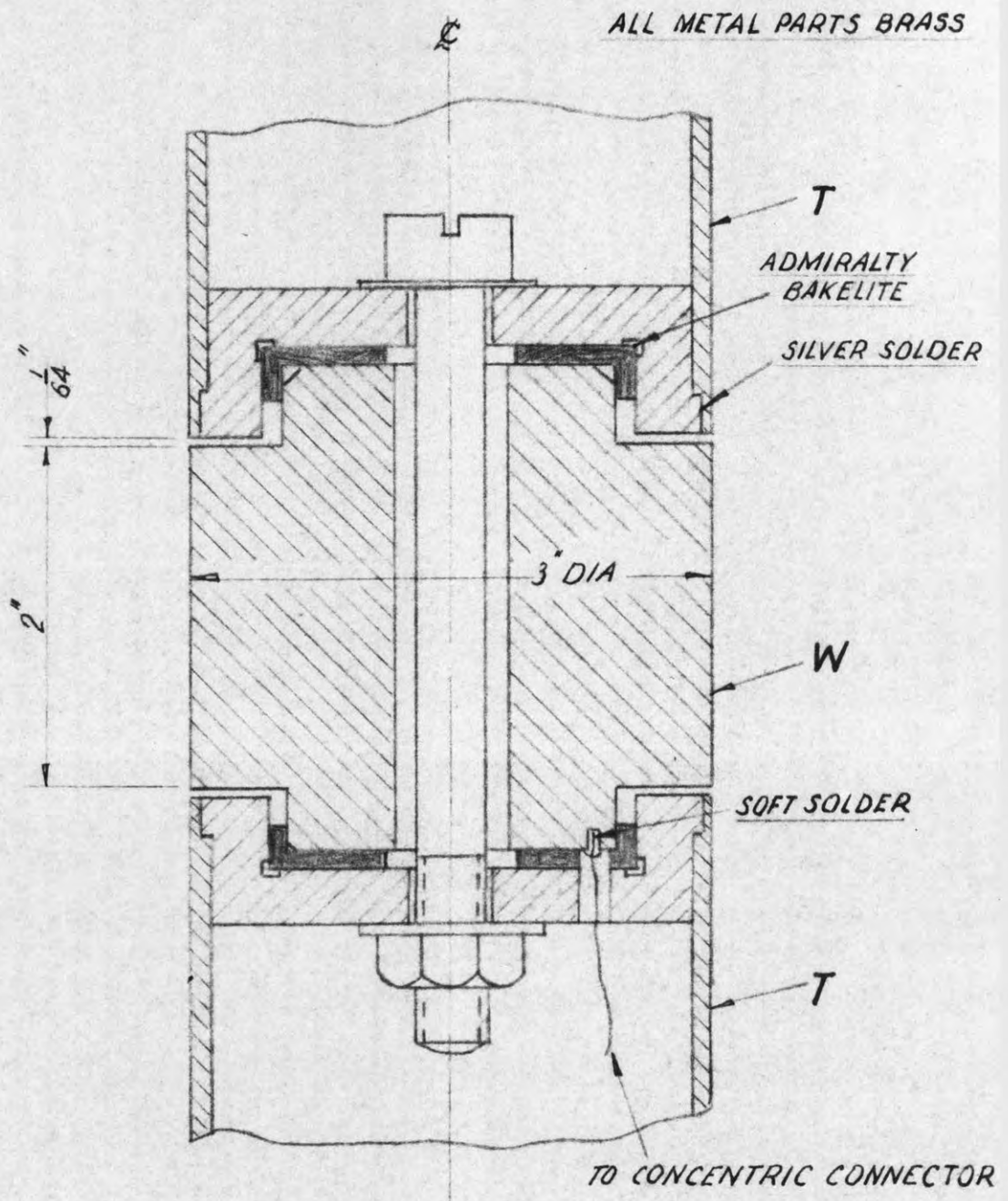


FIG. 70 PRINCIPLE OF HIDDEN INSULATION IN THE LOW VOLTAGE ELECTRODE ASSEMBLY OF A HIGH VOLTAGE 3 TERMINAL CAPACITOR

an easily constructed three terminal micrometer capacitor as shown in Fig. 71. This figure, which gives the main dimensions and materials is self explanatory but it should be mentioned that for ease of reading, a 3 V lamp, 2 torch cells and a press button are incorporated for the illumination of the micrometer scale. The micrometer spindle has a diameter of 0.682 cm and for a scale factor of 2/1000 pF per 1/1000 inch a diameter of the bore of 1.362 cm was computed from the well known expression of capacitance of cylindrical capacitors. This bore is close to 17/32 inch and using a drill of this size a scale factor of 0.00203 pF / 0.001 inch was obtained. The scale factor is constant within the range $\frac{1}{4}$ to $\frac{3}{4}$ inch and the range, without corrections, is therefore 1pF.

The inductive ratio arm is based on a universal transformer used throughout this thesis (e.g. see Fig : 5, 7, 17, 18, 25, 26, 35, 36, 74). This transformer which is in no way "special" is very convenient for laboratory work at 50 c/s and at audio frequencies and more than a dozen of these are used by the author's colleagues. It is regretted that this transformer which is ideal for a student's laboratory is not produced commercially. Its data are : No 95 Stalloy, crosssection 1.9 square inches, 4 turns per volt, windings and D.C. resistances : 240 V - 17 Ohms, Shield, 6 V - 0.08 Ohms, 240 V tapped at 100, 140, 200 - 104 Ohms, 240 V tapped at 100 140, 200 - 104 Ohms, Shield, 100 V tapped every 10 V by wander lug - 19 Ohms, 10 V tapped every 1 V by wander lug - 0.08 Ohms, 1 V tapped $\frac{1}{4}$, $\frac{1}{2}$, $\frac{3}{4}$ - 0.01 Ohm, Shield. The two 240 V windings are side by side to ensure equal impedances.

The bridge circuit is shown in Fig. 72. With the switch S on A the capacitance of C_1 will be $1300/(480:0.5) = 1.34$ pF which is well within the upper limit of the linear range of C_1 . Taking the lower limit as $\frac{1}{4}$ inch or 0.5 pF, capacitors C_x up to $1.34 - 0.5 \sim 0.85$ pF can be measured by connecting C_x in parallel to C_1 viz : S on B, F on D. For larger capacitances, say up to 3 pF, connection of F to C will result in a change of C_1 of $3 \times 100 / 480 = 0.625$ pF and a reading of C_1 of $1.34 - 0.625$ pF which is again in the linear range. For smaller values of C_x connection of F to other taps gives greater reading accuracy.

The detector sensitivity required for a fractional change of 0.1% can be computed using Thevenin's theorem. The detector voltage is the product of detector current and detector impedance. The current equals the

BRASS. D.N.P.

- ① $\frac{15}{16} \times 2 \times 1$; $\frac{17}{32}$ BORE.
- ② $\frac{9}{16} \times 2 \times 1$.
- ③ 20th WHOLE WIDTH OF BOX.

KERAMOT.

- ④ $\frac{15}{16} \times 2 \times \frac{5}{8}$
- ⑤ $\frac{9}{16} \times 2$
- ⑥ PUSH FIT ON MICROMETER.

BRASS. D.N.P.

AL. BOX.

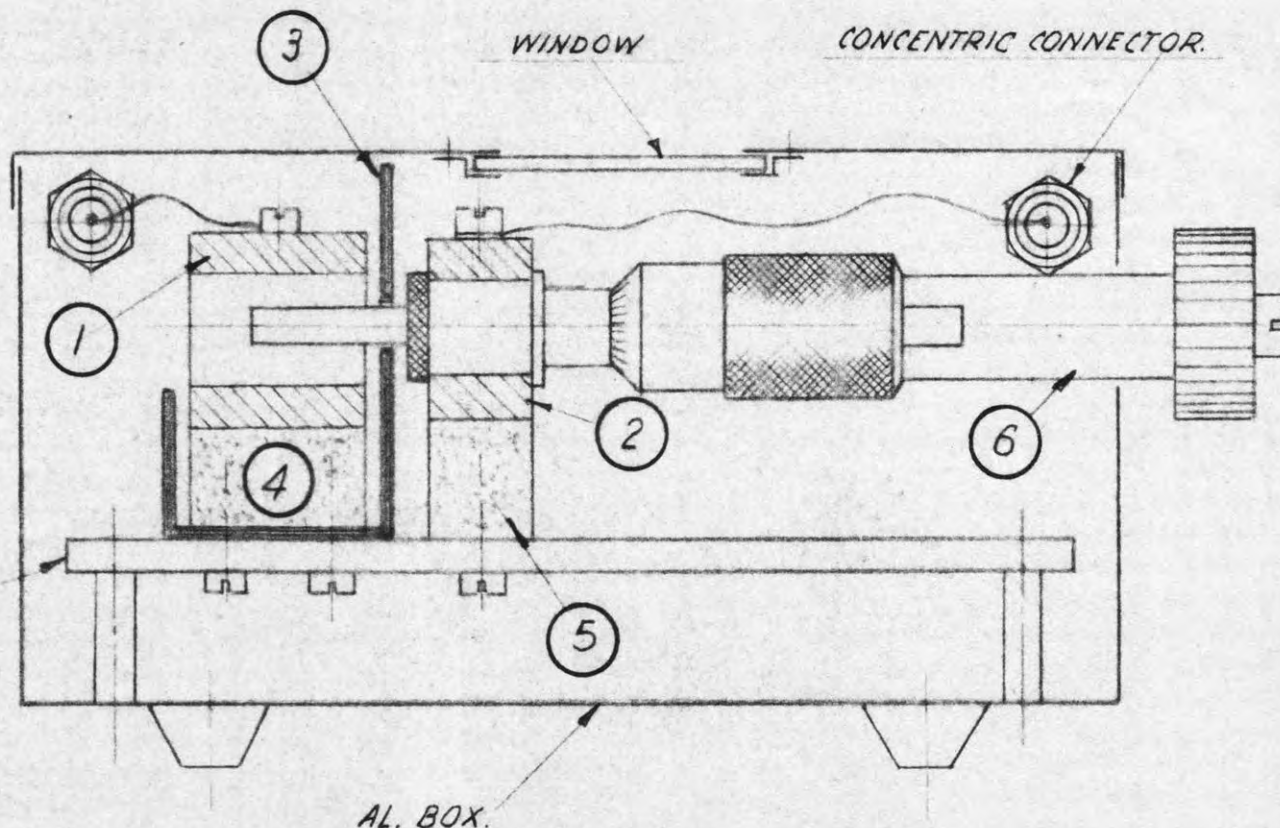
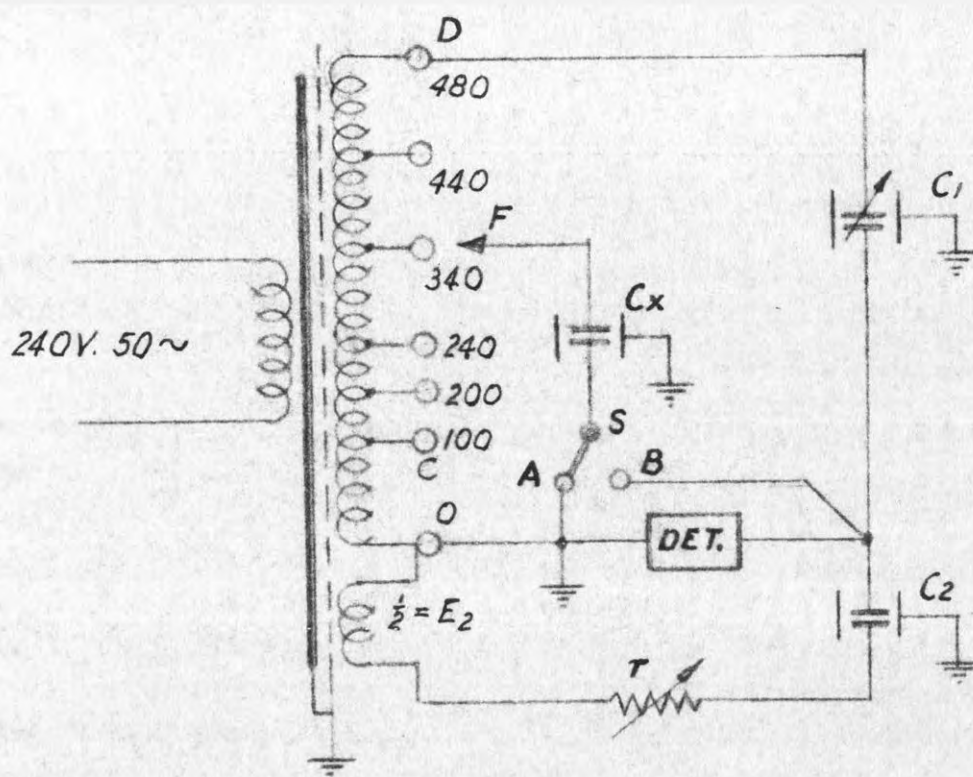


FIG. 71. THREE TERMINAL MICROMETER CAPACITOR.

FOLLOWING PAGE: 112



C_1 — MICROMETERCAPACITOR 0.5 pF TO 1.5 pF.

C_2 — 1300 pF, 3 TERMINAL AIRCAPACITOR.

R — 1111 Ω

DET. — 100 μ V r.m.s./ INCH. AT 50 c/s.

FIG. 72. TEST CIRCUIT

voltage on the detector points before connecting the detector impedance divided by the sum of detector impedance and Z_{c1} and Z_{c2} in parallel. $C_1 \ll C_2$ and therefore the voltage before connecting the detector impedance is approx. $d \times E_2$ wherein d is the fractional change required (1/1000). The detector impedance is, at 50 c/s, practically equal to the input resistance $R = 2$ Megohms (Fig. 12) and the voltage V_d on the detector for a change of d becomes approx. :

$$V_d \sim d E_2 \left(1 + \frac{1}{\omega^2 C_2^2 R^2} \right)^{-\frac{1}{2}}$$

In our case with $d = 1/1000$, $E_2 = \frac{1}{2}$ V, $\omega = 314$, $C_2 = 1300$ pF and $R = 2$ Megohms V_d yields 320 microvolts. The detector has thus ample sensitivity.

The resistance (r) in Fig. 72 serves for phase angle balance. It was sometimes found that the phaseangle of the lower part of the bridge was greater than that of the upper arm. In this case the latter angle was artificially increased by putting a carbon resistor in series with C_1 or C_x . A knowledge of the phase angle was not required for the tests described below.

The change of ratio of the ratio arm due to loading is negligible. A transformer of this type has a leakage inductance of the 480 V winding of less than 0.1 H μ . A loading with even 10000 pF would according to the expression given in Section 3.1.2.5.

$$\mu = L_s \cdot 100 \cdot \omega^2 C$$

give an error of $p = 0.01\%$ only. The ratio error between say the 100 V tap and the full 480 V winding was found to be well below 0.1% without any special winding arrangement. In the case of the more important investigations F was on D (Fig. 72) and that error had no influence on the result.

Fig. 72 illustrates the simplicity and ease obtainable with inductive ratio arms.

c) Capacitance and perturbation tests.

Table XI gives the capacitance as a function of spacing for three

high voltage electrode arrangements.

Table XI.

Spacing (cm)	one horizontal cylinder	two horizontal cylinders	
		spaced 1 inch	spaced $2\frac{1}{4}$ inch
	pF	pF	pF
1	2.32	1.63	1.22
2	1.46	1.31	1.03
3	1.04	1.03	0.88
5	0.68	0.73	0.66
7.5	0.45	0.52	0.50
10	0.34	0.40	0.39

At a spacing of 7.5 cm which was finally selected all three configurations have approximately the same capacitance.

In the finally chosen arrangement with two horizontal cylinders spaced 1 inch the capacitance increased by 1.3, 2.3, 3.2 and 3.8% when at the spacings 2, 4, 7.5 and 10 cm respectively the rear guard cylinder was left out.

Leaving out all three guard cylinders increased the capacitance to about 1 pF at a spacing of 7.5 cm.

Table XII gives the percentage change in capacitance when the angle of the high voltage electrode(s) was changed, zero degrees being horizontal.

Table XII.

Configuration	angle	spacing (cm)				
	degr.	2	3	5	7.5	10
One H. T. cyl.	10	-0.35	-0.25	-0.15	0.0	0.0
	45	-3.3	-3.0	-2.4	-1.7	-1.1
Two H. T. cyl.) spaced 1 inch)	10	+1.4	+1.0	+0.4	0.0	0.0
	45	+13.0	+7.8	+3.0	+0.1	-1.3
Two H. T. cyl.) spaced 2 $\frac{1}{4}$ inch)	10	+2.2	+1.4	+0.8	+0.5	0.0
	45	+27	+18	+7.5	+2.5	0.0

The above results are only approximately correct as some difficulty was experienced in adjusting the angle without altering the spacing. However the insensitivity of the configuration with two cylinders at a spacing of 7.5 cm was repeatedly checked and confirmed.

The percentage decrease in capacitance due to the proximity of a vertical grounded plate with dimensions 24 x 24 inches and having positions a, b and c as shown in Fig. 73a is given in Table XIII.

Table XIII.

Configuration	test	spacing (cm)		
		5	7.5	10
One H. T. cylinder	a	0.29	0.39	0.49
	b	0.39	0.49	0.59
	c	0.20	0.28	0.35
Two H. T. cyl. spaced 1 inch	a	0.30	0.36	0.42
	b	0.38	0.44	0.50
	c	0.19	0.23	0.27
Two H. T. cyl. spaced 2 $\frac{1}{4}$ inch	a	0.34	0.41	0.49
	b	0.39	0.48	0.56
	c	0.18	0.23	0.28

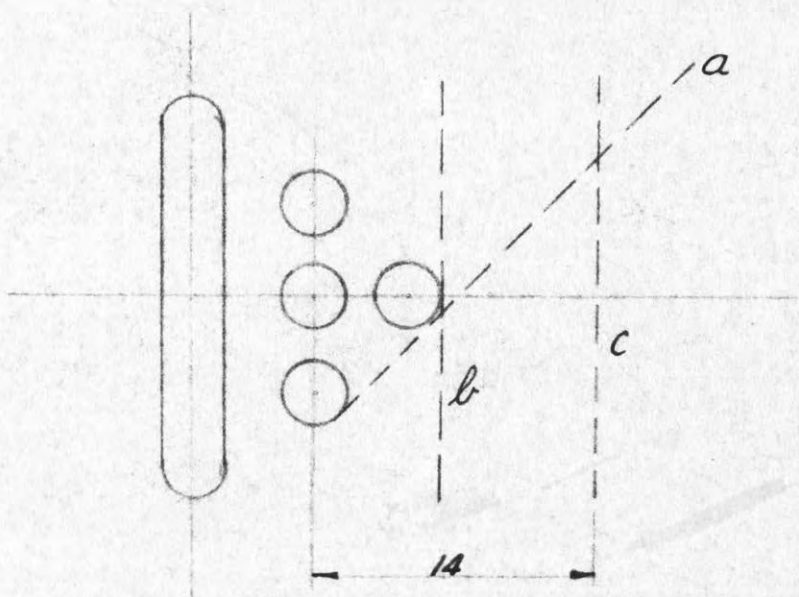


FIG. 73a

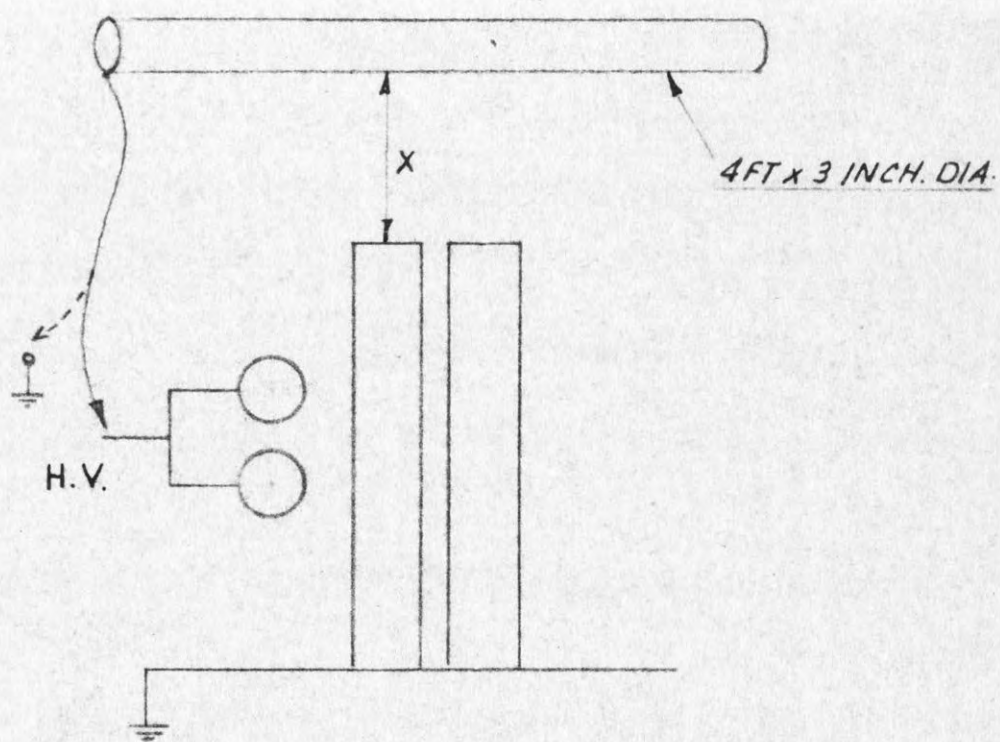


FIG. 73b

Of great practical importance is the change in capacitance due to a nearby high voltage conductor. The rather severe test arrangement is shown in Fig. 73b. A 3 inch diameter tube, 4 ft. long was hung above the capacitor at various distances (x). Table XIV gives the % increase in capacitance when the normally grounded tube was connected to the H. V. electrode.

Table XIV.

Configuration	distance (x)	Spacing (cm)		
	cm	5	7.5	10
One H. T. cylinder	20	0.40	0.84	1.6
	40	0.24	0.53	1.1
	60	0.20	0.41	0.88
Two H. T. cyl. spaced 1 inch	20	0.18	0.41	0.74
	40	0.07	0.22	0.47
	60	0.0	0.16	0.34
Two H. T. cyl. spaced $2\frac{1}{2}$ inch	20	0.18	0.36	0.69
	40	0.08	0.22	0.42
	60	0.0	0.10	0.28

Finally tests were made with a view to omit the three earthed guard cylinders which give the capacitor its rather peculiar appearance. The low voltage electrode was encircled by an earthed wrap of shim brass, 4 inches high, leaving only $3\frac{3}{4}$ inches of the circumference of the low voltage electrode exposed. However the figures given in Table XIII were higher and those in Table XIV up to 3 times larger. The original electrode configuration is therefore preferable. While the appearance may be unusual the system of guarding by means of three plain cylinders is much easier constructionally than the guarding system mentioned in the last test. The final model of the capacitor will have 3 plain guard cylinders and one low voltage electrode as per Fig. 70.

d) High voltage tests and comparison with computation.

50 c/s breakdown tests were not carried out as carefully and precisely as described in Section 3.1. for the measuring gap but it was thought

opportune to check the performance of a crossed cylinder gap using 3 inch diameter cylinders. In order to avoid end effects and the effect of the sharp edge of the shim brass low voltage electrode, initially, one horizontal and one plain vertical guard cylinder were used.

Within certain limits the puncture strength of air for several electrode configurations can be expressed by :

$$y = a(1 + b.x^{-\frac{1}{2}}) \dots\dots\dots (KV_p / cm)$$

whereby, for example in a uniform field for spacings (x) between 0.01 and 10 cm the author uses $a = 24.3$ and $b = 0.28$, for engineering accuracy. From the work by Pankow (4) who summarizes previous work on cylinders an approx. equation was derived in which $a = 27.0$ and $b = 0.33$ for $x = 0.5$ to 15 cm radius. However this work is based on doubtful measurements and on Schwaigers (1) assumption that $1/n$ is the same for crossed or parallel cylinders. (See Section 2). It appears therefore more accurate to compute the puncture strength of air for 7.6 cm (3 inch) diameter cylinders from the measured value of $33.35 KV_p / cm$ (see Section 3.1.6.) for 5 cm diameter cylinders and taking for b the figure of 0.33. This yields $32.2 KV_p / cm$ which figure differs by about 1% from Pankow's. Using this value for the expected puncture strength and the equation for $1/n$ in Section 2 the expected breakdown values shown in Table XV were computed. R. M. S. values are given for ease of measurement and because in this case great accuracy was not essential.

Table XV.

Spacing (cm)	KV r.m.s. expected	KV r.m.s. measured (mean of 10)
2	42.0	41.5
3	60.6	60.5
5	95.3	95.0
5.5	103.1	102.5
6	110.9	109.5
7.5	133	insulator flashover at 111 KV.

The discrepancies are thought to be due to the peakfactor which was known to be about 1.01 to 1.02. Also, above 100 KV two transformers in series had to be used with loss of measuring accuracy.

There was no significant change in breakdown voltage when the single horizontal H. T. cylinder was replaced by two cylinders spaced 1 inch. When however three vertical plain cylinders spaced 1 inch were used instead of the single one a significant reduction due to end effect occurred. This was expected from Table 1 in Section 3.1.5. For example at 3 cm spacing the reduction was about 2% but at 5.5 cm it rose to 12%. Generally it appears from the work done in this thesis that the length of the cylinders in a crossed cylinder gap should be 7 to 8 times the spacing. From this it must regretfully be concluded that the crossed cylinder gap, while ideal for voltages up to about 200 KV_p becomes an awkward structure at higher voltages.

A further reduction in breakdown voltage was observed when the cylinder with the low voltage electrode was added. This was expected and is due to the break in the surface caused by the shim brass. It is confidently expected that in the final model (Fig. 70) this will be insignificant. At the chosen spacing of 7.5 cm breakdown occurred always over the insulator at voltages between 105 and 115 Kv, the latter figure being obtainable immediately after washing the insulator with alcohol.

e) Discussion and application.

i) Discussion.

The configuration with two H. T. cylinders spaced 1 inch has been chosen because, firstly, the capacitance at larger spacings is nearly independent of the H. T. electrode configuration (Table XI), secondly because at the spacing of 7.5 cm required to safely withstand 100 KV r.m.s. the alignment is not at all critical (Table XII) and thirdly because the external influences as tabulated in Tables XIII and XIV are not unduly high. A configuration with one H. T. cylinder on each side was not tested because two insulators are required and because of the practical difficulty in paralleling the two cylinders.

The capacitor is not in the class of a fully shielded standard

capacitor but a comparison with the dimensions given in Plate 2 for the 85 KV capacitor shows the great advantage of using crossed cylinders and Table XIV shows that, if situated several feet from a H. T. line, its capacitance can be defined to about 0.1%. This is vastly superior to the monitor shown in Fig. 8 which can also be seen at the right in Plate 11.

Owing to the ease of capacitance measurement long term stability is not important and can hardly be expected from a capacitor which is meant to be dismantled for transport.

It is however of prime importance that the capacitor has an insignificant voltage coefficient of capacitance as otherwise a low voltage capacitance determination would be meaningless. An actual measurement of this has not yet been carried out but it was made quite sure that no unpleasant surprise would be encountered on the final model. Using simplifying assumptions the force of attraction was computed to be less than 50 grams. A force of double this amount produced an electrode movement of less than $\frac{1}{2}/1000$ inch as measured on a dial gauge. The dial gauge was then attached firstly to the low voltage electrode and then to the high voltage electrode and its reading observed by means of a telescope when the voltage on the capacitor was varied from 0 to 100 KV. The indication was much less than $\frac{1}{2}/1000$ inch in each case but even if the total movement is taken as $1/1000$ inch, at the chosen spacing of about 3 inches, the voltage coefficient of capacitance would be less than 0.03%. In the final model it is planned to measure the voltage coefficient of capacitance using the bridge of Fig. 10 in Section 3.1.2.6. with the unknown capacitor in parallel with the 5 pF/85 KV capacitor. The ratio of the testing transformer will then be measured say at 10 and 80 KV with the 0.5 pF capacitor on and off. If the 0.5 pF capacitor has no voltage coefficient of capacitance the ratios obtained should be the same with it on or off.

ii) Applications.

The capacitor is mainly used as a superb monitor superseding the one described in Section 3.1.2.3. In this case and in the applications described below an actual knowledge of the capacitance value is not

required. Neither is this accurately required for Schering bridge work because the main interest is usually the change of power factor as a function of applied voltage in order to determine the ionisation knee.

Fig. 74 shows a new method devised for peak factor measurement. This measurement which often must be carried out in the field checks if the A.C. wave form for material testing is within the limits specified in the B.S.S. viz : Peak value / r.m.s. value $\cdot \sqrt{2} = 1 \pm 0.05$. The circuit is based on the amplitude indicator described in Section 3.1.2.2. and Fig. 6 and the set up for peak voltage ratio measurement described in Section 3.1.2.9. and Fig. 14. The C.R.O. has a 50 c/s sinusoidal time base the voltage of which is taken from the same phase as the voltage V_x . With the switch in position "B" the 1.11 microfarad decade capacitor or, coarsely, the bias voltage of the amplitude indicator are adjusted until the diode just conducts. This manifests itself by a vertical line on one end of the time base. The reading of the r.m.s. meter, connected to the output terminals of the 20 W amplifier, at which the line just appears is noted. Let this reading be "B". The switch is then thrown to "A" and the attenuator adjusted until again an indication on the C.R.O. is observed. Let the reading of the r.m.s. meter, which in this case is caused by a pure sine wave, be "A". As in both cases the peak voltage is the same the peak factor of V_x is A/B. As expected, the measurement of a ratio requires no absolute knowledge of any quantity involved. The method therefore is superior to the measurement of peak and r.m.s. value individually. The scheme depends on the performance of the 20 W amplifier which has been described in Section 3.1.2.10.

The circuit of the sine wave source is shown in Fig. 75. A pure sine wave is obtained from the mains by filtering. A bridge with one nonlinear circuit element - the pilot lamp P_2 - reduces normal mains voltage fluctuations by a factor of 50. The filters are an L ... C filter with a Q of about 12 tuned to 50 c/s followed by a parallel "T" filter tuned to 150 c/s. The usual 2 to 3% distortion in the mains can be reduced to less than 0.01%. The 0.25 Megohm variable resistor serves as fine control when connected to the 2 Megohm attenuator. The maximum output voltage across 2 Megohms is approx. 1 Volt peak.

The rack seen in the background of Plate 11 carries, from top to bottom : the distortion meter (Fig. 16) the sine wave source (Fig. 75)

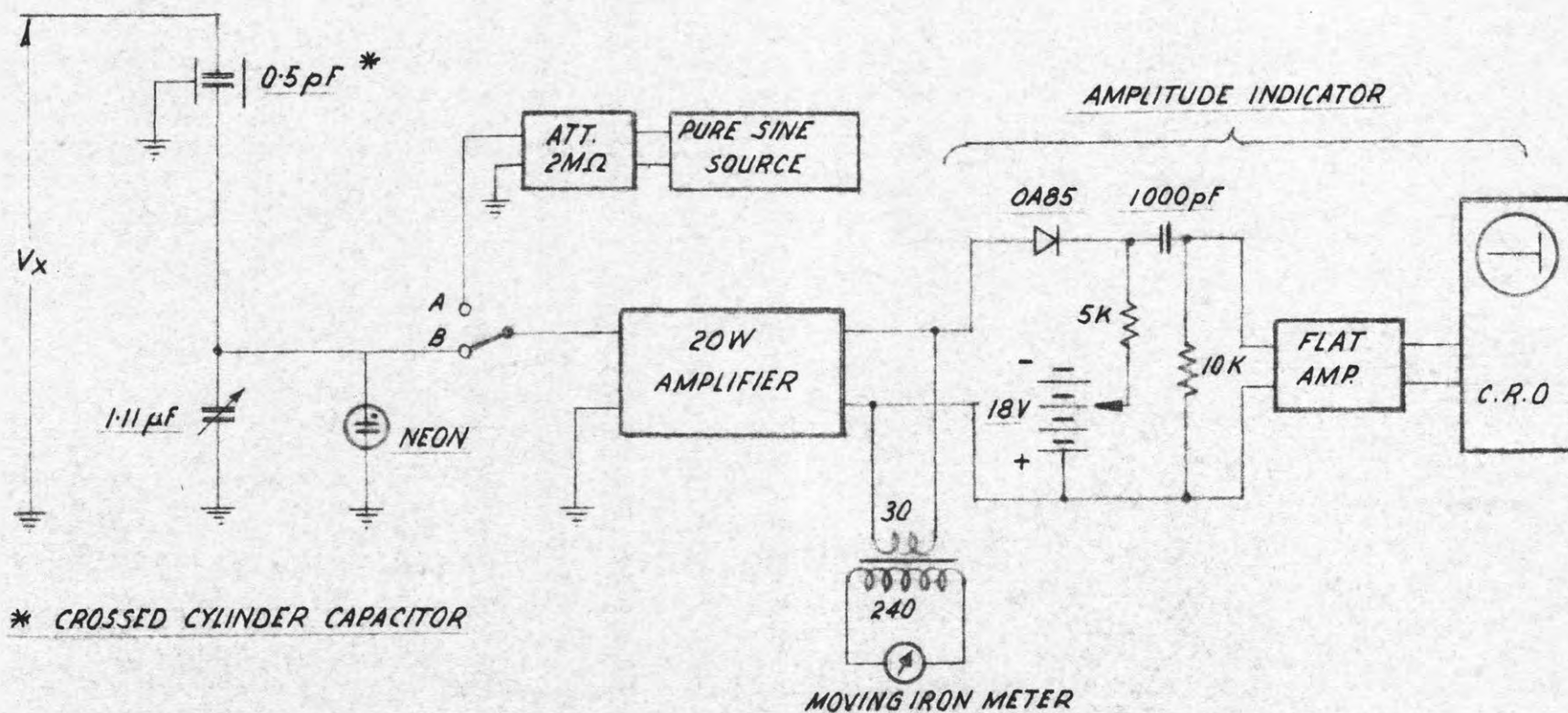


FIG. 74. ARRANGEMENT FOR PEAK FACTOR MEASUREMENT

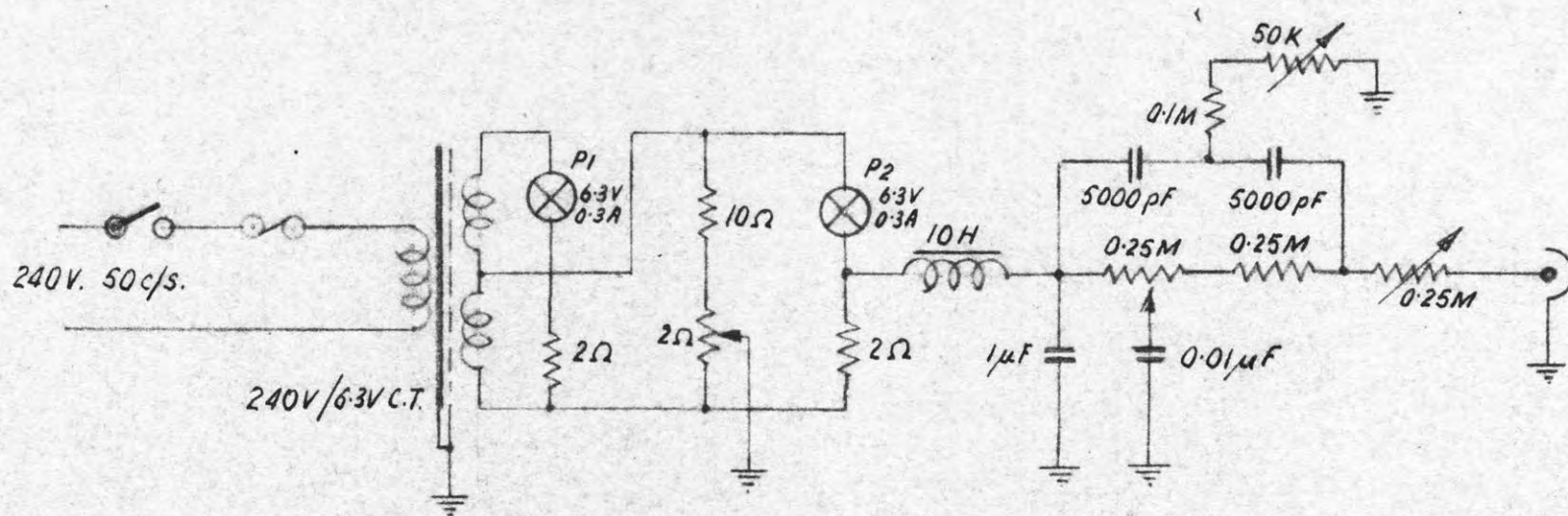


FIG. 75 CIRCUIT DIAGRAM OF SINE WAVE SOURCE

FOLLOWING PAGE: 120

the detector amplifier (Fig. 12) and the Mullard 20 W amplifier.

Another application is the calibration of a testing transformer in the field. The secondary r.m.s. voltage is required as a function of the reading of a primary or tertiary r.m.s. meter M_x . Fig. 76 shows the set up for calibrating a 100 KV, 100 KVA transformer in a cable factory. Up to 20 KV the calibration was carried out with a potential transformer 22000/110 V using the meter M_1 . Such a transformer is small and transportable. At 20.0 KV as known from M_1 the decade capacitor was set to say C_{21} to give a convenient reading on M_2 . This capacitance was about 0.1 microfarad, the capacitance ratio therefore about 200,000 and the voltage on the amplifier input about 0.1 V. With a gain of 80 the reading on M_2 was about 8 V. This reading was noted. The potential-transformer was then switched off and the voltage on the transformer under test was raised to the next required calibration point on its own voltmeter M_x . The decade capacitor was then adjusted until M_2 showed the same reading as before. Let this setting of C_2 be C_{22} . As $C_1 \ll C_2$ the transformer voltage is then :

$$V_x = 20,000 (C_{22} + C_g) / (C_{21} + C_g)$$

wherein C_g is the guard plus cable capacitance which was about 700 pF. As $C_g \ll C_{21}$ this capacitance need not be known accurately. It was assumed that the loading due to the potential transformer causes a negligible error. This assumption was checked by reading M_2 at a constant reading of M_x with the potential transformer on or off.

As, at 20 KV, C_2 was about 0.1 microfarad a capacitance of 0.5 microfarad was required at 100 KV. Owing to the use of the potential transformer an actual knowledge of the value of C_1 was not required.

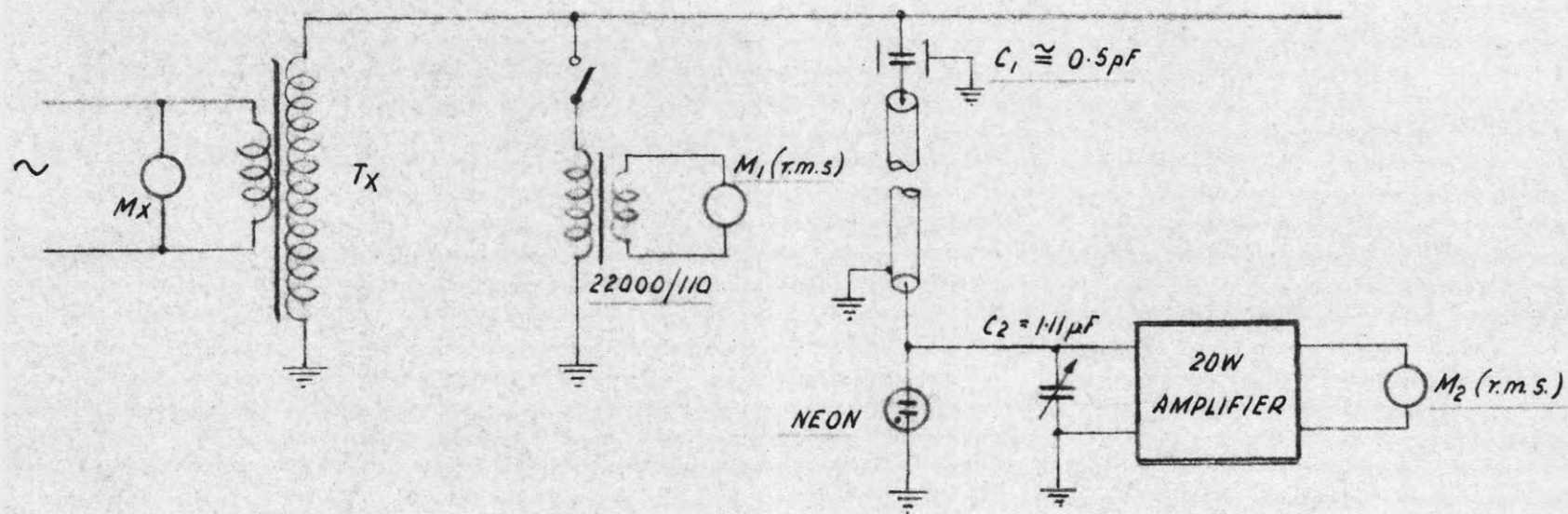


FIG. 76. ARRANGEMENT FOR THE *r.m.s.* VOLTAGE CALIBRATION OF TRANSFORMER T_x .

APPENDIX 6.

A simple method of impulse wave chopping.

a) Review of known methods.

Johnson (63) has pointed out the drawbacks of the commonly used rod gap. In order to avoid jitter and humidity dependance he proposed the method shown in Fig. 77a, in which the output circuit of an impulse generator is depicted. After a time determined by R and C the sphere gap G_2 sparks over and then G_1 . The spacings of the two gaps are equal and each spacing is larger than that required for $\frac{1}{2}$ the voltage but smaller than required for the full voltage. Both gaps are sphere gaps and G_2 can conveniently be the normally used measuring gap. Chopping is thus achieved by precise gaps with insignificant time lag.

Another approach is that by Auth and Schindelin (64). This is shown in Fig. 77b. Here, a shallow spherical calotte is placed over the earthed sphere of the existing measuring gap of the impulse generator. This calotte has a hole and a trigatron needle. The main gap is set to a voltage higher than the test voltage and after a time, to be chosen, a trigger unit produces a spark between the needle and the calotte which initiates the sparkover of the main gap thus chopping the wave. This scheme aims at not altering the measuring accuracy of the sphere gap by furnishing it with a hole to be used only when wave chopping is desired.

From the work described in Section 5.2. and from Table VI it appears doubtful if the measuring accuracy would suffer if the lower sphere had a hole which, if not required, could be plugged. However to test this is risky because of the high cost of large spheres. This is thought to be the reason why the authors mentioned above invented their "clip on" trigatron.

Another obvious solution would be the turning away of the hole from the sparking area if it is not required. Mechanically, crossed cylinders should be advantageous for this case. Alternatively, plugging of the hole could be done more precisely owing to the greater wall thickness as compared with spheres.

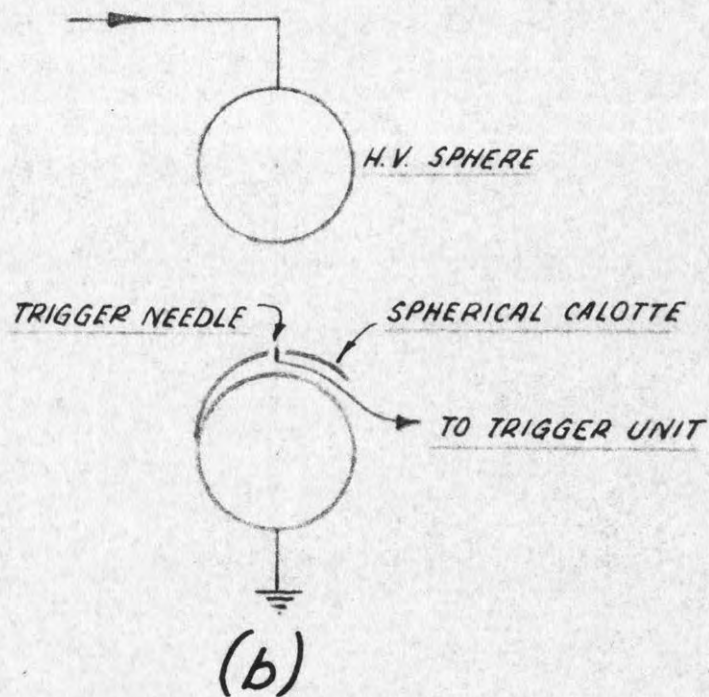
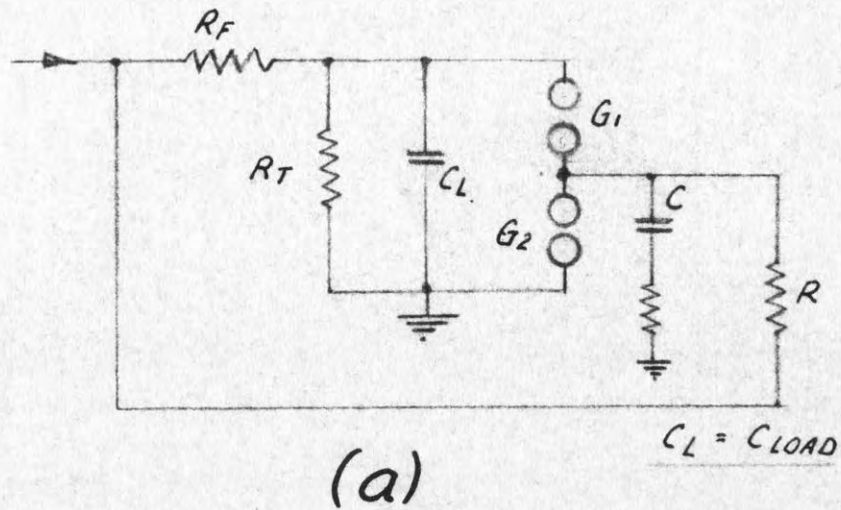


FIG. 77. CHOPPING METHODS

(a) Due to JOHNSON

(b) Due to AUTH and SCHINDELIN.

During a discussion on chopping methods Mr. R.H. Clarke of the School of Electrical Engineering pointed out that the Johnson method is expensive, G_1 and C having to be rated for at least $\frac{1}{2}$ the maximum required voltage. The author then proposed the method described below which does not require a complex trigger unit either.

b) Description of the new circuit and analysis.

i) Description.

The circuit is shown in Fig. 78a. A third sphere and a resistor are added to the existing measuring gap which may be connected to any type of impulse generator. The spacing 1...2 is greater than that required for breakdown at the maximum test voltage while the spacings 3...1 and 3...2 are equal and greater than required for breakdown at $\frac{1}{2}$ the test voltage. After a time determined by the voltage, the value of R and the capacitances C_{31} and C_{32} sparkover occurs between spheres 3 and 2 and then between 1 and 3. The capacitance C_{12} is part of C_L . The circuit may be regarded as the Johnson circuit with the two connected spheres replaced by one sphere and C replaced by the capacitances mentioned.

The cost of this arrangement is trivial. The resistor is a water resistor (Fig. 20) and the third sphere can be smaller than sphere 1 or 3 and it need not be finished well because it is not used for precise measurements. C_{32} can easily be altered by hanging a rounded metal object on the shank of sphere 3 thus giving fine control of the chopping time. Plate 12 shown clearly such an object, the water-resistor and the third sphere.

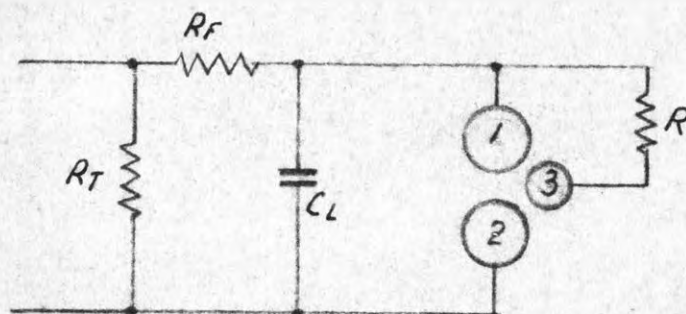
ii) Analysis.

As chopping is initiated by a breakdown between spheres 3 and 2 we require the voltage e_0 between spheres 3 and 2 as a function of the applied voltage. The circuit is re-drawn in Fig. 78b in the form of a network. If a step function would be applied to this network, at $t = 0$, the output voltage $e_0 = E.C_{31} / C_{31} + C_{32}$ and at time t :

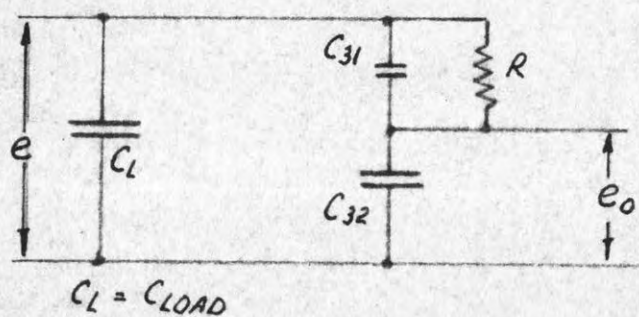


Plate 12 : The impulse chopping arrangement.

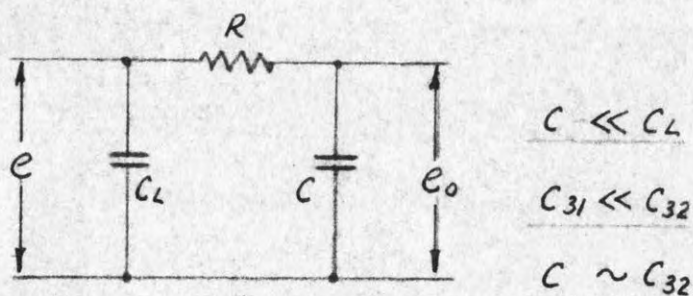
FOLLOWING PAGE: 123



(a)



(b)



(c)

FIG. 78. THE NEW CIRCUIT (a) AND EQUIVALENT DIAGRAMS (b, c)

$$e_0 = E \left[1 - \frac{C_{32}}{C_{31} + C_{32}} e^{-\frac{t}{R(C_{31} + C_{32})}} \right]$$

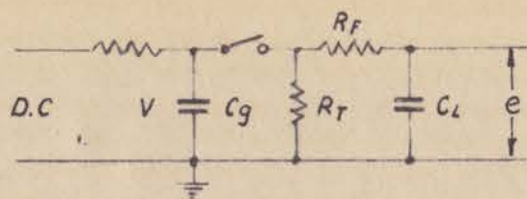
This differs little from:

$$E \left(1 - e^{-\frac{t}{RC_{32}}} \right)$$

if $C_{31} \ll C_{32}$.

The difference becomes smaller still if a function which rises less steeply is employed as is the case for the output voltage of an impulse generator for 1/50 microsecond waves. In order to obtain a reasonably simple expression for $e_0 = f(e)$ the network of Fig. 78b is approximated by the network of Fig. 78c, in which $C_{31} = 0$. It will be shown later that this is the case in practice because the ground capacitance of sphere 3 and shank plus water-resistor greatly exceeds the mutual capacitance.

The input voltage in Fig. 78 is the output voltage of the generator. From reference 39, page 129, the exact solution of the differential equation giving the output voltage (e) of a simplified impulse generator in which inductance is neglected is shown in Fig. 79.



V at $t = 0$.

$$e = V \frac{R_T C_g}{T_1 - T_2} \left(\varepsilon^{-\frac{t}{T_1}} - \varepsilon^{-\frac{t}{T_2}} \right)$$

T_2 = Time constant of wavefront.

T_1 = " " " wavetail.

SET : $V \frac{R_T C_g}{T_1 - T_2} = E \dots$ SEE FOOTNOTE

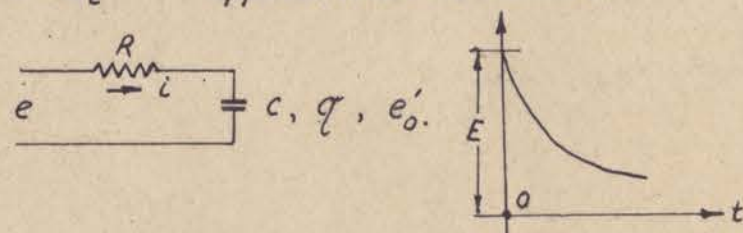
$$\frac{1}{T_1} = K_1$$

$$\frac{1}{T_2} = K_2$$

$$\therefore e = E \left(\varepsilon^{-K_1 t} - \varepsilon^{-K_2 t} \right)$$

FIRST WE SOLVE THE SIMPLER CASE :

$e = E \varepsilon^{-K_1 t}$ applied to an RC network.



$$Ri + \frac{q}{C} = e;$$

TAKING LAPLACE TRANSFORMS ON BOTH SIDES :

$$R\bar{i} + \frac{\bar{q}}{Cp} = \bar{e} = E \cdot \frac{1}{p+K_1}$$

FOOTNOTE : IN PRACTICE FOR $1/50 \mu$ SEC. WAVES

$$C_g \gg C_L; R_T C_g \sim T_1; T_1 \gg T_2;$$

$$\therefore V \sim E$$

because

$$\varepsilon^{-K_1 t} \supset \frac{1}{p+K_1} \text{ and}$$

$$i = \frac{dq}{dt}$$

$$\frac{dq}{dt} \supset p\bar{q} - q_0 = \bar{i}$$

$$\text{at } t=0 \rightarrow q_0 = 0; \bar{q} = \frac{\bar{i}}{p};$$

$$\bar{i} \left(R + \frac{1}{Cp} \right) = E \frac{1}{p+K_1}$$

$$\bar{i} = \frac{E}{R} \frac{p}{\left[p + \frac{1}{RC} \right] [p + K_1]}$$

$$= \frac{E}{R} \left(\frac{A}{p + \frac{1}{RC}} + \frac{B}{p + K_1} \right)$$

wherin from partial fractions (65):

$$A = \frac{1}{1 - K_1 RC}; B = \frac{K_1 RC}{K_1 RC - 1}$$

INVERTING:

$$i = \frac{E}{R} \left(A \varepsilon^{-\frac{t}{RC}} + B \varepsilon^{-K_1 t} \right)$$

$$e'_0 = e - iR$$

$$= E \left(\varepsilon^{-K_1 t} - A \varepsilon^{-\frac{t}{RC}} - B \varepsilon^{-K_1 t} \right)$$

$$e'_0 = E \left[(1-B) \varepsilon^{-K_1 t} - A \varepsilon^{-\frac{t}{RC}} \right]$$

$$1-B = A$$

$$e'_0 = \frac{E}{1-K_1 RC} \left(\varepsilon^{-K_1 t} - \varepsilon^{-\frac{t}{RC}} \right) *$$

BECAUSE ALL CIRCUIT ELEMENTS ARE LINEAR, BY SUPERPOSITION

$$e_0 = \frac{E}{1-K_1 RC} \left(\varepsilon^{-K_1 t} - \varepsilon^{-\frac{t}{RC}} \right) - \frac{E}{1-K_2 RC} \left(\varepsilon^{-K_2 t} - \varepsilon^{-\frac{t}{RC}} \right)$$

* CHECK : $K_1 = 0$, STEPFUNCTION:

$$\frac{E}{1-0} \left(\varepsilon^{-0} - \varepsilon^{-\frac{t}{RC}} \right) = E \left(1 - \varepsilon^{-\frac{t}{RC}} \right)$$

FIG. 79.

In using the expression for e_o derived in Fig. 79 the chopping time is desired and the constants of the generator, K_1 , K_2 etc. are given. Therefore $e_o = f(RC)$ but as the spacing (s) of the spheres depends on e_o and because (C) is a function of the spacing, $C = f(s)$ and $e_o = f(s)$ must be known also. Although the spheres have a different diameter the latter function can, with sufficient accuracy, be interpolated from calibration tables of sphere gaps e.g. the B.S.S. 358. $C = f(s)$ must be measured and it is fortunate that the capacitance of a practical gap does not change very much with spacing. (Compare Table IV in Section 3.4.2.1.).

Owing to the rather temporary nature of the generator this measurement was done only for a few spacings to test the principle of the chopping circuit. In one instance C_{31} was 4 and $C_{32} = C$ was 23 pF, the spacing between the 15 cm diameter sphere and the 25 cm spheres was 3.2 cm, R was 200,000 Ohms and t was 5 microseconds. For a 1/50 wave, from reference 39 : T_1 is about 70 and T_2 about 0.4 microseconds. These values in the expression of Fig. 79 yield $e_o = 0.604 E$. If, instead of the long formula a simple step function applied to an R..C network had been used :

$$e_o'' = E \left(1 - e^{-\frac{t}{RC}} \right) = 0.663 E$$

This indicates that, taking regard to the uncertainty with which the constants are known, it is feasible to use a much simpler way of computation. Even with t is 2 microseconds and R is 50,000 Ohms the difference between e_o and e_o'' is not too large it being 0.72 E and 0.82 E respectively.

As the method lends itself to easy experimental adjustment of the chopping time by putting rounded conducting objects on the shank of the third sphere and as the chopping time must be checked experimentally in any case an approximate calculation using a step function applied to an R...C network is sufficient in practice. This would however become quite erroneous for chopping at the wave front.

c) Performance and applications.

1) Performance.

The trace as seen on the C.R.O. screen is shown in Fig. 80. Owing to the lack of reasonably convenient access to photographic facilities no photo can be given. However, the author has demonstrated the performance to several workers with personal overseas experience in this field and no unfavourable comment was made. The generator shown in Fig. 27 was used at voltages between 120 and 220 KV_p. In order to test for jitter - at some risk of overloading the rectifiers - the circuit breaker was bridged and traces could be obtained in quick succession. Owing to the persistence of the screen it was possible to estimate that the jitter did not exceed 0.1 microsecond.

ii) Applications.

The main application at present is the qualitative comparison of voltage dividers for impulse voltage measurement and the termination of cables connected to them and the C.R.O.

The most important application, chopped wave testing of completed transformers, has not been undertaken and is not likely to be carried out in the foreseeable future. Firstly this is due to lack of photographic equipment and the need for several high speed C.R.O.'s and secondly these tests can now be made in the School of Electrical Engineering.

The following remarks are therefore not based on experience. If a transformer is given first several shots on the 1/50 wave, then several shots on a chopped wave and then tested again on the 1/50 wave to see if any damage has been done during the chopping, fault detection being carried out only at the 1/50 wave, no reason can be seen why the method described should not work just as well as the Johnson method provided ordinary care is taken that the lead to the test object does not significantly alter C₃₁. If however fault detection is to be carried out also on chopped waves and the results are to be compared at 50, 70, 90 and 110% of the test voltage all methods except the one by Auth and

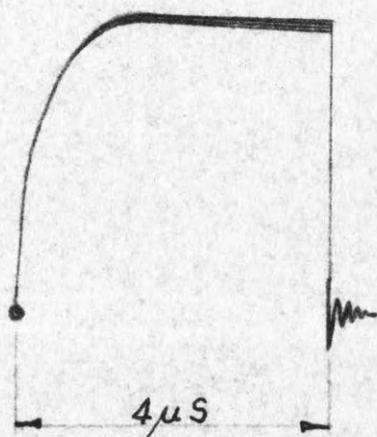


FIG. 80. C.R.O. TRACE

Schindelin (64) are unsuitable because in practice the chopping time could not be adjusted to be identical to permit inter-comparison of the photographs of the four cases. However, at the present state of the art conventional fault detection methods (e.g. neutral current, secondary voltage, differential) are not very satisfactory on chopped waves and require great skill in interpretation. On the other hand it is most likely that a fault, say a spark, may occur on chopped waves only and owing to the self-healing properties of an oil-filled transformer it will not show up on the subsequent 1/50 wave test thus making fault detection on chopped waves rather important. It is therefore the author's opinion that the fault detection method developed by Gaenger (66) will supersede, at least for chopped waves, the conventional methods. In that scheme a magnetic microphone is lowered into the tank and the pressure change due to a spark displayed on a C.R.O. A filter suppresses structural vibrations and external noise as may be caused by the gaps of the generator. All problems of high speed oscillography are eliminated.

If this method finds universal acceptance the simple and inexpensive chopping method described in this appendix would be suitable also in those cases where fault detection on chopped waves is required.

APPENDIX 7.

The use of corona detection apparatus for finding at low voltage the voltage distribution on high voltage insulators and the detection of internal sparking in resistors.

1) Introduction.

During developmental work on a 150 KV r.m.s. compressed gas capacitor of the type shown diagrammatically in Fig. 81a, a method was required to find that angle of the conical H.V. electrode which would bring about a tolerable surface stress on the outside of the Paxolin tube.

Fig. 81b and c show two well known methods. (Ref. 1, p.185 - 187, Ref. 10, p. 8 - 9, Ref. 12, p. 453 - 454). Referring to Fig. 81b, two wires (W) spaced 1 cm or 1 inch and arranged on an equipotential line around, say, a bushing (B) are connected to a measuring spark gap (G). By moving the wires to different positions the surface gradient anywhere along the surface can be measured. If the spark gap capacitance is so large that it appreciably alters the voltage between the wires the result obtained is in error.

The bridge method of Fig. 81c requires a high voltage divider (R). The detector may be a neon lamp or a small spark gap. Alternatively a wool fibre may be attached to W and its angle of deflection noted at a certain voltage V with the lead L disconnected. L is then connected and the slider on R adjusted until, at the same voltage V, the angle of the fibre is the same as before. From the divider ratio the voltage on W is then known.

Some experiments were first carried out with the circuit of Fig. 81c, but as no suitable voltage divider was available the circuit was arranged as shown in Fig. 81d. It was found difficult to obtain a clear null indication because the voltage on W is not only dependant on capacitances but also on the surface leakage thus giving a phase-angle which necessitates the insertion of a phaseshifter at P. Also, quite wrong results were obtained when there was any lead from W to D as this significantly altered the capacitances governing the voltage

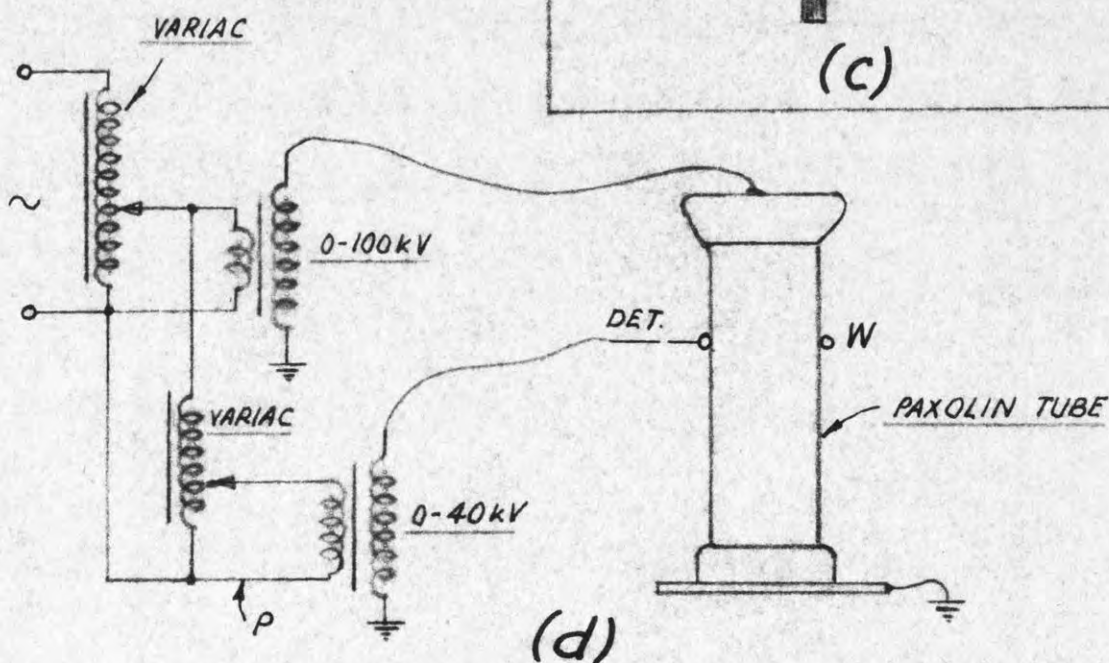
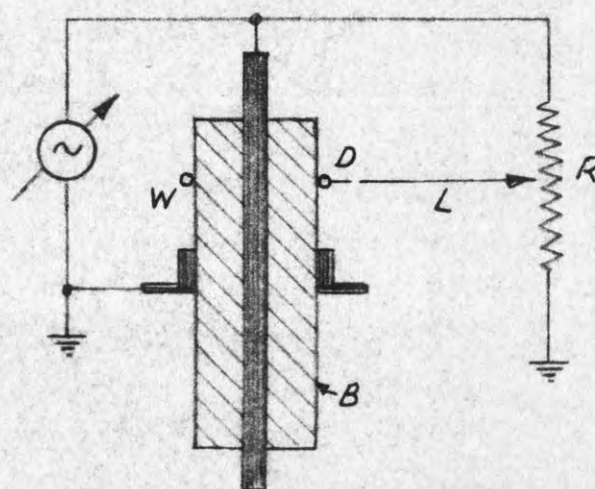
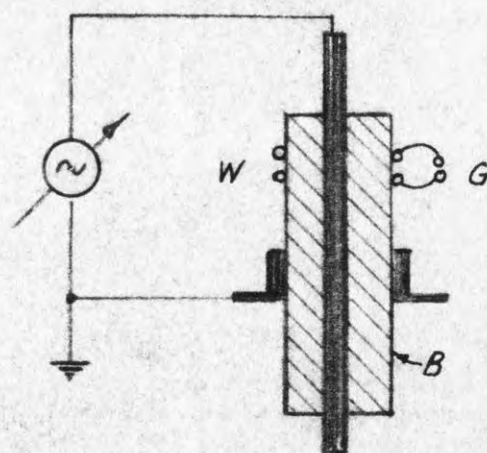
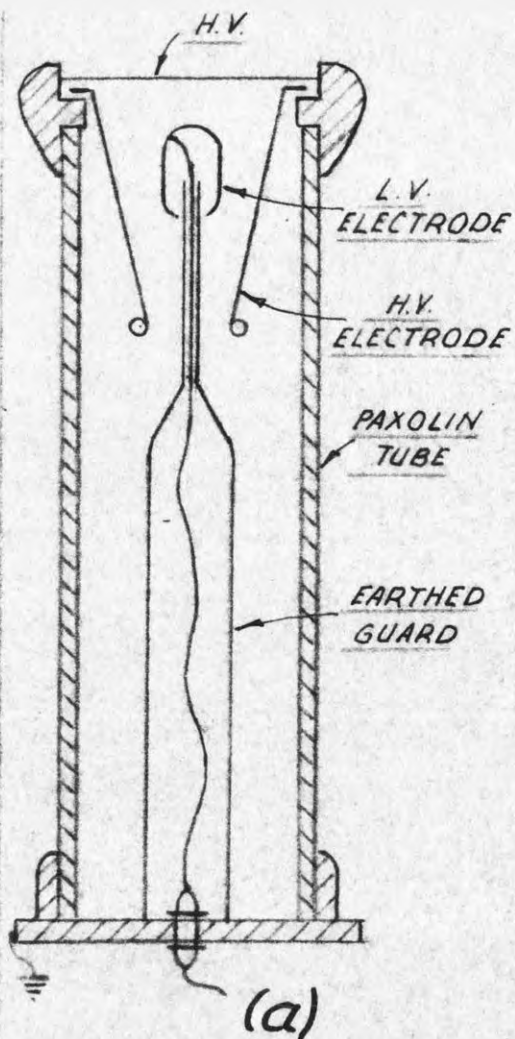


FIG. 81. ORTHODOX METHODS

distribution. A tiny gap right at W was found best. While, without doubt, this circuit could be refined the equipment requirements are rather extensive and it was thought more profitable to concentrate on the refinement of the circuit of Fig. 81b.

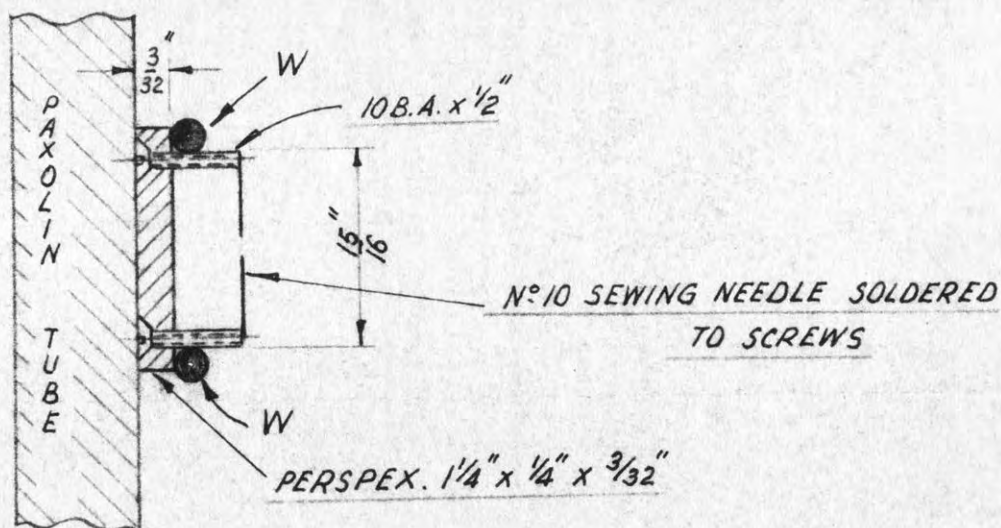
ii) Description of the new method for voltage distribution measurements.

Referring to Fig. 81b an obvious refinement is the use of a spark gap with very small capacitance. The gap shown in Fig. 82a has a capacitance of 0.08 pF and it is set to spark over at about 1100 Volts peak. The sewing needle electrodes were soldered to the screws with part of the gap submerged in water in order to prevent softening of the perspex. The latter material was chosen for its high surface resistivity. It was found quite important to arrange the needles as in Fig. 82a and not as in Fig. 82c as otherwise the sharpness of the sparkover onset voltage as detected in the arrangement described later was adversely affected.

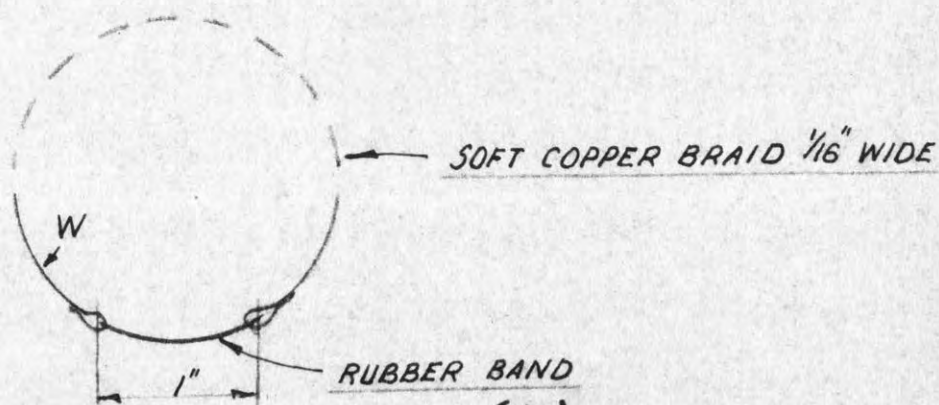
The wires (W) constructed as shown in Fig. 82b firmly encircle the tube and give contact with the 10 BA screws. The test method described below clearly indicates, by a different pattern on the C.R.O. screen, if this contact is insufficient.

The electrodes of such a small fine gap would quickly become burnt if the gap were used conventionally by observing a spark. Also, the sparkover onset would be hard to see and observation would have to be made in a darkened room using a telescope. Even then different observers obtained widely differing results.

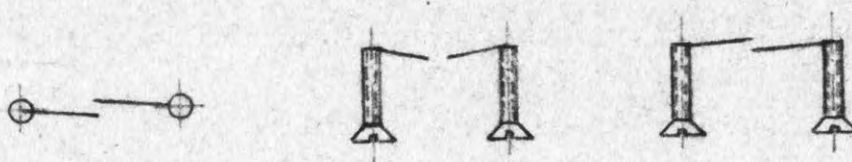
This difficulty has been overcome by using an electrical method. The circuit is identical with the one described before for the detection of sparks in voids of a dielectric (25 and 25a). Instead of the detector shown in reference 25a (see reprints attached) the simpler arrangement shown in Fig. 83a is suitable, the sensitivity requirements being much less than for corona detection in dielectrics. The sensitivity of the C.R.O. need not be better than 100 mV peak to peak per inch. Fig. 83a can be replaced by the equivalent diagram of Fig. 83b in which leakage resistances have been neglected. On breakdown of the gap, the



(a)

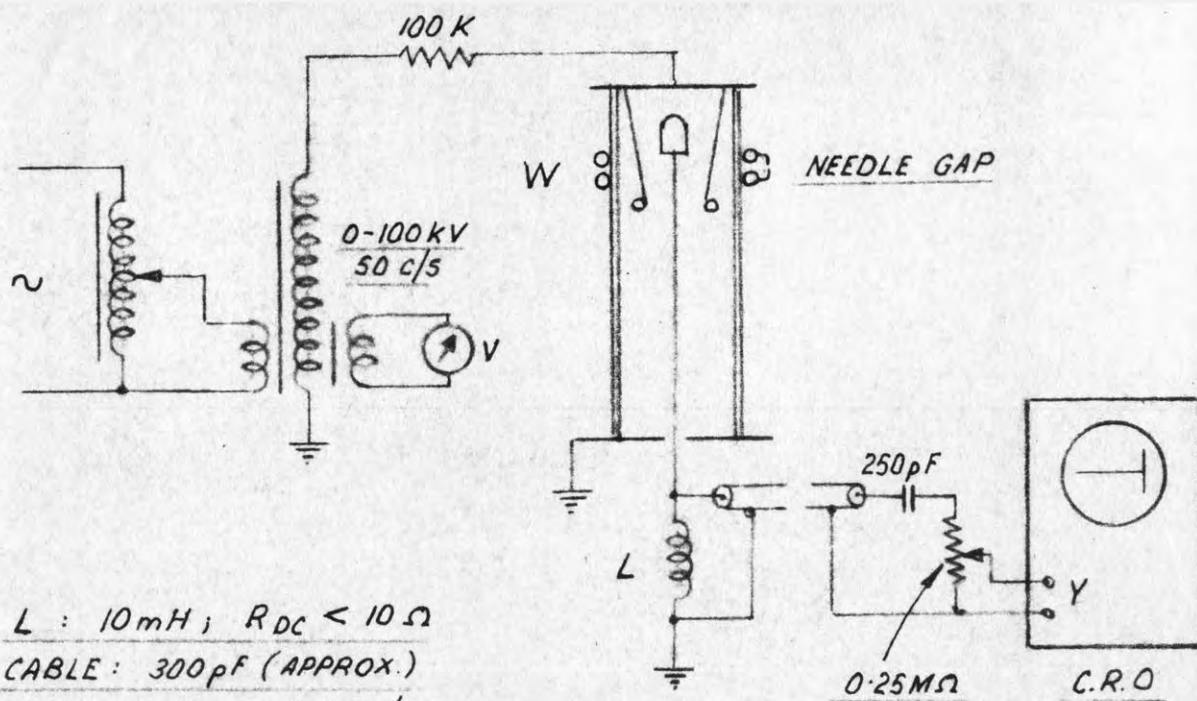


(b)

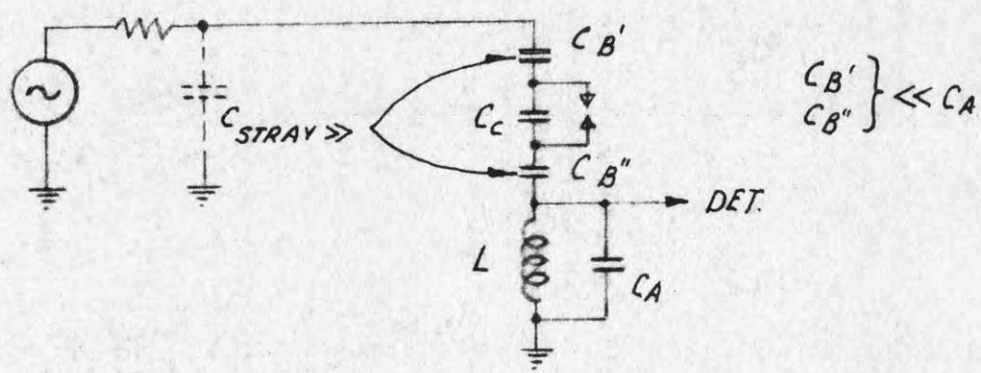


(c)

FIG. 82. PERTAINING TO NEEDLE GAP



(a)



(b)

FIG. 83. THE NEW CIRCUIT FOR VOLTAGE DISTRIBUTION MEASUREMENTS ON INSULATORS (a), AND ITS EQUIVALENT DIAGRAM. (b)
 FOLLOWING PAGE: 129

voltage on C_c drops in a very short time and the subsequent charge distribution leads to a change in voltage on the tuned circuit $L \dots C_A$ which is shock excited into a damped oscillation the frequency of which is in the order of 100 Kc/s for the component values given. The 50 c/s component is sufficiently attenuated by the coil L , the reactance of which is quite small at 50 c/s and by the 250 pF coupling capacitor. The time base of the C.R.O. is 50 c/s sinusoidal obtained by connecting the C.R.O. heater voltage to the horizontal input terminal. Because breakdown occurs at the peak of the cycle the damped oscillation will appear as vertical lines at the ends of the time base. This assumes that the C.R.O. is connected to the same phase as the testing transformer. Furthermore, as the discharge will commence at the peak of the negative cycle the display has only one vertical line as shown in Fig. 83a. This particular form of display is very helpful in discriminating against noise and r.f. signals picked up from other sources.

iii) Application of the method and tests.

The purpose of voltage distribution measurements is to find a design in which the voltage at the surface varies as linearly as possible with length. Assuming first this ideal of constant voltage gradient and assuming that the voltage at $1/10$ of the total insulator length is required the supply voltage must be 10 times the gap voltage viz : 11,000 V. In practice at $1/10$ of the length the voltage is unfortunately usually much higher than $1/10$ of the applied voltage and an even lower supply voltage is sufficient in most cases. Because mainly the points of highest gradient are of interest and because the gap strikes at a low voltage only a moderate voltage supply is necessary. This is quite important because at higher voltages corona (streamers) on the insulator under test modifies the voltage distribution. At moderate voltages the indication on the C.R.O. is also much clearer because the testing transformer and the leads are free of corona.

The test procedure consisted of recording at which value of applied voltage (V) an indication of gap breakdown could be observed. The accuracy of this was not limited by sensitivity because a change of $V/100$ could easily be seen. If the operating voltage of the insulator

is V_0 , the surface stress for the particular position of the wires (W) which are spaced 1 inch is : $(V_0 / V) \times 1.1 \text{ KV}_p / \text{inch}$. In this it is assumed that the capacitances and leakage resistances are independent of voltage which is reasonably true if the stress computed as above is not causing any surface streamers.

The method is easy to use and conducive to experiments with stress-distributors etc. to reduce surface stress.

It was remarked before that large errors could occur if the spark gap had a large capacitance. As it was not known a priori how small this capacitance should be tests were made in each case by observing the onset voltage with the capacitance doubled. This was done by connecting a similar structure as the gap shown in Fig. 82a in parallel with the gap. This structure had a larger spacing to prevent sparkover but it had strips instead of needles. Only in cases where the capacitances were very small as in case of a $\frac{1}{2}$ inch diameter conductor in the centre of an air-filled bakelite tube of 6 inches I.D. was an error of about 10% observed when the capacitance was doubled.

For greater accuracy the gap, which is not very sturdy, was frequently calibrated in situ by connecting the lower wire (W) to the not earthed side of (L) in Fig. 83a and the other wire to a source of variable voltage via a 2 Megohm resistor.

Experiments were also made to replace the spark gap by a neon lamp. Tests could then be made at still lower voltages. However, while the detector had enough sensitivity the available lamps had either too high a capacitance or their onset voltage was not well defined. In all cases their insulation resistance was quite low and surface treatment with methylchlorosilane had to be applied.

iv) Accidental finding of another method.

During work on a synthetic resin bonded paper bushing the lower part of which was submerged in oil the author happened to put oily fingerprints on the s.r.b.p. tube. Tests for streamer onset were made in the dark and a torch was used to read the meters. When the light of this lamp happened to illuminate the fingerprints the oily surface appeared crumbled and there was a very sharp transition from a smooth

OIL SMEAR

X

**FIG. 84. PERTAINING TO TEST METHOD FOR
STREAMER ONSET USING AN OIL SMEAR**

FOLLOWING PAGE: 131

oily surface to the crumbled surface at one particular voltage. Below this voltage the surface was smooth, above, it appeared crumbled.

This was then investigated more closely. An oil smear as shown in Fig. 84 was deliberately put on a clean bushing and illuminated by a sharply focussed light beam. At a voltage which could be determined to within 3% crumbling could be observed at the points of highest stress before any streamers could be noticed. Stress relieving measures could then be taken to increase the voltage at which crumbling occurred. This proved a very convenient and quick method to find experimentally the optimum size and position of stress rings.

The oil film was found to operate satisfactorily even after 40 minutes continuous application of voltage. Alternatively expressed, a slight reduction in voltage after 40 minutes immediately produced a smooth surface. Some practice is necessary in applying the film. Too thick a film will not produce the effect while a too thin one is hard to observe. It should be stressed that the onset voltage of "crumbling" is different for each film. In practice this does not matter because only one film is necessary to find improvements due to different shapes of the hardware.

The phenomenon is probably due to interaction of electric wind (ionic wind) and surface tension. In a horizontally arranged bushing covered with baby powder the powder was violently blown away from the points of highest stress, an oil drop placed in a shallow indentation was also blown away and wool fibres connected to the end of an insulated stick, when brought near points of high stress (X in Fig. 84) behaved as if they were placed near a fan. The electric wind explanation is supported by a remark by Goodlet, Edwards and Perry (67) who comment on the electric wind produced by streamers on a similar structure.

The method which has since been used often also on porcelain bushings is convenient and quick but the method described in (ii), while slower, is quantitative.

v) The detection of internal sparking in high voltage resistors.

Superficially it would seem that the method described in (ii) should be directly applicable to detect sparking between the turns of

the carbon track of a high voltage resistor (e.g. I.R.C., MV types) as used in gap type "B". (Section 4.2.1.). Sparking between turns should be equivalent to sparking of the gap in Fig. 83a. The difficulty which arises stems from the fact that there must be no sparking at the highest voltage, in this case 100 KV r.m.s., and that at such a voltage corona in the testing transformer or on leads may be confused with sparking in the resistor. As, a priori, the sensitivity required to detect sparking in the resistor is not known, it is most likely that too much sensitivity will be used thus adding to the confusion. The scheme described below aims at finding out the sensitivity required.

Although several 20 Megohm resistors as used in gap type "B" were available a method was preferred which did not necessitate any damage to the resistor.

As shown in Fig. 85a two resistors were connected in series via a 0.5 Megohm resistor which was shunted by the spark gap shown in Fig. 82a. High voltage was applied via a $\frac{1}{2}$ inch diameter copper tube. At a voltage of approx. $(2 \times 20/0.5) \times 1.1 / 2^{\frac{1}{2}} \sim 62$ KV r.m.s. breakdown of the gap could be observed on the C.R.O. screen and the sensitivity could be adjusted to give a very clear indication of the gap breakdown as compared with circuit corona. The gap shunt resistor was then reduced and gap breakdown at 94 KV was quite clearly observed. When the gap and its shunt resistor were tried at points B and T (Fig. 85a) equally sharp indication of gap breakdown was obtained. During these tests, suddenly, at lower voltage, an indication equal in appearance to a gap breakdown was observed and it was found that one resistor had become faulty. In the dark at elevated voltages a tiny spark could be seen.

Without change in the sensitivity setting of the C.R.O. the 100 KV line was then connected to the resistor to be tested (Fig. 85b) and the voltage raised to 100 KV r.m.s. The resistor had 46 turns or approx. 3 KV_p between turns. No sign of sparking could be observed although the sensitivity was, from the previous test, known to be high enough to show a spark at 1.1 KV_p . Six resistors were tested including the one which failed in air. As the result was negative in all cases the design adopted for the series resistor of gap type "B" was considered satisfactory.

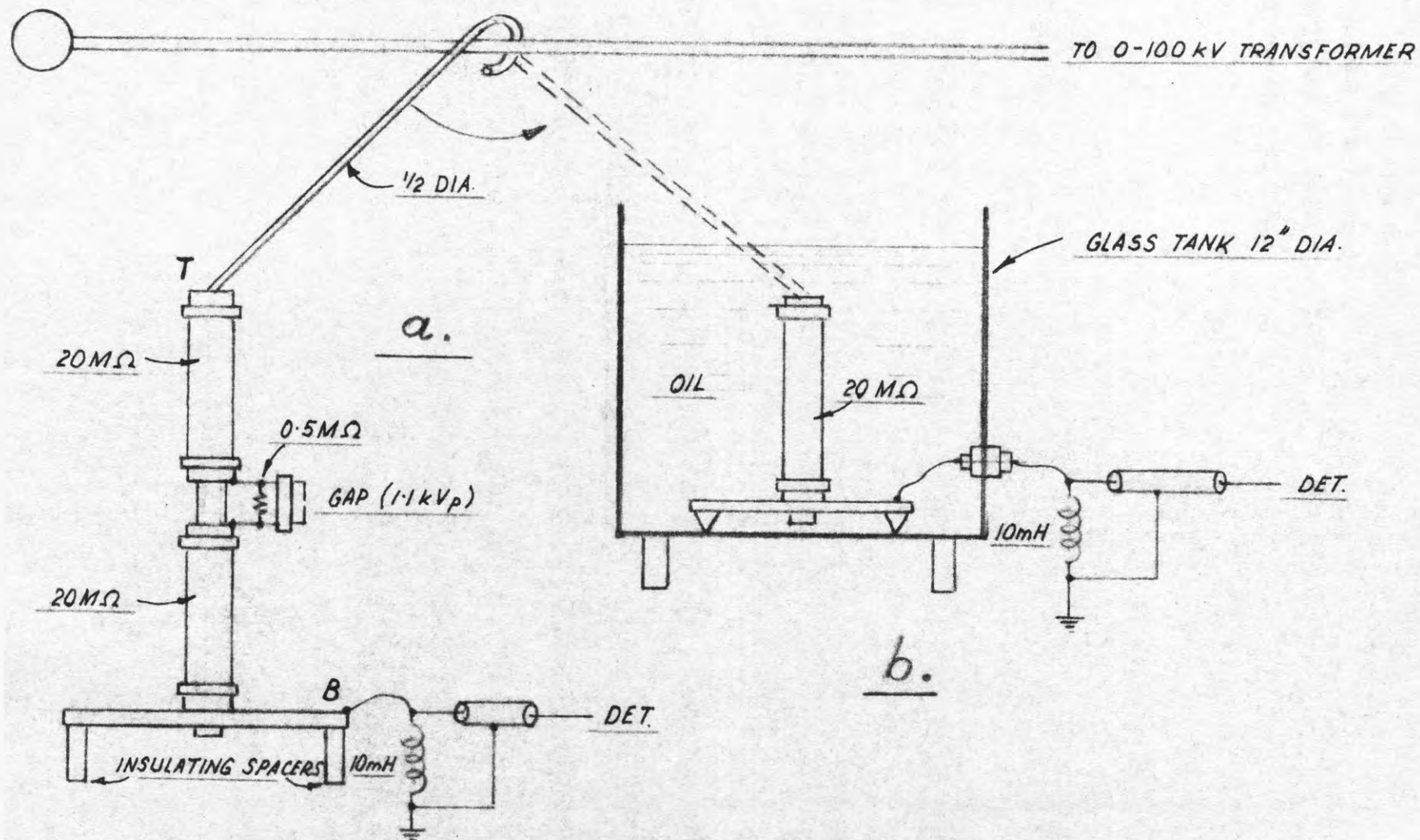


FIG. 85. METHOD FOR THE DETECTION OF INTERNAL SPARKING IN RESISTORS

FOLLOWING PAGE: 133

In a similar manner tests were made on ten 10 Megohm wire wound resistors made by Sprague (USA) and used in an oil-filled resistor, rated 100 KV and 100 Megohms, now being used to measure the charging voltage of the impulse generator.

8. References pertaining to the appendices.

- (58) R.G. Wylie and A.F.A. Harper
An analysis of the galvanometer amplifier
Austr. J. of Sc. Res. Series A, Vol. 4, No. 4, p.560, 1951.
- (59) E.W. Golding
Electrical Measurements
3rd ed. p. 443, Pitman 1942
- (60) W.K. Clothier
A fixed gas dielectric capacitor of high stability
Proc. I.E.E. vol. 101, part II No. 82, p.453, August 1954
- (61) "Huetten" the Engineers Handbook
23rd ed. vol. 1 1920, p.132
- (62) P.K. Mc-Elroy and R.F. Field
How good is an iron cored coil?
General Radio Experimenter, March 1942.
- (63) G.H. Johnson
An impulse generator for chopped wave tests on transformers
Trans. A.I.E.E. Vol. 72, 1953 part III, p.839
- (64) W. Auth and H. Schindelin
Method of controlling the chopping time of a chopped wave
E.T.Z. (A) Vol. 76, 1.6. 1955, p. 386
- (65) R.W. Dull
Mathematics for engineers
Mc Graw Hill, New York, p. 315
- (66) B. Gaenger
The Brown Boveri oil pressure detector employed for fault location during impulse tests on transformers
Brown Boveri Review, vol. 44, August 1957, p. 336
- (67) B.L. Goodlet, F.S. Edwards and F.R. Perry
Dielectric phenomena at high voltages
J.I.E.E. vol. 69, p. 695, 1931.

9. A general remark, clarifications and recent changes in the equipment described.

1) General remark.

At the time when application was made for enrolment as an M. E. student at least 10 appendices were contemplated and it was envisaged that those appendices describe the measurement techniques. The reason why this thesis has only 7 appendices is due to the inclusion of the main techniques in the body of the thesis in Sections 3.1.2.1. to 3.1.2.10.

1i) Clarifications.

Section 1: The investigation of gap type "A" did not only aim at the extension of previous work on A.C. to D.C., impulse and symmetrical A.C. voltages but also to give all dimensions of a practical gap, based on perturbation tests, and to improve the accuracy of calibration.

Section 2: The decision to use 5 cm diameter cylinders was subsequently proved correct because Fig. 29 shows that any measure which would lead to increased spacing sharply increases the polarity effect.

Section 3.1.2: The stress at the rounded edges of the H.V. electrode of the capacitor shown in Plate 2 was computed by approximating the configuration "cylinder in a torus" by crossed cylinders (1).

Section 3.1.2.5: The negative leakage inductance concept is described in Blume's book on transformer engineering. In a three winding transformer it manifests itself as a voltage decrease on loading with a capacitance.

Section 3.1.2.7: The tests on 40 c / S were made after the loading tests and after the equivalent diagram has been drawn and after the self-capacitance of the transformer has been determined as otherwise the relevant corrections could not have been applied.

Section 3.1.6: The figure for puncture strength of air using 5 cm diameter crossed cylinders given in the third column of Table II is slightly lower than the figure which can be interpolated from Werner's work (3) which is re-published by Pankow (4). This is to be expected because both authors use the stress - multiplication-factor for parallel cylinders which,

according to equations 3 and 4 in Section 2, is slightly higher than for crossed cylinders.

Appendix 6: The expression for the output voltage of an impulse generator taken from reference 39 and given in Fig. 79 is valid if the tail resistor is either across C_g or C_L .

Section 2 and later : It is regretted that semisphere was used instead of hemisphere.

Section 2 : Although the use of 10 cm diameter spheres is recommended only up to 5 cm spacing, for comparison purposes , the spacing of 5.67 cm has been used because it is common practice to use 10 cm spheres at least up to 140 KV_p and because calibration data are given in the BSS 358.

Section 1 and page 118 : In the statement that crossed cylinders must be long it is assumed that small proximity and polarity effects are desired. If this is not the case the length may be reduced. The limiting case is the sphere gap with zero cylindrical length.

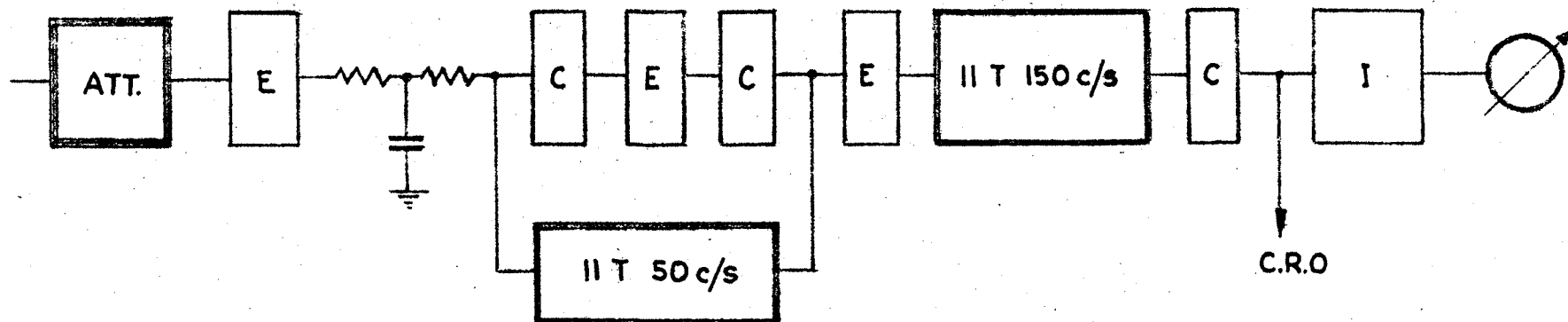
iii) Recent changes in equipment.

The tail resistor of the impulse generator (Fig. 27) has been replaced by a "Silko" ribbon made of constantan wire and situated in an oil filled bakelite tube. A tap at $1/400$ of the resistance has been provided for use of the tail resistor as an resistive impulse voltage divider.

Water resistors are now made using distilled water and sodium chloride. This was done because copper deposits were noticed on the electrodes.

The detector amplifier of Fig. 12 and Section 3.1.2.6. plus the shielded transformer described in Section 3.1.2.10 have been lent to Mr. Williams of the Sydney County Council for Schering bridge work. Subsequently Mr. C.E. Ranger suggested the development of a transistorised instrument. The principle embodied in the valve amplifier was used again and Fig. 86 is a block diagram of a breadboard model. Final circuit values cannot be given as yet because there may still be some alterations after tests in the field.

In order to reduce noise the first stage is "hushed" by using very low collector voltage. The components of the "parallel T" Filters could be kept small (0.05 microfarad) by suitable impedance matching. For this, use is made of the low output and high input impedance of grounded collector stages. The phase shift in the loop containing three transistors is 180 degrees which is equivalent to the valve version of Fig. 12. The indicator may be a C.R.O. or, if both bridge detector points are above ground, a C.R.O. connected to the emitter circuit of the last grounded collector stage through a transformer of the type described in Section 3.1.2.10. It should be stressed that magnetic shielding is far less important in this case because the gain after the transformer is low and relatively few turns are required to match into a low impedance circuit. Alternatively the indicator unit may be used making the detector completely self contained. This unit consists of two transistors with the last one in a circuit which is the transistor equivalent of the anode bend detector. This has been described before (68). Using a Philips 6M 5655 C.R.O. at max gain, an input of one microvolt gives an oscillogram 4 cm high. The same input gives $\frac{3}{4}$ of full scale deflection on a 200 microampere meter of the indicator unit.



E : *GROUNDING Emitter.*
 C : *GROUNDING Collector.*
 I : *INDICATOR UNIT.*

FIG. 86. TUNED DETECTOR AMPLIFIER
 USING TRANSISTORS

FOLLOWING PAGE: 138

The noise referred to the input is 0.1 microvolt with the input shorted and 0.2 microvolt with the input open. The input resistance is about 10,000 Ohms. At the harmonic frequencies $f_n \geq 150$ c/s about 1000 microvolts are required to give the same output as one microvolt at 50 c/s.

The sensitivity and input resistance of this detector make it suitable for the usual low impedance A.C. bridges as well as for high impedance bridges e.g. Fig. 10 Section 3.1.2.6. and Fig. 72 in Appendix 5.

Power consumption is 4.5 volts at 1.2 mA.

Reference 68:

L. Medina and F.C. Hawes

An indicator employing a transistor for the detection of live high voltage conductors and faulty insulators

Australian Journal of Instrument Technology
Vol. 12, Aug 1956 p.111.



Reprints of References :

11

13

14

18 a

19

19 a and 26 a.

20

21

22

25

25 a

26

41

68

(11)

Reprinted from the
AUSTRALIAN JOURNAL OF APPLIED SCIENCE
VOLUME 6, NUMBER 4, PAGES 453-457, 1955

THE DETECTION OF CORONA DISCHARGES IN HIGH VOLTAGE AIR
CAPACITORS

By L. MEDINA



Reprinted for the
Commonwealth Scientific and Industrial Research Organization
Australia

THE DETECTION OF CORONA DISCHARGES IN HIGH VOLTAGE AIR CAPACITORS

By L. MEDINA*

[Manuscript received April 4, 1955]

Summary

When an air capacitor was connected to a source of alternating voltage it was observed that an increase in power factor due to corona was accompanied by the appearance of a D.C. component in the current through the capacitor. This provides a convenient method for discharge detection.

Measurements on three-terminal air capacitors rated at 5 pF/33 kV, 17 pF/10 kV, and 50 pF/11 kV indicate that a D.C. component can be detected when the increase in power factor due to discharges exceeds 2 parts in 10^6 . The order of magnitude of the D.C. current to be detected is 10^{-11} A.

The detector can be arranged to be insensitive to discharges outside the electrode system under test.

The apparatus required consists of a low-pass filter and a high sensitivity D.C. vacuum tube voltmeter.

I. INTRODUCTION

Three-terminal high voltage air capacitors, widely used as standards in power frequency bridges, may, due to corona, show an appreciable rise in power factor with voltage. Corona is caused by overstressing the air on edges or at protuberances on the surfaces of the electrodes and even when the electrodes are well finished and their geometry is chosen so that sparkover should precede corona, the presence of dust or fibres may still cause corona to occur before sparkover. In order to avoid errors due to this effect when using a high voltage air capacitor, the power factor should be checked as a function of voltage.

The power factor increase may be detected by comparison tests using another capacitor known to be free from corona losses, but such a standard is not always at hand, as, for example, when developmental work is being carried out on a new capacitor having a higher voltage rating than that of any available standard.

Methods based on the detection of high frequency currents set up by the discharges, while not requiring a comparison standard, do not permit discrimination between (i) discharges occurring between the high voltage and the low voltage electrode, and (ii) discharges on insulators or in the power supply. In general, the latter discharges are difficult to avoid and although they are permissible in a properly guarded and correctly used three-terminal capacitor their presence precludes corona detection by radio frequency methods. Moreover, filter elements free of corona up to the required test voltage are required when the radio frequency method is used.

These difficulties have been overcome by an alternative method described in Section II.

* Division of Electrotechnology, C.S.I.R.O., University Grounds, Sydney.

II. DISCHARGE DETECTION METHOD

The technique is based on the following experimental observation: when a source of alternating voltage was connected to an air capacitor the increase in power factor above a certain critical voltage was accompanied by the appearance of a D.C. component in the current through the capacitor.

A rectifying effect of this sort may be anticipated from the observations of many workers on the difference in onset voltage for positive and negative corona. For example, Peek (1929) states that on alternating voltage the sign of the net unidirectional flow depends on the spacing, shape of electrodes, and voltage. Gaenger (1953) reports that in the case of stranded or roughened conductors, such as used for transmission lines, the onset voltage for negative corona was lower because negative discharges are more sensitive to local field concentrations on the surfaces of the electrodes. This result is relevant to the case of a capacitor having the imperfections referred to in Section I.

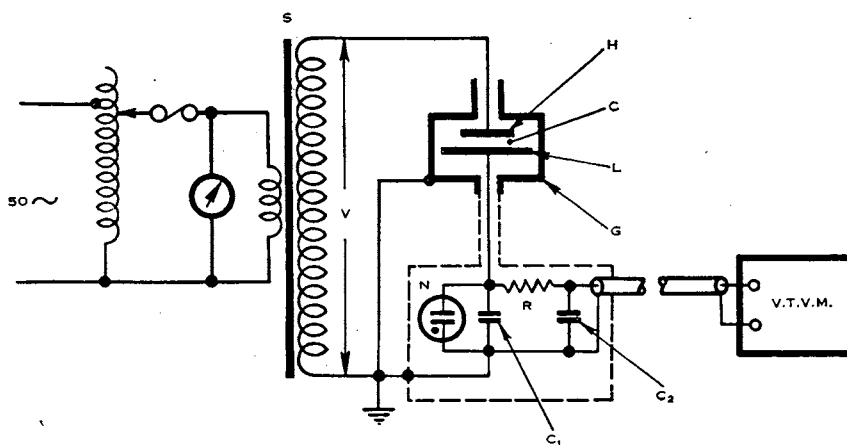


Fig. 1.—Discharge detection circuit.

S, source of variable A.C. voltage; *C*, capacitor under test; *H*, high voltage electrode; *L*, low voltage electrode; *G*, guard electrode; *C*₁, 0.5 μ F 350V D.C.W polystyrene dielectric; *C*₂, 0.1 μ F 350V D.C.W polystyrene dielectric; *R*, 1M Ω 1W cracked carbon type; *V.T.V.M.*, D.C. vacuum type voltmeter, "Philips" GM6010; *N*, rare gas cartridge: ignition voltage, 200V; max. current, 10A for 3 sec.

The correlation between power factor increase and the appearance of a D.C. component was observed on capacitors differing in form (parallel plate and cylindrical), voltage rating (10 to 33 kV), and capacitance (5 to 50 pF).

A suitable test circuit is shown in Figure 1. *S* is a source of smoothly variable A.C. test voltage of value *V*, *C* is the capacitor under test, and *C*₁, *C*₂, and *R* are the components of a low-pass filter for the separation of the D.C. component in the current through the capacitor.

The presence of direct current is indicated by a vacuum tube voltmeter. On its most sensitive range the instrument used has a voltage sensitivity of 1×10^{-5} V/div, a current sensitivity of approx. 2×10^{-11} A/div, and, with a voltage of 0.05V A.C.

50 c/s applied to its input terminals, the deflection is less than $\frac{1}{2}$ div. If this is the limiting allowable alternating voltage V_0 at the meter input, then, since $V_0 \cong VC/C_1\omega C_2R$, for $\omega = 2\pi 50$ and the values shown in Figure 1, we obtain $V \cdot C \cong 780 \text{ kV} \cdot \text{pF}$. This permits the test of a capacitor of say 5 pF at a maximum voltage of 156 kV. More filtering must be provided if higher values of $V \cdot C$ are required.

III. EXPERIMENTAL RESULTS

To determine the sensitivity of the method, the power factor change and the D.C. component were measured for several capacitors as a function of voltage at 50 c/s. Three standard capacitors rated at 50 pF/11 kV, 5 pF/33 kV, 5 pF/85 kV, and an experimental capacitor rated at 17 pF/10 kV were used. The power factor was measured in a high voltage bridge by substituting the capacitor under test for a standard capacitor of higher voltage rating. Provision was made for rapid change-over to the circuit of Figure 1.

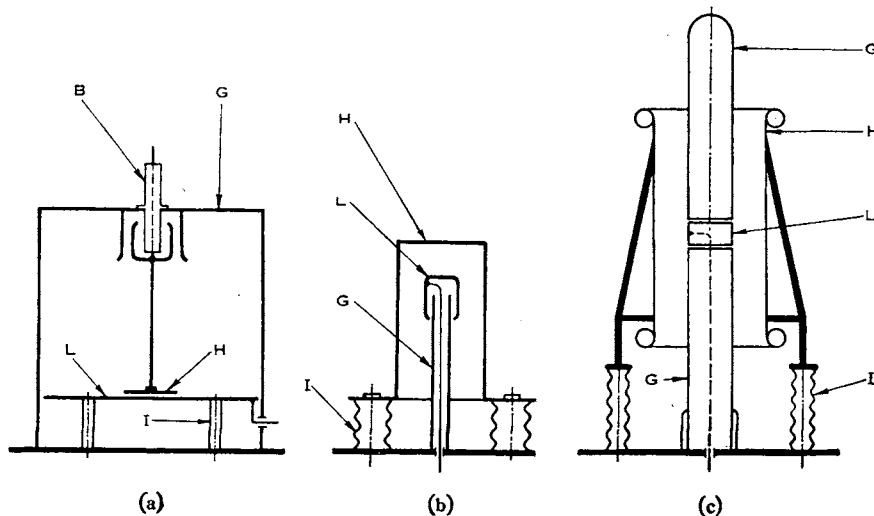


Fig. 2.—Form of some of the capacitors investigated.

- (a) Experimental parallel-plate capacitor, 17 pF/10 kV.
 $\left. \begin{array}{l} H-4 \times 4 \times 0.125 \text{ in.} \\ L-15 \times 10 \times 0.125 \text{ in.} \end{array} \right\} \text{Spacing } 0.3 \text{ in.}$
- (b) Cylindrical capacitor 5 pF/33 kV. $H\text{-I.D.} = 5.75 \text{ in.}$ $L\text{-O.D.} = 2.3 \text{ in.}$
- (c) Petersen type cylindrical capacitor, 5 pF/85 kV. $H\text{-I.D.} = 16 \text{ in.}$ $L\text{-O.D.} = 6 \text{ in.}$
 H , high voltage electrode; L , low voltage electrode; G , guard electrode; B , bushing;
 I , insulators.

The experimental parallel-plate type capacitor is shown in Figure 2(a) and typical results obtained are given in Table 1 for (i) a high-voltage electrode, the edges of which were carefully rounded and buffed, and for (ii) an electrode with its edges rounded by filing.

When the buffed electrode was replaced by an apparently identical one no change in power factor could be detected up to 6 kV, but at higher voltages both the direct current and the power factor were higher than shown in Table 1. This discrepancy was traced to the presence of minute fibres and when these were removed the results agreed closely with those given in the table. A similar fault has been observed in the cylindrical capacitor shown in Figure 2(b). This capacitor is usually free of discharges up to 37 kV. Twice, however, during the past few years, the power factor and the direct current increased sharply at a voltage as low as 18 kV. Cleaning restored the original performance.

TABLE 1

Condition of Electrode	Applied Voltage (kV)	Power Factor Increase ($\times 10^{-5}$)	D.C. Component ($\times 10^{-11}$ A)
Edges rounded and buffed	6	0	0
	8	1.0	1
	10	2.5	2
Edges rounded by filing	6	1.5	2
	8	6.5	24
	10	16.5	52

In some cases a gradual decrease with time of power factor and direct current was observed when a voltage was applied high enough for discharges to occur and sometimes this "conditioning" action was completed in a few minutes. When strong discharges occurred the direct current was unsteady and occasionally there was a sudden increase causing a large deflection of the meter. However, in all cases, it was found that an increase in power factor was accompanied by an increase in direct current, and from many measurements on capacitors ranging from 5 to 50 pF it was concluded that a power factor increase of about 2 parts in 10^5 could be detected by the D.C. technique.

The power factor change of the 85 kV capacitor shown in Figure 2(c) could not be measured as no standard of higher voltage rating was available, but since no direct current was observed, this capacitor is thought to be free of discharges within its working range.

Although developed specifically for the convenient checking of capacitors, the technique is suitable for general use in testing various electrode configurations for freedom from discharges, provided the electrodes can be arranged in the form of a guarded three-terminal air capacitor.

It should be stressed that the method is applicable only when the direct air path is not intercepted by solid insulation.

IV. PRECAUTIONS

In order to avoid spurious direct current due to dielectric absorption and electrolytic effects, sealed filter capacitors with polystyrene dielectric* were used. Even with this type of capacitor, however, it was observed that the filter could produce some direct current when the alternating voltage on C_1 was more than a few volts. C_1 should therefore be of sufficiently high value to ensure that only a low alternating voltage appears across it. Spurious direct current may also appear for other reasons, for example, solder flux residue on connecting leads.

V. REFERENCES

- PEEK, F. W. (1929).—"Dielectric Phenomena in High Voltage Engineering." 3rd Ed. p. 103. (McGraw-Hill Book Co. Inc.: New York.)
- GAENGER, B. (1953).—"Der Elektrische Durchschlag von Gasen." pp. 516-7. (Springer Verlag: Berlin.)

* Obtainable from U.C.C., 433 Punchbowl Road, Enfield, N.S.W.

Reprinted from the
AUSTRALIAN JOURNAL OF APPLIED SCIENCE
VOLUME 5, NUMBER 2, PAGES 141-144, 1954

A PEAK VOLTMETER WITH A LONG TIME CONSTANT

By L. MEDINA

Reprinted for the
Commonwealth Scientific and Industrial Research Organization
Australia

A PEAK VOLTMETER WITH A LONG TIME CONSTANT

By L. MEDINA*

[Manuscript received October 20, 1953]

Summary

A peak voltmeter which retains its reading for a considerable time is described. Power frequency breakdown phenomena may be studied without distraction and the breakdown voltage read afterwards at leisure. The discharge time constant is 10,000 sec.

I. INTRODUCTION

The instrument was developed for voltage measurements in connection with high voltage puncture and flash-over tests at mains frequency. When the object under test breaks down, the voltage on it collapses, the transformer supplying the variable test voltage being protected either by a limiting impedance or being switched off by an overload device. If a voltmeter is available which retains the breakdown voltage reading for a reasonably long period after breakdown has occurred, then the operator can concentrate solely on the observation of the breakdown phenomena and read the breakdown voltage afterwards at leisure.

Instead of measuring the high tension voltage on the object under test, it is simpler and often sufficiently accurate to measure the primary voltage, or preferably the voltage on a specially provided measuring winding (tertiary) of the testing transformer. The secondary voltage is then obtained from the known transformation ratio. The instrument described in Section II is intended for this application.

II. CIRCUIT DESCRIPTION

The circuit diagram is shown in Figure 1. The voltage to be measured is applied to the terminals *A* and *B*, charging the capacitor C_1 via the diode V_1 . The resistors R_2 and R_3 form a voltage divider giving two voltage ranges, 100 and 400 V peak (70 and 280 V r.m.s. sine wave). The voltage on C_1 , which is negative with respect to ground, is measured by means of an inverted triode vacuum tube voltmeter in which the grid is connected to a source of positive potential, the plate being used as control electrode (Terman 1928). An increase in applied voltage causes the plate of V_2 to become more negative and this reduces the grid current, its change being a measure of the applied voltage. The resistors R_6 , R_7 , R_8 , and zero adjustment resistor R_9 serve to balance out the initial grid current of V_2 . The change of grid current with plate voltage is made nearly linear by inserting the resistor R_5 into the grid circuit of V_2 .

With the switch S_2 open the charge on C_1 will leak away only slowly, the leakage resistance being made up by the insulation resistances of C_1 , V_1 , and V_2 , and the back resistances of the valves. In the present instrument this resistance amounts to 50,000 M Ω , and with C_1 at 0.2 μ F the discharge time constant was 10,000 sec. Closing S_2

* Division of Electrotechnology, C.S.I.R.O., University Grounds, Sydney.

discharges C_1 through R_4 . The value of R_4 has been chosen so that the instrument may also be used as a peak voltmeter with a short time constant of 2 sec when S_2 is closed (Rider 1941). For the particular application of the instrument mentioned earlier, in which the source impedance is nearly zero, the resistor R_1 ensures approximately the

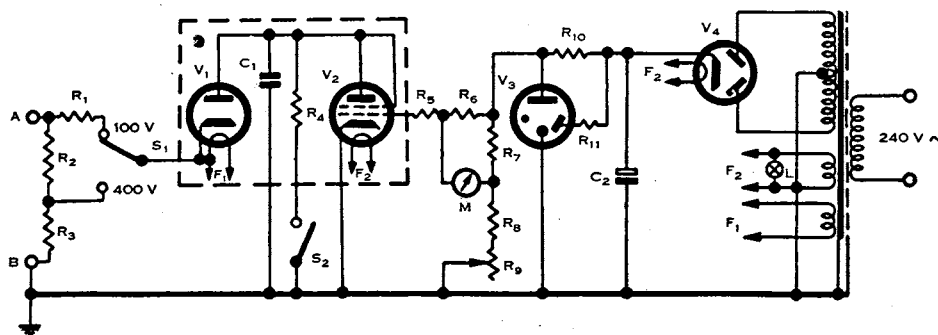


Fig. 1.—Circuit diagram.

Resistors: R_1 , 3.3 k Ω , 1 W carbon, ± 5 per cent.; R_2 , 15 k Ω , and R_3 , 5 k Ω , both 8 W W/W, matched, $R_3 = \frac{1}{3}R_2$; R_4 , 10 M Ω , 1 W carbon, ± 10 per cent.; R_5 , 4.5 k Ω , 3 W (see text) W/W; R_6 , 22 k Ω , 1 W carbon, ± 5 per cent.; R_7 , 33 k Ω , 1 W carbon, ± 5 per cent.; R_8 , 6.8 k Ω , 1 W carbon, ± 5 per cent.; R_9 , 1 k Ω , 1 W W/W, ± 5 per cent.; R_{10} , 20 k Ω , 8 W W/W, ± 5 per cent.; R_{11} , 220 k Ω , 1 W carbon, ± 5 per cent.

M , meter, 0.0–5 mA; L , pilot lamp, 6.3 V; T , transformer: primary 240 V, secondary 250/250 V, 6.3 V, 5 V.

Valves: V_1 , EA50; V_2 , 6V6G; V_3 , QS95/10; V_4 , 6X4.

Capacitors: C_1 , 0.2 μ F, 350 V, polystyrene dielectric; C_2 , 8 μ F, 525 V, electrolytic.

same charging time constant of about 1 msec for both positions of S_1 . The filament of V_1 is underheated. This increases the back resistance without undue increase in forward resistance (Hibbard 1947). The valve types were chosen for their high back resistance and smooth grid current-plate voltage characteristic.

III. CONSTRUCTIONAL DETAILS

The component values are shown in Figure 1 and the instrument in Figure 2. The socket of the valve V_2 was removed and the glass envelopes of V_2 and V_1 were made water-repellent with methylchlorosilane in order to ensure high surface-leakage resistance even in humid conditions (Meakins, Mulley, and Churchward 1950). The components surrounded by dashed lines were mounted on a "Perspex" plate, the surface of which was cleaned with benzol. The switch S_2 consists of a clicker plate, a shaft, and a piece of silver-plated phosphor-bronze wire. In the position "short time constant" this wire makes contact with a silver-plated contact on the "Perspex" plate. The resistor R_5 was adjusted for full-scale deflection of the meter M with 100 V applied to terminals A and B . The deviation of the calibration curve from a straight line was found to be less than half a division in 100, so that it was possible to fit the moving coil meter M with a linear scale.

IV. PERFORMANCE

Normally the instrument is used to measure the tertiary voltage of a 15 kVA, 240/100,000 V testing transformer, the primary voltage of which is adjusted by means of a continuously variable autotransformer. A resistor of 20Ω , rated 3 kW, permanently connected to the primary terminals, dissipates the energy stored in the core and prevents switching surges when the transformer is being switched off. Occasionally the instrument has been used to measure the primary voltage of smaller testing transformers not fitted with a tertiary winding. Terminal *B* was then connected to the earthy primary terminal.



Fig. 2.—Completed instrument.

The meter indication decreases by only 1 per cent. in 100 sec, following the removal of the applied voltage. This provides ample time for taking a reading. In consecutive flash-over tests, time may be saved by not discharging C_1 completely before commencing the next test. No appreciable zero shift was found during tests lasting several hours.

The initial calibration was found to be within 0.5 per cent. after 8 months' service. Using this calibration, the overall accuracy of the instrument is 1 per cent. of full-scale deflection.

V. ACKNOWLEDGMENT

The author wishes to thank Mr. P. T. Rudge for his help in the development and construction of the instrument.

VI. REFERENCES

- HIBBARD, L. U. (1947).—*J. Sci. Instrum.* **24**: 181.
MEAKINS, R. J., MULLEY, JOAN W., and CHURCHWARD, VIVIENNE R. (1950).—*Aust. J. Appl. Sci.* **1**: 113.
RIDER, J. F. (1941).—"Vacuum Tube Voltmeters." p. 24. (John F. Rider Publisher Inc.: New York.)
TERMAN, F. E. (1928).—*Proc. Inst. Radio Engrs. N.Y.* **16**: 447.

Ein Verzerrungserzeuger mit einstellbarer Wellenform

Von Leo Medina, Sydney*)

DK 621.373.43 : 621.317.7.089.6

In Hochspannungs-Prüf- und Versuchsanlagen benötigt man zum Messen des Scheitelwertes direktzeigende Meßeinrichtungen. Zum Prüfen dieser Scheitelwert-Meßeinrichtungen eignet sich das im folgenden beschriebene Verfahren zur Erzeugung verzerrter Spannungen.

Allgemeines

Der nachfolgend beschriebene Verzerrungserzeuger mit einstellbarer Wellenform für die Untersuchung der Kurvenfehler von Meßinstrumenten bei 50 Hz wurde ursprünglich für Lehrzwecke entwickelt. Er gestattet, den Einfluß typischer, zur Nulllinie symmetrischer Wellenformen auf die Anzeige von Effektivwert-, Mittelwert- und Scheitelwert-Instrumenten vorzuführen. Konstanz und Einstellbarkeit der Ausgangsspannung reichen aus zum Feststellen von Differenzen von 1 % gegen ein Normalinstrument. Die Anordnung dient jetzt zur laboratoriumsmäßigen Untersuchung der Kurvenfehler von Meßwerken und Meßeinrichtungen.

Arbeitsweise

Die Schaltung des Verzerrungserzeugers zeigt Bild 1. Der Transformator 1, dessen Primärwicklung für die Netzspannung ausgelegt ist, liegt über den Kondensator C und den Widerstand R am Netz oder — für Präzisionsmessungen — an den Ausgangsklemmen eines Netzspannungs-Stabilisators. Durch partielle Reihenresonanz ist die Spannung am Transformator 1 höher als die Netzspannung, und der Magnetisierungsstrom ist stark verzerrt. Der Magnetisierungsstrom, der auch durch C und R fließt, verursacht eine verzerrte Spannung am Transformator, selbst wenn das Netz sinusförmige Wellenform hat. Bild 2a zeigt die Form der Spannungswelle am Transformator 1. Andere Wellenformen, z.B. die der Oszillogramme b, c und d in Bild 2, können durch Addition erzeugt werden: Zu der auf der Sekundärseite des Transformators abgenommenen verzerrten Spannung wird die an dem einstellbaren induktiven Spannungsteiler 2 abgegriffene sinusförmige Netz-

spannung addiert. Dabei wird die gewünschte Wellenform durch den Abgriff an 2 eingestellt. Bei den in Bild 2e und 2f gezeigten Wellenformen muß der Umschalter 4 nach Stellung II umgeschaltet werden. Der zweite

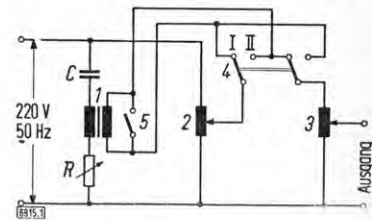


Bild 1. Schaltung des Verzerrungserzeugers.

Transformator 1: 220/70 V 880/280 Windungen, 15/1,5 Ω
Eisenquerschnitt 12 cm²,
Eisenvolumen 300 cm³

induktive Spannungsteiler 2 und 3: 250 V, 500 VA

C: 2 μ F

R: Schiebewiderstand 200 Ω , 1 A

einstellbare induktive Spannungsteiler 3 dient zum Einstellen der Höhe der Ausgangsspannung.

Die unverzerrte Spannung erhält man am Ausgang, wenn die Sekundärwicklung des Transformators 1 mit Hilfe des Schalters 5 kurzgeschlossen ist.

Auslegung der Schaltung

Für die Auslegung der Schaltung reicht die von Klinkhamer [1] angegebene rechnerische Erfassung der Ferroresonanz nicht aus, da das an sich schon schwierige Problem im vorliegenden Falle noch komplizierter wird durch die Bedingung, daß die Kurvenform der Spannung an der Sekundärseite des Transformators 1 nur einen ausgeprägten

*) Dipl.-Ing. L. Medina ist Dozent für elektrische Meßkunde an der Technischen Universität von Neu-Süd-Wales/Australien.

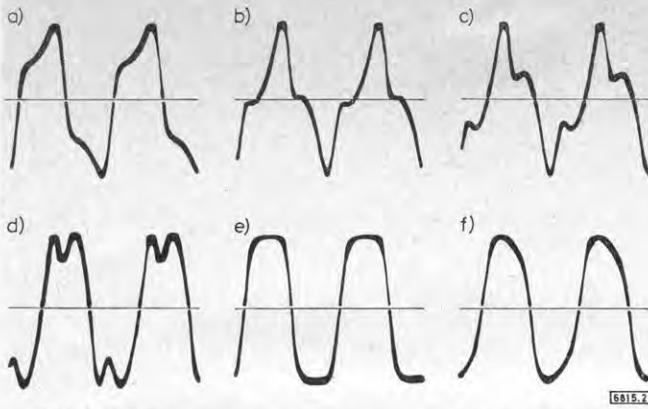


Bild 2. Oszillogramme, aufgenommen am Ausgang der Schaltung nach Bild 1. $U_{\max} = 100 \text{ V} = \text{konst.}$

Kurve	a	b	c	d	e	f
effektive Spannung am Abgriff des Spannungsteilers 2 V	0	60	95	160	55	120
gemessen bei Schalterstellung	I	I	I	I	II	II

Höchstwert haben darf, damit die in Bild 2 gezeigten Wellenformen durch Addition einer Sinusspannung erzeugt werden können. Die Werte von C , R und für den Transformator 1 können aber, wie Versuche mit verschiedenen Eisensorten und verschieden großen Kernen gezeigt haben, verhältnismäßig einfach experimentell gefunden werden. Der Transformator 1 (Übersetzungsverhältnis 220/70 V) hat bei Speisung mit 220 V eine magnetische Induktion von etwa 10 kG. Der Wert von C wird in Stufen von $1 \mu\text{F}$ so lange geändert, bis die effektive Spannung an C etwa 520 bis 560 V beträgt. Am Transformator 1 wird dann eine effektive Spannung von etwa 330 bis 360 V sein. Schließlich wird R eingestellt, bis die Kurvenform der Spannung am Transformator 1 einen ausgeprägten Scheitelwert haben wird. Wenn die Spannung an C hierdurch unter die oben angegebenen Werte sinkt, wird der nächst größere Wert von C gewählt. Bei Transformatorblech mit einer Verlustziffer V_{10} von mehr als etwa 1,2 W/kp ist R manchmal überhaupt unnötig. Doch sollte man, wenn eine große Stabilität der Ausgangsspannung erwünscht ist, die Über-temperatur des Transformators niedrig halten und hochlegiertes Blech verwenden.

Bei gleichförmigem Eisenquerschnitt ist die Ausgangsleistung dem Eisenvolumen des Transformators 1 verhältnismäßig. Bei der Schaltung nach Bild 1 beträgt die größte Scheitelspannung am Ausgang etwa 100 V. Der Verzerrungserzeuger kann mit einem Wirkwiderstand von 500Ω — parallel mit einem Kondensator von $4 \mu\text{F}$ oder einer Induktivität von 1,75 H — belastet werden, ohne daß sich die Wellenform wesentlich ändert. Der Scheitelfaktor U_{\max}/U_{eff} läßt sich in den Grenzen zwischen 1,15 und 1,9 einstellen.

Um den Verzerrungserzeuger besser an den Meßbereich der zu untersuchenden Meßinstrumente anzupassen — besonders bei der Prüfung von Strommessern —, benötigt man einen Anpassungstransformator zwischen dem Ausgang des Verzerrungserzeugers und der angeschlossenen Bürde.

Messungen mit dem Verzerrungserzeuger

Als Normalinstrumente für die Untersuchung von Effektivwertmessern wurden eisenlose Dynamometer oder Instrumente mit Thermoumformern verwendet. Scheitelwertmesser wurden in der Schaltung nach Bild 3 verglichen. Bei unverzerrter Ausgangsspannung werden zunächst mit Hilfe des induktiven Spannungsteilers 3 (Bild 1) ein Skalenpunkt am Prüfling und dann der aus den Widerständen R_1 und R_2 bestehende induktionsarme Spannungsteiler so eingestellt, daß der Stromfluß durch die Diode am

Spannungsscheitel einsetzt. Dies erkennt man daran, daß auf dem Schirm des Kathodenstrahl-Oszillographen scharfe Zacken in der durch das Kippgerät erzeugten Linie erscheinen. Man kann nun mit Hilfe des induktiven Spannungsteilers 2 (Bild 1) eine andere Wellenform wählen, am Spannungsteiler 3 die Ausgangsspannung so einstellen, daß wieder die Zacken gerade einsetzen, und beobachten, ob sich die Anzeige am Prüfling geändert hat. Mit der in Bild 3 angegebenen Schaltung konnte eine Scheitelwertänderung von 1 % noch gut festgestellt werden.

Anwendungsgebiete

Die praktische Verwendung des Verzerrungserzeugers erstreckte sich unter anderem auf die Untersuchung der folgenden Kunschtaltungen für Effektivwertmessung: Gleichrichteranordnung nach Boucke [2], in der die Ladezeitkonstante etwa 3- bis 4mal kleiner ist als die Entladezeitkonstante; Brückenschaltungen mit nichtlinearen Widerständen; Anordnungen mit Gleichrichterröhren, die im Sättigungsgebiet arbeiten, und Schaltungen, in denen durch zweckmäßige Kombination von Gleichrichtern und Widerständen eine angenähert quadratische Beziehung zwischen Strom und Spannung besteht.

Mit Hilfe der Untersuchungen an Scheitelspannungsmessern konnten Glühmühlröhren ausgewählt werden, die als Scheitelspannungsnormale geeignet sind. Andere Versuche dienten dazu, die Größe der zu erwartenden Meßfehler beim Anschluß von Scheitelspannungsmessern an die Ausgangsklemmen von Meßverstärkern¹⁾ zu ermitteln. Bei Geräten, die nach dem Prinzip der Messung des Entladestromes

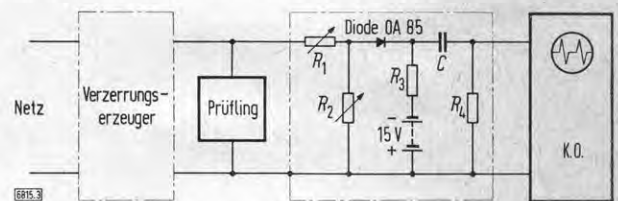


Bild 3. Schaltung zum Vergleich von Scheitelwertmessern.

R_1, R_2 : Kurbelwiderstand 1111 Ω

R_3 : 5 k Ω

R_4 : 20 k Ω

C : 1 nF

KO: Kathodenstrahl-Oszillograph mit einer Meßempfindlichkeit von $u_{\max} = 3 \text{ mV/cm}$

eines von einer Diode geladenen Kondensators arbeiten, sinkt der Scheinwiderstand in der Nähe des Wellenscheitels, was bei zu hohem Ausgangswiderstand des Verstärkers zu Verzerrungen und Fehlmessungen führen kann. Dagegen ist bei dem von Chubb [3] angegebenen Prinzip, bei dem der Mittelwert des durch einen Kondensator fließenden Stromes mit einem Drehspulinstrument und mit vorgeschalteter Diode gemessen wird, der Scheinwiderstand zwar praktisch konstant, doch können Meßfehler auftreten, wenn die Welle mehr als einen Scheitel hat und wenn die Summe aller anderen im Stromkreise befindlichen Scheinwiderstände nicht viel kleiner ist als der Scheinwiderstand des Kondensators.

Zusammenfassung

Typische, bezüglich der Nulllinie symmetrische Wellen deren Form stetig veränderlich ist, erhält man durch die Addition der Netzspannung zur Spannung eines ferroresonanten Stromkreises. Der beschriebene, nach diesem Prinzip arbeitende Verzerrungserzeuger kann aus üblichen Laboratoriumsgeräten zusammengestellt werden.

Schrifttum

- [1] Klinkhamer, H. A. W.: Equivalent network with highly saturated iron cores with special reference to their use in the design of stabiliser. Philips Techn. Rev. Bd. 2 (1937) S. 276–281.
- [2] Boucke, H.: Ein neuartiger Effektivwert-Gleichrichter mit verminderten Kurvenfehler. Arch. elektr. Übertr. Bd. 4 (1950) S. 267–270.
- [3] Chubb, L. W.: The crest voltmeter. Trans. Amer. Inst. electr. En. Bd. 35 (1916) S. 109–116.

¹⁾ Dieser Fall tritt in der Praxis auf, wenn zur Hochspannungsmessung ein Spannungsteiler und ein Meßverstärker verwendet werden.

Berechnung der Induktivität bifilar angeordneter Blechbänder

Von Leo Medina, Sydney

DK 621.3.011.3

In dieser Zeitschrift hat unlängst H. Schering [1] ein Rechenverfahren angegeben, mit dem man einen vom Verfasser der vorliegenden Arbeit seit einiger Zeit verwendeten Ausdruck für die Induktivität einer bifilaren Blechbandschleife sehr einfach überprüfen kann.

Aus der klassischen Formel für die Streuinduktivität L_o von Transformatoren mit Röhrenwicklungen ergibt sich mit den Bezeichnungen von Bild 1 a und Angabe der Abmessungen in Zentimetern

$$L_o = \mu_0 \frac{D \pi}{h} w^2 \left(d_L + \frac{d_1 + d_2}{3} \right) k \quad \text{H,} \quad (1)$$

worin $\mu_0 = \frac{4 \pi}{10} 10^{-8}$ H/cm die Permeabilität des Vakuums, w die Windungszahl und $k = 0,9$ ein von Story [2] angegebener Korrekturfaktor ist. Setzt man nach Bild 1 b mit den von Schering [1] verwendeten Bezeichnungen $d_1 = d_2 = d$ und $d_L = s = m - d$, ferner die Windungszahl $w = 1$ und divi-

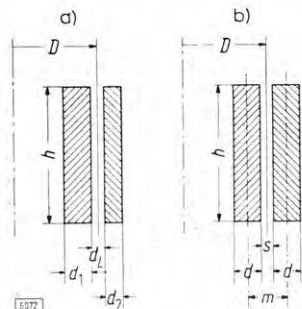


Bild 1. Querschnitt durch ein Paar konzentrischer Spulen oder paralleler Blechbänder a) mit den bei Transformatoren mit Röhrenspulen gebräuchlichen Bezeichnungen, b) mit den Bezeichnungen nach Schering.

diert die Streuinduktivität L_o durch den Umfang πD , so erhält man für die auf die Längeneinheit bezogene Induktivität

$$\frac{L_o}{\pi D} = \lambda \approx \frac{3,8 (3 m - d)}{h} \frac{nH}{cm}. \quad (2)$$

Gl. (2) gilt für $m/h < 0,1$.

In der Ableitung von L_o nach Gl. (1) ist angenommen, daß der Streufluß sich im Eisen über einen Weg sehr kleinen magnetischen Widerstandes schließen kann. Dies erklärt wohl auch, weshalb Gl. (2) nur für $m/h < 0,1$ gilt, wenn kein Eisen vorhanden ist. Mit wachsendem h überwiegt nämlich infolge des vergrößerten Luftquerschnittes die Abnahme des magnetischen Widerstandes für den Feldrück-schluß die Zunahme des magnetischen Widerstandes in dem durch $(2d + s)$ und h begrenzten Kanal.

Gl. (2) wurde auch mit dem von Orlich angegebenen Ausdruck¹⁾ verglichen. Die beiden ersten Glieder der Formel von Orlich lauten:

$$\lambda = \frac{4 \pi}{3} \frac{3 s + 2 d}{h} - 4 \left(\frac{s + d}{h} \right)^2 \left(\frac{25}{12} + \ln h \right) + \dots \frac{nH}{cm}. \quad (3)$$

Berücksichtigt man nur das erste Glied dieser Gleichung, dann ergibt sich mit den hier benutzten Bezeichnungen nach Bild 1 b

$$\lambda \approx \frac{4 \pi}{3} \frac{(3 m - d)}{h} \frac{nH}{cm} \approx \frac{4,2 (3 m - d)}{h} \frac{nH}{cm}, \quad (4)$$

also ein rd. 10 % größerer Wert als nach Gl. (2). In Tafel 1 sind Zahlenwerte der Induktivitäten bifilar angeordneter Blechbandschleifen für verschiedene Abmessungen der Blechbänder und für verschiedene Abstände angegeben. Dabei wurden die nach der Formel von Schering²⁾ und für einige Fälle auch die nach der Formel von Orlich¹⁾ — unter Berücksichtigung der Korrekturglieder — berechneten Werte mit den aus der einfachen Formel nach Gl. (2) ermittelten verglichen.

¹⁾ [1], S. 335, Gl. (6).

²⁾ [1], S. 337, Bild 2.

(18a)

Vor dem Erscheinen der Arbeit von Schering wurde der Ausdruck für λ in zeitraubender Weise nach dem von Grover [3] angegebenen Verfahren überprüft. Für Bänder mit $h = 5,08$ mm und $h = 2,54$ mm, $d = s = 0,127$ mm und

Tafel 1. Induktivitäten bifilarer Blechbänder.

Abmessungen nach Bild 1b			$x = \frac{m}{h}$ $y = \frac{d}{m}$		$\frac{\lambda}{x}$ nach Schering ²⁾	$\frac{\lambda}{x}$ nach Orlich ¹⁾	$\frac{\lambda}{x} \approx \frac{1}{x} \frac{3,8(3m-d)}{h}$ nach Gl. (2)
h	d	m			$\frac{nH}{cm}$	$\frac{nH}{cm}$	$\frac{nH}{cm}$
2,5	0,1	0,2	0,08	0,50	9,2	9,5	9,5
	0,1	0,3	0,12	0,33	9,6		10,2
	0,5	0,6	0,24	0,83	6,5		8,25
	0,5	0,7	0,28	0,71	6,7		8,7
	0,5	0,7	0,28	0,71	6,7		8,7
5	0,1	0,2	0,04	0,50	9,6	9,9	9,5
	0,1	0,3	0,06	0,33	10,1		10,2
	0,5	0,6	0,12	0,83	7,5		8,25
	0,5	0,7	0,14	0,71	7,7		8,7
	0,5	0,7	0,14	0,71	7,7		8,7
10	0,1	0,2	0,02	0,50	10,1	10,1	9,5
	0,1	0,3	0,03	0,33	10,55		10,2
	0,5	0,6	0,06	0,83	8,15		8,25
	0,5	0,7	0,07	0,71	8,4		8,7
	0,5	0,7	0,07	0,71	8,4		8,7
10	0,1	0,7	0,07	0,14	11,1	10,8	10,85
	0,6	0,7	0,07	0,86	7,85		8,15

eine Schleifenlänge von 100 cm ergaben sich nach Grover Induktivitäten von 48 nH für das breitere und von 90 nH für das schmalere Band. Nach Gl. (2) findet man 47,5 nH für das breitere und 95 nH für das schmalere Band.

Außer den naheliegenden praktischen Anwendungen für Widerstände geringer Induktivität und für bifilare Verbindungsleitungen in Wechselstrombrücken dient die Formel für λ nach Gl. (2) auch zum Berechnen induktiver Brücken-zweige.

In einer üblichen Ausführung trägt ein Kern aus Mu-Metall³⁾ oder Ferroxcube⁴⁾ eine Erregerwicklung, die der

3) Mu-Metall enthält 76 % Ni, 17 % Fe, 5 % Cu und 2 % Cr.

4) Ferroxcube ist die Markenbezeichnung eines magnetisch weichen Ferrites mit hoher Anfangspermeabilität und besonders kleinen Verlusten.

gewünschten Stromquelle angepaßt ist. Die Brücken-zweige mit der Übersetzung 1:1 bestehen aus zwei miteinander gekoppelten Wicklungen. Wenn die Kopplung sehr fest ist, z. B. wenn zwei verdrehte Drähte verwendet werden, beträgt der Streublindwiderstand, den man sich mit jeder der beiden Wicklungen in Reihe geschaltet denken muß, etwa die Hälfte des induktiven Blindwiderstandes der verdrehten Drahtschleife, wobei das Vorhandensein des Eisenkernes und die Tatsache, daß die Schleife aufgespult ist, wenig ausmacht.

Bei Verwendung dünner Blechbänder, die z. B. durch Polyäthylenband voneinander isoliert seien, verringert sich der Streublindwiderstand und der Verlustwiderstand. Je kleiner diese beiden Größen sind, desto kleiner werden der Übersetzungsfehler und der Fehlwinkel, wenn man die induktiven Brücken-zweige dazu benutzt, Scheinwiderstände, die ungleiche Erdkapazitäten haben, miteinander zu vergleichen. Für gegebene zulässige Werte der Fehler gestattet die Verwendung von Blechbändern eine Erweiterung des Frequenzbereiches.

Da es beim Entwurf solcher Brücken-zweige immer darauf ankommt, für eine gegebene Meßaufgabe eine Kompromißlösung zu finden, ist die einfache Formel nach Gl. (2) ein hierfür willkommenes Hilfsmittel.

Zusammenfassung

Eine vom Verfasser dieser Arbeit angegebene einfache Formel für die Induktivität bifilar angeordneter Blechbänder wird unter Beschränkung auf dünne Blechbänder mit einer auf völlig anderem Wege abgeleiteten genaueren Formel von Schering und mit einem von Orlich gegebenen Ausdruck verglichen. Die Genauigkeit der einfachen Formel reicht für viele praktische Fälle aus.

Schrifttum

- [1] H. Schering: Die Induktivität von zwei geraden parallelen Leitern mit gleichen Rechteckquerschnitten. ETZ-A Bd. 75 (1954) S. 335 ... 338.
- [2] J. G. Story: Berechnung von Audiotransformatoren. Wireless Engr. Bd. 15 (1938) S. 69 ... 80.
- [3] F. W. Grover: Induktanz-Berechnung. Verlag D. van Nostrand, New York 1946.

(18a)

(19)

THE NEW SOUTH WALES
UNIVERSITY OF TECHNOLOGY

FINAL EXAMINATION, 1957

25TH NOVEMBER

ELECTRICAL ENGINEERING DEGREE COURSE

Professional Elective—Measurements

Time allowed—Three hours.

Answer *five* questions only.

The questions are of equal value.

Slide rules, mathematical tables and instruments may be used.

1. A bridge with a 1 : 1 inductive ratio-arm is to be used to measure Q and L of a Ferroxcube coil at 50 c/s as a function of flux density. The coil is expected to have $L = 10$ Hy and $Q = 25$. The cross-sectional area of the core is 2 cm^2 and the number of turns is 2,000. The investigation is to be carried out over the range 10 to 100 lines per cm^2 .
 - (a) Give a suitable circuit, the relevant equations, estimate the range of components required and give the order of detector sensitivity required for 1 per cent accuracy.
 - (b) By means of an equivalent diagram give a suitable method of measuring the leakage inductances of an inductive ratio-arm.

2. An iron cored reactor to be used at 50 c/s has a layer wound coil with the following data : length of coil 4", mean circumference 10", number of layers 20, thickness of layer insulation 0.008", permittivity of insulation, 3.

- (a) Compute the self-capacitance of this coil and derive from first principles the expression used.
- (b) Give the circuit and proof of one method of self-capacitance measurement.

3. A D.C. milliammeter with 1 mA full scale deflection is to be used as an A.C. meter at 50 c/s with a full scale deflection of 5 amperes.

- (a) Give the steps in the design of a suitable current transformer for a measuring accuracy of 2 per cent.
- (b) Give and explain briefly the circuit of a testing set for measuring the errors of a current transformer using a relative method.
- (c) Give the circuit and explain briefly a method for nullifying the effect of the capacitance of the supply transformer when testing current transformers as under (b) at low primary currents. The use of screens or low capacitance windings is not acceptable.

4. A 66 kV condenser bushing of 100 pF. capacitance is to be tested in a high voltage Schering bridge. The frequency is 50 c/s. A compressed gas capacitor of 50 pF. is available as standard. For reasons of mechanical simplicity its guard electrodes are solidly grounded.

- (a) Give a circuit and compute suitable component values for a bridge in which the error caused by earthing the guards can be compensated for.
- (b) Sketch schematically a compressed gas capacitor and state the main points of interest, viz: usual type of gas, gas pressure, regions of highest electrical stress and optimum electrode dimensions.

5. (a) Explain briefly an electrostatic Ohm meter and state its advantages and applications.
 - (b) Derive the functional equation of an attracted disc type electrostatic voltmeter, schematically sketch the usual form of the instrument, state usual ranges and the precautions necessary when using the instrument.
 - (c) Show in the form of a block diagram the apparatus required in addition to the voltmeter as per (b) for measuring the peak-factor of a high voltage A.C. wave. State measurement procedure and give reasons for the necessity of peak-factor measurement.
6. A four-stage impulse generator has 4 capacitors of 0.1 microfarad each. The maximum capacitance of any test object envisaged is 1,000 pF.
 - (a) Give a circuit in which a trigatron, the drilled electrode of which is earthed, is used for firing.
 - (b) Compute the component values for a 1/50 wave using approximate expressions and state briefly the advantages and disadvantages of the various ways of arranging the front and tail-resistor.
 - (c) Give and explain briefly means of producing precisely controlled chopped waves on an impulse generator as per (a). A rod-gap is not acceptable.
7. A resistor of 20,000 ohm is to be measured at 1 Mc/s using a bridged "T" network.
 - (a) Give the circuit of the arrangement and derive a general expression for R_x in terms of the other components of the network.
 - (b) Give the range of components required.
8. The flux in the airgap of an electrodynamic loudspeaker is to be measured by means of an electronic fluxmeter.
 - (a) Give a block diagram and briefly explain operation.
 - (b) For a maximum flux density of 10,000 lines/cm.² in the gap give reasonable values of search coil area, search coil turns and full scale deflection of the fluxmeter.
 - (c) Show means of calibrating the fluxmeter and give values of suitable components.

(19a)
(26a)

THE NEW SOUTH WALES
UNIVERSITY OF TECHNOLOGY.

ANNUAL EXAMINATION, 1955.

28TH NOVEMBER.

ELECTRICAL ENGINEERING DEGREE CONVERSION
COURSE.

Professional Elective—Electrical Measurements.

Time allowed—Three hours.

Five questions only to be attempted.

The questions are of equal value.

Slide rules, mathematical tables and instruments may be used.

1. A resistive voltage divider of value $10R$ has 10 fixed ratios, 0.2, 0.3, 1.0.
 - (a) Devise a circuit with a common connection between one input and one output terminal, using as few resistors as possible.
 - (b) Show in tabular form the method of ratio calibration by build up, using a D.C. Wheatstone bridge of moderate accuracy. Continue only as far as required to show the principle.
 - (c) State the advantages of the build up principle and mention briefly two other applications.

182—66432

P.T.O.

2. (a) Discuss the influence of the connections of source and detector on the error of A.C. bridges, firstly, with one terminal of the source at earth potential; and, secondly, with one detector terminal earthed.
- (b) Explain the Wagner earth principle and give one circuit.
- (c) Discuss the advantages and characteristic requirements of inductive ratio-arms and give the equivalent circuit of a transformer, the secondary of which is used as inductive ratio-arm.

3. (a) A two-terminal resistor of value r shows an insulation resistance R between its terminals and its metal container. Derive an expression for the effective D.C. resistance, assuming that the insulation resistance is uniformly distributed and that in use one terminal of the resistor is connected to the container.
- (b) Suggest an electronic method of measuring an insulation resistance, the order of which is one million Megohms.

4. The secondary of a small current transformer feeding a bridge rectifier type meter has a resistance of 100 Ohms. The D.C. movement has 0.9 mA at full scale deflection. The ratio error at full scale deflection is 1%.
 - (a) Estimate the value of the loss-component in the exciting current of the transformer.
 - (b) Show a suitable arrangement to measure this current directly by means of an A.C. meter scaled 0—10 mA. Give approximate values of the components employed and the turns ratio of any transformer used.
 - (c) What governs the choice of the impedance in series with an iron cored coil, the core loss of which is to be determined?

5. (a) Give the circuit and vector diagram for an arrangement using resistors, a capacitor and a transformer in which the angle between current and voltage is exactly 90 degrees.
- (b) Give the circuits, the main functional equations and the physical arrangement of the following instruments:—A dynamometer synchronoscope, a dynamometer phase angle meter, a dynamometer frequency meter and a moving iron frequency meter.

6. For a single phase induction motor type watt-hour meter give—
- (a) the main functional equations;
 - (b) means for friction error compensation;
 - (c) means for achieving exact quadrature between pressure coil voltage and current (illustrate by a vector diagram);
 - (d) means to reduce the error due to creep;
 - (e) the influence of temperature on the accuracy of indication.
7. (a) Give and explain a simplified circuit for a recurrent surge oscillograph. State the purpose of such an instrument.
- (b) Compute the component values of the surge generator part for a 1/50 wave, assuming that the capacitance of the test object does not exceed 1,000 pF.
- (c) Remark on the required writing speed of the cathode ray tube.
8. In connection with rectifier type instruments—
- (a) derive an expression for the storage capacitor in a peak reading meter when the required voltage range, the frequency, the tolerable error and the full scale current of the D.C. movement are given;
 - (b) briefly give and explain a circuit for a peak-to-peak reading instrument;
 - (c) explain the purpose and the arrangement of a current transformer having a $\frac{1}{4}$ turn primary;
 - (d) show a simple and economical method of linearizing the low voltage scale of a multi range AC/DC meter;
 - (e) give a simple expression which permits an estimate of the waveform error of an average reading instrument;
 - (f) show a circuit and give the main design equation for a rectifier type meter reading nearly correct r.m.s. values of a wave with an appreciable third harmonic content.

9. (a) Give circuit and component values and derive the balance equations for a high voltage Schering bridge. Explain its use for the detection of corona discharges in dielectrics.
- (b) Give a circuit and its limitations of a corona discharge detector based on the display of the r.f. generated and give and interpret an equivalent diagram of a piece of electrical insulation in which discharges occur.
- (c) Explain possible means to differentiate between corona in the sample and corona external to it.

10. Compute the value of a non-reactive resistor from the following:—

The primary of an r.f. transformer is connected to the "L" terminals of a "Q" meter, the frequency dial of which is set to 10 Mc/s. With the secondary on open circuit resonance occurs at 100 pF and the Q value is 200. When the secondary is shorted, resonance occurs at 400 pF. With the unknown resistor connected to the secondary the Q value is 50. The inductance of the secondary is 1 microhenry and its Q value greater than 10. Derive the formulas used in the computation.



(20)

THE INSTITUTION OF ELECTRICAL ENGINEERS

FOUNDED 1871: INCORPORATED BY ROYAL CHARTER 1921

SAVOY PLACE, LONDON, W.C.2

THE ABSOLUTE CALIBRATION OF VOLTAGE TRANSFORMERS

By

W. K. CLOTHIER, B.Sc., M.E., Associate Member, and L. MEDINA, Dipl.Ing.



Reprint from

THE PROCEEDINGS OF THE INSTITUTION, VOL. 104, PART A, NO. 15, JUNE 1957

*The Institution is not, as a body, responsible for the opinions expressed by individual authors
or speakers*

THE ABSOLUTE CALIBRATION OF VOLTAGE TRANSFORMERS

By W. K. CLOTHIER, B.Sc., M.E., Associate Member, and L. MEDINA, Dipl.Ing.

(The paper was first received 30th May, and in revised form 14th August, 1956. It was published in November, 1956, and was read before the MEASUREMENT AND CONTROL SECTION 4th December, 1956.)

SUMMARY

An account is given of equipment and measuring techniques in use at the National Standards Laboratory, Australia, for calibrating voltage transformers. The equipment employs 3-terminal air-dielectric capacitors to form a voltage divider, the ratio and phase defect angle of which are determined by a self-contained build-up technique. Owing to the use of virtually loss-free capacitors, the phase angle of the divider is negligibly small.

Two methods are described for calibrating transformers. In one, ratio balance is obtained by means of a small auxiliary variable-ratio voltage transformer, and phase balance by current injection into one of the detector bridge junctions. In the other method, ratio balance is provided by a variable 3-terminal air-capacitor in the low-voltage arm of the divider, and phase balance by voltage injection in series with that arm, a feedback amplifier providing a low-impedance injection circuit. In both methods the accuracy of measurement is approximately 2 parts in 10^5 in ratio and 0.05° in phase angle.

The air-dielectric capacitors used in the voltage divider are tested to ensure that they have no significant voltage coefficient of capacitance or loss angle.

LIST OF SYMBOLS

- C = Capacitance in phase-balancing circuit, farads.
- C_1 = Capacitance in high-voltage arm of capacitance voltage divider, farads.
- C_2 = Capacitance in low-voltage arm of capacitance voltage divider, farads.
- D = N/N_2 .
- I_1 = Current in C_1 , amp.
- I_2 = Current in C_2 , amp.
- I_R = Current in R , amp.
- K_a = Ratio of transformer under test.
- K_n = Nominal ratio of transformer under test.
- N = $N_2 - N_1$.
- N_1 = Primary turns on auxiliary transformer T_2 .
- N_2 = Secondary turns on auxiliary transformer T_2 .
- R = Resistance in phase-balancing circuit, ohms.
- V = Voltage on C_2 , volts.
- V_p = Primary voltage of transformer under test, volts.
- V_s = Secondary voltage of transformer under test, volts.
- α = Fraction of the voltage V on R .
- ϕ = Phase angle, rad.
- ω = Angular frequency, rad/sec.

(1) INTRODUCTION

During recent years measuring facilities have been set up at the National Standards Laboratory, Australia, for testing voltage transformers, principally those of high precision required for use as standards in the various government, semi-government and industrial laboratories throughout Australia. In considering possible methods for testing these transformers, the use of an absolute technique was regarded as mandatory, not only because of the Laboratory's particular responsibilities as a standardizing authority, but also because of its distance from the corresponding

laboratories of other countries, which might otherwise have been called upon to provide calibrations had a relative method been adopted.

Of the various absolute methods considered, those involving a null balance in a bridge circuit were the only ones showing promise of satisfactory accuracy. In general, absolute null methods make use of some form of voltage divider for comparing the primary and secondary voltages of the transformer under test. Resistance dividers^{1,2,3} have been used for voltages up to about 150 kV, but owing to the measures that must be taken to control unavoidable capacitances, the bulk of this type of divider, together with its shield, is very considerable, even when its rating is only a few tens of kilovolts. With available resistance alloys there seems little prospect of extending the working voltage of highly precise resistance dividers much beyond 50 kV.

As appreciably higher voltages were of immediate interest, and as facility for extension to still higher voltages was desirable, attention was turned to other forms of divider, in particular to circuits employing air or compressed-gas capacitors in the high-voltage arm. The methods due to Churcher,⁴ Dannatt,⁵ Yoganandam⁶ and Gopalakrishna,⁷ shown in Fig. 1, are of this

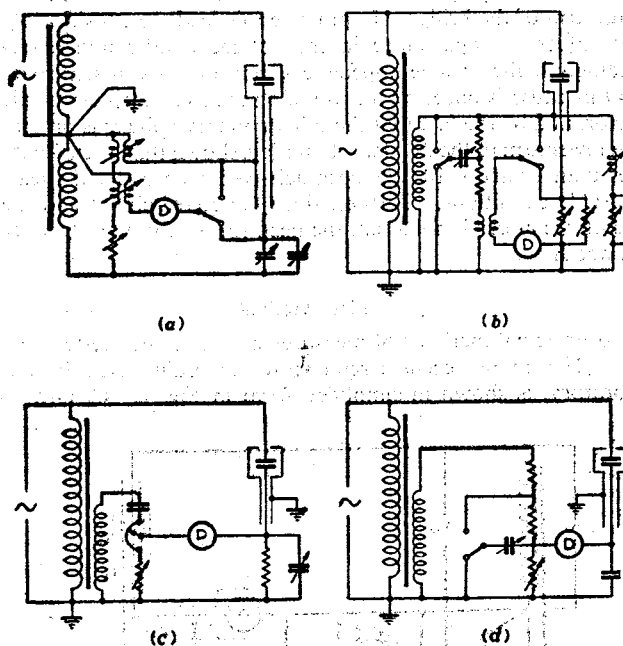


Fig. 1.—Voltage transformer testing circuits.

- (a) Churcher's circuit.
- (b) Dannatt's circuit.
- (c) Yoganandam's circuit.
- (d) Gopalakrishna's circuit.

type. In Churcher's circuit [Fig. 1(a)] the ratio balance control is a variable mica capacitor in parallel with a variable air capacitor and the phase control comprises a mutual inductor and resistor, either of which may be varied. The other circuits, although

differing in principle of operation, use for the ratio control a variable resistor and for the phase control a variable mica capacitor. In addition to the balance controls, each circuit except Churcher's makes use of at least two other components—resistors, mica capacitors or mutual inductors—the values of which enter with first-order importance into the equations for ratio balance.

In two of the circuits [Figs. 1(a) and 1(b)] a subsidiary balance is required to bring the voltage of the guard to the same value as that of the detector. Yoganandam and Gopalakrishna omit the second balance, and the resulting error due to the voltage difference between the detector and the earthed guard is kept small by limiting the impedance in the lower arm of the high-voltage divider. This results, however, in reduced sensitivity in tests at low primary voltages.

(2) CHOICE OF METHOD

An attempt has been made to devise a test method suitable for all transformer ratios from 1/1 upwards, using a simple capacitance divider as in Churcher's method, but avoiding the use of mica capacitors and mutual inductors. The former require corrections, both in capacitance and in power factor, when used for precise measurements at power frequencies, and, in the case of switched mica capacitors, the corrections are apt to be different for each setting of the dials. Mutual inductors, unless fully astatic, are inconvenient as major circuit elements determining the bridge balance, owing to their susceptibility to interference from stray magnetic fields. These component limitations have been avoided in the present equipment, principally by the use of a capacitance voltage divider in which 3-terminal air-dielectric capacitors are employed in the low-voltage as well as in the high-voltage arm of the bridge. In practice this leads to considerably lower values of capacitance in the voltage divider and correspondingly higher bridge impedances, but any loss in sensitivity from this cause is offset by the use of a sensitive tuned electronic detector, and by the fact that the full secondary voltage is present in the lower arm of the divider. Later it is shown that a sensitivity better than 1 part in 10^5 has been achieved even under the least favourable conditions. Further, since the guard circuit and the detector are at earth potential, the need for a subsidiary balance does not arise.

(2.1) First Method

Two principal methods of measurement have been tested very fully. The more recent circuit, now generally used in this Laboratory, is shown in simplified form in Fig. 2. C_1 and C_2

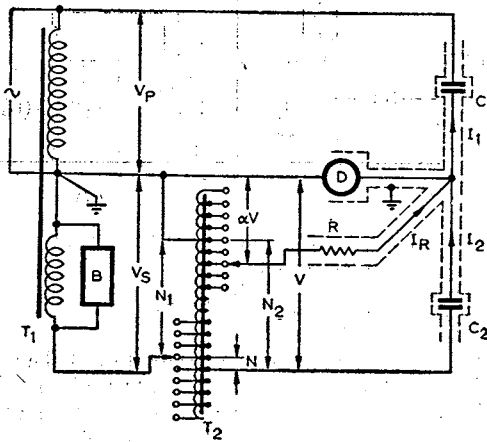


Fig. 2.—Simplified circuit of first method.

are 3-terminal loss-free capacitors forming a voltage divider whose ratio is adjusted, by choice of C_1 and C_2 , to equal the nominal ratio of the transformer under test, T_1 . The primary and secondary of T_1 are connected in series aiding. Errors in the ratio of T_1 are balanced by means of an auxiliary transformer T_2 , whose ratio can be adjusted a little above or below unity using decade switches to control the primary turns.⁸ Errors in phase angle are balanced by supplying a current I_R through a high resistance R to the junction of C_1 and C_2 . I_R is in phase with the secondary voltage and therefore in quadrature with the current in C_2 . Its value is adjusted by means of a switch operating on a winding on T_2 . The tuned electronic detector D is connected between the earthed junction of the primary and secondary of T_1 and the junction of C_1 and C_2 .

Since the detector voltage is zero at balance, the current in R is $\alpha V/R$, where αV is the voltage on R with respect to earth and V is the voltage on C_2 . Since αV can have either sign, both positive and negative phase angles can be measured.

$$\text{At balance} \quad I_1 = I_2 + I_R$$

$$\text{and, since } I_1 = j\omega C_1 V_p, \quad I_2 = j\omega C_2 V \text{ and } I_R = \alpha V/R$$

$$\text{therefore} \quad j\omega C_1 V_p = j\omega C_2 V(1 + \alpha/j\omega C_2 R)$$

$$\text{or} \quad \frac{V_p}{V_s} = \frac{C_2}{C_1} \frac{V}{V_s} \left(1 - \frac{j\alpha}{\omega C_2 R}\right) \quad (1)$$

Assuming that the phase angle of the auxiliary transformer may be neglected and that its voltage ratio is very nearly equal to the turns ratio (see Section 2.1.4), then, if N_1 and N_2 are respectively the numbers of turns on the primary and secondary of T_2 , and if $N = N_2 - N_1$,

$$\frac{V}{V_s} = \frac{N_2}{N_1} = \frac{N_2}{N_2 - N} = \frac{1}{1 - N/N_2} = \frac{1}{1 - D}$$

where D is the turns difference expressed as a fraction of the secondary turns N_2 .

From eqn. (1), the phase angle is given by

$$\phi \simeq \tan \phi = \alpha/\omega C_2 R \quad (2)$$

following the sign convention for phase angle of B.S. 81:1936.

The ratio K_a of the transformer under test is given by

$$K_a = \frac{|V_p|}{|V_s|} = \frac{C_2}{C_1} \frac{1}{1 - D} \sqrt{\left(1 + \frac{\alpha^2}{\omega^2 C_2^2 R^2}\right)} \quad (3)$$

$$\simeq \frac{C_2}{C_1} \frac{1}{1 - D} \sqrt{1 + \phi^2}$$

If the ratio of the capacitance divider is adjusted so that C_2/C_1 is equal to the nominal ratio K_n of the transformer, eqn. (3) becomes

$$K_a/K_n = \sqrt{(1 + \phi^2)/(1 - D)} \quad (4)$$

$$\simeq 1 + D + D^2 + \frac{1}{2}\phi^2$$

the approximation being justified since D and ϕ are both small.

In the majority of cases, the simpler approximation

$$K_a/K_n = 1 + D$$

gives sufficient accuracy.

(2.1.1) Detailed Description.

The detailed circuit is shown in Fig. 3. The low-voltage capacitor comprises a number of fixed air-dielectric units, 500_b, 500_c and 1000_a — 1000_e (the numerals indicating the capacitances in micromicrofarads) which can be paralleled as required

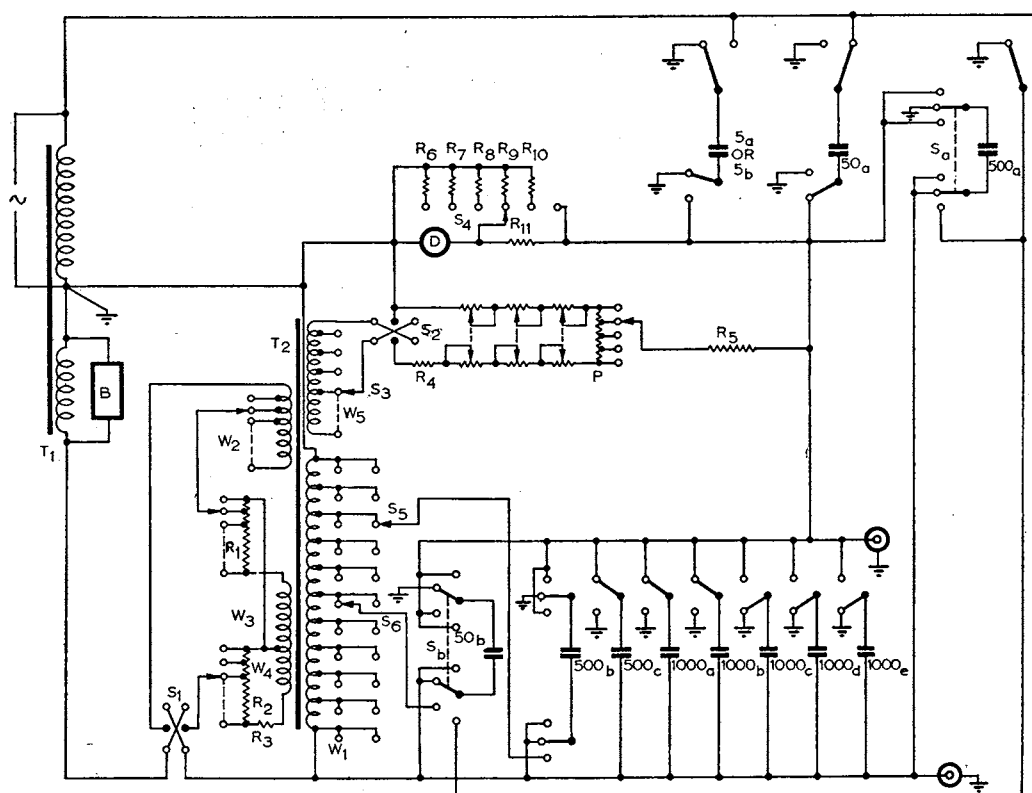


Fig. 3.—Detailed circuit diagram.

to give capacitances from $500\mu\text{F}$ to $6000\mu\text{F}$ in steps of $500\mu\text{F}$. The voltage rating of these units is 1.1 kV , although the voltage applied to them in normal use does not exceed 121 volts. High-voltage capacitors 500_a (1.1 kV), 50_a (11 kV), 5_a (33 kV) and 5_b (75 kV) are available for the upper arm, whilst two units, 500_a and 50_b (1.1 kV), can be connected into either arm. (A 150 kV compressed-gas capacitor is at present under construction.) All these capacitors are of 3-terminal construction with the solid insulation intercepted by the earthed guards. Since their power factors do not exceed a few parts in 10^6 the phase angle errors of the capacitance dividers may be neglected. The capacitor 50_b and those of $500\mu\text{F}$ and $1000\mu\text{F}$ capacitance are structurally similar to the units described by one of the authors⁹ except that they are not hermetically sealed. The capacitors 50_a , 5_a and 5_b are described briefly in Section 5.1. As the capacitors are required only to define a ratio, their absolute capacitance need not be known except in so far as it enters into the phase angle relationship of eqn. (2), and here it is required only to low accuracy. Hence, variations in capacitance due to changes in temperature or in moisture content and pressure of the atmosphere are of no consequence, provided that all capacitors are affected in the same degree. This is sensibly the case for all open-type units. On the other hand, a compressed-gas capacitor would be expected to show slight changes relative to the open units, but it would be unusual for this effect to exceed 1 or 2 parts in 10^4 , and in any event the change would be observed and allowed for in the build-up calibration described in Section 2.1.2.

For simplicity, full details of the guarding arrangements are not shown in Fig. 3, but it should be stressed that the capacitors and the wiring to the high-impedance detector bridge point must be completely guarded. However, since each capacitor has its own earthed metal case, no large screened enclosures are

necessary. The various units are interconnected by coaxial leads with the outer conductors serving as guards, and, as an additional precaution, the wiring to the low-voltage capacitors, on the side remote from the detector, is also carried out in coaxial leads in order to reduce the stray electric field in the vicinity of the more sensitive high-impedance circuits. The usual metal-braided coaxial conductor falls short of the ideal owing to the small openings between the strands of the braid. To avoid trouble from this cause, the wiring to the detector point is carried out in double-braided coaxial conductors.

By means of the switches shown in Fig. 3 the lower-arm capacitors are connected to give a capacitance ratio equal to the nominal ratio of the transformer under test, using as required a $500\mu\text{F}$, a $50\mu\text{F}$ or a $5\mu\text{F}$ capacitor connected into the high-voltage arm. The capacitor 500_a can be transferred to this arm at the lowest position of its control switch S_a .

Additional capacitors can be connected into the lower arm for special purposes. For example, by means of a $1250\mu\text{F}$ 3-terminal variable air-capacitor the lower-arm capacitance can be adjusted continuously throughout the range from 500 to $7250\mu\text{F}$. In addition, a 3-terminal micrometer capacitor is available for applications requiring fine sub-division of capacitance.

It will be noticed that the lower-arm capacitors not connected to the detector are switched to earth. This allows simple switches to be used, since all contacts of the switch are at earth potential in both positions and therefore inter-contact capacitances are of no significance. Also, a constant capacitance load is maintained in the lower arm, a result of value when the equipment is used for measurements of exceptional accuracy, as for instance in the capacitance build-up calibration described in the next Section.

The ratio balance is obtained by adjusting the number of turns in the primary circuit of the auxiliary transformer T_2 . Winding

W_2 is tapped in increments of 0.1% giving a total range of 1% by means of a decade dial. Two additional decades give steps of 0.01% and 0.001% by means of low-resistance voltage dividers supplied from the windings W_3 and W_4 . The dials are engraved to indicate the amount by which the quotient true-ratio/nominal-ratio differs from unity, and the sign of this difference is indicated by the position of the reversing switch S_1 controlling the connections to the winding. The auxiliary transformer is described more fully in Section 5.2.

Phase difference is balanced by means of a 5110-ohm switch-dial voltage divider P and 2-megohm resistor R_5 supplied from the secondary W_5 of the auxiliary transformer, and the sign of the phase angle is controlled by the position of the reversing switch S_2 . The coarsest dial of the phase control covers a range of 40' in steps of 10', and three additional decade dials give steps of 1', 0.1' and 0.01'. The total range is thus 51.1'. For the phase angle dials to be direct reading there must be appropriate correspondence between the tapping used on the winding W_5 and the total capacitance in the lower arm, which in normal testing does not exceed $5000\mu\text{F}$. To provide for this, W_5 has 10 equal sections and the selector switch S_3 is set so that the number of active sections is equal to $C_2/500$, where C_2 is the total capacitance in the lower arm in micromicrofarads. W_5 has an additional winding of one-tenth the turns of the other sections, and when connection is made to this winding in the first position of S_3 the phase angle dials are direct reading when the capacitance in the lower arm is $50\mu\text{F}$, a circuit condition that occurs during the build-up calibration.

For convenience in adjusting the detector sensitivity, an attenuator network, R_6 – R_{11} , controlled by the switch S_4 , is included in the measuring unit; R_{11} is short-circuited when the switch is in the position for maximum sensitivity. The impedance of the tuned amplifier can be regarded as infinite since it has no grid leak, the d.c. grid-cathode return being provided by the bridge itself through the 2-megohm phase-circuit resistor R_5 . The sensitivity of the amplifier is such that $10\mu\text{V}$ can be detected at the input. This sensitivity is ample for all conditions of use of the equipment, including the build-up calibration described in the next Section. In the course of normal transformer calibration, at rated voltage, the voltage on the detector exceeds $200\mu\text{V}$ for 1 part in 10^5 unbalance of the bridge.

The equipment is suitable for measurements on transformers at any frequency between 20 and 60 c/s, the auxiliary transformer T_2 and the tuned detector having been designed for use over this frequency range. The phase angle dials are direct reading on 50 c/s. At any other frequency, f , their readings must be multiplied by $50/f$.

The burden on the secondary of the transformer under test, due to the decade transformer T_2 and the total lower-arm capacitance load, is approximately 0.04 VA at 110 V, 50 c/s.

(2.1.2) Capacitance Build-up.

The build-up calibration provides for the rapid intercomparison of all capacitor units so that every capacitance ratio is determined by a completely self-contained measurement. The control switches on the capacitors (Fig. 3) enable the equipment to be used both for normal testing and for the build-up calibration. The only item additional to the normal measuring equipment is a good-quality 1100/110-volt voltage transformer which throughout the build-up takes the place usually occupied by the transformer under test.

The successive steps in the build-up will be described by reference to the functional diagrams of Fig. 4, in which the actual switching operations are represented, for simplicity, as being performed by single-pole selector switches. The switching is in fact more complicated than this (see Fig. 3) owing to the provision

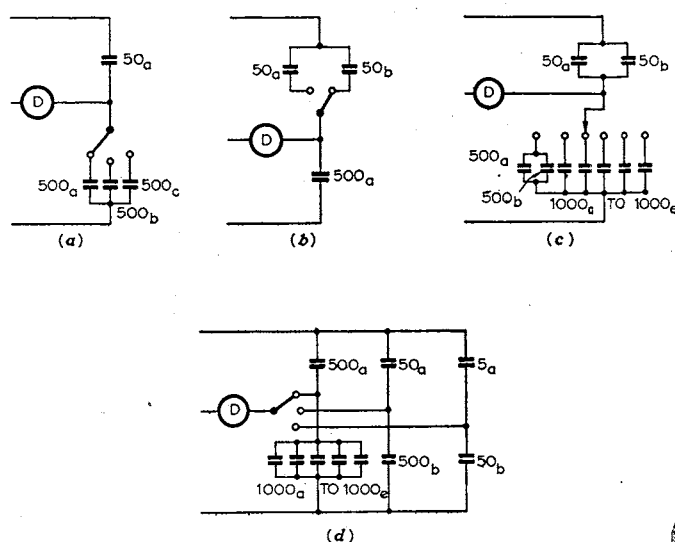


Fig. 4.—Capacitance build-up.

that must be made for earthing any capacitors that are not connected to the detector point. Fig. 4 accurately represents, however, the actual bridge-arm connections at each stage of the build-up.

Commencing with the capacitance divider arranged as in Fig. 4(a) and with one of the $50\mu\text{F}$ capacitors in the upper arm, the three $500\mu\text{F}$ capacitors, 500_a , 500_b and 500_c , are substituted in turn in the lower arm. From the dial readings at balance the relative capacitances and loss-angle differences of the $500\mu\text{F}$ capacitors are known. The $50\mu\text{F}$ units, 50_a and 50_b , are next intercompared as shown in Fig. 4(b). Capacitors 50_a and 50_b are then paralleled to give a nominal capacitance of $100\mu\text{F}$ in the upper arm as in Fig. 4(c), and the $1000\mu\text{F}$ capacitors, 1000_a to 1000_e , are compared with 500_a and 500_b in parallel in the lower arm.

The measurements of Figs. 4(a) and 4(c) give the relative values of all the $500\mu\text{F}$ and $1000\mu\text{F}$ capacitors. By transferring one of the $500\mu\text{F}$ capacitors, (500_a), to the upper arm and paralleling the five $1000\mu\text{F}$ units in the lower arm, a voltage divider of known ratio—nominally 10/1—is now formed and, as shown in Fig. 4(d), this is compared in turn with each of the two dividers of the same nominal ratio formed from the 50_a and 50_b capacitors and the 5_a and 5_b capacitors.

From the ratio balances obtained, the relative values of all capacitors are now known and the true value of any divider ratio formed from the capacitors can be determined with high precision. At each stage of the build-up the phase circuit switch S_3 , Fig. 3, is positioned in accordance with the nominal capacitance in the lower arm, and the phase balance readings then remain unchanged throughout the build-up. Any change of significant magnitude would be evidence of anomalous power loss in one of the capacitors.

It has been found convenient to trim all capacitors by means of small external fixed trimmers so that their actual ratios are very close to nominal. The build-up procedure then becomes simply a check, and no readings need be taken nor corrections applied, provided that the balance does not change significantly at any step.

Since the capacitance build-up is basic to any subsequent measurements carried out with the equipment, adequate sensitivity must be available at each stage. The most exacting conditions occur during the substitution of the $50/5\mu\text{F}$ ratio, when the bridge impedance is a maximum. Under these conditions the

voltage change at the detector for 1 part in 10^5 capacitance unbalance is approximately $25 \mu\text{V}$. This, however, is very easily detected using modern tuned amplifiers,^{10, 11, 12, 13} and at least one has been described that is capable of detecting $1 \mu\text{V}$ under the same conditions.¹² For all other steps of the build-up the sensitivity available is 10 or more times greater.

The high sensitivity has been found useful in maintaining a closer check on the stability of the capacitors than is required merely for transformer testing, but if the equipment is to be used specifically for a purpose such as this, the 1100/110-volt transformer must have exceptional stability. It has been found best in applications such as these to use a transformer excited from a separate primary winding, the 1100/110 ratio being supplied by closely coupled secondary windings. In this way the ratio error and phase difference of the secondaries with respect to one another can be reduced to a few parts in 10^5 or less and the stability is improved to a corresponding degree.

(2.1.3) Stability of Capacitors

During the period of approximately five years since the capacitors were first put into service, the relative values of the various $500 \mu\text{F}$ and $1000 \mu\text{F}$ units have remained unchanged within 1 part in 10^5 at all times. Similar stability has been observed for the $50 \mu\text{F}$ and $5 \mu\text{F}$ capacitors under normal laboratory conditions, but under exceptional conditions—rapidly changing temperature or relative humidity—temporary changes up to 3 parts in 10^5 have occurred in ratios involving the use of these units. Since the complete build-up calibration can be carried out in quite a short time—less than 10 min—a check for any change in ratio is very easily made.

(2.1.4) Errors in the Measuring Circuit.

Owing to various small errors arising in the measuring circuit, the actual ratio and phase angle of a transformer may differ slightly from the values computed from eqns. (2) and (3). In Tables 1 and 2 the various sources of error for 50 c/s operation

Table 1
RATIO ERROR

Cause of error	Dial settings for maximum error	Maximum error
Ratio error of auxiliary transformer	All ratio dials set at 10	10×10^{-6}
Phase error of auxiliary transformer	Setting $50'$	$\sim 2 \times 10^{-6}$
Reactance of R	Setting $50'$	$< 5 \times 10^{-6}$

Table 2
PHASE ANGLE ERROR

Cause of error	Dial settings for maximum error	Maximum error
Phase error of auxiliary transformer	All ratio dials set at 10	$\sim 0.015'$
Ratio error of auxiliary transformer	Setting $50'$	$\sim 0.006'$
Change in resistance of phase-balance circuit with dial setting	Approx. $25'$	$\sim 0.035'$

are given; also the conditions under which the error is a maximum and the magnitude of this maximum. Errors due to inaccuracy of adjustment of the resistors in the phase-angle and ratio circuits are not included in the Table since they are neg-

ligibly small. It is seen that under the least favourable conditions the total errors arising in the measuring circuit do not exceed 2 parts in 10^5 in ratio and $0.05'$ in phase angle.

The error in ratio of 5×10^{-6} given in Table 1 as due to the reactance of R is based on an assumed time-constant of 10^{-6} sec for the resistor, which is wire wound and has a value of 2 megohms. A time-constant lower than this is easy to achieve, either by the form of the winding or by the use of compensation, but the wiring of the resistor into the bridge must be carried out carefully to avoid additional stray capacitance in shunt with the resistor. The judicious use of a shield is helpful in this connection.

(2.1.5) Non-Standard Ratios.

The equipment as described above provides for the calibration of transformers with nominal ratios of 1/1, 2/1, 3/1, 4/1, 5/1, 6/1, 7/1, 8/1, 9/1, 10/1, 11/1, 12/1, also 10-fold and 100-fold multiples of these ratios. In tests at intermediate ratios the effective capacitance of one or more of the fixed units is varied in steps of 10% of its maximum value by connecting it to tappings on the winding W_1 of the auxiliary transformer T_2 in Fig. 3. In this way one of the $500 \mu\text{F}$ units (500_b), using the switch S_5 , provides capacitances from $50 \mu\text{F}$ to $500 \mu\text{F}$ in steps of $50 \mu\text{F}$, and a $50 \mu\text{F}$ unit (50_b), using the switch S_6 , gives values from $5 \mu\text{F}$ to $50 \mu\text{F}$ in steps of $5 \mu\text{F}$. By means of these two capacitors, together with the other fixed units, effective lower-arm capacitances from $500 \mu\text{F}$ to $6050 \mu\text{F}$ can be selected in steps of $5 \mu\text{F}$. This degree of sub-division is sufficient to allow a bridge balance to be obtained for any ratio by means of the ratio controls of the measuring circuit. The accuracy depends upon the precision of sub-division of voltage in the tapped winding W_1 . Taking into account the errors of this transformer, and bearing in mind that the contribution to the total effective lower-arm capacitance by the capacitors connected to the tappings on W_1 never exceeds 50%, it is found that the errors do not exceed 2×10^{-5} in ratio and $0.1'$ in phase angle.

An alternative method for testing transformers with non-standard ratios makes use of a 3-terminal variable air capacitor in the lower arm to provide a capacitance ratio equal to the nominal ratio of the transformer under test.

(2.2) Second Method

The second principal method of testing voltage transformers that has been investigated in detail is shown in Fig. 5. The

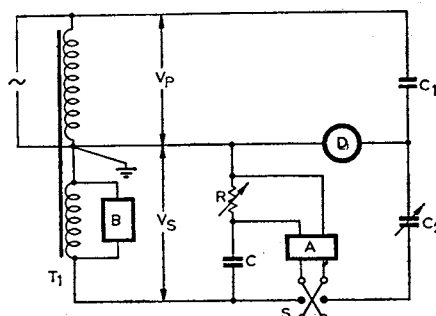


Fig. 5.—Simplified circuit of second method.

capacitance divider is identical with that previously described except that one of the $1000 \mu\text{F}$ fixed capacitors is replaced by a $1250 \mu\text{F}$ 3-terminal variable air capacitor, thus enabling the capacitance in the lower arm to be adjusted continuously throughout the range from $500 \mu\text{F}$ to $6250 \mu\text{F}$. Ratio balance is obtained by varying this capacitor, finer sub-division being provided, when necessary, by means of a micrometer capacitor connected in parallel.

Phase balance is obtained by injecting a quadrature correcting-voltage in series with the lower arm. This voltage is derived from a variable resistor R and capacitor C shunted across the secondary of the transformer under test, T_1 . The voltage on R is applied to the input of a feedback amplifier, A , with a gain of unity, and the output appears in a winding of an output transformer in the feedback loop. Reversal of the phase of the injected voltage is carried out by reversing the connections to this winding.

The voltage on the phase-balancing resistor R is

$$j\omega CRV_s/1 + j\omega CR$$

Since A has a gain of unity, the voltage on C_2 at balance is $V_s \pm j\omega CRV_s/1 + j\omega CR$, the sign depending upon the position of the reversing switch, S , in the output circuit of the amplifier.

The current in C_2 , therefore, is

$$j\omega C_2 V_s (1 \pm j\omega CR/1 + j\omega CR) = j\omega C_1 V_p$$

since the currents in C_1 and C_2 are the same at balance.

Hence

$$\begin{aligned} V_p/V_s &= \frac{C_2}{C_1} \left(1 \pm \frac{j\omega CR}{1 + j\omega CR} \right) \\ &= \frac{C_2}{C_1} \left(1 \pm \frac{\omega^2 C^2 R^2 + j\omega CR}{1 + \omega^2 C^2 R^2} \right) \\ &= \frac{C_2}{C_1} \left(\frac{1 + 2\omega^2 C^2 R^2 + j\omega CR}{1 + \omega^2 C^2 R^2} \right) \text{ or } \frac{C_2}{C_1} \left(\frac{1 - j\omega CR}{1 + \omega^2 C^2 R^2} \right). \quad (5) \end{aligned}$$

From eqn. (5), the phase angle ϕ of the transformer is given by

$$\tan \phi = - \frac{\omega CR}{1 + 2\omega^2 C^2 R^2}, \text{ or } \omega CR \quad (6)$$

respectively, for negative and positive phase angles in accordance with the sign convention of B.S. 81: 1936.

For most purposes the term $2\omega^2 C^2 R^2$ is negligible and it is sufficient to use the approximation

$$\phi \simeq \tan \phi \simeq \mp \omega CR \quad (7)$$

Neglecting 4th and higher powers of ωCR , eqn. (5) gives for the ratio K_a

$$\begin{aligned} K_a = \left| \frac{V_p}{V_s} \right| &= \frac{C_2}{C_1} (1 + \frac{1}{2}\omega^2 C^2 R^2) \text{ or } \frac{C_2}{C_1} (1 - \frac{1}{2}\omega^2 C^2 R^2) \\ &\simeq \frac{C_2}{C_1} (1 + \frac{1}{2}\phi^2) \text{ or } \frac{C_2}{C_1} (1 - \frac{1}{2}\phi^2) \quad (8) \end{aligned}$$

In the majority of cases the terms in ϕ^2 can be neglected so that

$$K_a \simeq \frac{C_2}{C_1}$$

In practice there are small departures from the relationships of eqns. (7) and (8) due chiefly to the phase-defect angle of C and the finite output impedance of the amplifier. The former gives a ratio error proportional to the product of the phase-defect angle and the indicated transformer phase angle. With a mica capacitor of reasonable quality for C , the defect angle is less than 10^{-3} rad and the error in ratio is then less than 10^{-5} at an indicated phase angle of $35'$. The error due to capacitance current flowing in the output impedance—approximately 10 ohms resistance—of the amplifier is almost constant at $0.07'$ for 50 c/s operation. No significant error occurs owing to incorrect amplifier gain since it differs from unity by less than 0.1% .

The capacitance build-up calibration is carried out by a

procedure generally similar to that described in Section 2.1.2 for the first method.

(2.3) Comparison of the Methods

Both methods of testing described above are capable of high accuracy, and in this respect there is little to choose between them. Experience with the fixed capacitors, however, showed their stability to be considerably superior to that of the best available variable air capacitors, and the advantages of this high stability could be more fully realized in the first method. At the same time, the use of decade switches for the ratio dials and the elimination of any form of valve amplifier from the main bridge network were considered to be points in favour of this method. For these reasons the first method was adopted for general testing work.

It is worth noting that alternative combinations of the techniques described for ratio and phase measurement have certain advantages, in particular one employing the ratio control of the first method and the phase control of the second, but a discussion of these alternatives is beyond the scope of the paper.

(2.4) Auxiliary Tests

A number of useful check tests have been employed at various stages in the development of the equipment, and some have been adopted as routine because of their value in periodical checking.

(2.4.1) Tests for Variation of Capacitance with Voltage.

One of the more important tests is that used to confirm that the capacitances are independent of the applied voltage up to their maximum working limits. It was pointed out earlier that, in the build-up calibration, the maximum voltage on the $10\mu\text{F}$ and $5\mu\text{F}$ capacitors is 1100 volts, whereas the working voltages on these units during transformer testing are very much higher—11 kV (nominal) for the $50\mu\text{F}$ unit; 33 kV and 75 kV for the $5\mu\text{F}$ units.

The 11 kV and 33 kV capacitors were tested in the following way. Using a voltage transformer to provide ratio arms in the circuit of Fig. 3, the bridge was first balanced using a capacitance divider with the test capacitor in the upper arm. This divider was then replaced by another of the same nominal ratio, but with a higher-rating capacitor in the upper arm, and the bridge was rebalanced. By repeating the substitution at various voltages up to the limiting working voltage of the test capacitor, any alteration in its capacitance or power factor could be detected. In this way, for example, the 11 kV $50\mu\text{F}$ capacitor, with $5000\mu\text{F}$ in the lower arm, is tested by comparison with the 33 kV $5\mu\text{F}$ capacitor, with $500\mu\text{F}$ in the lower arm, up to the maximum working voltage of 11 kV + 10% applicable to the $50\mu\text{F}$ unit. The 33 kV $5\mu\text{F}$ capacitor, with a suitable value of capacitance in the lower arm, is then compared with the 75 kV $5\mu\text{F}$ capacitor using any convenient voltage transformer capable of supplying 33 kV + 10%.

There remains the 75 kV $5\mu\text{F}$ capacitor to be checked at voltages above 33 kV + 10%. In the absence of other 3-terminal capacitors to cover this range, recourse must be had to indirect methods of test, and two such methods have been used. Both are based upon the observation that, in 3-terminal capacitors of sound design, any capacitance change or increase in power loss with increase in the applied voltage is invariably associated with corona discharge which appears abruptly at a particular voltage and then increases rapidly with rising voltage. In one method the assumption is made that, when testing a good-quality transformer by means of the capacitor under examination, the absence of any anomalous change in the measured ratio or phase angle with increasing voltage is evidence of satisfactory capacitance

behaviour. The second test has been described by one of the authors¹⁴ and is found to be very reliable, for both high- and low-voltage capacitors. In this test, discharges are detected under normal a.c. conditions by observing the existence of a d.c. component in the current to the guarded electrode. Such a direct current has invariably been found associated with discharges in air-dielectric capacitors, and, unlike r.f. detection methods, the d.c. technique discriminates between discharges to the guard and to the working electrode.

The tests described above have given complete agreement when used for determining the safe working limits of voltage on the capacitors for measuring purposes.

(2.4.2) Check Tests using a Calibrated Transformer.

Having carried out the build-up calibration and the checks for voltage independence, the capacitors can, if desired, be used to calibrate one or more transformers, and then, reversing the order, subsequent tests on the transformers can serve as a check on the capacitors, at least within the limits of stability of the transformers. This procedure has been adopted as routine in the Laboratory, and before testing a voltage transformer a check test on the same nominal ratio and at the maximum working voltage is carried out on a suitable laboratory voltage transformer reserved for the purpose. Experience has shown that the measured ratio and phase angle of the check transformers remain constant to better than 1 part in 10^5 under laboratory conditions with controlled air temperature.

(2.4.3) Check on the Capacitance Build-up.

The Laboratory has available a high-quality 6.6 kV 150 000-ohm resistance divider, constructed for another purpose, and this has been used to check the capacitance build-up at reduced voltages. At voltages up to half the nominal rating of the divider the actual divider ratios agree with the nominal within 1 part in 10^5 , and, by suitable interconnections, all the standard ratios and a large number of non-standard ratios are available. The capacitance ratios were checked using the transformer ratio bridge shown in Fig. 6. With the detector switched to the

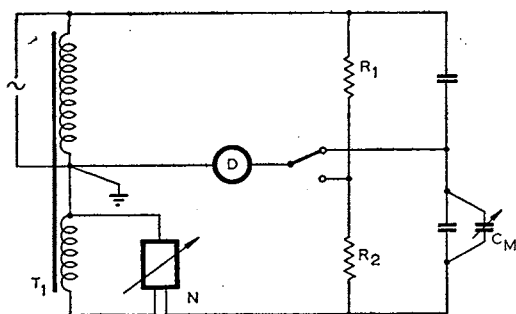


Fig. 6.—Check of capacitance ratio against resistance divider.

resistance divider, the bridge was first balanced by adjusting the magnitude and phase controls of a low-impedance correcting network, N, on the secondary of a voltage transformer, T_1 , of nominal ratio equal to the resistance ratio. The detector was then transferred to the capacitance divider and the latter was adjusted to the same ratio by means of the micrometer capacitor C_M , any necessary phase adjustment again being taken up by means of the phase control. In this way the capacitance ratio was adjusted for equality with the resistance ratio. The capacitance ratio obtained by means of the resistance divider agreed with that given by the capacitance build-up within the limits of accuracy of the measurements, i.e. approximately 1 part in 10^5 .

The resistance divider does not provide a useful check on the

power factor of the capacitors, since the phase angle of the divider is relatively large and varies with the ratio. Because of its excellent stability, this divider has at times been used as a reference standard for setting the ratio of the capacitance divider when testing transformers with non-standard ratios.*

(2.4.4) Influence of Primary and Secondary Interconnections.

In the methods of calibration described above, the transformer primaries and secondaries are connected in series aiding. To check for a possible effect of dielectric admittance currents on the ratio or phase angle, depending upon the interconnection used, a carefully balanced 110/110-volt isolating transformer was connected in cascade with the secondary of the transformer under test and the ratio and phase angle of the combination were measured for the series-aiding and series-opposing connections of the test transformer secondary. No significant difference has been observed in many tests carried out in this way.

On the other hand, appreciable changes have been observed when the primaries of high-voltage transformers are reversed. For example, out of eight 33 kV transformers with fully insulated primaries, seven showed measurable changes, the greatest however being only 1.7 parts in 10^4 in ratio and 0.09° in phase angle, and this result was obtained in a test at a frequency of 50 c/s on a transformer rated at 25 c/s. In every case the reversal effect was very small, so much so that in order to measure the effect it was essential to maintain a close control on voltage and frequency.

(3) CONCLUSIONS

Two absolute methods have been developed for the precise measurement of the errors of voltage transformers. The standard of ratio employed is a capacitance voltage divider of negligible phase angle formed from 3-terminal air-dielectric capacitors, the relative values of which are determined by a build-up calibration. The sensitivity and accuracy are such that ratio can be measured to 2 parts in 10^5 and phase angle to an equivalent accuracy.

(4) REFERENCES

- (1) DAVIS, R.: 'The Design and Construction of a Shielded Resistor for High Voltages', *Journal I.E.E.*, 1931, **69**, p. 1028.
- (2) SILSBEE, F. B.: 'A Shielded Resistor for Voltage Transformer Testing', *Scientific Papers of the Bureau of Standards*, No. 516, 1925.
- (3) DE LA GORCE, P.: 'La réalisation d'une résistance pour les mesures en très haute tension', *Comptes Rendus*, 1930, **191**, p. 1297.
- (4) CHURCHER, B. G.: 'The Measurement of the Ratio and Phase-Displacement of High Alternating Voltages', *Journal I.E.E.*, 1927, **65**, p. 430.
- (5) DANNATT, C.: 'The Testing of Voltage Transformers for Ratio and Phase-Angle', *Metropolitan-Vickers Gazette*, 1931, **13**, p. 62.
- (6) YOGANANDAM, G.: 'A Ready Method of Measuring the Voltage Ratio and Phase-Angle of High Voltage Transformers', *Journal I.E.E.*, 1930, **68**, p. 192.
- (7) GOPALAKRISHNA, H. V.: 'A Precise Method of Determining the Ratio and Phase Angle Errors in High Potential Instrument Transformers', *Journal of the Indian Institute of Science*, 1955, **37**, Sect. B, p. 16.
- (8) CLOTHIER, W. K., and MEDINA, L.: 'A Portable Voltage Transformer Testing Set', *Australian Journal of Applied Science*, 1954, **5**, p. 145.

* The authors' attention has been drawn to a paper on the absolute calibration of voltage transformers (*VDE-Fachberichte*, 1953, 17) by H. E. Linckh, who describes a detailed technique for calibrating a capacitance divider by comparison with a resistance divider of known ratio and phase angle.

- (9) CLOTHIER, W. K.: 'A Fixed Gas-Dielectric Capacitor of High Stability', *Proceedings I.E.E.*, Paper No. 1679 M, August, 1954 (101, Part II, p. 453).
- (10) RAYNER, G. H.: 'A Selective Detector Amplifier for 10–10000 c/s', *Journal of Scientific Instruments*, 1953, 30, p. 17.
- (11) LOOMS, J. S. T.: 'A Null-Detector for Power Frequency Bridges', *ibid.*, 1953, 30, p. 290.
- (12) CLOTHIER, W. K., and SMITH, W. E.: 'A Tuned Detector-Amplifier for Power Frequency Measurements', *ibid.*, 1955, 32, p. 67.
- (13) CLOTHIER, W. K., and HAWES, F. C.: 'A Tuned Differential Amplifier for Low Frequency Bridges', *Australian Journal of Applied Science*, 1956, 7, p. 38.
- (14) MEDINA, L.: 'The Detection of Corona Discharges in High Voltage Air Capacitors', *ibid.*, 1955, 6, p. 453.

(5) APPENDICES

(5.1) High-Voltage Capacitors

The electrode arrangements and the approximate proportions of the 11 kV, 33 kV and 75 kV capacitors are shown in Fig. 7. Leading dimensions are given on the diagrams. All capacitors are of 3-terminal construction, and in each case the location of the solid insulating material is such that it has no appreciable influence on the direct capacitance or power factor.

The 11 kV 50 μ F unit [Fig. 7(a)] is a parallel-plate capacitor with the two assemblies of crossed rectangular plates supported on ceramic insulators from a heavy metal base. The electrodes of the 33 kV 5 μ F unit [Fig. 7(b)] are concentric cylinders, closed at the upper ends, the outer cylinder serving as the high-voltage electrode. The 75 kV 5 μ F, Petersen-type capacitor [Fig. 7(c)] has been constructed to satisfy a temporary need until a compressed-gas capacitor becomes available. Although of very simple construction it has given completely satisfactory performance. The inner cylindrical low-voltage electrode and guard electrodes are made from brass tubing, and the outer cylinder from rolled brass sheet.

(5.2) The Auxiliary Transformer

The auxiliary transformer (T_2 in Fig. 3) has a $2\frac{1}{2}$ in core of Telcon type 113N 0.015 in Mumetal laminations, singly interleaved. Details of the windings are given in Table 3, the notation being the same as in Fig. 3. The winding order is the order of entry in the Table, W_2 being the innermost winding. The ten sections of W_1 are connected in a sequence giving minimum errors in sub-division of voltage. Denoting the ten sections by 1 to 10, the sequence of connections is 6–5–7–4–8–3–9–2–10–1.

The primary current of T_2 at 110 volts is 0.25 mA at 50 c/s

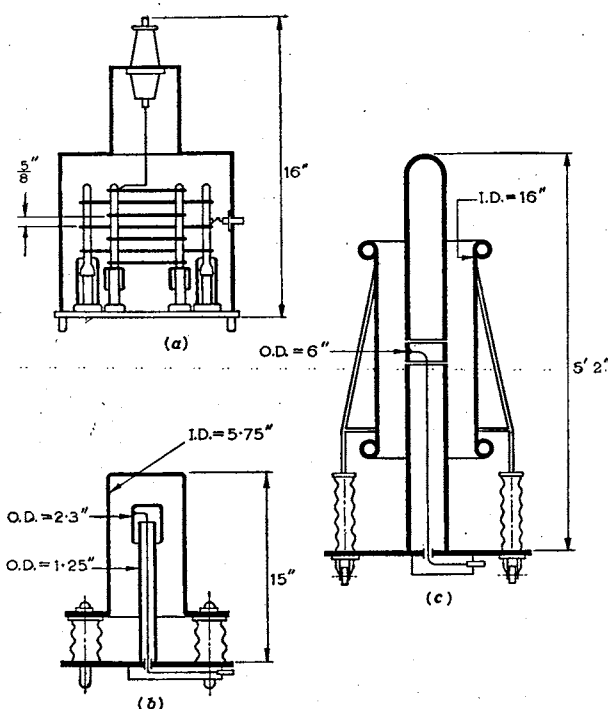


Fig. 7.—High-voltage capacitors.

- (a) 50 μ F 11 kV capacitor.
- (b) 5 μ F 33 kV capacitor.
- (c) 5 μ F 75 kV capacitor.

Table 3

Winding	Number of turns	Taps at	Wire
W_2	30	Every 3 turns	16 B. & S. S.S.E.
W_3 and W_4 ..	4	3 turns	0.005 in shim copper 2 in wide
Electrostatic shield	1	—	0.002 in shim brass
W_1	10 × 300	—	29 B. & S. S.S.E.
Electrostatic shield	1	—	0.002 in shim brass
W_5	150	1½ turns and every 15 turns	23 B. & S. S.S.E.

and 0.5 mA at 20 c/s. These figures are for the transformer loaded with the resistors R_1 , R_2 and R_3 and with the voltage divider P bridging the whole of winding W_5 . The influence of the capacitance load due to the low-voltage capacitors and guard circuits is to modify the primary current at 110 volts to 0.35 mA at 50 c/s and 0.45 mA at 20 c/s.

DISCUSSION BEFORE THE MEASUREMENT AND CONTROL SECTION, 4TH DECEMBER, 1956

Mr. D. Edmundson: Nothing is easier than to design a bridge circuit, but nothing is more difficult than to design a good one. The first of the two described in the paper is singularly free from almost any kind of objection.

A bridge circuit is judged not only—or even primarily—on its accuracy but also on such matters as the following. Is it direct-reading? Does the screen require a separate balance? Are the two adjustments independent? Can a spurious balance be obtained? The authors' circuit is satisfactory on all these counts. Its most important innovation is the use of a gas-dielectric condenser at the l.v. end of the divider, made possible by developments in amplifier-galvanometers. The objection to the mica condenser universally used is not that its phase angle,

differing from zero, introduces inaccuracies: such an error, which need be only of the order of 0.1% or less, say 1–3 min, can be accurately known and allowed for. It is that, since a correction has to be made, the bridge is not direct-reading. Again, the introduction of the auxiliary transformer, made possible by the development of high-permeability alloys, makes direct reading possible in all normal circumstances. The authors disarm criticism by referring to its negligible burden, but more detail of its design would be appreciated.

In the second circuit, which is only briefly referred to, the authors give no details of the amplifier. I do not doubt that it can be made, but, in work of this sort, the point has hardly been reached where an amplifier—which, after all, is an essential

part of the circuit—can be represented by a rectangle without reference to its design.

How far use can be made of the accuracy now achieved by the authors is perhaps a philosophical question. Occasionally, a voltage transformer has to be calibrated in a laboratory for use as a secondary standard, but the calibration accuracy would depend on its stability. Or, for a special measurement, e.g. that of the heat-rate of a turbine, extremely accurate integrators may justify a corresponding accuracy in associated equipment. Again, in measuring the short-circuit loss of a large power transformer, the circuit phase-angle of perhaps 3° or 4° requires a very low phase-angle error in the instrument transformers. Most voltage transformers are, however, designed to supply relays or meters of commercial accuracy, and it is doubtful if present methods of calibration have ever introduced significant errors. It is on the other grounds which I have mentioned that I hope to see the authors' circuit introduced into this country as general practice in the transformer industry.

Mr. H. D. Hawkes: I think it would be advisable to call the authors' method of calibration a 'direct method' as opposed to the 'difference methods' using a standard transformer for reference. In both these methods, where the out-of-balance signal has to be resolved into active and reactive components, high accuracy is approached only where the error signal is relatively small.

The authors claim an accuracy of 2 parts in 10 for both⁵ ratio and phase angle for their method, which is dependent on both frequency and waveshape. I should like to ask if this is realistic in view of the h.t. supply required.

I should like to see the national laboratories develop a direct method of measurement which would give errors of voltage transformer under practical conditions of, say, 1% or 2% harmonic distortion in the supply voltage. This method would, of course, be complex and could only be undertaken by a national concern, but it could produce some valuable information. It would mean using a device other than a fundamental detector, which covers a multitude of sins.

Table 1 of the paper gives the cumulative errors due to an auxiliary transformer. It would be interesting to know the actual errors of this transformer and how they were measured. In Section 2.4.1, in contradiction to the title of the paper, the use of an absolute transformer for checking a calibration method is mentioned, and the authors make a somewhat hazardous assumption in respect of a voltage transformer on increasing voltage. A 50% increase or decrease in voltage on a good transformer (class A) can give a change in error in ratio of 1 part in 10^4 and a phase-error change of 1.5 min.

Mr. A. Felton: The methods of calibration described have achieved an accuracy far beyond anything that has been obtained before on voltage transformers, and there is no doubt that the paper will become a classic on the subject. Further, by careful attention to every detail, the authors have anticipated every reasonable criticism.

One of the very few technical objections to the method is that the transformer is not tested under the conditions of use. In the first place, the primary and secondary are connected in series aiding, and although no differences due to dielectric admittances have yet been found, it cannot be assumed that all transformers will be equally good in this respect. Secondly, one side of the primary is earthed, whereas in some 3-phase transformers both terminals are, in normal use, at a high potential to earth. It must, of course, be admitted that this defect is shared by all the well-known voltage-transformer testing circuits, and hitherto, with the limited accuracy that has been obtainable, any differences between conditions of use and conditions of test have been considered to be negligible. But with the greatly

improved accuracy achieved by these new circuits the differences may be significant, and if the authors are considering any further work they might direct some attention to this aspect of the subject.

Mr. J. K. Webb: For use at the high voltages which the authors consider, instrument transformers must be quite large and expensive. It would enhance the value of the paper if the illustrations of the high-voltage capacitors shown in Fig. 7 were supplemented by similar illustrations of the transformers. An economical procedure is to provide a tertiary winding on a mains transformer so that it can be used both to supply power and to serve as a means of measuring the output voltage. This method became popular in the cable industry about 1930, when a modified Schering bridge was used to measure voltage which was given directly in terms of the tertiary voltage and the bridge settings at balance. The circuit was similar to that of Yoganandam shown in Fig. 1(c), and an accuracy of 1 part in 1000 was claimed. Would the authors, in the light of their investigation, agree with this figure, or do they think that there is anything much to be gained from their rather more elaborate circuit, bearing in mind the deficiencies involved in using a mains transformer as an instrument transformer?

Mr. G. W. Bowdler: I have recently measured the errors of voltage transformers with the aid of *ad hoc* equipment, using the circuit of the authors' Fig. 1(a). The procedure is equally applicable to any circuit in which a small fraction of the primary voltage is balanced against a fraction of the secondary. Ample sensitivity is obtained if these fractions are of the order of 1 volt.

Before the transformer test, the voltage dividers which it is proposed to use are connected together (Fig. A) to form a

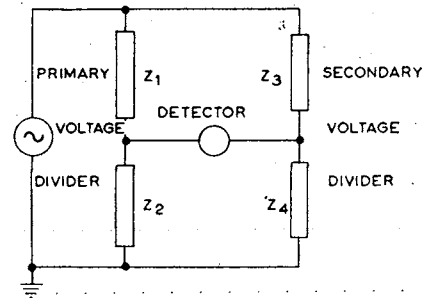


Fig. A

simple bridge which may conveniently be fed from the transformer secondary winding and balanced by adjustment of Z_2 or Z_3 . The voltage across Z_2 and Z_4 under these circumstances will be only about $1/k$ volt, where k is the transformer ratio. Nevertheless, with a high-impedance detector sensitive to $1\mu\text{V}$, the bridge can still be balanced correct to 1 part in 10^4 for values of k up to 100. For transformers with higher ratios it may be necessary to operate the bridge at correspondingly higher voltages.

$$\text{At balance, } \frac{Z_1}{Z_2} = \frac{Z_3}{Z_4} \quad \dots \quad (\text{A})$$

The transformer is then tested by connecting the dividers across their respective windings and balancing the bridge by alteration of Z_4 to a value Z'_4 ($\approx kZ_4$), keeping Z_1 , Z_2 and Z_3 unchanged.

$$\text{At balance, } \frac{V_p}{V_s} = \frac{Z_1 + Z_2}{Z_2} \frac{Z'_4}{Z_3 + Z'_4} \quad \dots \quad (\text{B})$$

Eqns. (A) and (B) give

$$\frac{V_p}{V_s} = \frac{Z'_4}{Z_4} \frac{Z_3 + Z_4}{Z_3 + Z'_4} \quad \dots \quad (\text{C})$$

Since Z_3 is large compared with Z_4 and Z'_4 , the second fraction of eqn. (C) is nearly unity and the transformer ratio and phase angle are determined almost entirely by the relative magnitudes and phase angles of Z_4 and Z'_4 .*

In tests on a 66000/110 volt transformer, the divider on the primary side might consist of a 50 pF standard high-voltage capacitor in series with a $2\mu\text{F}$ mica capacitor, giving a nominal divider ratio of 40000 : 1. With a resistive secondary divider, a standard 4-terminal 1-ohm shunt of short time-constant would be used for Z_4 in the preliminary balance, which would be effected by adjustment of the magnitude (approximately 40 kilohms) and phase angle of Z_3 . This value of Z_3 would impose a negligible burden on the transformer in the subsequent test, in which

balance would be obtained by adjustment of the magnitude (approximately 600 ohms) and phase angle of Z'_4 .

It is not difficult to ensure that the impedances Z_1 , Z_2 and Z_3 remain constant throughout the tests, and this is the only demand made on them; their actual values are immaterial and a tedious intercomparison of these values is therefore unnecessary.

In conclusion I should like to ask the authors whether they have experienced any difficulty in obtaining a good balance when their detector is switched to full sensitivity. There must be a small unbalance of harmonic components of the voltage wave which, in spite of the sharply tuned detector, might prevent the attainment of a null reading.

THE AUTHORS' REPLY TO THE ABOVE DISCUSSION

Messrs. W. K. Clothier and L. Medina (*in reply*): Both Mr. Edmundson and Mr. Hawkes raise, with some justification, the question as to what use can be made of the high accuracy of our method of measurement. This may to many be a philosophical question, but we feel that to the national laboratories, charged with the maintenance of standards of measurement, it is a matter of very practical importance. In the experience of most standardizing laboratories the work of calibration is more reliable and more economical of time and effort when a factor of perhaps 5 or 10 in accuracy is in hand, over and above the accuracy demanded by virtue of the quality and performance of the instrument under test. In our equipment we have done little better than to achieve this objective for the important class of high-quality transformers used as reference standards. At the same time we have had in mind other important applications of the equipment, e.g. the calibration of transformer testing sets. Where somewhat lower accuracy is sufficient, a simpler circuit

* If a potentiometer type of divider were used on the secondary winding, the second fraction of eqn. (C) would be exactly unity, and a direct reading of ratio could be obtained.

arrangement is possible in which only one capacitor is used in the lower arm, its effective value being adjusted in steps by means of tapings on the secondary of the auxiliary transformer, in the manner described in Section 2.1.5.

The following additional information is given with reference to the auxiliary transformer and the associated resistance dividers. R_1 is in 10 sections each of 0.2 ohm, R_2 is in 10 sections each of 0.1 ohm, R_3 and R_4 are 2.33 and 360 ohms, respectively. At 50 c/s the maximum ratio error of this transformer with W_1 as primary and $W_2 + W_3 + W_4$ as secondary is 0.1%, and under the same conditions the ratio error between W_1 and W_5 is 0.11%. The corresponding phase differences are about 0.5'. These errors were measured in a circuit similar to that of Fig. 5, using the auxiliary transformer in the place of the transformer under test, T_1 .

The amplifier A in Fig. 5 was designed some years ago, and with the modern valves and electronic techniques now at one's disposal alternative circuits would be preferred. However, the amplifier has given reliable service, and the circuit, shown in Fig. 3, is of

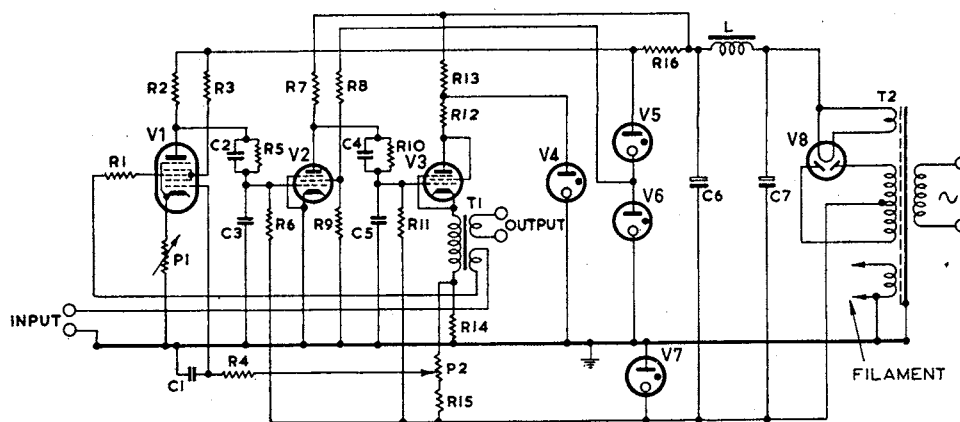


Fig. B—Feedback amplifier.

R_1, R_{12}	5 k Ω	C_1	4 μF
R_2	220 k Ω	C_2	0.0005 μF
R_3	60 k Ω	C_3	0.004 μF
R_4, R_5, R_{10}	0.5 M Ω	C_4	0.0001 μF
R_6	1.5 M Ω	C_5	0.005 μF
R_7	0.4 M Ω	C_6, C_7	16 μF
R_8	25 k Ω	V_1	6SA7
R_9	7 k Ω	V_2	6SJ7
R_{11}, R_{15}	1 M Ω	V_3	6AC7
R_{13}	9 k Ω	V_4, V_6, V_7	VR150
R_{14}	250 Ω	V_5	VR75
R_{16}	4.7 k Ω	V_8	5Y3G

T_1 : 126 pairs of Telcon type 24T Mumetal laminations butt-jointed. Primary, 1800 turns 34 s.w.g. SSE wire; each secondary, 360 turns 26 s.w.g. SSE wire. Primary inductance with 8 mA d.c., 35 H.

T_2 : 240/2 \times 385 V, 6 V, 5 V.

L : 20 H.

P_1 : 1 k Ω } Preset adjustment.

P_2 : 15 k Ω

interest. The three amplifier stages are directly coupled, using positive and negative stabilized voltage sources in order to keep the grid potentials near earth potential. For stabilizing the d.c. levels a d.c. feedback path is provided from the cathode of the last stage to the No. 1 grid of the 6SA7 pentagrid valve, and a low-pass filter prevents a.c. feedback via this path. It should be noted that the transconductance of the No. 1 grid of the 6SA7 is negative with respect to its anode, thus giving correct phasing of the feedback circuit. The output is taken from the secondary of a 5/1 step-down transformer, the primary of which is in the cathode circuit of the last stage. A.C. feedback is provided by another secondary of equal turns symmetrically disposed with respect to the primary and connected between the input terminal and the No. 3 grid of the input valve. The problem of achieving stability at low frequencies is eased, since the filter in the d.c. feedback path is a single-section *RC* network terminated by the grid impedance of a valve. High-frequency stability is assisted by the use of small capacitors in the grid circuits of the second and final stages. The amplifier output impedance of 10 ohms is almost entirely due to the d.c. resistance of the output winding.

In reply to Mr. Hawkes, our experience is that the ratio of a normal good-quality transformer determined with reference to the fundamental components of primary and secondary voltage is not influenced significantly by 2% of harmonic in the supply voltage. On the other hand, there may be some influence on the ratio of the r.m.s. voltages, the most serious effect arising from the simultaneous presence of harmonics in the supply together with harmonic generation of the same frequency within the transformer. It can be shown that the fractional effect on the r.m.s. ratio due to this may have a maximum value, depending on phase considerations, equal to the product of the two harmonic components. For example, with 2% of third-harmonic in the supply and a typical value of 0.25% generated third-harmonic voltage, the maximum difference between the r.m.s. ratio and the fundamental ratio could be approximately 0.005%.

With reference to Mr. Hawkes's comments on Section 2.4.1, we would emphasize that the transformers referred to there are in no sense employed as 'absolute' transformers. In the one case the transformer merely provides arbitrary ratio arms for convenience in intercomparing the ratios and phase angles of two capacitance dividers at successively higher voltages. The test for changes with voltage referred to in the third paragraph of Section 2.4.1 is based on the observation that in a good transformer the ratio and phase angle plotted as functions of voltage are smooth curves. Onset of corona in the high-voltage capacitors is easily recognized as a sharp change in the shape of the plot, especially in the case of phase angle.

We agree with Mr. Felton that work along the lines suggested should be carried out, particularly in the case of high-voltage transformers, in which capacitance effects would be more pronounced.

In reply to Mr. Webb, we have had limited experience with the circuit referred to for measuring the secondary voltage of a testing transformer, but we feel that an accuracy limit of at least 1 part in 10^3 would arise in the measurement of tertiary voltage alone if this is done with an indicating instrument. We do not think much would be gained by the use of our circuit solely for this application, though it could readily be adapted for the purpose. On fundamental grounds, however, we prefer to take measurements of peak voltage directly on the high-voltage secondary.

We are much impressed with the simplicity and economy of Mr. Bowdler's method of measurement, having as it does some of the properties and advantages of a substitution method.

We have had no difficulty in obtaining a good detector balance, even when testing transformers working at high flux density, contributing reasons no doubt being that the detector amplifier provides third-harmonic attenuation of approximately 3000 relative to the fundamental, and that we use a cathode-ray oscillograph indicator which makes it possible to observe the balance of the fundamental in the presence of a certain amount of residual harmonic.

Zur Messung der Leerlaufverluste von Kleintransformatoren für 50 Hz

Von Dipl.-Ing. L. Medina, Sydney, Australien

Während der Entwicklung, wie auch zur Kontrolle der Gleichmäßigkeit der Erzeugung ist die Messung der Leerlaufverluste notwendig. Eine Substitutionsmethode und eine Brückenschaltung werden besprochen und ihre Meßfehler geschätzt. Als Beispiele werden Messungen an einem Kleintransformator mit etwa 0,3 W Leerverlust und einem Stromwandler mit 10 Mikrowatt Eisenverlust angeführt. Zur Abgleichanzeige dient ein auf 50 Hz abgestimmter Röhrenverstärker. Die Arbeit enthält praktische Hinweise für den Bau der Apparatur mit geringem Aufwand.

In der Erzeugung von Kleintransformatoren können Mehrverluste auftreten, die auf Mängel im Fabrikationsprozeß zurückzuführen sind, wie zum Beispiel die Verwendung von Lamellen mit Grat, Bolzen und Lamellen mit beschädigter Isolation oder gar Lamellen einer falschen Eisensorte. Abgesehen von der Temperaturerhöhung sind die Eigenschaften des Kernes oft für die richtige Arbeitsweise von Bedeutung, wie etwa im Falle von Stromwandlern, deren Stromfehler in erster Annäherung den Kernverlusten proportional sind.

Um die für Entwicklungszwecke und Fabrikationsüberwachung erwünschte Kenntnis der Kerneigenschaften zu vermitteln ist es ferner wichtig, daß die Meßschaltung auch die Leerlaufblindleistung zu messen gestattet.

Eine Meßgenauigkeit von etwa 2% ist meist ausreichend. Zur größenordnungsmäßigen Abschätzung der erforderlichen Empfindlichkeit der Meßanordnung sei als praktischer Extremfall ein Stromwandler mit folgenden Daten angenommen: Bürde 10^{-3} VA, Sekundär EMK 1 V, Kernverlust 10^{-5} W. Um eine Verlustdifferenz von 1% bestimmen zu können, muß die Empfindlichkeit 10^{-7} W betragen.

Ferner ist es mit Rücksicht auf die oft rauen Prüffeldbedingungen in Kleinbetrieben erwünscht, erschütterungsempfindliche Spiegelinstrumente mit Bändchenaufhängung zu vermeiden.

Aus diesem Grunde und wegen der hohen Empfindlichkeit kommen weder Meßgeräte mit nichtlinearen Widerständen (Thermistors¹ und Metallfadenlampen²) noch thermische Instrumente in Frage. Als Beispiel sei auf ein von Fischer³ beschriebenes Thermoelement-Wattmeter hingewiesen, das bei einem Meßbereich von 10^{-2} W ein empfindliches Spiegelgalvanometer benötigt.

Röhrenwatt^{4,5} und Phasenmesser⁶ erscheinen für den vorliegenden Fall weniger einfach als die unten beschriebenen Schaltungen, in denen Röhren so verwendet werden, daß eine Änderung des Arbeitspunktes nur die Empfindlichkeit beeinflusst.

Wechselstromkompensatoren und Brücken erfüllen die oben erwähnten Bedingungen. Die

erforderliche Empfindlichkeit wird durch einen auf 50 Hz abgestimmten Röhrenverstärker erzielt, der zur Abgleichanzeige ein robustes Drehspulinstrument oder einen Kathodenstrahlindikator speist.

Im Falle von Messungen an Transformatoren geben aber alle Schaltungen, in denen auf die Meßfrequenz abgestimmte Abgleichanzeigergeräte verwendet werden, zu Meßfehlern Anlaß, die durch die Oberwellen der Spannungsquelle und des Leerlaufstromes hervorgerufen werden.

Einfache Meßschaltungen, deren Fehler klein und meist vernachlässigbar sind, werden im folgenden beschrieben.

Ausgeführte Meßschaltungen und Abschätzung der Meßfehler

In Abb. 1 ist T_A ein stetig veränderlicher Autotransformator und T_I ein Isoliertransformator, dessen Sekundärspannung so gewählt wird, daß mit T_A die erforderliche Prüfspannung (U) des zu untersuchenden Transformators T_X eingestellt werden kann. Es ist vorläufig angenommen, daß U

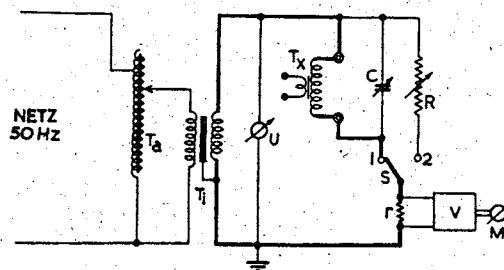


Abb. 1. Substitutionsschaltung

sinusförmig ist. In Serie mit T_X liegt r , ein Widerstand kleiner Ohmzahl. Wenn der veränderliche Kondensator so eingestellt wird, daß der kapazitive Strom gerade so groß ist wie der induktive Strom der Grundwelle der Leerlaufstromblindkomponente, dann wird der durch r fließende Strom ein Minimum sein und nur aus der Verlustkomponente und den Oberwellen bestehen. Parallel zu r liegt ein auf 50 Hz abgestimmter Verstärker, dessen Verstärkung für Oberwellen geringer als etwa 1/500 der Verstärkung für 50 Hz ist. Daher ist die durch das Instrument M angezeigte Ausgangsspannung ein Maß der Verlustkomponente J_{ov} des Leerlaufstromes J_o . Die Oberwellen von J_o sind wattlos, da U sinusförmig angenommen wurde.

Die Verlustmessung von T_X wird so durchgeführt, daß in Schalterstellung 1 mit Hilfe von C auf den Minimalausschlag von M eingeregelt wird und dann in Schalterstellung 2 der Widerstand R

verändert wird, bis M den gleichen Ausschlag zeigt. Die Ohmzahl von R stellt dann den Parallelverlustwiderstand R_{vp} von T_X dar und der Leerlaufverluststrom J_{ov} ist angenähert:

$$J_{ov} \approx \frac{U}{R_{vp}} \approx \frac{U}{R} \quad (1)$$

Die durch diese Annäherung unter praktischen Verhältnissen auftretenden Meßfehler können wie folgt geschätzt werden.

Der Effektivwert des durch r fließenden oberwelligen Stromes sei J_H . Da $r \cdot J_H^2$ von einer sinusförmigen Spannungsquelle nicht gedeckt werden kann, muß T_X als Frequenzwandler⁸ wirken und einen Teil der aufgenommenen Leistung in $r \cdot J_H^2$ umformen. Der gemessene Verlustwiderstand R_{vp} ist also kleiner als im Falle der normalen Verwendung des Transformators, wenn $r = 0$. Um die Größe dieses Fehlers abzuschätzen, sei der für Kleintransformatoren hohe Oberwellengehalt $J_H = 0,3 \cdot J_o$ angenommen. In der Praxis ist gewöhnlich $J_{ov} = 0,2$ bis $0,5 \cdot J_o$, so daß man in grober Annäherung sagen kann: $J_H \approx J_{ov}$. Praktisch wird in dieser und in allen folgenden Schaltungen

$$r \leq \frac{R_{vp}}{200} \quad (2)$$

gewählt. Aus (1) und (2) ergibt sich:

$$r \cdot J_{ov} \leq \frac{U}{200} \quad (3)$$

und da $J_{ov} \approx J_H$, $r \cdot J_H^2 \approx J_{ov} \cdot U/200 \approx W/200$. Der durch das Vorhandensein von r in Serie mit T_X hervorgerufene Fehler in der Bestimmung der Leerverlustleistung (W) ist daher in der Größenordnung von $1/2\%$.

In Wirklichkeit ist die Spannung U nicht sinusförmig, und die aufgenommene Leistung:

$$W = U_1 \cdot J_{o1} \cdot \cos \varphi_1 + U_3 \cdot J_{o3} \cdot \cos \varphi_3 + U_5 \cdot J_{o5} \cdot \cos \varphi_5 + \dots$$

An Netzen großer Städte ist aber der Oberwellengehalt der Spannung gering. In einem typischen Fall wurden folgende Werte gemessen: dritte Oberwelle...3%, fünfte...1,25%, siebente...1%, neunte...0,75% und elfte...0,25%. Zum Zwecke der Schätzung seien für den Oberwellengehalt von J_o folgende Werte angenommen, die im Falle von Kleintransformatoren wohl selten überschritten werden. Dritte Oberwelle...30%, fünfte...12 1/2%, siebente...7%. Nimmt man ferner den praktisch unmöglichen ungünstigen Fall an, daß $\cos \varphi_3 = \cos \varphi_5 = \cos \varphi_7 = \dots = 1$, so ergibt sich ein Meßfehler in der Größenordnung von 1%. Die Streureaktanzen und Widerstände von T_A und T_i können hier klein genug gewählt werden, so daß der Oberwellengehalt des Netzes nur unbedeutend erhöht wird. Die beiden obgenannten Meßfehler haben entgegengesetztes Vorzeichen.

Durch die Einschaltung von r liegt T_X nicht an der vollen Spannung. In der Annäherung $J_{ov} \approx U/R$ ist angenommen, daß $R = R_{vp}$ ist konstant. Für einen kleinen Spannungsbereich ($U_{Tx} \geq 0,995 \cdot U$)

ist das gerechtfertigt, da die Eisenverluste $V_{FE} \approx K \cdot B^n \approx K' \cdot U^n$, worin der Exponent meist wenig von 2 abweicht.

Für den durch die Mitmessung des Verluststromes von C bedingten Fehler kann eine Korrektur angewendet werden, wenn der Leistungsfaktor (p%) des Kondensators bekannt ist. Für Papierkondensatoren liegt p meist zwischen 0,2 und 0,7%. Mit erlaubten Vernachlässigungen gilt in Ω , μF und % für 50 Hz:

$$R_{KORR} \approx R \left(1 + \frac{3,14 \cdot R \cdot C \cdot p}{10^6} \right).$$

Zur Messung von U ist ein Effektivwert-Instrument vorzuziehen, denn die maximale Fehlanzeige (f%) eines den Mittelwert anzeigenden Voltmeters beträgt für q% einer n-ten ungeraden Querwelle⁹: $f = \pm q/n$.

Die Phasenreinheit der Widerstände R und r ist hier weniger wichtig als in Brückenschaltungen, da nur die Impedanz, nicht aber der Phasenwinkel in das Resultat eingeht.

Was die Bestimmung der Blindkomponente J_{oB} des Leerlaufstromes J_o betrifft, ist es zu ungenau, diese aus: $J_{oB} = 314 \cdot U \cdot C$ zu errechnen, da sich die Anzeige von M nur mehr wenig ändert, wenn die Spannung an r schon fast in Phase mit U ist. Es ist besser J_{o1} zu messen und $J_{oB} = \sqrt{J_{o1}^2 - J_{ov}^2}$ zu berechnen. J_{o1} mißt man, indem man C abschaltet, in Schalterstellung 1 den Ausschlag von M notiert, und in Schalterstellung 2 mit R (Ablesung R') auf den gleichen Ausschlag einstellt. Die Grundwelle des Leerlaufstromes ist dann:

$$J_{o1} \approx \frac{U}{R' + r} \quad (4)$$

Bei Transformatoren mit hoher Induktion ist J_o stark spannungsabhängig. Es soll daher r so klein wie möglich gewählt werden, um den durch den Abfall in r hervorgerufenen Fehler zu verkleinern.

Zur Trennung der Leerkupferverluste und Eisenverluste wäre zwar die Kenntnis des Effektivwertes der verzerrten Stromwelle erwünscht, doch sind die Leerkupferverluste meist nur wenige % der Gesamtleerverluste, und selbst wenn man 30% Oberwellen annimmt, beträgt die Differenz der Effektivwerte zwischen der verzerrten Stromwelle und der Grundwelle nur etwa 5%, womit der Fehler, den man in der Bestimmung der Eisenverluste macht, vernachlässigbar wird.

Wenn der Widerstand R geeicht ist, kann man mit diesem r eichen. Demnach ist es möglich, mit Hilfe eines geeichten Voltmeters und eines geeichten Widerstandes J_{ov} und J_{oB} zu bestimmen.

Für den Röhrenverstärker hat sich eine Spannungsverstärkung von 5000 bewährt. In dem bereits erwähnten Extremfall eines Transformators für 1 V wird nach Gleichung 3 der Abfall an r...5 mV und die Ausgangsspannung 25 V. Ein solcher Verstärker ist kaum komplizierter als der übliche Niederfrequenzteil eines Radioapparates.

Der Widerstand R ist zweckmäßigerweise ein Dekadenkurbelwiderstand mit 5 Dekaden

(111 110 Ω). Um Überlastung dieses Widerstandes im Falle der Messung von Transformatoren mit einigen Watt Verlust zu vermeiden, empfiehlt es sich, eine Kombination aus festen, geeichten Drahtwiderständen und dem Dekadenwiderstand zu verwenden. Als veränderlicher Kondensator ist ein Dekadenkurbelkondensator am bequemsten. Man kann aber auch 14 Papierkondensatoren (billige Radiotypen) und 14 einpolige Schalter zu einem in 1 nF*-Stufen veränderlichen Kondensatorkasten von 4,111 μF Maimalkapazität zusammenbauen.

In der Praxis — zur Prüfung außerhalb des Laboratoriums — hat es sich bewährt, für jeden erzeugten Transformatortyp einen fixen Wert von C, R und r in einen Kasten zu bauen und nur den Teil von C und R veränderlich zu machen, der der Erzeugungstoleranz entspricht. Meist wurde auch für jeden Typ ein sorgfältig erprobtes Modell in denselben Kasten gebaut und in der Erzeugung die Differenz zwischen diesem Modell und dem Serienfabrikat bestimmt.

Abb. 2 zeigt einen Spezialfall der Abb. 1 für die Verlustmessung von Netztransformatoren für Radio- und ähnliche Elektronenröhrengeräte.¹⁰ Für

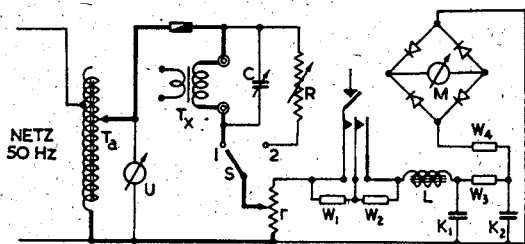


Abb. 2. Spezialfall der Schaltung nach Abb. 1 zur Verlustmessung von Radio-Netztransformatoren

220 V-Transformatoren mit Verlusten zwischen 1 und 10 W wurden folgende Bestandteilwerte gewählt: Empfindlichkeitsregler $r = 20 \Omega$, $K_1 = 4 \mu\text{F}$, $K_2 = 0,1 \mu\text{F}$, $W_1 = 10\,000 \Omega$, $W_2 = 1000 \Omega$, $W_3 = W_4 = 25\,000 \Omega$, $M \dots 50 \mu\text{A} \dots 2500 \Omega \dots 1 \text{ mA}$. Trockengleichrichter, $L = 2,5 \text{ Hy}$ mit einem Verhältnis von Reaktanz zu Serienverlustwiderstand vom mindestens 15.

Das Filter ($L \dots K_1$) wird durch Veränderung des Luftspaltes von L auf 50 Hz abgestimmt. Der Abschwächungsfaktor der dritten Oberwelle ist dann etwa 100. Bei der Messung von Transformatoren unter etwa 2 W Verlust empfiehlt es sich mit T_x einen genau bekannten Widerstand parallel zu schalten, um den Ausschlag von M zu vergrößern und hiemit den Einfluß des Ablesefehlers auf das Resultat zu verringern.

Während in der Schaltung nach Abb. 1 das Instrument nicht gefährlich überlastet werden kann, da der Verstärker eine begrenzte Ausgangsspannung hat, ist es in dieser Schaltung anzuraten, eine Schutzaste anzubringen, die zur Ablesung betätigt wird, und erst W_1 und dann W_2 kurzschließt.

* 1 nF = 10^{-9} F .

Beide Schaltungen haben den Nachteil, daß R und C für die totale Leerverlust- bzw. Blindleistung von T_x dimensioniert sein müssen. In der Resonanzbrücke nach Abb. 3 muß nur C für die Blindleistung von T_x bemessen sein. Unter Benützung

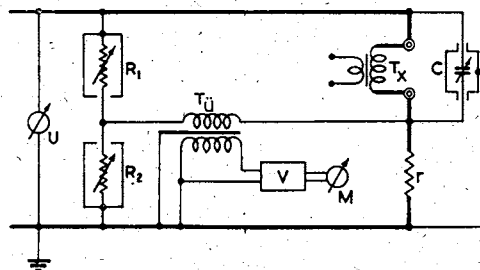


Abb. 3. Resonanz-Brücke

der Symbole der Abb. 3 und mit den früher gemachten Annäherungen gilt für Stromlosigkeit von

$$M: J_{ov} \approx \frac{U}{R_{vp}} \approx \frac{U \cdot R_2}{r \cdot R_1} \quad \text{und} \quad J_{OB} \approx 314 \cdot U \cdot C.$$

An Netzen konstanter Frequenz ist die Abgleichung dieser Brücke sehr einfach, da R und C unabhängig voneinander einjustiert werden können. Die erste Dekade des Kondensators muß hier ein stetig veränderlicher 1 nF-Drehkondensator sein. Der Übertrager T_a dient zum Anschluß des einseitig geerdeten abgestimmten Verstärkers. Die Bestandteilwerte für diese Brücke sind die gleichen wie für die Brücke nach Abb. 5.

Eine Brücke, in der der kostspielige veränderliche Kondensator vermieden wird, hat Schering¹¹ zur Verlustmessung von Zählerwinden verwendet. Die Brücke hat drei Widerstände und zwei Spulen mit fixer gegenseitiger Induktion.

Wegen der im Transformatorprüffeld oft beträchtlichen Streufelder sind aber Schaltungen mit Kapazitäten vorzuziehen.

Goldstein¹² hat die Maxwellbrücke nach Abbild. 4, in der die Blindleistung von C nur ein kleiner Bruchteil der Blindleistung T_x ist, dazu benützt, um die Leerverluste eines 20 000 kVA-Transformators zu messen. Eine wattmetrische Messung ergab nur 1 1/2 % Differenz. Die Bedingungen für die Stromlosigkeit des von einem Oberwellen-Filter gespeisten Galvanometers sind:

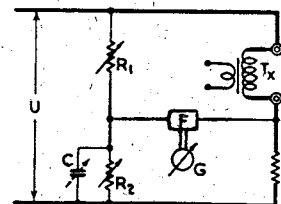


Abb. 4. Prinzipschema der von Goldstein zur Verlustmessung verwendeten Maxwellbrücke

$$R_{vs} = \frac{r \cdot R_1}{R_2} \quad \text{und} \quad L = C \cdot r \cdot R_1,$$

worin R_{vs} und L die Serienkombination von Verlustwiderstand und Induktivität von T_x ist. Umwandlung in die Parallelkombination ergibt:

$$J_{ov} \approx \frac{U \cdot R_{vs}}{(\omega \cdot L)^2 + R_{vs}^2} \approx \frac{U \cdot R_2}{r \cdot R_1} \left(\frac{1}{\omega^2 \cdot C^2 \cdot R_2^2 + 1} \right) \quad \text{und}$$

$$J_{oB} \approx \frac{U \omega C}{(\omega \cdot L)^2 + R_{vs}^2} \approx \frac{U \cdot \omega \cdot C}{r \cdot R_1} \left(\frac{R_2^2}{\omega^2 \cdot C^2 \cdot R_2^2 + 1} \right).$$

Die quadratischen Glieder machen die Auswertung zeitraubend.

In der Brücke nach Abb. 5 wird das vermieden. Wie leicht gezeigt werden kann, sind die Nullbedingungen hier:

$$R_{vp} = \frac{r \cdot R_1}{R_2} \quad \text{und} \quad L = C \cdot r \cdot R_1,$$

worin die Symbole der Abb. 5 verwendet wurden und L die Induktivität von T_x ist, der der Parallel-

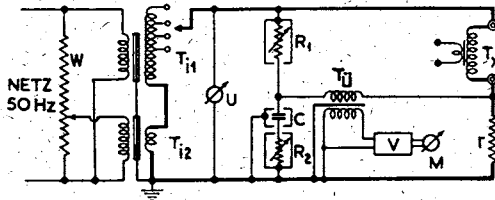


Abb. 5. Brücke mit Fixkondensator und einfachen Gleichungen für Leerwirk- und Blindstrom

verlustwiderstand R_{vp} parallel liegt. Mit den früher erörterten Annäherungen gilt dann für 50 Hz:

$$J_{ov} \approx \frac{U}{R_{vp}} \approx \frac{U \cdot R_2}{r \cdot R_1} \quad (6)$$

und

$$J_{oB} \approx \frac{U}{314 \cdot L} \approx \frac{U}{314 \cdot C \cdot r \cdot R_1} \quad (7)$$

Die konstante Korrektur für den Leistungsfaktor p des Festkondensators C ist für 50 Hz in Ω , μF und %:

$$R_{2 \text{ KORR}} \approx R_2 + \frac{10^4 \cdot p}{314 \cdot C} \quad (8)$$

Ein meist unbedeutender Nachteil dieser Anordnung ist, daß man Transformatoren, deren Leerlaufleistungsfaktor nahe 1 ist, nicht messen kann; denn für $\cos \varphi = 1$, $L = \infty$ und endliche Werte von r und R_1 , wird $C = \infty$. Die Division von (6) durch (7) ergibt: $J_{ov}/J_{oB} = 314 \cdot R_2 \cdot C$ und wenn wie früher $r \leq R_{vp}/200$, so wird $R_2 \leq R_1/200$ und $J_{ov}/J_{oB} = 314 \cdot C \cdot R_1/200$. Setzt man für R_1 den Wert 111 100 Ω und für C 8 μF ein, so wird $J_{ov}/J_{oB} \approx 1,4$ und der Leistungsfaktor $\cos \varphi = \frac{1,4}{\sqrt{1 + (1,4)^2}} \approx 0,8$. Dieser Wert ist viel größer als der normale $\cos \varphi$ im Leerlauf.

Aus obigem ist auch ersichtlich, daß, solange R_1 nicht überlastet wird, zur Bereichumschaltung nur r geändert werden muß.

Wenn der stetig veränderliche Autotransformator T_A (Variac) nicht zur Verfügung steht, kann wie in Abb. 5 gezeigt, U mit dem Stufentransformator T_{t1} grob und mit T_{t2} und W fein eingestellt werden. T_{t2} ist ein Transformator, dessen Sekundärspannung etwa $U/10$ ist. Der Rheostat $W \leq 250 \Omega$. R_1 und R_2 sind zweckmäßigerweise induktionsfreie abgeschützte Vierdekadenkurbelwiderstände mit 111 100 Ω , bzw. 1111 Ω . Der Widerstand r besteht aus Nickelindraht, bifilar ge-

wickelt. Unter Berücksichtigung der Gleichung 2 ergibt sich für R_2 ein Höchstwert von $111\,100/200 \approx 555 \Omega$. Der verwendete Übertrager T_A hat einen Kern aus 0,35 mm starken MU-Metall-Lamellen, einen Eisenquerschnitt von 1 cm², eine mittlere Eisenweglänge von 7,5 cm und 650 Primär- und 650 Sekundärwindungen aus 0,15 mm starkem Emaildraht. Die Isolation zwischen Kern und Wicklung und Wicklung und geerdetem Schirm hat eine Dicke von 1 mm und eine Dielektrizitätskonstante $\epsilon \leq 3$. Gegen Streufelder ist der Übertrager durch Einbau in eine 1 mm starke MU-Metalldose abgeschirmt. Die Impedanz bei 50 Hz und 0,1 Gauß ist etwa 3500 Ω . Dieser Wert ist einigemal größer als r und R_2 und bedingt nur einen geringen Empfindlichkeitsverlust.

Im allgemeinen kann man erzielen, daß $r \leq R_{vp}/200 \leq 1000 \Omega$ wird, und zwar auch im Falle von Transformatoren für hohe Spannung (R_{vp} hoch), indem man von der Niederspannungsseite aus mißt.

In allen Abbildungen wurde die Verbindung des Kernes offen gelassen. Diese Verbindung und der Anschluß von unbenützten Wicklungen und Schirmen beeinflusst die Kapazitäten von T_x und damit J_{oB} . Meist werden der Kern und die offenen Wicklungen geerdet. Die Erdkapazitäten liegen dann teilweise parallel zur Spannungsquelle (kein Meßfehler) und teilweise parallel zu r . Die Werte von r und R_2 sind, wie oben erwähnt, in der Praxis so klein, daß die Reaktanz der Streukapazitäten meist einige tausend Male größer ist, wodurch der Phasenfehler vernachlässigbar wird.

Wenn in der Serienfabrikation die Brücke zu Vergleichsmessungen verwendet wird, ist es vorteilhaft, Transformatoren mit hoher Induktion bei verminderter Spannung zu vergleichen, um den Einfluß von Netzspannungsschwankungen zu verringern.

Für den oben erwähnten Extremfall von T_x für 1 V wird $r \cdot J_{ov} = 5$ mV und für 1% Abgleichgenauigkeit ist die Eingangsspannung am Verstärker etwa 50 μV .

Der abgestimmte Verstärker

Abb. 6 zeigt das Schaltschema. P_1 ist der Empfindlichkeitsregler. Zwischen Anode und Gitter der ersten Röhre liegt ein „T“ Sieb ($R_1 - R_2 - R_3 - C_1 - C_2 - C_3$), das auf 50 Hz abgestimmt ist. Für alle anderen Frequenzen wird die Verstärkung der ersten Röhre gering, da Gegenkopplung erfolgt. R_9 und C_9 bilden ein Dämpfungsglied für die höheren Oberwellen, und $R_{11} - R_{12} - R_{13} - C_{10} - C_{11} - C_{12}$ sind ein „T“ Sieb, das auf 150 Hz, die stärkste Oberwelle, abgestimmt ist. Das Verhältnis (Verstärkung bei 50 Hz) : (Verstärkung der Oberwellen) ist etwa 3000 für 150 Hz und 300 bis 500 für die nächstfolgenden Oberwellen. Diese Filteranordnung hat sich für den vorliegenden Fall als ausreichend erwiesen und ist stabiler als Schaltungen, in denen das „T“ Sieb im Gegenkopplungskreis mehrerer Stufen liegt, oder Kaskadenschaltungen von mehreren Stufen mit auf 50 Hz abge-

stimmten Filtern zwischen Gitter und Anode. Schalterstellung 1 ist für die Meßschaltung nach Abb. 1 gedacht. In Schalterstellung 2 ist der Vorwiderstand verkleinert und diese Stellung ist für die Brücke nach Abb. 3 und 5 geeignet. In Schalterstellung 3 ist der Verstärkerausgang mit einer Buchse verbunden, an die ein Kathodenstrahlindikator (magisches Auge) oder am besten der Vertikalverstärker eines Kathodenstrahloszillographen angeschlossen werden kann. Im letzteren Falle ist es vorteilhaft, das Kippgerät mit der Netzfrequenz zu synchronisieren. Um den hauptsächlich im Gitterkreis der ersten Röhre verbleibenden Rest der 50 Hz-Störspannung, den man durch Abschirmung nicht mehr weiter verkleinern kann, zu kompensieren, wird mit Hilfe von P_2 und P_3 eine der Größe und Phase nach veränderliche Kompensationsspannung an das Bremsgitter der zweiten Röhre gelegt. Diese Spannung wird der 6 V-Heizstromquelle entnommen. Die Werte der verwendeten Teile sind in Abb. 6 angegeben. Die Röhren sind amerikanische 6J7 Typen, doch ist kaum eine Schwierigkeit zu erwarten, wenn andere Röhren (steile Hochfrequenzpentoden mit $R_i \geq 1 \text{ M}\Omega$) verwendet werden. Wählt man in dem 50 Hz-Filter $C_1 = C_2 = 1 \text{ nF}$ (Glimmerkondensator), so muß $C_3 = 2 C_1 = 2 \text{ nF}$ sein. Da $R_1 = 1/\omega \cdot C_1$, wird $R_1 = R_2 = 3,18 \text{ M}\Omega$ und $R_3 = R_1/2 = 1,59 \text{ M}\Omega$. Im 150 Hz-Filter wurde $C_{10} = C_{11} = 0,5 \text{ nF}$ gewählt.

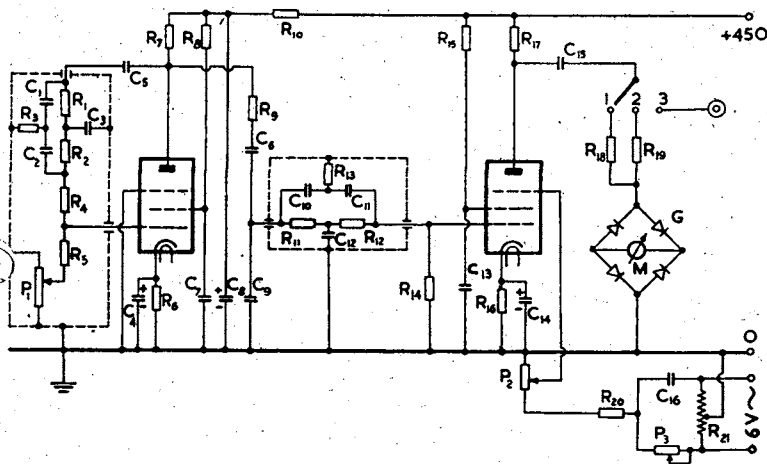


Abb. 6. Schaltschema eines auf 50 Hz abgestimmten Verstärkers

$R_1 - R_2 - R_3$ siehe Text, $R_4 = R_{14} = 3 \text{ M}\Omega$ ($\frac{1}{2} \text{ W}$); $R_5 = 2 \text{ M}\Omega$ ($\frac{1}{2} \text{ W}$); $R_6 = R_{16} = 2000 \Omega$ (1 W); $R_7 = 0,25 \text{ M}\Omega$ (1 W); $R_8 = 1,5 \text{ M}\Omega$ (1 W); $R_9 = R_{20} = 1 \text{ M}\Omega$ ($\frac{1}{2} \text{ W}$); $R_{10} = 10000 \Omega$ (2 W); $R_{11} - R_{12} - R_{13}$ siehe Text, $R_{15} = 3 \text{ M}\Omega$ (1 W); $R_{17} = R_{18} = 0,5 \text{ M}\Omega$ (1 W); $R_{19} = 0,1 \text{ M}\Omega$ (1 W); $P_1 = P_2 = 0,1 \text{ M}\Omega$; $P_3 = 0,5 \text{ M}\Omega$; $R_{21} = 50 \Omega$ (1 W) mittelangezapft; $C_1 - C_2 - C_3$ siehe Text, $C_4 = C_{14} = 100 \mu\text{F}$ (12 V); $C_5 = C_6 = 0,01 \mu\text{F}$ (600 V); $C_7 = 0,5 \mu\text{F}$ (600 V); $C_8 = 16 \mu\text{F}$ (600 V); $C_9 = 5 \text{ nF}$ (600 V); $C_{10} - C_{11} - C_{12}$ siehe Text, $C_{13} = 0,25 \mu\text{F}$ (600 V); $C_{15} = 0,1 \mu\text{F}$ (600 V); $C_{16} = 0,1 \mu\text{F}$ (200 V); $M = 50 \mu\text{A}$; $G = 1 \text{ mA}$

$C_{12} = 1 \text{ nF}$ und $R_{11} = R_{12} = 2 R_{13}$ wird $2,12 \text{ M}\Omega$. Diese Werte wurden aus einigen Radiohochohmwidständen hergestellt. Die Widerstände wurden künstlich gealtert, indem sie etwa durch zwei Wochen während des Tages auf 75°C erhitzt wurden, und in der Nacht abkühlten.

Anwendung und Meßresultate

a) Der Leerlaufstrom von hundert 240/10 V-100 VA-Transformatoren wurde gemessen. Die Werte lagen zwischen 70 und 160 mA, woraufhin der Auftraggeber die Übernahme verweigerte. Dann wurden nach Abb. 2 die Leerverluste bestimmt, deren Extremwerte nur zwischen 1,05 und 4,45 Watt schwankten. Die durch die höhere Blindleistung hervorgerufenen Mehrkupferverluste waren vernachlässigbar und die Transformatoren wurden übernommen.

b) Ein Stromwandler 2 A/1,11 mA (für ein 1 mA Drehspulinstrument mit Trockengleichrichter) wurde in der Schaltung nach Abb. 1 untersucht. Die folgende Tab. zeigt das Resultat:

Tabelle 1

U	r	R	C	J_{ov} Gl. (1)	R'	J_{o1} Gl. (2)
1 V	500 Ω	105 000 Ω	0,096 μF	9,5 μA	31000 Ω	31,7 μA

Da die ersten zwei Dekaden von C aus Glimmerkondensatoren bestanden, wurde auf eine Korrektur des Leistungsfaktors von C verzichtet. Auch wurde in der Bestimmung von J_{o1} der parallel zu r liegende Eingangswiderstand des Verstärkers ($10^5 \Omega$) vernachlässigt. Das Kerngewicht war 0,181 kg und B war 145 Gauß. Unter Vernachlässigung der Kupferverluste ergibt sich $U \cdot J_{ov} / 0,181 = 0,052 \text{ mW/kg}$. Die von der Erzeugerfirma der Lamellen (Mu-Metall) angegebenen Grenzwerte sind 0,044 bis 0,077 mW/kg für obige Induktion.

c) Ein Kleintransformator, der als Übersetzungsnormal in einer Brücke dienen sollte, wurde in der Schaltung nach Abb. 5 untersucht. Um die Richtigkeit der Messung zu prüfen, wurden dem Transformator genau bekannte Widerstände (R_3) parallelgeschaltet und von dem gemessenen Wert J_{ov} der Stromwert U/R_3 abgezogen. Die vorletzte Zeile der Tabelle zeigt das Resultat. In der letzten Kolonne ist die Messung mit $R_3 = \infty$ wiederholt, wobei r auf das fünffache erhöht wurde. Die gute Übereinstimmung läßt darauf schließen, daß die Phasenfehler in den Armen vernachlässigbar waren. Ein weiteres Hilfsmittel, um die Phasenreinheit von R_1 zu prüfen und die günstigste Verbindung

der Abschätzung von R_1 zu finden, besteht darin, daß man einen Kohlewiderstand (Radio-type) mit einer Ohmzahl von etwa $0,9 R_1$ mit R_1 in Serie schaltet, die Brücke neu abgleicht und aus der Änderung von R_2 auf die Phasenreinheit von R_1 schließt.

Tabelle 2

$R_s \parallel T_x$	Ω	∞	100 000	50 000	20 000	∞
U	V	120	120	120	120	120
r	Ω	100,0	100,0	100,0	100,0	500,0
R_1	Ω	93 920	93 700	93 930	93 650	18 730
R_2	Ω	200,0	293,0	388,5	668,0	201,8
C	μF	7,60	7,60	7,60	7,60	7,60
p	%	0,7	0,7	0,7	0,7	0,7
$R_s KORR$ Gl. (8)	Ω	202,9	295,9	391,4	670,9	204,7
U/R_s	mA	0	1,20	2,40	6,00	0
J_{ov} Gl. (6)	mA	2,59	3,79	5,00	8,59	2,62
$J_{ov} - U/R_s$	mA	2,59	2,59	2,60	2,59	2,62
J_{oB} Gl. (7)	mA	5,35	5,36	5,35	5,37	5,37

Literaturverzeichnis

- ¹ Becker-Green-Pearson, Transact. A. I. E. E. 65 (1946), S. 711. — ² H. Hochrainer, Eund M 64 (1947), H. 9/10, S. 148. — ³ J. Fischer, Arch. f. Elektrotechn. 33 (1939) S. 242. — ⁴ Turner-McNamara, Proc. I. R. E. (U. S. A.) 18 (1930) S. 1743. — ⁵ R. J. Wey, Wireless Engineer 14 (1937) S. 490. — ⁶ Opitz, Günthers Fortschritte der Funktechnik 2 (1937) S. 59. — ⁷ Greig-Parton, Engineering (1938), Oktober, S. 431. — ⁸ Greig-Kayser, Journal I. E. E. 95 (1948), zweiter Teil, Nr. 44, S. 205. — ⁹ I. Wolff, Proc. I. R. E. (U. S. A.) 19 (1931) S. 647. — ¹⁰ Medina, Proc. I. R. E. (Aust.) 7 (1946) Nr. 9, S. 13. — ¹¹ H. Schering, Zeitschr. f. Instrumentenkunde 42 (1922) S. 106. — ¹² J. Goldstein, ETZ 45 (1924) S. 1270, und B. Hague, Wechselstrombrückenmethoden, Verlag Pitman.

In den obgenannten Literaturstellen sind Hinweise auf andere Arbeiten enthalten, von denen leider die Mehrzahl dem Verfasser nicht zur Verfügung stand.

An Instrument for the Detection of Short-Circuited Turns in Coils

By L. Medina,* Dipl. Ing., A.M.I.E. (Aust.), M.I.R.E. (Aust.)

Summary.

The instrument is mains-operated and consists of two units, namely a test jig and a detector. The test jig contains two identical laminated open cores of small cross-section, each of which carry primary and secondary windings. The primaries are excited in series at mains frequency and the secondaries are connected in series opposition to the input terminals of the detector. The detector consists of a high gain amplifier tuned to the mains frequency, the output being displayed on the screen of a cathode ray tube. The coil to be tested is slipped over one core. A short-circuited turn causes an out-of-balance EMF which after amplification tilts the trace on the screen of the cathode ray tube. Capacitive currents in the coil under test merely open the trace into an ellipse. The instrument can detect one shorted turn of 5 ohms resistance (approximately 1 foot of 48 SWG copper wire).

1. Design Considerations.

The instrument was built to cater for the needs of a coil-winding shop manufacturing small transformers and reactors mainly for use in electronic apparatus. It was desired to find shorted turns in coils before laminating.

The design of the instrument is based on a method described by Brown¹. Two open core transformers ("X" and "ST" in Figure 1) carry primary and secondary windings. The primaries are connected in series and are excited at mains frequency. The secondaries, in series opposition, are connected to the input terminals of an amplifier. If both transformers were identical, the output of the amplifier would be zero. In practice, null balancing controls must be provided. From the many methods of doing this² the following was chosen. Transformer "ST" is deliberately unbalanced by means of a small additional coil (4 turns, Figure 1). In series with the main secondary coil (1,000 turns) is another coil (18 turns) the output voltage from which is adjustable by means of R.5. Thus the magnitudes of the secondary voltages can be made equal. Phase adjustment is effected by R.7. This control, called the loss control, must be placed across transformer "X" in order to equalize the load on "ST" by resistors R1, R2, R3, R5, R6.

If a coil to be tested is slipped over transformer "X", a shorted turn will cause an out-of-balance EMF practically in quadrature with the secondary voltage. This EMF is amplified in an amplifier tuned to the mains frequency,

the output voltage of which is applied to the vertical plates of a cathode ray tube (Figure 1). Voltage at mains frequency is applied to the horizontal plates via the phase shifter R.60, C.22, which can be so adjusted that shorted turns will cause a tilt of the horizontal trace. The test for shorted turns then resolves itself into the observation whether or not the trace tilts when the coil to be tested is slipped over transformer "X".

In practice, however, a complication occurs owing to the fact that in coils with many turns of fine wire capacitive currents of considerable magnitude flow even at 50 c/s. These currents produce an out-of-balance EMF practically in phase with the secondary voltage. The out-of-balance EMF's caused by shorted turns and capacitive currents are in quadrature to each other. Therefore, a coil without shorted turns but having a significant capacitance causes the trace to open into an ellipse with a horizontal main axis. A tilted ellipse is indicative of the presence of shorted turns as well as capacitive currents. The capacitance effect is sometimes so great that it is not possible to decide if the ellipse is tilted or not. In this case all that is required is adjustment of R.5, called the quadrature control, until the ellipse closes. If there is then no residual tilt the coil has no shorted turns.

A further complication is due to the fact that the coil capacitances are not loss free and that there will be coils in which the dielectric losses are equal to the loss in a shorted turn.

Another consideration of importance arises if it is necessary to detect shorted turns in coils which possess a static shield. It is possible to accomplish this by making the cores long relative to the expected coil length and placing the coil under test approximately in the centre of the core where the flux is uniform and will not introduce eddy current losses in a shield concentric with the core.

It can be shown that for a given core the sensitivity is proportional to the flux density, the number of secondary turns and the number of short-circuited turns and inversely proportional to the resistance of one shorted turn. To reduce electric shock hazard, it was thought unwise to exceed 5 mV/turn. For a coil under test of 10,000 turns this leads to an induced EMF of 50 volts. The primaries were designed for excitation from the amplifier filament supply, and the flux density was chosen such that the heat dissipation in the cores is not large enough to cause serious zero drift.

*Officer of Division of Electrotechnology, C.S.I.R.O., Australia.
Manuscript received by the Institution 19/6/51.
U.D.C. number 621.317.613: 621.318.4.

1. Brown, E.B., "Two simple methods of detecting short-circuited turns in coils," *Journal of Sci. Instr.*, 25, 1948, 282.
2. Brailsford, F., "An improved tester for the routine detection of internal short circuits in coils," *Metropolitan Vickers Elec. Co. Ltd., Descriptive Leaflet 904/8-1*, 1940.

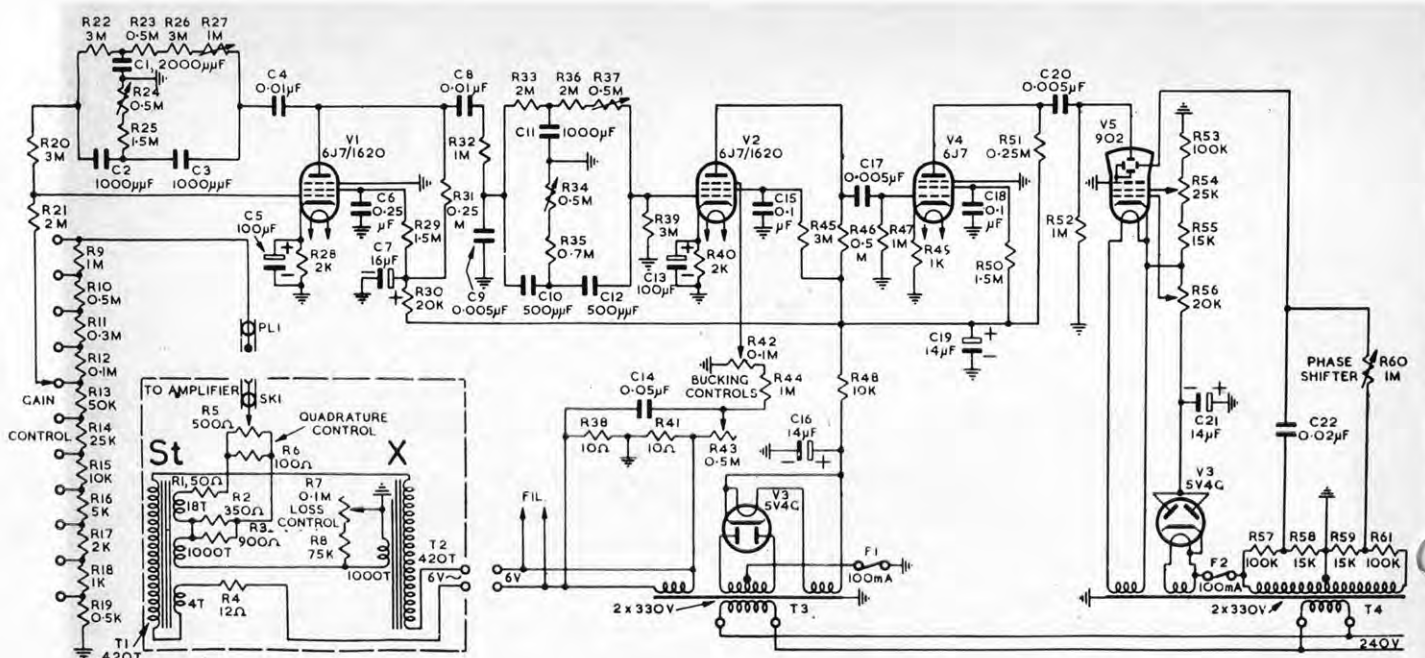


Figure 1—Circuit diagram.

The amplifier and cathode ray tube indicator was built as a separate unit so that it could also be used as a null-detector for mains frequency bridge measurements. Experience has shown that for this purpose the unit should have a sensitivity of 10 microvolts, an input resistance of 2 megohms, an attenuation of 60 to 70 db. for the 3rd harmonic and 45 to 55 db. for the higher order odd harmonics. An amplifier of this kind, the sensitivity and selectivity of which has been found stable over a period of several years, has been described elsewhere³. A similar circuit was adopted for this instrument.

Selectivity is obtained by means of the parallel-T feedback amplifier stage VI tuned to the mains frequency in series with another parallel-T network adjusted to give maximum reduction of the third harmonic. Further attenuation of the higher harmonics is effected by R32 and C9. The residual mains frequency voltage, which with proper layout amounts to between 10 and 20 microvolts can be cancelled by a voltage, adjustable in magnitude and phase (R42 and R43) which is injected into the suppressor grid of V2.

2. Constructional Details.

(a) The Test Jig.

Transformers "X" and "ST" are identical. The core consists of strips 11 inches x $\frac{3}{8}$ inch cut from 29 gauge good quality silicon iron. The cross-section is $\frac{3}{8}$ inch x $\frac{3}{8}$ inch. The strips are stuck together with varnish and baked. The core is covered with 2 wraps of 0.003 inch oil silk, a shim brass strip 13 inches x $\frac{3}{16}$ inch x 0.002 inch being inserted between the wraps to form the return conductor for the single layer primary winding. This winding has 420 close wound turns of 24 SWG enamelled copper wire, placed symmetrically on the core. The secondary of 2

inches length is placed in the centre of the core and has 1,000 turns of 42 SWG SSC copper wire. The insulation between primary and secondary consists of 1 wrap of 0.003 inch oil silk and the inter-layer insulation of 1 wrap of 0.001 inch jewellers tissue. The cores and coils are thoroughly shellacked and dried.

Transformers "X" and "ST" are arranged astatically with a centre to centre distance of $7\frac{1}{2}$ inches. They are supported in a wooden housing with detachable panels (Figure 2). Transformer "X" is protected by a bakelite tube, $\frac{3}{4}$ inch by $\frac{3}{4}$ inch outside, $\frac{1}{8}$ inch thick. The tube is filled with paraffin wax and held in position by means of a wooden clamp and brass screws. The centre of the core of "X" is 3 inches above the top covering panel. Two white lines at a distance of 1 inch on either side of the core centre are painted on the bakelite tube to indicate approxi-

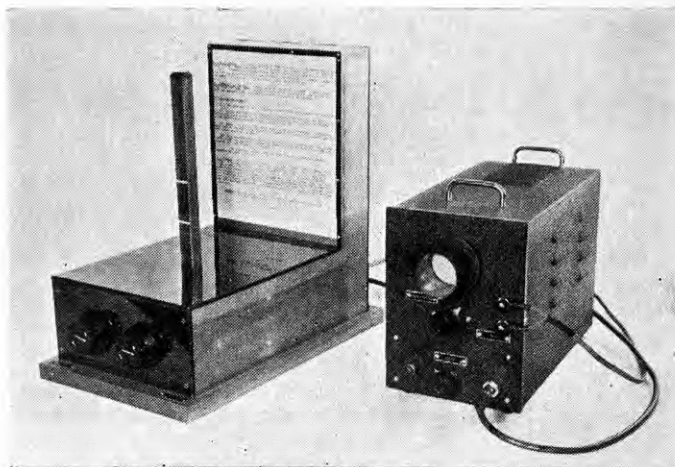


Figure 2—Test jig and detector.

3. Medina, L., "On the measurement of no-load losses in small transformers for 50 c/s," E. and M. (Vienna), 67, 1950, 99.

mately the correct position for the coil under test. The top of the bakelite tube is closed by a bakelite cap with rounded edges. Transformer "ST" is enclosed in the rear portion of the box and held by wooden clamps. The coils with 4 and 18 turns were added after assembly, the number of turns having been found by experiment. The 4 turn coil simply consists of four turns of the leadwire of the primary held in position with shellac. The 18 turn coil consists of 7/0.005 inch cotton-insulated stranded wire wound round the primary near the upper wooden clamp. The box also contains the quadrature and loss controls and associated resistors. The rear panel carries 2 terminals for the excitation voltage and a concentric connector for the shielded connection to the amplifier. A sheet with operating instructions is attached to the panel facing transformer "X".

(b) *The Tuned Detector and Cathode Ray Oscilloscope.*

This unit is built into a steel case $12\frac{1}{2}$ inches long, $8\frac{3}{4}$ inches high and $6\frac{3}{8}$ inches wide. The front panel carries the gain control, the phase shifter (R60), the 6 V terminals for the excitation of the test jig, the concentric input connector, and contains a hooded aperture for the C.R. tube. The focus, brilliance and humbucking controls R54, R56, R42 and R43, respectively, have screw driver adjustment and are accessible after detaching a small coverpanel on the side of the case. No position controls are used, the spot position having been adjusted by a small Alnico magnet mounted on a bracket near the C.R. tube. The two identical power transformers are mounted near the rear end of the chassis and symmetrical to the C.R. tube. Their primaries are so polarized that the resultant mains frequency field in the region of the C.R. tube is so small that magnetic shielding of the tube can be dispensed with. Care has been taken to avoid large loops in the grid circuit of the first tube. The gain control and the first parallel-T filter are mounted in shim brass shield boxes under the chassis but the screwdriver controls R24 and R27 are accessible from the top of the chassis. The second parallel-T filter is mounted in a small brass box on top of the chassis. The rectifier tubes are kept as far away as possible from the filters in order to reduce heating of their components. The values in Figure 1 are for a man's frequency of 50 c/s and all components have ordinary commercial tolerances. The component values of the parallel-T filters were computed⁴. In adjusting the first parallel-T to a null for 50 c/s and the second to a null for 150 c/s, additional parts (e.g. R23) may have to be added to make up for parts with large tolerances.

(c) *Calibrating Turns.*

A number of wires about 10 to 12 inches long and joined at the ends, so that each wire forms a shorted turn, are required for the successful application of the instrument. The gauges used should represent the majority of wire gauges used in the coil winding shop for which the instrument is intended. In this particular instance, 9 shorted turns were prepared ranging from 22 SWG to 42 SWG. These turns were clamped between 2 thin bakelite plates having holes sufficiently large to clear the bakelite tube of transformer "X".

3. Practical Use and Limitations of the Instrument.

A large mass of metal near the test jig or stray electromagnetic fields may make zero balance impossible. A distance of 2 feet between the test jig and the detector—C.R.O. unit was found appropriate. The warm-up drift is very small and the instrument is ready for zero adjustment as soon as the trace is visible on the screen of the C.R. tube. Zero adjustment should be carried out at maximum gain for the "zero" to be valid for any other position of the gain control. However, it has been found in practice that more than one-quarter of the available gain is rarely employed probably because very fine wire is not used on coils for which this instrument is intended. Zero adjustment at $\frac{1}{4}$ maximum gain is less laborious and this is usually employed.

The trace of the C.R. tube is adjusted until it is a horizontal line by means of the loss control (which tilts the trace) and the quadrature control (which closes the ellipse). One of the calibrating turns, corresponding to the finest wire used in the coil to be tested, is then slipped over transformer "X" and held between the white lines. If a calibrating turn of the correct gauge is not available, the one with the next finer gauge should be used. The gain control is then so adjusted that the tilt observed is approximately 45° , and without moving the loss or quadrature control the phase shifter (R60) is adjusted until the trace becomes a line tilted at approx. 45° . The instrument is now ready for use.

If the coil to be tested is now slipped over transformer "X", and there is no tilt, or the tilt is less than that produced by the calibrating turn, the coil has no shorted turns. As already mentioned, capacitive currents in the coil under test will open the trace into an ellipse. If this ellipse becomes so large that it is not possible to observe the amount of tilt with sufficient accuracy, the quadrature control must be readjusted for closure of the ellipse into a line. This adjustment must be carried out while the coil is held in the test position. This, of course, necessitates a new zero adjustment for the next coil to be tested. A slight tilt often remains owing to losses in the dielectric. No hard and fast rule can be given for the limiting case when the loss in one shorted turn equals the dielectric loss. However, it may safely be assumed that this case will be very rare in practice.

During the one and a half years the instrument has been in operation, a watch was kept for such a case. The shop which uses the instrument makes coils of a great variety but only a few of each type; the test conditions are therefore more severe than in the general case of mass production of only a few types. Only one badly impregnated coil wound several years ago has so far been found which did produce this limiting condition. This coil had altogether 16,400 turns, the wire gauges being 42 and 38 SWG. The power factor of the capacitance was of the order of 20 per cent. at 50 c/s. However, it was possible to test a small batch of coils, physically much larger than the one mentioned, each having 15,200 turns of 40 SWG wire without any doubt remaining. Coils suitable for cores up to 8 square inches cross-sectional area have been tested.

4. Henny, K., "Radio Engineering Handbook," McGraw-Hill, New York, 3rd edition, 1941, 229.

The Author :



Mr. Medina was born in Austria in 1908. He graduated Dipl. Ing. in Electrical Engineering from the Technical University of Vienna in 1932. While still an undergraduate he was Assistant Technical Editor of several radio periodicals. Mr. Medina is the author of numerous papers dealing mostly with the results and practical applications of electrical measurements. After graduation he was a senior receiver design engineer in several radio factories in Poland, Czechoslovakia and Austria. In 1938, while still in Europe, he was engaged by Thom and Smith Pty Ltd., and he arrived in Australia early in 1939. As Assistant Chief Engineer of this Company he was responsible for the electrical design and development of radio receivers, amplifying equipment, two-way mobile installations, transceivers, and MF, HF and VHF transmitters for FM and AM, mostly for the Armed Services. In 1946 he joined the staff of the Division of Electrotechnology, C.S.I.R.O., where he is mainly concerned with the development of equipment for precise measurements and with the design of special transformers.

Spurious indication due to eddy currents in a static shield has not been found troublesome. Coils up to 3 inches long, possessing shields of 0.002 inch shim brass, have been tested without obtaining false indications, even at maximum gain. However, in these cases it is necessary to move the coil under test along transformer "X" until minimum tilt is obtained. In practice, longer coils can be tested because maximum gain is hardly ever required. It will also be appreciated that the influence of a shield can be studied by slipping a "dummy shield" over transformer "X".

The most serious limitation is due to the fact that one can only detect short-circuited turns which are present at the time of the test. Most short-circuits occur, however, due to the stresses set up during the impregnating and laminating process. If the wound coils are impregnated, tested and then laminated, the instrument is useful, but when the coils are wound, tested, laminated and then impregnated, additional methods of detecting short circuited turns should be used⁵.

4. Acknowledgments.

The work described in this Report was carried out in the Division of Electrotechnology, Commonwealth Scientific and Industrial Research Organization. The help of Mr. F. P. Paine and Mr. H. Bairnsfather in the construction of the instrument is gratefully acknowledged.

5. Medina, L., "A device for the measurement of no-load losses in small power transformers," Proc. I.R.E. (Aust.), 7, 1946, 13.



It has not been possible to be completely digitised all information on next 2 pages due to tight book fold binding.

Please see the original journal for a complete manuscript.

Reprinted from "Proceedings of the Institution of Radio Engineers Australia," Vol. 15, No. 5, May, 1954

Prevention of Ionization in Small Power Transformers

L. Medina.*

ary.

all air-cooled transformers often fail in service because their operating voltage is above the ionization onset voltage, thus causing rapid aging. Since the ionization voltage gradient decreases with increasing insulation thickness, a higher ionization voltage can be obtained for a given total thickness if, by means of foils in the insulation, it is split up into n sections with $1/n$ of the voltage maintained on each section.

Results of tests and design details for a typical transformer are

Total Insulation Thickness of Sample (inches)	Ionization Onset Voltage (R.M.S. volts)	Ionization Voltage Gradient (volts/mil)
0.005	500	100
0.01	750	75
0.02	1,000	50
0.04	1,500	37
0.08	2,200	27

Discussion.

Several small, air-cooled transformers, 240/2 x 2,500 volts, used in power supplies for electronic apparatus had to be redesigned because of insulation breakdown after about one year's service.

In investigation of similar types of transformer it was found that the insulation was ample for the usual one minute over-voltage test but ionization in the insulation commenced at 35 to 50 per cent. of the operating voltage.

It is well known that small quantities of ozone and oxides of nitrogen are produced when air between the sheets of insulation is entrained or occluded within the insulating material is ionized. Ozone causes accelerated aging of organic materials whilst the oxides of nitrogen may, in the presence of moisture, form nitrous and nitric acids which attack these materials and metals. Even in the case of materials highly resistant to chemical attack, ionization is objectionable owing to the RF interference created.

Table 1 gives figures for the ionization onset voltage of various dielectric materials and points out that this voltage for the case of transformers should be 20 to 30 per cent. of the operating voltage, contrary to the usual practice of allowing a factor of safety on the one minute over-voltage test. Carroll² shows that the ionization onset voltage can be raised by the use of low permittivity material and also by employing many thin sheets, thus reducing the size of residual air voids.

Construction of Ionization-free Transformers.

In order to obtain information for the redesign of the above-mentioned transformers, the ionization onset voltage of the material used for the insulation was measured. The following figures were obtained and found to vary little, for samples in which the individual sheets of material varied in thickness between 0.005 and 0.010 inch. The sheets were pressed together tightly to reduce air films.

Since the ionization voltage gradient decreases with increasing insulation thickness, it would be expected that for a given total thickness a higher ionization voltage could be obtained if the insulation could be split up into n sections with $1/n$ of the voltage maintained on each section. As in condenser bushings, the splitting-up of the dielectric can be achieved by placing metal foils into the insulation thus forming several series-connected capacitors. In practical transformers the reactance of these capacitors is much smaller than their insulation resistance thus ensuring that the foils control the voltage distribution.

Complete advantage of this principle can only be realised if the construction is such that the high voltage insulation can be pulled tight in order to reduce air-films.

A typical shell-type transformer with concentric coils, 230, 240, 250/2 x 2,500 volts, used with the centre tap at earth potential, was constructed as follows. The low voltage winding was arranged nearest to the core and the taps were placed on the inside to reduce irregularities in the outer surface. For the same reason the last layer was fully wound. Above the primary was placed the usual electrostatic shield, forming one electrode of the first of the capacitors which constituted the high voltage insulation. It was split up into three sections as shown in detail in Figure 1. The outer shield was connected to the start of the high-voltage winding. As the windings did not fill the available window space no special insulation was required between the finish of the high voltage winding and the core. If this had not been the case further high voltage insulation similar to that shown in the figure could have been used on the outside of the high-voltage winding.

This type of insulation has been used on many transformers which have given satisfactory service for several

* Division of Electrotechnology, National Standards Laboratory, R.O., Sydney, Australia.
Manuscript received by the Institution 30/7/53.
P.C. number 621.314.2.

1. Lee, R., "Electronic Circuits and Transformers", Wiley, New York, 1947.
2. Carroll, J. S., 11th Report, 1948/1949, Ryan Lab., Elect. Eng. Dept., Stanford University.

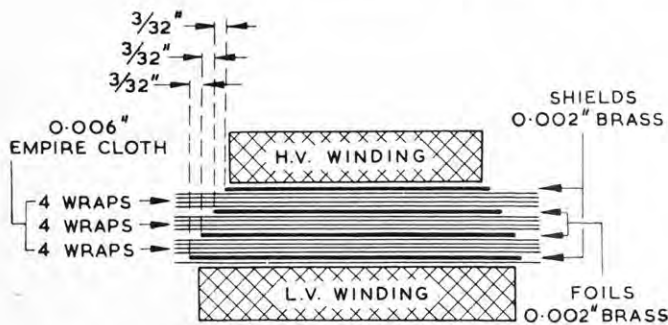


Figure 1.—Arrangement of the high-voltage insulation for an ionization-free transformer.

years. The ionization voltage was found to lie between 3,200 and 3,500 volts. For a thickness of 4×0.006 inch, one would expect, from the values given in the table, an ionization onset voltage of approximately 1,100 volts and for three sections 3,300 volts. This is in fair agreement with the measured values. As the circuit voltage was 2,500 volts, the margin of safety is reasonable.

3. Ionization Testing.

The transformers and insulating materials were tested using Quinn's circuit³ in a slightly modified form (see Figure 2). At the onset of ionization, spikes appear on

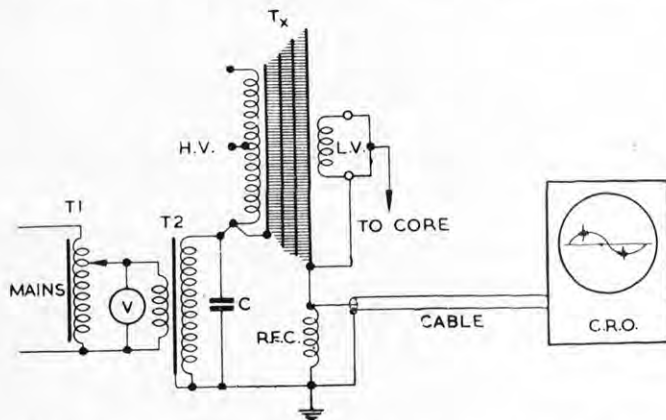


Figure 2.—Circuit used for testing ionization onset voltage.

T_1 : Variable autotransformer.

T_2 : 240/10,000 volt transformer.

T_3 : Transformer under test.

V : Voltmeter.

C : $0.02 \mu F$.

Radio-frequency choke: 10 millihenry, 40 ohms.

Cable: About 10 ft. $22 pF/ft$.

C.R.O. sensitivity: $15 mV$ R.M.S./cm at 100 kc/s.



Mr. Medina was born Austria in 1908. He graduated Dipl. Ing. in Electrical Engineering from the Technical University of Vienna in 1932. While still an undergraduate he was Assistant Technical Editor of several radio periodicals. Mr. Medina is the author of numerous papers dealing mostly with the results and practical application

of electrical measurements. After graduation he was a senior receiver design engineer in several radio factories in Poland, Czechoslovakia and Austria. In 1938, while still in Europe, he was engaged by Thom and Smith Pty. Ltd., and arrived in Australia early in 1939. As Assistant Chief Engineer of this Company he was responsible for the electrical design and development of receivers, amplifying equipment, two-way installations, transceivers, and MF, HF and VHF transmitters for FM and AM, mostly for the Army Services. In 1946 he joined the staff of the Division of Electrotechnology, C.S.I.R.O., where he is mainly concerned with the development of equipment for precise measurements, the design of special transformers and with high voltage engineering.

the trace of the cathode-ray oscilloscope, the time of which is locked to the supply frequency.

Since the voltage required for this work was low, difficulty was found in avoiding ionization external to the test piece. It was not necessary therefore to use the more complicated detection methods⁴ in which the effects of external discharges are balanced out. The equipment was tested for freedom from external discharges up to 7.5 kilovolts by replacing the test piece with a sphere gap consisting of two balls, 13 millimeters diameter, spaced 8 millimeters apart. A convenient method on the operation of the detection circuit may be obtained by means of a needle gap consisting of two crossed sewing needles, 0.5 millimeters in diameter, spaced 5 millimeters apart for which the ionization onset voltage was found to be approximately 2,300 volts.

4. Acknowledgment.

The constructional work was carried out by Mr. Paine, whose help is gratefully acknowledged.

(25a)

Apparatus for the Detection of Corona Discharges in the Insulation of Electrical Equipment

L. Medina*

Summary.

The useful life of many insulating materials is reduced by discharges occurring in gas-filled voids.

Apparatus is described for the detection of such discharges by observing the shock excited oscillations in a tuned circuit when a void breaks down.

Samples ranging in capacitance from a fraction of 1 pF to 1 μ F can be accommodated and the sensitivity of the equipment is such that discharges in the solid insulation of a 0.2 pF capacitor can be detected when it is shunted by a 20,000 pF capacitor free of discharges.

Self-checking methods, typical displays, circuit details and constructional data are given.

1. Introduction.

It has been known for some time that discharges occurring in voids within solid insulation or in voids between solid insulation and metal electrodes reduce the useful life of the insulation. Only recently, however, the results of life tests on a large number of insulating materials have been published by Dakin, Philofsky and Divens¹. To quote only one example from their paper, a 0.005 inch Nylon film, operated at twice the discharge inception voltage at 60 c/s, will break down after about 500 hours. Mason² mentions the inherent danger of A.C. over voltage proof tests which may cause considerable deterioration by discharges and a similar view is expressed by Hagenguth and Liao³ who state that in transformers built by their company corona has been largely eliminated even at test levels.

Discharge detection is therefore an important field of electrical testing. The test voltage may be either D.C. or A.C. When, in the case of testing with D.C., a void in a dielectric breaks down the boundary surface becomes

charged and further discharges cannot occur till the charge has leaked away. The discharge repetition rate is low and indeterminate for high grade insulation. D.C. testing is also unsuitable for A.C. insulation designed to be capacitatively stress-controlled⁴.

A.C. voltage at 50 c/s is employed in the apparatus to be described. The circuitry used is a refined version of that outlined before⁴ and it is based on the detection of oscillations in a tuned circuit excited by the discontinuous nature of the discharges.

An instrument has been built for the routine detection of discharges in small transformers for electronic apparatus, and while for this purpose a maximum test voltage of 5 kV r.m.s. was considered adequate, the detector in conjunction with suitable supply transformers has been used at much higher voltages to find discharges in transformers, bushings, mica, paper and ceramic capacitors and in structures supporting high voltage equipment.

2. Principle of Operation.

In practice a particular dielectric medium may contain many voids randomly distributed. However, to discuss the principle of operation and to determine the sensitivity requirements we shall use a simple model in which only one void exists. Such a model—solid insulation between two metal electrodes A and B—is shown in Fig. 1a. The

*Officer of the Division of Electrotechnology, C.S.I.R.O., Sydney, N.S.W.

Manuscript received by the Institution 4/10/55.

U.D.C. number 621.313.3.018.532.

1. Dakin, T. W., Philofsky, H. M. and Divens, W. C., "Effect of electric discharges on the breakdown of solid insulation," *Communications and Electronics*, No. 12, May, 1954, p. 155.

2. Mason, J. H., "Breakdown of insulation by discharges," *Proc. Instn. Elec. Engrs.* 100, Pt. IIA, 1953, p. 149.

3. Hagenguth, J. H., and Liao, T. W., "Impulse corona-detection, measurement of intensity, and damage produced," *A.I.E.E. Transactions*, 71, Pt. III, 1952, p. 461.

4. Medina, L., "Prevention of ionization in small power transformers," *Proc. Instn. Radio Engrs. (Aust.)* 15, No. 5, May, 1954, p. 114.

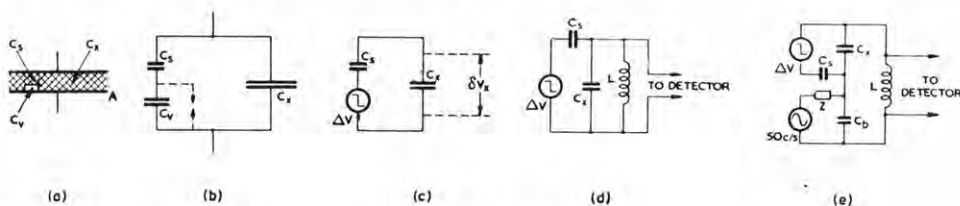


Figure 1.

- (a) Physical concept of a model containing one void.
 (b) Model circuit.
 (c) Equivalent diagram of the model.
 (d) The combination of (c) with a coil and a detector forms the elementary test circuit.
 (e) Elementary test circuit including the source of test voltage and its bypass-capacitor.

capacitance of the void is C_v , the capacitance of the dielectric in series with the void is C_s and the capacitance of the remainder of the dielectric is C_x . This concept yields the circuit of Fig. 1b, and it is assumed that $C_s \ll C_v \ll C_x$. When the void breaks down, the voltage on C_v drops suddenly by ΔV and this is equivalent to connecting a zero impedance step-function generator with a voltage ΔV in series with C_s . This is shown in Fig. 1c and by inspection $\delta V_x = \Delta V C_s / C_x$ where δV_x is the change of voltage on C_x .

As eventually δV_x is used to produce a damped oscillation in a tuned circuit connected to the detector (Fig. 1d) it follows that the sensitivity required to detect a discharge of a given magnitude must be greater for a larger value of C_x . For example, if a specimen of insulation is diluted by a shunt capacitance free of discharges, the sensitivity required to detect discharges in the specimen is higher. The discharge energy which may be regarded as a measure of the damage produced is $\frac{1}{2} \cdot \Delta V^2 \cdot C_v$. Let V be the applied voltage at which discharges occur, then since $C_s \ll C_v$, $C_v \cong C_s \cdot V / \Delta V$. Combining with $\delta V_x \cong \Delta V \cdot C_s / C_x$, the discharge energy becomes $\frac{1}{2} \delta V_x \cdot C_x \cdot V$ and it is proportional to the voltage on the detector, to the sum of specimen and diluting capacitance and to the applied voltage.

The elementary circuit of Fig. 1e includes the source of test voltage which may represent a high impedance (Z in Fig. 1e) at the natural frequency of the tuned circuit. A bypass capacitor C_b is therefore required.

The ionisation time of the spark gap represented by the void is less than 0.1 microsecond and it is known that spectral components of the surge voltage which appears at the terminals of C_x have been detected at frequencies up to 100 Mc/s. There is thus a wide choice in the resonance frequency of the tuned circuit consisting of L and the series combination of C_x and C_b (Fig. 1e). At low frequencies the rejection of the mains frequency and its harmonics is more difficult while higher frequencies necessitate a more complicated detector amplifier. A limit is also imposed by the capacitance and inductance of the test objects. A frequency range of 15 kc/s to 100 kc/s was found to be a suitable compromise. An untuned amplifier for this range is easy to construct, its response to low frequencies can be cut conveniently and only two values of L and C_b are required to test specimens varying in capacitance from a fraction of 1 pF to 1 μ F. In that

frequency range it is also easy to obtain a "Q" value which is high enough to give damped oscillations lasting several cycles.

3. Circuit Description.

Figs. 2a, 2b and 2c show three test circuits appropriate to different conditions of test. In Fig. 2a the specimen C_x is earthed and this connection is often convenient. For specimens up to 20,000 pF the inductor L has a value of 10 mH and the bypass capacitor is 10,000 pF. The lowest resonance frequency is then approximately 20 kc/s. In the case of very small specimens of a few pF only, the resonance frequency is approximately 100 kc/s and it is

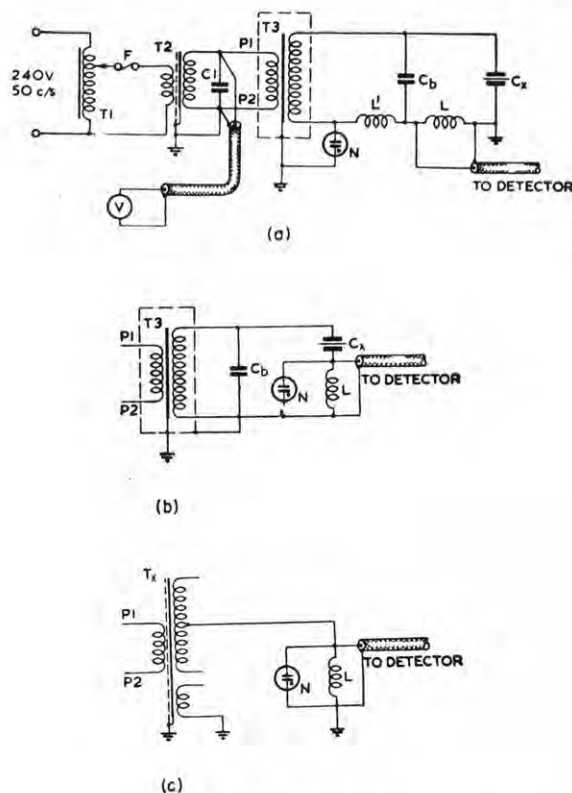


Figure 2.

- (a) Test circuit with specimen earthed.
 (b) Test circuit for specimens which can be insulated from earth.
 (c) Circuit for testing a Transformer (T_x) which supplies its own test voltage.

mainly determined by the capacitance of the polythene insulated connecting cable and the input capacitance of the amplifier, a total of approximately 250 pF. For specimens in the range 20,000 pF to 1 μ F, L is changed to 0.25 mH and C_b to 0.5 μ F.

The test voltage is supplied by the transformer T_3 . Often, for reasons of economy, the insulation between the "earthy" side of the secondary and the primary is designed to withstand a small voltage only and consequently the interwinding capacitance is large and lossy. The dilution effect of this capacitance is made small by the insertion of the inductor L' of value 10 L. The rare gas cartridge N prevents damage to T_3 and a dangerous voltage at the detector terminals in case of an accidental open circuit in L' or L .

Not only the capacitance of the test specimen but all capacitances associated with T_3 , the bypass capacitor C_b and the capacitance of the high tension wiring can be represented by the circuit of Fig. 1c if discharges occur in them. Several corona generators would then be in the circuit and all would cause a signal at the detector input. In order to be sure that only discharges in C_x are indicated it is essential that T_3 , C_b and the high tension connecting lead are free of corona up to the required test voltage.

A simpler circuit, shown in Fig. 2b, is possible when C_x can be insulated from ground. In this case dilution due to the transformer capacitances does not occur. The same values for L and C_b as given above are used. A further simplification is possible for specimens with a capacitance of less than about 300 pF. In this case the capacitance of the high tension terminal to the earthed tank together with the self-capacitance of the secondary provide an adequate bypass and makes C_b superfluous. This is particularly valuable at very high voltages when it may be quite difficult to obtain a corona-free bypass capacitor.

Another simplification applicable only when the specimen is a transformer which has a high voltage winding is shown in Fig. 2c. Here the transformer T_x under test supplies its own test voltage and discharges in the insulation between the secondary and any other winding may be detected. In a well-designed transformer no discharges should occur at the operating voltage. If it is desired to find the actual onset voltage, a voltage higher than the normal primary voltage must therefore be applied to the terminals P_1 and P_2 in Fig. 2c. An increase of 25 per cent is usually permissible before core saturation occurs but if this is insufficient a test voltage of higher frequency e.g. 150 c/s may be used. This complication is outweighed by the advantage that corona-free components are not required.

In all circuits the test voltage is adjusted by a variable auto-transformer T_1 . An isolating transformer T_2 with a static shield and terminals and leads so arranged as to minimise the direct primary to secondary capacitance is interposed between T_1 and T_3 in order to prevent r.f. mains noise from reaching the detector. The leakage inductance of this transformer together with C_1 forms a filter for audio and supersonic noise in the mains.

The voltmeter V measures the secondary voltage in terms of primary voltage and turns ratio

4. The Detector Amplifier.

The circuit is shown in Fig. 3 and an external view in Fig. 4. A 400 V power supply is the high tension source for both the amplifier and the cathode ray tube, the grid voltage of which is obtained from a variable back bias resistor which serves as an intensity control. A variable focus control was found unnecessary for discharge detection. Shift controls were omitted and the spot was centred by means of a small Ferroxdure magnet attached to the chassis. The sensitivity at 15, 50 and 100 kc/s is 430, 260 and 350 μ V r.m.s./cm. respectively. The noise voltage of the detector referred to the input is less than 20 μ V and is just noticeable.

The time base is sinusoidal and is derived from the power supply transformer. As corona onset occurs at the peak of the test voltage discharges are seen as pulses at the end of the time base trace. While the phase angle between the time base voltage and the test voltage is usually so small that the pulses appear at or very near

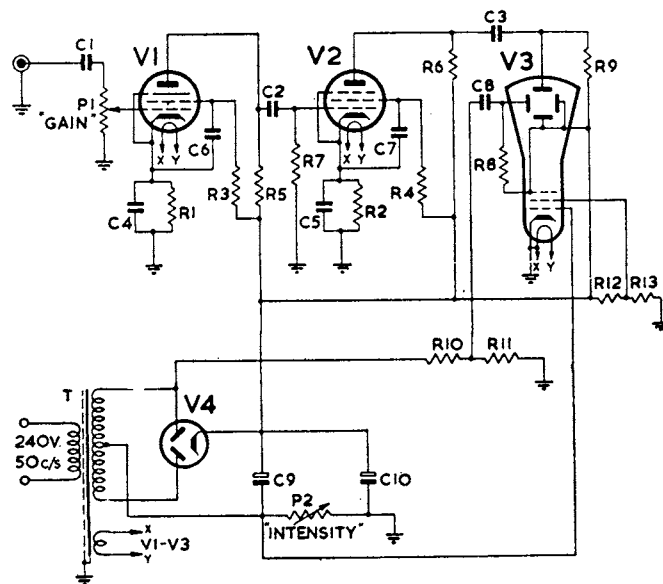


Figure 3.—Circuit diagram of the detector amplifier.

V_1, V_2	6BX6
V_3	902
V_4	6X4
T	240/2 \times 325/6.3V
P_1	0.25 M Ω
P_2	5000 Ω
R_1, R_2	470 Ω
R_3, R_4	470 k Ω
R_5, R_6	100 k Ω
R_7, R_8, R_9	220 k Ω
R_{10}	680 k Ω
R_{11}	150 k Ω
R_{12}	250 k Ω
R_{13}	75 k Ω
C_1, C_2, C_3	250 pF
C_4, C_5	0.05 μ F
C_6, C_7	0.01 μ F
C_8	0.25 μ F
C_9, C_{10}	8 μ F

the ends of the trace, it is necessary to feed the detector and the test voltage supply from the same phase when three phase mains are used.

The rejection of the 50 c/s test voltage is achieved by the coil L (Fig. 2), the 50 c/s voltage drop on which is quite small, and by small coupling and small bypass capacitors in the amplifier which reduce the gain at 50 c/s to considerably less than unity.



Figure 4.—The detector amplifier.

5. Testing.

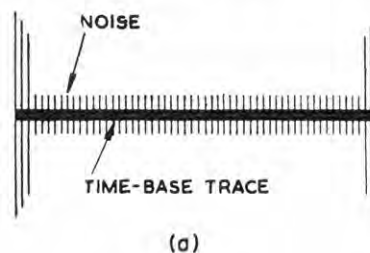
Freedom from discharges in T_3 (Fig. 2) may be checked using the circuit of Fig. 2c. Discharges in paper, empire-cloth, silicone-varnished glass fibre cloth, polythene, micanite, etc., will generally appear as shown in Fig. 5a. The pulses—which are damped oscillations lasting a few cycles of the resonance frequency of the tuned circuit—appear suddenly when the voltage is increased and the onset voltage can usually be determined with an accuracy of a few per cent. Discharges in oil are characterised by intermittent occurrence, lack of a definite phase relationship with the applied voltage and by a large difference in onset and offset voltage.

In a completed transformer discharges may occur not only within the winding insulation but also in a bushing and at points of high stress at the bushing surface, or they may emanate from sharp points, e.g., a terminal lug. If the bushing consists of a conductor with insulation moulded or wrapped around it, the display will be as in Fig. 5a. If however, there is an air space between conductor and insulating shell, a polarity effect as shown in Fig. 5b is usually observed. Surface discharges and discharges from sharp points produce pulses of large magnitude with a strong rectification effect⁵ and over a wide voltage range the display appears as shown in Fig. 5c. In oil-filled

transformers below 50 kV the most likely limitation is due to discharges in the bushing. To quote one drastic example, in the porcelain bushing of a 240/22,000 V transformer discharges commenced at 5.5 kV and while these are quite harmless in inorganic material the use of the transformer in discharge detection apparatus had to be restricted to voltages below 5.5 kV.

Discharges in the high voltage wiring may be checked using the circuit of Fig. 2a or Fig. 2c by connecting to the high voltage terminal of T_3 the lead which is to be used in connecting the specimen. The end of the lead must be protected by a well-rounded metallic body or bent back on itself in a rounded loop. Corona is displayed as shown in Fig. 5c. It was found that for voltages up to 10 kV bare 20 S.W.G. wire is satisfactory. For higher voltages copper tubing is used.

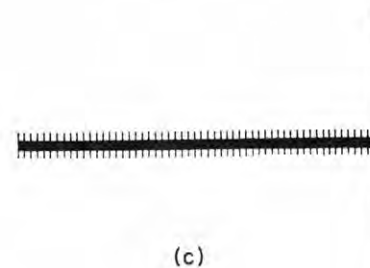
No self-checking method is available to test the bypass capacitor. A rough check may be made using the circuit of Fig. 2b with C_b in place of C_x but the sensitivity is reduced due to the absence of a bypass capacitor. It is therefore advantageous to use a bypass capacitor made up of three equal capacitors, each of value $C_b/3$, in parallel.



(d)



(b)



(c)

Fig. 5.—Diagrammatic representation of displays.

(a) Voids in a dielectric.

(b) A bushing with an air space between conductor and porcelain shell.

(c) A sharp point or surface discharge.

5. Peek, F. W. (1929) "Dielectric phenomena in high voltage engineering" 3rd ed. p. 103 (McGraw-Hill Book Company Inc.: New York).

The Author:

Mr. Medina was born in Austria in 1908. He graduated Dipl. Ing. in Electrical Engineering from the Technical University of Vienna in 1932. While still an undergraduate he was Assistant Technical Editor of several radio periodicals. Mr. Medina is the author of numerous papers dealing mostly with the results and practical applica-

tion of electrical measurements. After graduation he was a senior receiver design engineer in several radio factories in Poland, Czechoslovakia and Austria. In 1938, while still in Europe, he was engaged by Thom and Smith Pty. Ltd. and he arrived in Australia early in 1939. As Assistant Chief Engineer of this Company he was responsible for the electrical design and development of radio receivers, amplifying equipment, two-way mobile installations, transceivers, and MF, HF and VHF transmitters for FM and AM, mostly for the Armed Services. In 1946 he joined the staff of the Division of Electrotechnology, C.S.I.R.O., where he is mainly concerned with the development of equipment for precise measurements, the design of special transformers and with high voltage engineering.

Two in series acting as C_b can then be used to test the third one as C_x and by interchanging all may be checked.

To test the sensitivity of the equipment the circuit of Fig. 2a was used. Four small capacitors in which discharges commenced at voltages between 1 and 2 kV were made by placing several sheets of Empire cloth, Kraft-paper, polythene and glassine respectively between small spherical electrodes. The effective capacitance through the dielectric was approximately 0.2 pF in each case. The ionisation onset voltage was determined for each capacitor and the specimen under test was then shunted with a capacitor of 20,000 pF known to be free of discharges. In all cases the onset voltage was only a few per cent higher than without the shunt. This dilution ratio of 10^5 may be visualised as occurring in practice in a capacitor in which the impregnating agent fills all the voids except in $1/10^5$ of the area of the dielectric. Paper was found to be the most difficult material and the indication at high dilution ratios was rather feeble. Without the shunt capacitor or at low dilution ratios only a fraction of the available gain was required to detect the onset of discharges.

While no difficulty was experienced in testing capacitors up to 1 μ F at relatively low voltages, extraneous noise became troublesome when capacitors of a high kVA rating

were tested, because a shielded isolating transformer of suitable rating was not available (T_2 in Fig. 2). In this case it was found helpful to compare the display obtained from the specimen with the display observed when four capacitors nominally equal to the specimen and connected in series parallel were substituted for it. It was also found important to keep the brush of T_1 (Fig. 2) in good condition in order to avoid confusing transients.

In all work with the exception of a few tests on 150 c/s the test frequency was 50 c/s. However, as it is known⁶ that the discharge inception voltage is nearly independent of frequency up to 100 kc/s, it should be sufficient to test, say, the insulation of a transformer used in flyback type E.H.T. supplies at 50 c/s.

The circuits described have been used by the author for several years and during that time experiments were carried out with a view to further improvement. While it is realized that more rigorous filtering and screening—the latter often quite impracticable in high voltage work—and a tunable detector of narrow bandwidth may be advantageous, it was felt that details of the apparatus in its present form should be given because it is simple to construct, positive in its indication and convenient to use.

6. Constructional Details.

Ferroxcube pot cores D 36/22 of III B 3 grade were used for the 10 mH and 0.25 mH coils. The cores had no airgap and a gap was provided by a sheet of bakelite approximately 0.03 inch thick. The coils had 220 and 35 turns wound with 27 x 47 S.W.G. and 27 x 38 S.W.G. litz wire respectively. The D.C. resistances were 4 ohms and 0.1 ohms. It can be shown that the core flux density at 50 c/s will remain below 2,000 lines/cm² if the current in the 10 mH coil is less than 0.4A and less than 2.5A in the 0.25 mH coil. The coil L' (Fig. 2a) was used only for specimens of less than 20,000 pF because all larger specimens were capacitors for which the simpler arrangements of Fig. 2b was used. The inductance of L' was 0.1 H, its D.C. resistance was 5 ohms and it was built as a low capacitance air coil.

The rare gas cartridge N (Fig. 2) rated 10A for 3 seconds had an ignition voltage of 100 V.

Although various types of transformers were used for T_2 (Fig. 2) it was found that a value of 4 μ F for C_1 was sufficient and not critical.

7. Acknowledgments.

The author is grateful to Mr. C. Gett (Science student, University of Sydney) for his help in the developmental work and to Mr. F. P. Paine (Division of Radiophysics, C.S.I.R.O.) for his part in the construction of the apparatus.

6. Hopkins, R. J., Walters, T. R. and Scoville, M. E., "Development of corona measurements and their relation to the dielectric strength of capacitors." *A.I.E.E. Transactions*, 70, 1951, Pt. II, p. 1643.



(26)

A Recurrent Surge Oscillograph for Surge-Voltage Distribution Measurements on Transformers

F. C. HAWES*

Summary.

The apparatus comprises a thyatron surge generator combined with a CRT display unit. The generator supplies 1/50 microsecond pulses of 450 V peak to the transformer under test at a repetition rate of 50 times per second. The display unit, consisting of a measuring probe, a variable capacitance attenuator, video amplifier and double beam cathode ray tube, provides simultaneous comparison of the waveshape at any point along a winding with the applied voltage wave or with a timing wave. Means are provided for measuring the voltages on taps of windings as a percentage of the applied voltage. The instrument features simple design and construction from readily available components.

1. Introduction.

Since some electrical equipment is susceptible to damage by lightning or switching surges, tests in which these surges are simulated are becoming increasingly common. To standardize testing, B.S. 923:1950 defines, with appropriate tolerances, the test waveform as a pulse which rises from zero to maximum voltage in 1 microsecond and decays to one half its maximum value in 50 microseconds. This test waveform is generally known as a 1/50 microsecond wave.

For the design engineer to provide insulation capable of withstanding surges of specified peak value (e.g. 95 kV for 11 kV equipment), the surge-voltage distribution must

* Department of Motor Transport, N.S.W., formerly with C.S.I.R.O., Division of Electrotechnology.

Manuscript received by the Institution March 15, 1957.

U.D.C. number 621.317.75.015.1.

be known. Impulse testing equipment comprising a high voltage impulse generator together with its associated potential divider, oscillograph and sphere gap is very costly and hence is usually available only in the laboratories of large manufacturing concerns or testing authorities.

It has been shown that generally a transformer winding behaves as a linear network for the duration of the $1/50$ wave. Thus, the surge distribution, which is mainly governed by the series and earth capacitances of the various windings, is very nearly independent of the applied voltage and relative measurements of the voltages appearing on coils may be made at any convenient level of applied voltage.

The Recurrent Surge Oscillograph (RSO), which comprises a surge generator delivering low voltage (<1 kV) recurrent pulses and an oscillographic display unit, is extremely useful in determining the surge-voltage distribution in transformers. It can be constructed in portable form and on account of its small size can be used in almost any location. The presentation of a steady trace on the screen of the cathode ray tube enables the designer to observe immediately the effects of small changes in winding arrangements. This is of particular importance during the development of a new type of transformer.

With a knowledge of the surge-voltage distribution and of the impulse strength of materials, the designer can predict with reasonable accuracy the performance of transformers when submitted to full scale voltage tests.

The construction is simple and the circuits are not critical, readily available components being used throughout.

2. Circuit Distribution.

2.1 Simplified Circuit.

The circuit is based in part on the work of Rohats¹ and is shown in Fig. 1. Slightly before the peak of the positive half-cycle of the 50 c/s mains frequency source S , the thyatron V_1 conducts and supplies current to the network, RC_1 . The voltage developed across the capacitor C_1 is used as the time base for the cathode ray tube V_5 . The storage capacitor C which is negatively charged during the opposite half-cycle by diode V_2 , is discharged into a pulse shaping network R_7, R_t, C_t when thyatron V_3 is triggered from the cathode of V_1 . The $1/50$ microsecond wave developed across R_t is applied to the transformer under test.

The measuring circuit contains a probe consisting of a high impedance capacitance attenuator C_s, C_p and a cathode follower V_6 , which is connected by a coaxial cable to a video amplifier stage V_7 , the output of which is displayed on the Y_2 plate of the CRT, V_5 .

V_1 also triggers the thyatron V_4 which provides reference timing frequencies on the Y_1 plate.

The surge generator output is available in 10% steps at a calibration terminal and also, by suitable switching, may be applied to the Y_1 plate for measuring, as a percentage of the applied voltage, the amplitude of the surge-voltage appearing on the windings.

2.2 The Time Base. The complete circuit of the RSO is shown in Fig. 2. The firing angle of V_1 is controlled by a DC bias voltage derived from the 6.3 V AC heater supply by means of germanium diode D_1 and is adjusted in magnitude so that conduction occurs slightly before the peak positive value of the 50 c/s supply voltage from T_1 . An RF choke is placed in the anode circuit of V_1 to improve firing stability and to suppress high frequency oscillations on the surge wavefront. Sweep durations of 10, 50 and 100 microseconds, approximately, are selected by $S3_{(1)}$, the fastest sweep being obtained with only the stray capacitances of the switch and wiring. Generally, the greatest stress on transformer windings occurs a few microseconds after the application of the surge and hence the quasi-logarithmic sweep provided by the time base is advantageous because it permits detailed observation of the wavefront while still presenting the whole wave².

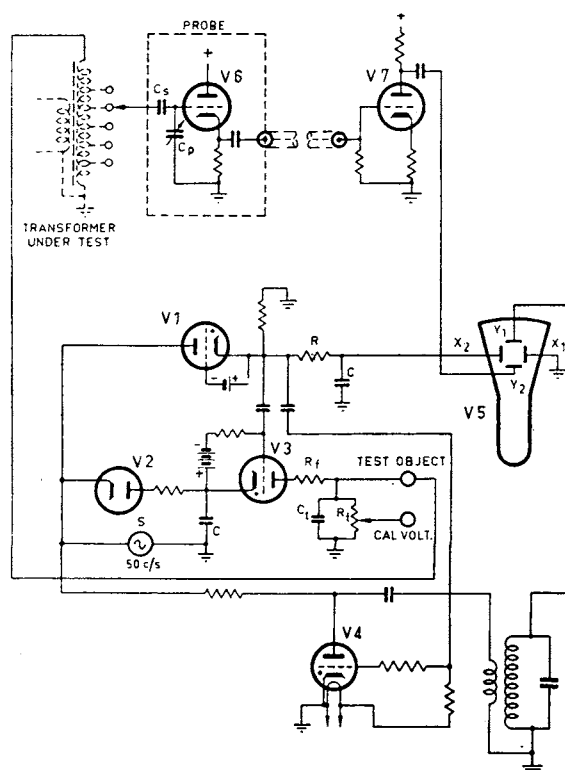


Figure 1.—Simplified Circuit.

Brightening of the CRT trace is achieved by applying a positive pulse to the grid of V_5 through the coupling capacitor C_{10} , the pulse length being chosen by $S3_{(2)}$. Germanium diodes D_2 and D_3 in series function as level clamp diodes between grid and cathode of V_5 .

2.3 The Surge Generator.

Hold-off bias for V_3 has, for simplicity, been obtained from a battery the current drain on which is negligible. The energy stored in C_5 is discharged into the pulse-shaping network $R_{14}, C_{11-13}, R_{15-24}$ when V_3 is triggered

1. Rohats, N., "The Oscillographic electric transient analyser", *G. E. Review*, 39, 1936, 146.

2. Creed, F. C., Kusters, N. L. and Purvis, W. J., "The modernization of the N.R.C. impulse testing facilities", *Engineering Journal (Canada)*, April 1954.

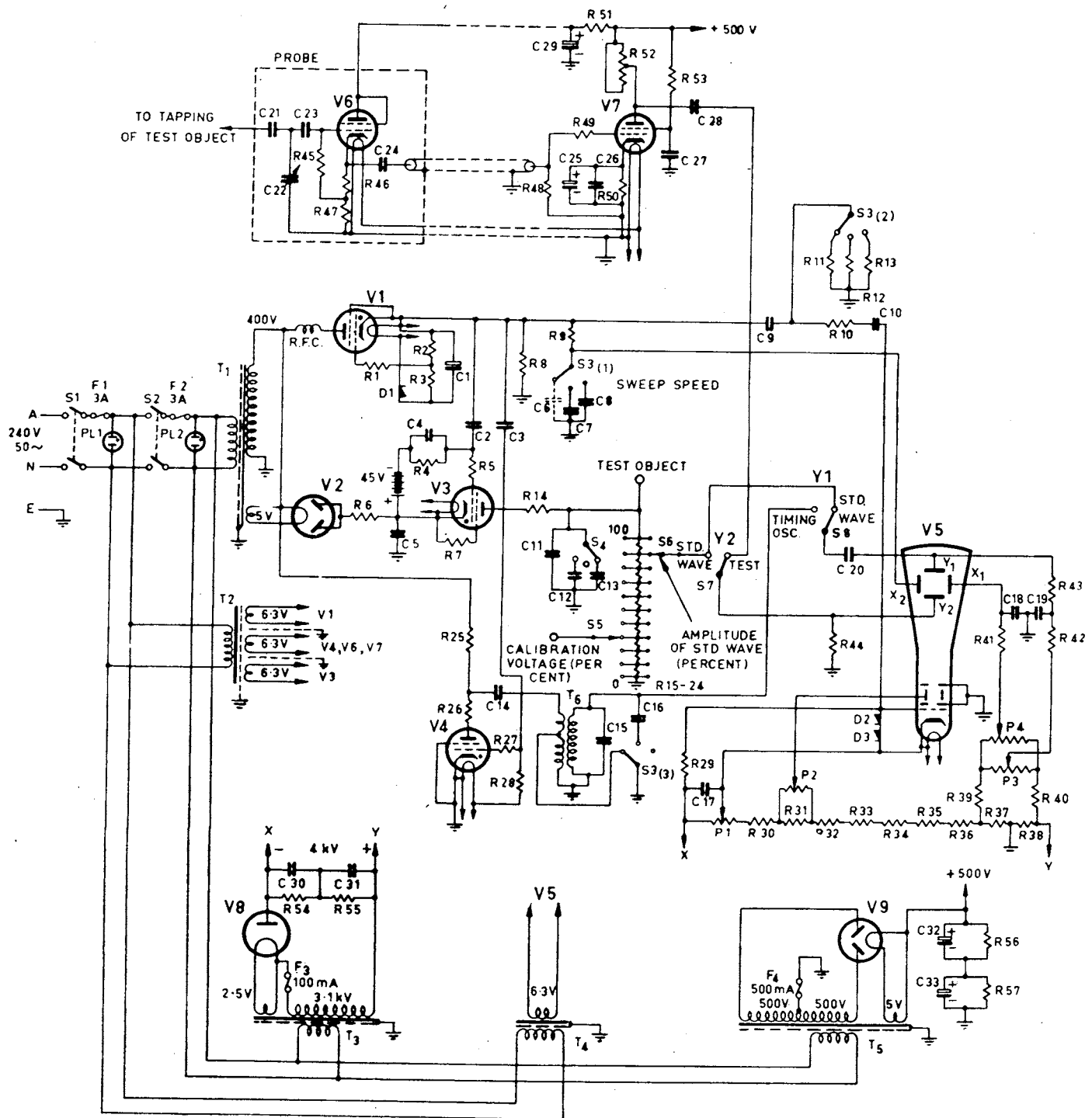


Figure 2.—Circuit Diagram.
All resistors carbon if not marked wire wound (WW).

$R_1, R_4, R_{27}, R_{28} \dots 100 \text{ k}\Omega \frac{1}{2} \text{ W}$. $R_2 \dots 18 \text{ k}\Omega \frac{1}{2} \text{ W}$.
 $R_3 \dots 33 \text{ k}\Omega \frac{1}{2} \text{ W}$. $R_5 \dots 10 \text{ k}\Omega \frac{1}{2} \text{ W}$. $R_6, R_{25} \dots 50 \text{ k}\Omega 2 \text{ W}$.
 $R_7 \dots 4.7 \text{ k}\Omega \frac{1}{2} \text{ W}$. $R_8 \dots 2 \times 100 \text{ k}\Omega 2 \text{ W par}$.
 $R_9 \dots 18 \text{ k}\Omega 1 \text{ W}$. $R_{10} \dots 220 \text{ k}\Omega 2 \text{ W}$. $R_{11} \dots 15 \text{ k}\Omega 1 \text{ W}$.
 $R_{12} \dots 82 \text{ k}\Omega 1 \text{ W}$. $R_{13}, R_{29}, R_{41}, R_{42}, R_{43} \dots 1 \text{ M}\Omega 1 \text{ W}$.
 $R_{14} \dots 220 \Omega 1 \text{ W}$. $R_{15} \text{ to } R_{24} \dots 680 \Omega \frac{1}{2} \text{ W}$.
 $R_{26} \dots 680 \Omega 1 \text{ W}$. $R_{30} \dots 150 \text{ k}\Omega 2 \text{ W}$.
 $R_{31} \dots 180 \text{ k}\Omega 2 \text{ W}$. $R_{32} \dots 250 \text{ k}\Omega 2 \text{ W}$.
 $R_{33}, R_{34}, R_{35} \dots 330 \text{ k}\Omega 2 \text{ W}$. $R_{38}, R_{39} \dots 100 \text{ k}\Omega 2 \text{ W}$.
 $R_{37}, R_{38} \dots 500 \text{ k}\Omega 2 \text{ W}$. $R_{40} \dots 470 \text{ k}\Omega 1 \text{ W}$.
 $R_{44} \dots 2.2 \text{ M}\Omega \frac{1}{2} \text{ W}$. $R_{46} \dots 10 \text{ M}\Omega \frac{1}{2} \text{ W}$.
 $R_{48} \dots 100 \Omega 1 \text{ W and } 220 \Omega 1 \text{ W par}$. $R_{47} \dots 4.7 \text{ k}\Omega 2 \text{ W}$.
 $R_{48} \dots 220 \text{ k}\Omega \frac{1}{2} \text{ W}$. $R_{49} \dots 330 \Omega \frac{1}{2} \text{ W}$.

$R_{50} \dots 12 \Omega \text{ WW}$. $R_{51} \dots 20 \text{ k}\Omega 2 \text{ W}$.
 $R_{52} \dots 10 \text{ k}\Omega$, I.R.C. type EPA. $R_{53} \dots 15 \text{ k}\Omega 20 \text{ W, WW}$.
 $R_{54}, R_{55} \dots 5 \times 1 \text{ M}\Omega 2 \text{ W, ser}$.
 $R_{56}, R_{57} \dots 100 \text{ k}\Omega 2 \text{ W}$.

Carbon Potentiometers.

$P_1 \dots 100 \text{ k}\Omega$. $P_2, P_3, P_4 \dots 2 \text{ M}\Omega$.

Capacitors.

(E = electrolytic, M = mica, P = paper, K = ceramic)
 $C_1 \dots 100 \mu\text{F } 40 \text{ V}$, E. $C_2, C_3 \dots 200 \text{ pF } 2.5 \text{ kV}$, M.
 $C_4, C_{10} \dots 1,000 \text{ pF}$, 600 V, M.
 $C_5, C_{14}, C_{23} \dots 0.01 \mu\text{F}$, 600 V, M. $C_6 \dots 25 \text{ pF approx. (wir. cap)}$.
 $C_7 \dots 700 \text{ pF}$, 2.5 kV, M.
 $C_8 \dots 2,000 \text{ pF}$, 2.5 kV, M. $C_9, C_{12} \dots 500 \text{ pF}$, 2.5 kV, M.

Figure 2. Caption (continued)

$C_{10} \dots 500 \text{ pF}$, 5 kV, M. $C_{11}, C_{13} \dots 1,000 \text{ pF}$, 2.5 kV, M.
 $C_{15} \dots 500 \text{ pF}$, 600 V, M. $C_{16} \dots 0.05 \text{ } \mu\text{F}$, 600 V, P.
 $C_{17}, C_{18}, C_{19}, C_{26} \dots 0.1 \text{ } \mu\text{F}$, 600 V, P.
 $C_{20}, C_{24}, C_{28} \dots 0.02 \text{ } \mu\text{F}$, 600 V, M.
 $C_{21} \dots 5 \text{ pF}$, 600 V, K.
 $C_{22} \dots 30 \text{ to } 750 \text{ pF}$, two-gang air variable.
 $C_{25} \dots 500 \text{ } \mu\text{F}$, 12 V, E.
 $C_{27} \dots 0.5 \text{ } \mu\text{F}$, 600 V, P.
 $C_{29}, C_{32}, C_{33} \dots 14 \text{ } \mu\text{F}$, 600 V, E.
 $C_{30}, C_{31} \dots 2 \text{ } \mu\text{F}$, 2.5 kV, P.
Indicator Lamps.
 PL_1, PL_2 , Neon indicator 240 V.
Fuses.
 $F_1, F_2 \dots 3 \text{ A}$, $F_3 \dots 0.1 \text{ A}$, $F_4 \dots 0.5 \text{ A}$.
Valves.
 $V_1, V_3, V_4 \dots$ PL 5727.
 $V_2 \dots 5Y3\text{-GT}$.
 $V_5 \dots 89D$ — CR tube — Cossor.
 $V_6 \dots EF 80$.

$V_7 \dots EL 34$.
 $V_8 \dots AV 11$.
 $V_9 \dots 5U4\text{-G}$.

Diodes.

$D_1 \dots GEX 66$, D_2, D_3 OA 85.

Transformers.

T_1 : 240/400 V, 40 mA, 5V, 2 A.
 T_2 : 240/6.3 V, 1 A; 6.3 V, 3 A; 6.3, 1 A.
 T_3 : 240/3,100 V, 10 mA; 2.5 V, 5 A.
 T_4 : 240/6.3 V, 2 A Sec. insul. 5 kV.
 T_5 : 240/500—0—500 V, 0.3 A; 5 V, 3 A.
 T_6 : Core: G.E.C. alloy Dust core No. 3.
 Prim: 74 turns tapped at 6, 27/47 litz-wire.
 Sec.: 80 " " "
 RFC: 75 mH — 350 Ω .

Switches.

$S1, S2, 10 \text{ A} — 240 \text{ V}$.
 $S3 \dots 3$ pole 3 pos.
 $S4 \dots 1$ pole 3 pos.
 $S5, S6 \dots 1$ pole 11 pos.
 $S7 \dots 1$ pole 2 pos. (low capacitance).
 $S8 \dots 1$ pole 2 pos.

by a positive pulse from the cathode of V_1 via C_2 . The ratio of the capacitive voltage divider C_4, C_2 is chosen to ensure that V_3 is triggered after the sweep has commenced. The surge generator constants are derived from the following approximate expressions (referring to Fig. 1):

$$\begin{aligned}
 t_{\text{front}} &\simeq 2C_t R_f \text{ seconds;} \\
 t_{\text{tail}} &\simeq R_t (C + C_t) \log_e 2; \\
 C &\simeq 5 C_t.
 \end{aligned}$$

and for critical damping: $R_f \simeq 2\sqrt{L/C_t}$ whereby L is the inductance of the leads and components in series with R_f . The screwdriver control $S4$ provides for a reduction in generator output capacitance so that transformers with high capacitance can be accommodated whilst still producing a surge waveform within specification tolerances.

2.4 The Timing Oscillator.

AC bias from the 6.3 V heater supply is used for V_4 which is normally non-conducting. C_{14} is charged during the positive half-cycle of the supply voltage from T_1 and V_4 is triggered by the pulse from V_1 via C_3 thus discharging C_{14} through the primary of the RF transformer T_6 . The secondary is tuned to 500 kc/s or 50 kc/s, the appropriate timing oscillator frequency being selected by $S3_{(3)}$.

2.5 The Probe and the Video Amplifier.

The probe consists of a high impedance capacitance attenuator $C_{21}\text{--}C_{22}$ and cathode follower V_6 . This arrangement provides an input capacitance of approximately 5 pF so that the effect of the probe on the waveshape is small. Since the input pulse is negative the cathode resistor R_{47} of V_6 has been kept small so that distortion due to clipping is negligible. The output from the cathode of V_6 is connected to the grid of V_7 by a coaxial cable. V_7 constitutes a single stage video amplifier giving a peak output voltage of 200 V and having a frequency response 3 db down at 2 Mc/s. This is adequate for all significant components of the 1/50 microsecond wave³.

$S7$ is a low capacitance switch enabling a portion of the surge generator output from $S6$ or the output of the video amplifier V_7 to be switched to the Y_2 plate of V_5 . $S8$ allows a timing oscillator frequency or the output of $S6$ to be displayed on the Y_1 beam.

2.6 Power Supplies.

Cathode ray tube and amplifier supply voltages are provided by conventional power supplies with rectifiers V_8 and V_9 .

3. Performance.

The surge generator delivers a 1/50 microsecond surge of peak value 450 V to the transformer under test. The CRT displays the 1/50 microsecond wave approximately 3 inches long and 1 inch high, thus giving reasonable reading accuracy. A writing speed of about 3 cms/ μsec . is achieved using a conventional double beam tube operating at a plate voltage of 4 kV. The performance of the measuring circuit may be checked simply by connecting the probe to the "Calibration Voltage" terminal and adjusting the attenuator so that the output of V_7 is superimposed on the standard wave shown on Y_1 over the whole length of the trace. By this method, which checks both the high and low frequency response, it was found that the measuring circuit time-delay is about 0.05 microsecond.

Fig. 3 (a) shows the waveshape of the surge generator output as selected by $S6$, the waveshape at a tap of the secondary winding, and a 500 kc/s timing wave. Fig. 3 (b) shows the applied wave, a typical waveform on a tapping, and a 50 kc/s timing wave. Fig. 3 (c) shows the waveform on the transformer tapping and the 500 kc/s timing wave superimposed by means of the shifts so that the traces intersect at approximately one microsecond after the application of the surge.

4. The Use of the Instrument.

The determination of the surge-voltage distribution in transformers necessitates the measurement of voltages between tapping points and earth. Care must be taken to keep capacitances between measuring leads and other circuits or earth to a minimum so that the measuring

3. Miles, J. G., "Frequency spectra of standard impulse wave-shapes", *Metropolitan Vickers Gazette*, 25, Sept. 1954, 367-9.

circuit does not influence the voltage waveshape on theappings. The addition of a known small capacitor across the winding quickly shows if any error is to be expected from the measuring probe.

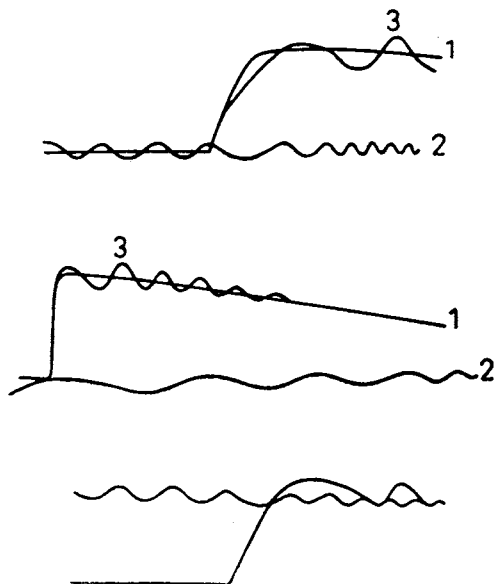


Figure 3.—Typical Displays.

- (a) 1 — Applied $1/50 \mu$ sec. wave.
2 — 500 Kc/s timing wave.
3 — Voltage at 25% of the winding from earthed end.
- (b) 1 — Applied impulse.
2 — 50 Kc/s timing wave and 50 μ sec. time base.
3 — Voltage at 25% of the winding from earthed end.
- (c) 500 Kc/s timing wave superimposed on voltage wave at a tapping so that the traces intersect at approx. 1μ sec. after the application of the impulse.

The instrument enables qualitative comparison of the waveshape onappings— Y_2 —and the standard $1/50$ micro-second wave— Y_1 —to be made. Quantitative measurements of the surge-voltage distribution may be carried out by switching Y_1 to the output of the timing oscillator and adjusting the Y_1 -shift until the timing wave intersects the voltage waveshape onappings— Y_2 —at any chosen time interval after the application of the surge-voltage (See Fig. 3 (c)). A magnifying lens and pointer assembly is then adjusted so that the point of intersection of the two beams and the end of the pointer are aligned. The measuring probe is then transferred to the calibration terminal. The calibration surge-voltage and the X-shift are then adjusted so that the peak of the calibration surge wave is in line with the pointer. Although the calibration surge-voltage may be adjusted only in 10% steps, it is possible to estimate to within a few per cent. In these measurements care must also be taken to avoid overloading the amplifier.

This procedure is then repeated for several time-intervals and several tapping points so that distribution curves corresponding to each nominal time interval may be obtained. Fig. 4 (a) shows the surge-voltage distribution

for a typical well designed transformer and Fig. 4 (b) for a transformer in which a large proportion of the surge voltage appears on the first coil of a 4-coil transformer.

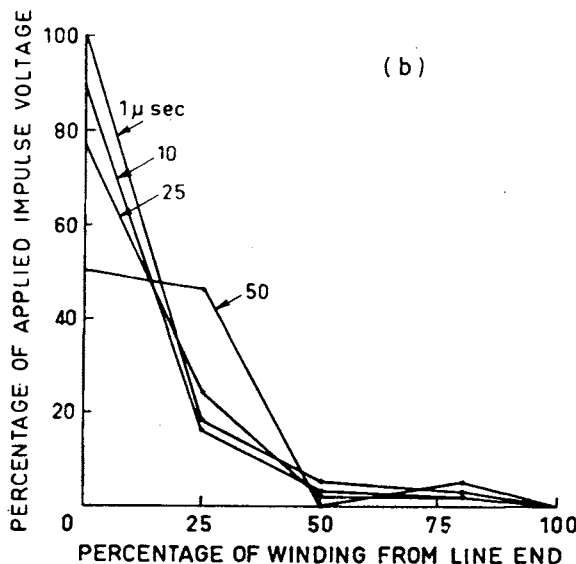
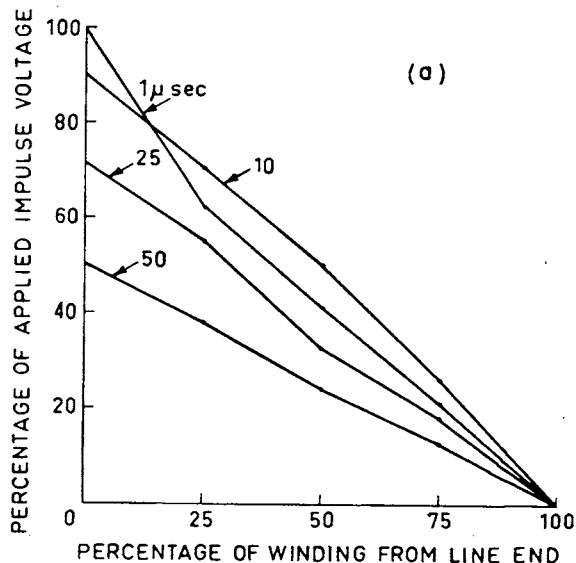


Figure 4.—Surge Voltage Distribution in H.T. Windings.

- (a) For a typical well-designed transformer.
- (b) For a four-coil winding in which nearly all the surge stress appears on one coil.

5. Constructional Details.

The Recurrent Surge Oscillograph has been built as a portable unit as shown in Fig. 5. All bulky components, including the DC power supplies, are housed in the lower unit, while the surge generator, video-amplifier and oscillograph unit are contained in the non-detachable upper unit which is set at an angle for convenient observation.

All controls are carried on the sloping front panel while "Heater" and "HT" switches and fuses are located on a lower vertical panel. For simplicity all connections

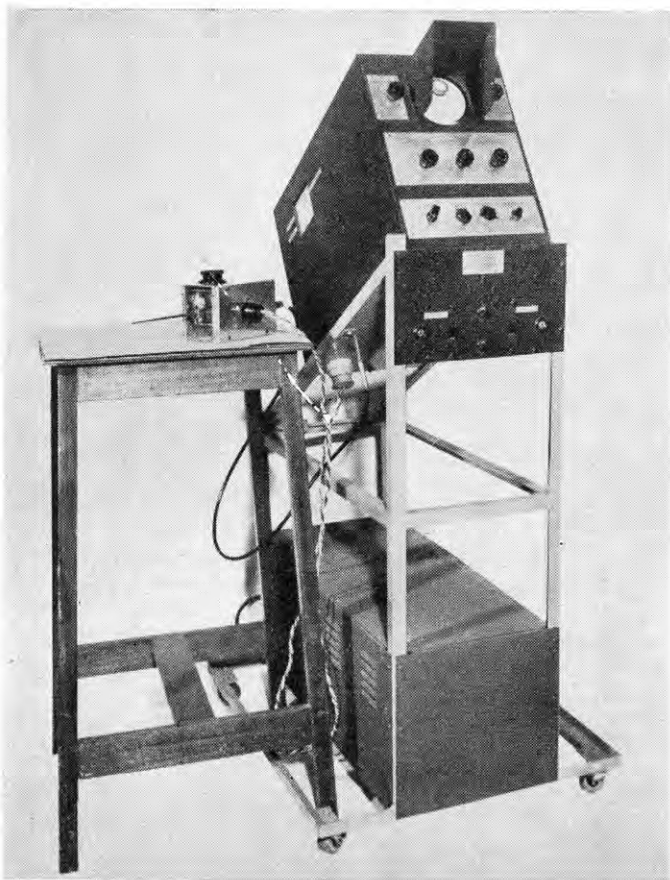


Figure 5.—Exterior View of the Instrument.

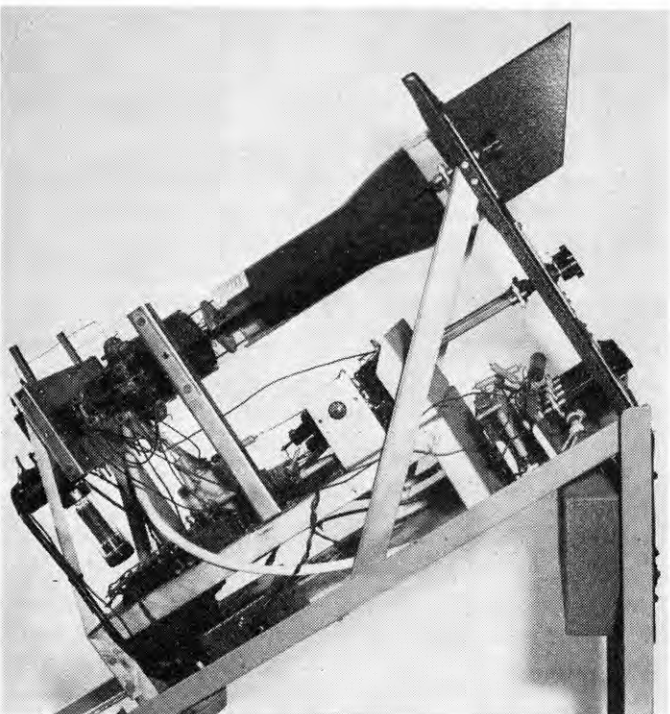


Figure 6.—Interior View of the Instrument.

The Author :



F. C. Hawes was born at Maclean, N.S.W. in 1927 and was educated at Marist Brothers High School, Eastwood. In 1944 he joined the staff of the Division of Electrotechnology, C.S.I.R.O., and was engaged on precise measurements at D.C. and power frequencies.

Upon obtaining a Diploma in Electrical Engineering at the Sydney Technical College in 1951, Mr. Hawes was transferred to the High Voltage Laboratory where he was concerned with the development of high voltage measuring equipment and with high voltage techniques.

In 1956, he joined the staff of the Traffic Engineering Section of the Department of Motor Transport, N.S.W. and is engaged in the design, construction and maintenance of traffic control signals and associated equipment in New South Wales.

between the two units are made by means of fixed cables, the HV cable being made by placing three PVC sleeves over PVC insulated hook-up wire. The layout of the upper unit has been chosen for ease of servicing as shown in Fig. 6.

The CRT voltages are obtained from a half-wave rectifier V_8 fed from a corona-free HT transformer T_3 (see Fig. 2), 240/3,100 V, 10 mA, in which capacitance shields control the voltage distribution in the insulation⁴.

Owing to the tolerances in the resistors R_{30} to R_{40} it may be necessary to alter some values slightly to obtain a sufficient range of the controls P_1 to P_4 .

T_2 is a special heater transformer 240/6.3 V, 1 A, 6.3 V, 3 A, and 6.3 V, 1 A, with electrostatic shields between the windings and appropriate HV insulation between the shields and the windings which feed V_1 and V_3 .

All wiring capacitances are kept to a minimum particularly at the anode of V_7 . The plate load of V_7 , R_{52} , is an IRC type EPA 10,000 ohm wire-wound resistor in which the centre tap is taken direct to the plate, the ends being connected together and to the supply voltage. This eliminates the capacitance due to the mounting brackets. The total capacitance measured at the plate of V_7 by a probe-type capacitance meter was 35 pF of which 17 pF were contributed by the CRT V_5 . The residual inductance of R_{52} was 160 μ H. This inductance is sufficient to provide the required amount of high frequency compensation, no additional series inductance being required. The capacitance of the cable from the probe to the video stage including all connectors was 150 pF.

6. Acknowledgment.

The author wishes to thank Mr. L. Medina of the C.S.I.R.O., Division of Electrotechnology, who initiated the development programme and whose helpful advice during many discussions is gratefully acknowledged.

4. Medina, L., "Prevention of ionization in small power transformers", *Proc. I.R.E. (Aust.)*, **15**, May 1954, 114.

(41)

Two Probe-type Capacitance Meters

L. Medina*

Summary.

Two types of instrument are described, suitable for the measurement of wiring and component earth capacitances in electronic apparatus. The instruments have a range of 50 pF and consist of a probe and an indicator unit.

In the first instrument a substitution method is used. The unknown capacitance can be read on the dial of a small variable capacitor contained in the probe. The accuracy of the instrument depends only on the stability of this capacitor. An estimate of the parallel loss resistance of the unknown capacitance is possible.

In the second instrument a moving coil meter gives a direct indication of capacitance. The accuracy is ± 5 per cent or ± 1 pF, whichever is greater.

1. Introduction.

The performance of many types of electronic apparatus is affected by the earth capacitances of its components and wiring. An instrument for the convenient measurement of these capacitances is not only useful for developmental work but is often essential for quality control in mass production. Wiring capacitances which form an integral part of a network can be checked and adjusted, variable trimmers can be preset to save alignment time and the capacitance between coupled coils can be compared with a standard sample.

With the first instrument to be described, capacitance is measured by a substitution method. The unknown capacitance detunes a parallel resonant circuit, and the capacitance change required to restore resonance is read from the dial of a small variable capacitor contained in the probe. This instrument is particularly suitable for developmental work, its stability of calibration being dependent on the stability of one capacitor only. Also, it makes possible an estimate of the parallel loss resistance of the unknown capacitance.

For production purposes, however, there is a need for another type of instrument with a direct indication of capacitance and with a smaller probe which does not require a variable capacitor. In this, the second instrument to be described, the accuracy depends on the stability of several components.

2. Description of First Instrument.

The circuit diagram is shown in Figure 1. The components surrounded by dashed lines are in the probe. In the octode V_1 , grids 1 and 2 are used as an oscillator. C_4 and L_2 determine the frequency, which is approximately 2 Mc/s. When the resonant frequency of C_1 L_1 approaches the oscillator frequency a voltage of this frequency appears on C_1 L_1 due to space charge and capacitance coupling.

Grid rectification occurs and, due to the flow of current in R_1 , there is a drop in plate current which is indicated by M. This effect has been used by Alexander¹. The magnitude of the plate current change can be adjusted by means of C_2 and it can be spread over the scale of a 0–1 mA moving coil instrument by means of the compensation circuit R_4 R_5 . The unknown capacitance C_x is placed across C_1 , thus detuning C_1 L_1 . The capacitance difference required to restore the plate current minimum equals C_x and can be read on the dial of C_1 . It is convenient to include in the probe a small variable trimmer so that the plate current minimum can be adjusted to occur with C_1 near maximum. If the dial of C_1 is marked zero when C_1 is near maximum, this dial can be calibrated directly in C_x .

A capacitance change of 0.1 pF can be detected and this is less than the reading error of a small dial marked 0.50 pF.

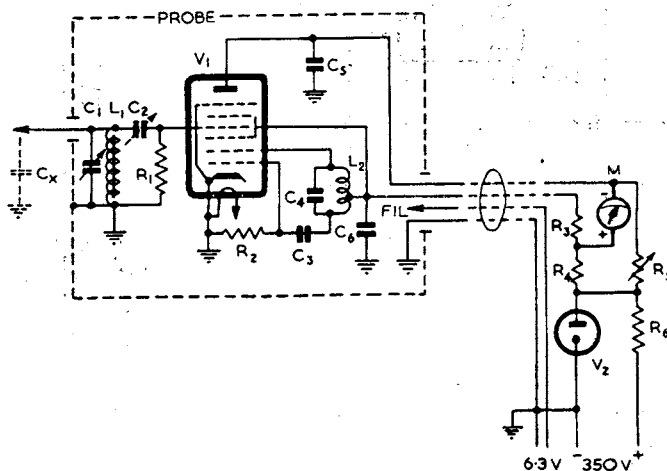


Figure 1.—Circuit Diagram of the first type of capacitance meter.

C_1	: 60 pF (air-dielectric variable capacitor).
C_2	: 25 pF
C_3, C_4	: 50 pF
C_5, C_6	: 0.01 μ F
R_1	: 3 M Ω
R_2	: 0.1 M Ω
R_3	: 10 K Ω
R_4	: 1 K Ω
R_5	: 2 K Ω
R_6	: 10 K Ω
V_1	: EK2 or EK32
V_2	: VR150/30
L_1	: $Q \geq 100$
L_2	: tapped at 1/3
} to resonate at approx. 2 Mc/s.	

*Division of Electrotechnology, C.S.I.R.O., Australia.

Manuscript received by the Institution 5/12/52.

U.D.C. number 621.317.7 : 621.3.011.4.

1. ALEXANDER, W., "An Electronic Ultramicro-meter," Electronic Engineering, 23, Dec. 1951, 479.

The magnitude of the plate current drop diminishes with a decrease in the "Q" of $L_1 C_1$. The table below gives the measured influence of parallel resistance added to $L_1 C_1$ the "Q" of which was 100. R_5 was adjusted for 1000 μA deflection on M with $L_1 C_1$ completely detuned. C_2 was set to 23 pF.

TABLE I.

Added Parallel Resistance, $M\Omega$...	∞	3	0.5	0.1	0.04	0.02
Indication of M, μA ...	120	200	500	620	800	870

Before the advent of "Q" meters, the dependence of the plate current change on the parallel resistance of the control grid circuit as indicated in Table I was used by the author for the comparison of parallel-tuned-circuits².

A suitable probe for this instrument is a box $2\frac{1}{4} \times 2\frac{1}{4} \times 7\frac{1}{2}$ inches, made of brass. In the front portion are C_1 , C_2 , L_1 and R_1 . The octode is in the centre and the oscillator circuit and cable terminations are in the rear part. In order to eliminate hand capacitance the probe tip should be arranged so that the box acts as a screen between the knob of C_1 and the probe tip.

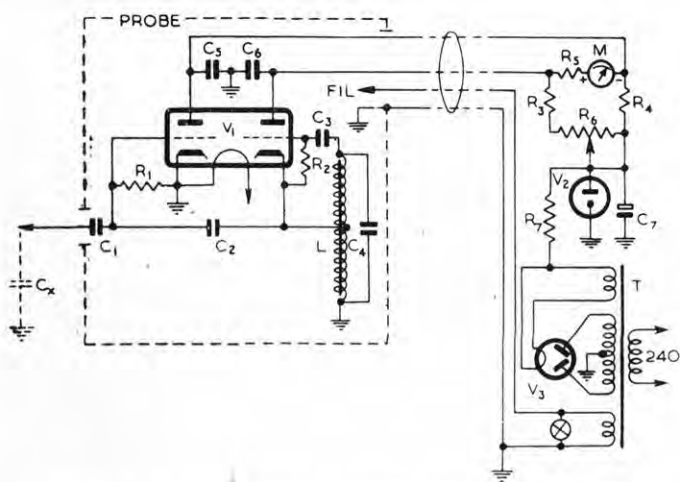


Figure 2.—Circuit diagram of second type of capacitance meter.

C_1	: 100 pF
C_2	: approx. 2 pF (twisted pair of 26 SWG enamelled wires).
C_3	: 10 pF
C_4	: 50 pF
C_5, C_6	: 0.01 μF
C_7	: 8 μF
R_1	: 3 $M\Omega$
R_2	: 0.25 $M\Omega$
R_3	: 1500 Ω
R_4	: 750 Ω
R_5	: approx. 900 Ω (by trial).
R_6	: 500 Ω
R_7	: 7500 Ω
V_1	: 12AU7
V_2	: VR150/30
V_3	: 5Z4
T	: 2 \times 330 V, 6.3 V, 5 V
L	: centre-tapped, to resonate at approx. 2 Mc/s.

Representative electrode currents for an EK2 tube are given in Table II.

TABLE II.

Electrode.	Electrode current in mA.	
	At plate current minimum.	L_1, C_1 completely detuned.
plate	—	4.0
grid 3/5	2.85	2.7
grid 2	0.55	0.5
grid 1	0.10	0.08

The maximum current through M during the warm-up period was 1.2 mA.

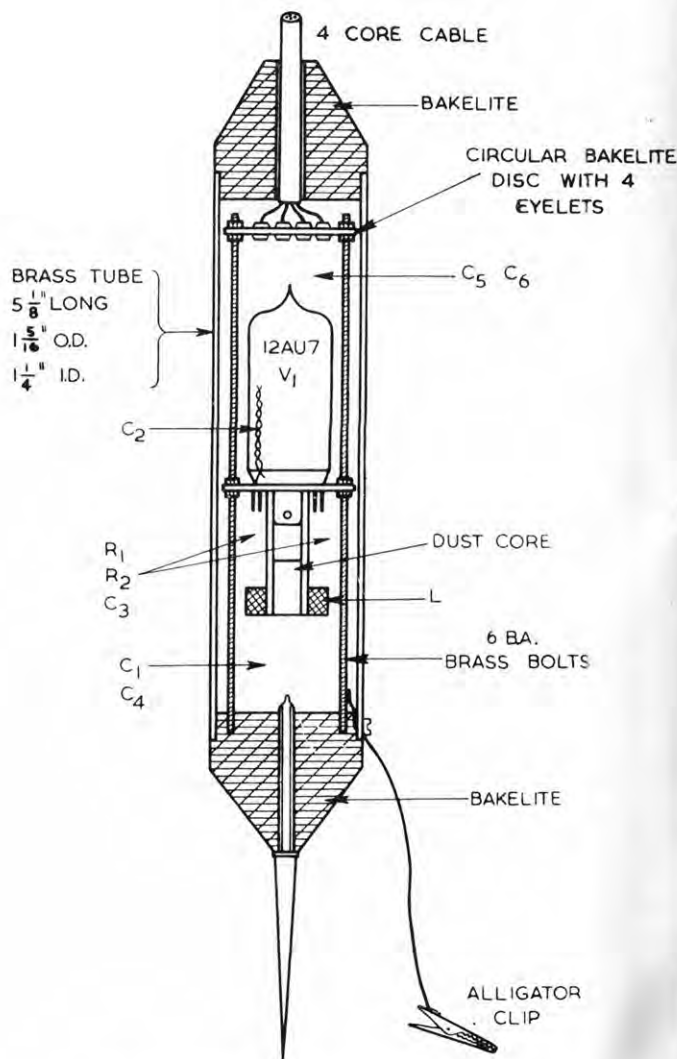


Figure 3.—The second type of capacitance meter.

3. Description of Second Instrument.

The circuit diagram is shown in Figure 2. The components surrounded by dashed lines are in the probe. V_1 is a double-triode, the right half of which is used as a Hartley oscillator coupled by means of C_2 to the left triode which serves as a grid-rectification type vacuum tube voltmeter. R_3 , R_4 and zero control R_6 are chosen in such a way that the plate potentials can be made equal. An unknown capacitance C_x forms, with C_2 , a voltage divider for the V.T.V.M. grid voltage. The resulting change in plate current of the V.T.V.M.-tube is indicated by M which can be calibrated in capacitance. C_1 is in series with C_x and prevents overloading of M when the tip of the probe is shorted to ground. Also, by means of C_1 the scale can be made open at low values of C_x and constricted at the higher values. Table III below indicates the scale shape obtained in the instrument shown in Figure 4.

TABLE III.

Capacitance, pF	5	10	15	20	30	40	50
Per cent deflection of M	...	15	29	41	51	69	86	100	

Because both plates of V_1 are at earth potential for RF the capacitance coupling between oscillator and V.T.V.M. within the tube is negligibly small.

The instrument reading is influenced slightly by the power factor of C_x but the error resulting from this is small. For example, the error is $\frac{1}{2}$ per cent for a power factor of 10 per cent in C_x .

The stability of calibration depends on several components of the circuit and on V_1 . A conservative estimate of the accuracy, based on tests, is ± 5 per cent or ± 1 pF, whichever is greater.

The construction of the instrument can be seen from Figures 3 and 4. Typical operating currents are given in Table IV.

TABLE IV.

V.T.V.M. plate current...	4.3 mA
Oscillator plate current	2.1 mA
Reversed current during warm-up period	0.5 mA
Current through M with probe shorted			2.3 mA

Changing V_1 does not require a new scale, but merely adjustment of components, mainly C_2 and R_5 .

Calibration and Range Extension.

The calibration may be carried out by means of a variable standard capacitor or by series and parallel combinations of 5 mica capacitors of 10 pF.

The Author :



Mr. Medina was born in Austria in 1908. He graduated Dipl. Ing. in Electrical Engineering from the Technical University of Vienna in 1932. While still an undergraduate he was Assistant Technical Editor of several radio periodicals. Mr. Medina is the author of numerous papers dealing mostly with the results and practical application of electrical measurements. After graduation he was a senior receiver design engineer in several radio factories in Poland, Czechoslovakia and Austria. In 1938, while still in Europe, he was engaged by Thom and Smith Pty. Ltd., and he arrived in Australia early in 1939. As Assistant Chief Engineer of this Company he was responsible for the electrical design and development of radio receivers, amplifying equipment, two-way mobile installations, transceivers, and MF, HF and VHF transmitters for FM and AM, mostly for the Armed Services. In 1946 he joined the staff of the Division of Electrotechnology, C.S.I.R.O., where he is mainly concerned with the development of equipment for precise measurements and with the design of special transformers.

The range of 50 pF was found to cover most requirements in practice. On the rare occasions when this was insufficient, a series capacitor of 100 or 70 pF was attached to the probe, thus extending the range to 100 or 200 pF.

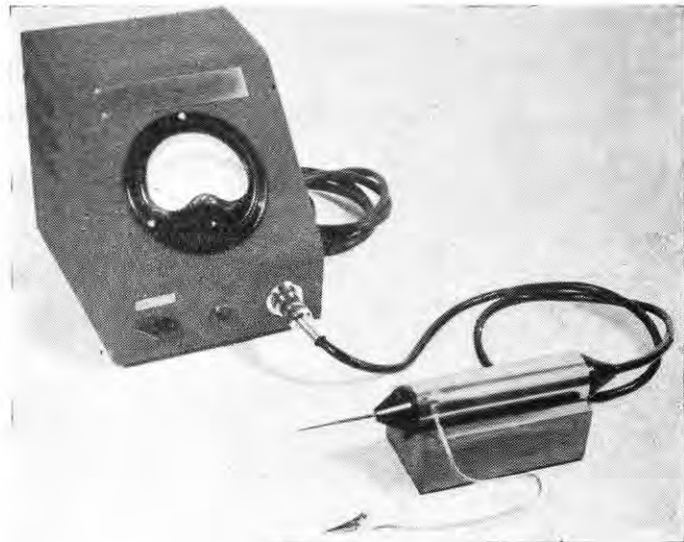


Figure 4.—Construction of the probe of the second type of capacitance meter.

COMMONWEALTH OF AUSTRALIA
COMMONWEALTH SCIENTIFIC AND INDUSTRIAL RESEARCH
ORGANISATION

AN INDICATOR EMPLOYING A TRANSISTOR FOR THE DETECTION OF LIVE HIGH VOLTAGE CONDUCTORS AND FAULTY INSULATORS

By

L. MEDINA and F. C. HAWES



*Reprinted from the "Australian Journal of Instrument
Technology," Vol. XII + No. 3 + Page Nos. 111-116
August, 1956*

An Indicator Employing a Transistor for the Detection of Live High Voltage Conductors and Faulty Insulators

By L. MEDINA, Dipl. Ing., A.M.I.E. (Aust.)* and
F. C. HAWES, A.S.T.C., Grad. I.E. (Aust.)*

SUMMARY.

A transistor amplifier, a single torch cell, and a d.c. mA meter are contained in a small metal housing located at the end of an insulating rod. When the instrument is connected to a live conductor, the charging current of the housing is amplified and indicated, the reading being proportional to voltage.

The detector may also be used to compare the voltage distribution of suspension insulator strings and the impedances of pin type insulators.

The voltage range is 2 to 40 kV_{rms} to earth and temperature compensation up to 45 deg. C. is provided in addition to protection against severe overload.

Several alternatives are described including a two-stage detector which gives an indication without contacting the conductor.

INTRODUCTION

A common type of live line detector[†] (see Fig. 1) consists of a resistor R located in an insulating tube I, a rectifier type mA meter M in a metal housing H, a rod S of insulating material and a trailing earth lead E. In some instruments the earth wire is omitted because it is an encumbrance when climbing a pole and it constitutes a hazard if it becomes open-circuited. A more sensitive indicator must then be used to detect the capacitance current flowing from H to ground.[†]

A neon lamp has been used as a sensitive indicator for this purpose, but observation is difficult in bright sunlight and furthermore a meter reading is preferable, if quantitative use is to be made of the indication, as is the case when testing insulators. A rectifier type micro-ammeter or an electrostatic voltmeter are considered insufficiently robust for field use; also it is desirable to use standard and readily available components for small quantity production.

A detector fulfilling these requirements has been made using a transistor amplifier to drive a robust 0-0.5 mA d.c. meter, the unit being supplied from a single torch cell located in the meter housing.

CIRCUIT DESCRIPTION

The circuit diagram of a detector with a voltage range of 2 to 40 kV (3.3 to 66 kV three-phase line voltage) and suitable for operation at temperatures up to 45 deg.C. is shown in Fig. 2.

*Division of Electrotechnology, National Standards Laboratory, C.S.I.R.O.

†The capacitance of H (usually 5 to 10 pF) and therefore the indicated voltage are nearly independent of the distance to ground if H is more than 3 ft. above earth.

Connection to the H.V. voltage conductor is made at I. The voltage drop on the resistor R_2 caused by the charging current of the

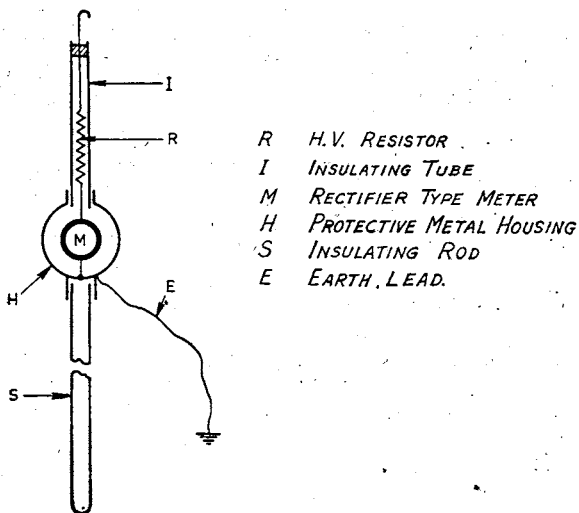


FIG 1: DIAGRAMMATIC REPRESENTATION OF A LIVE LINE DETECTOR WITH EARTH LEAD.

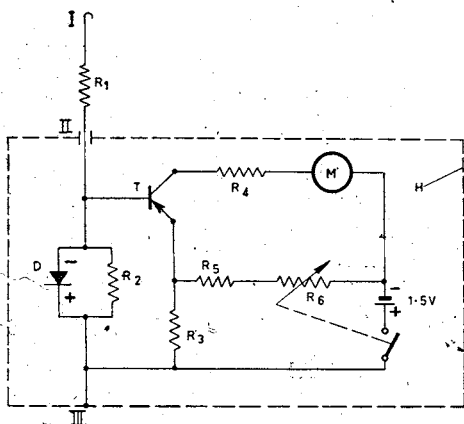


FIG 2 SINGLE STAGE CIRCUIT

R_1	$20 \times 1 M\Omega$	M	DC MILLIAMMETER 0-0.5 mA
R_2	$47 k\Omega$	D	DIODE, CV425 OR OA85.
$R_{3,5}$	50Ω	T	TRANSISTOR, OC70
R_4	470Ω	H	METAL HOUSING
R_6	$5 k\Omega$, POT. LOG. (FITTED WITH ON/OFF SWITCH.)		

metal housing H is rectified, in the base-emitter circuit and the amplified base current is indicated by the meter M in the collector circuit. This meter is scaled in units of deflection rather than voltage because any voltage calibration would change with temperature owing to its influence on the transistor parameters. Control R_6 provides variable negative emitter bias and permits adjustment of the no-signal collector current. This is required because the no-signal indication, which at temperatures below 25 deg.C. does not exceed 0.05 mA, rises to between 0.3 and 0.6 mA at 45 deg.C., the range of values being due to differences in transistors. R_3 and R_4 are chosen such that negligible degeneration occurs in the base emitter circuit and that at ordinary temperatures, when R_6 is at its maximum value, the emitter bias is nearly zero. The resistors R_1 , R_4 and the diode D prevent damage to the transistor and meter in case of a severe momentary overload as may occur if the housing H contacts a second line in a three-phase system.

PERFORMANCE

The graphs of Fig. 3 show typical meter readings in per cent. of full scale deflection as a function of voltage at 20 deg.C., 30 deg.C., 40 deg.C. and for two settings of R_6 .

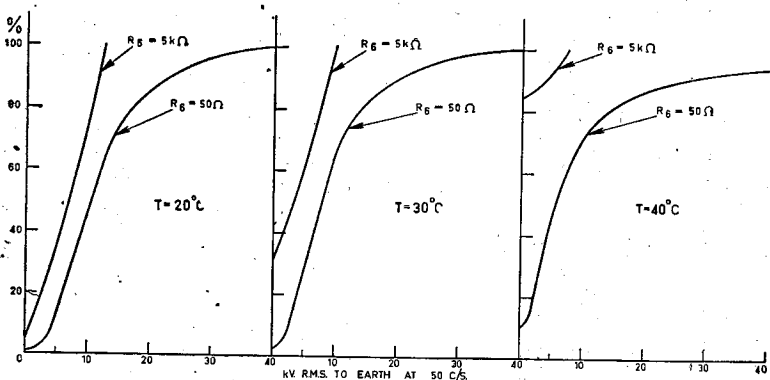


FIG 3. TYPICAL METER READINGS IN % OF FULL SCALE DEFLECTION.
AS A FUNCTION OF APPLIED VOLTAGE

The capacitance of the housing (measuring 4 x 4 x 4 in) plus the metal fitting for the insulating rod was about 9 pF and approximately the same readings were obtained when 1/1000 of the voltage was applied via a capacitor of 9 000 pF to II and III (Fig. 2). This artifice was used to observe the performance at elevated temperatures with the detector placed in an oven.

To check the influence of a near-by conductor on the indication, the detector was connected to a line, the voltage of which was adjusted to give a meter reading of 50 per cent. of full scale. When a second line adjusted to the same voltage as the first line, but with a phase-difference of ± 120 deg. was brought to within 7 in. of the meter housing the readings obtained were 45 per cent. and 55 per cent. respectively.

The battery current is less than 1 mA at ordinary temperatures and about 15 mA at the limit of the temperature range.

APPLICATIONS

Live Conductor Detection

Since the "safe" condition of high voltage conductors is indicated by a "zero" reading, this represents a danger should the detector be inoperative. A check immediately before and after the testing of conductors is therefore required.

At temperatures above 15 deg.C., the no-signal collector current and its change with the setting of R_3 (Fig. 2) provides a useful check of the circuit. An overall check may be carried out using an ignition coil and an interrupter or by means of the ignition system of a car. In this case I should be connected to the output of the ignition coil and III to the body of the car. An alternative is to use a 500 V "Megger" with its negative terminal connected to I and its positive terminal on III.

When testing for "live" conductors the maximum sensitivity should be used, with R_3 at its maximum value. If, however, the temperature is so high that the no-signal collector current exceeds 0.1 mA, R_3 should be adjusted to give a meter reading of 0.05 to 0.1 mA and no attempt should be made to "zero" the meter with R_3 , as this reduces the sensitivity. The overload capacity of the detector is such that no harm can be done by contacting a live line at maximum sensitivity.

Live Line Insulator Testing

Suspension insulator strings or insulator stacks may be tested by observing the potential differences between the metal caps and ground. Faulty disks are shown up by an abnormal voltage distribution.

The impedance of a single pin-type insulator mounted on a dry wooden pole or crossarm may be compared with the impedances of other similarly mounted insulators, or with that of an insulator known to be satisfactory, by connecting the detector first to the line and then to the pin. In these comparison tests it is convenient to set the meter to a cardinal scale point by means of control R_4 .

When testing insulators it is desirable to obtain readings on that part of the scale where a change of voltage causes a large change in deflection. At 66 kV/ $\sqrt{3}$, and to a lesser degree at 33 kV/ $\sqrt{3}$, range compression occurs (see Fig. 3) and in order to see differences more clearly the voltage on the transistor may be reduced by connecting a resistor externally between II and III (Fig. 2). A typical value is 3 k Ω .

ALTERNATIVE CIRCUITS

A simpler circuit for the range 2 to 40 kV is possible if operation at ordinary temperatures only is required. R_3 , R_5 and R_6 may then be omitted, but R_4 must be increased to 1 k Ω . With selected transistors this detector operates satisfactorily up to 30 deg.C.

In some cases a more linear relationship between voltage and deflection may be preferable. For the range 5 to 40 kV this may be achieved by omitting R_4 , R_5 and R_6 , by increasing the battery voltage to 4½ V and by increasing R_3 to 2 k Ω and bypassing it with a capacitor of 100 μ F. The meter movement should then be 0.1 mA. Adjustable temperature compensation is not required up to 30 deg.C.

In many high voltage reticulation networks the line voltage is 11 kV and a detector giving full scale deflection at approximately 7 kV would be preferable. This may be obtained by reducing the value of R_4 to 220 Ω and by using a type OC71 transistor in the

circuit of Fig. 2. For operation above 40 deg.C. transistors with a no-signal collector current of less than 1 mA at 45 deg.C. must be selected. To accommodate transistors with more than 1 mA, the range of the temperature compensation may be increased by decreasing R_2 to 22 k Ω but this in turn reduces the sensitivity and furthermore a large amount of compensation is not considered good practice.

The circuit of an experimental detector with still higher sensitivity is shown in Fig. 4. An amplifier stage precedes the arrangement of Fig. 2. Negative a.c. feedback, forward bias and stabilization of the operating point is obtained by connecting the resistor R_3 (Fig. 4) between base and collector. A portion of the bias developed

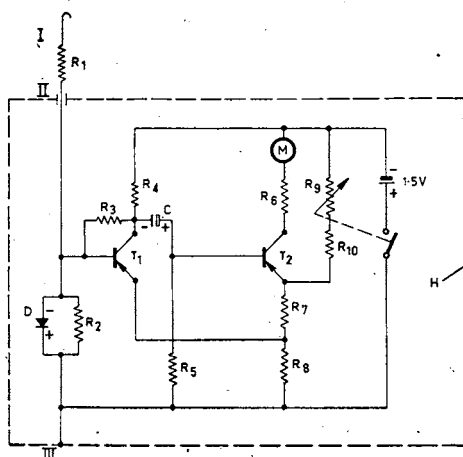


FIG. 4 TWO STAGE CIRCUIT

R_1	20x1M Ω	R_{10}	50 Ω
R_2	47 k Ω	M	D.C. MILLIAMMETER 0-0.5 mA
R_3	130 k Ω	D	DIODE. CV425 OR OA85.
$R_{4,5}$	10 k Ω	$T_{1,2}$	TRANSISTOR OC70
R_6	470 Ω	C	B.U.F
$R_{7,8}$	25 Ω	H	METAL HOUSING
R_9	2.5k Ω POT, LOG. (FITTED WITH ON/OFF SWITCH)		

on R_7 and R_8 is also applied to the emitter of the first stage for temperature compensation. Owing to the stabilization by means of R_3 the additional compensation of the first stage is less critical and with some transistors satisfactory operation at 45 deg.C. has been obtained with the emitter of T_1 connected to III. In the case of a very temperature-sensitive transistor it was found necessary to shift the connection of the emitter of T_1 to the junction of R_7 and R_{10} if operation above 40 deg.C. was desired. Instability due to positive feedback in this connection could not be observed.

The range of the two-stage detector is 0.5 to 40 kV. At 20 deg.C. and with R_9 at its maximum value the deflection was 10 per cent.

of full scale at 0.5 kV and 30 per cent at 1 kV. Owing to the higher sensitivity an indication is given without contacting the high voltage conductor. For example, at 5 kV to earth a reading of 10 per cent. of full scale was obtained at a distance of 5 in. from a line; at 40 kV and at a distance of 18 in. the reading was 60 per cent.

For insulator testing on 66 kV and 33 kV lines a typical value of shunt resistance to be connected between II and III is 2 k Ω .

ACKNOWLEDGMENT

The authors wish to thank Mr. E. P. Gough of D. E. Taplin Pty. Ltd., who carried out numerous field tests on the prototype detector and who supplied representative insulators for test.

REFERENCE.

1. Shotter, G. F. and Hutchins, E. E., *Potential Indicators for Live Conductor Detection*, E.R.A. Report Ref., F/T 133 (1940).